

Some pages of this thesis may have been removed for copyright restrictions.

If you have discovered material in AURA which is unlawful e.g. breaches copyright, (either yours or that of a third party) or any other law, including but not limited to those relating to patent, trademark, confidentiality, data protection, obscenity, defamation, libel, then please read our [Takedown Policy](#) and [contact the service](#) immediately

**THE USE OF FLOW CONTROL DEVICES TO
IMPROVE THE FLOW PATTERN AND
THROUGHPUT OF SIEVE TRAYS**

A THESIS SUBMITTED

BY

RAB NAWAZ KHAN, B-Eng, MSc.

A Candidate for the degree of

Doctor of Philosophy

DEPARTMENT OF CHEMICAL ENGINEERING

AND

APPLIED CHEMISTRY

ASTON UNIVERSITY

SEPTEMBER 1998

This copy of the thesis has been supplied on the condition that anyone who consults it is understood to recognise that its copyright rests with its author and that no quotation from the thesis and no information derived from it may be published without the author's prior written consent.

UNIVERSITY OF ASTON IN BIRMINGHAM

THE USE OF FLOW CONTROL DEVICES TO IMPROVE THE FLOW PATTERN
AND THROUGHPUT OF SIEVE TRAYS

A THESIS SUBMITTED BY

RAB NAWAZ KHAN B.ENG., MSc.,

A candidate for the degree of Doctor of Philosophy- October 1998

SUMMARY

Compared to packings trays are more cost effective column internals because they create a large interfacial area for mass transfer by the interaction of the vapour on the liquid. The tray supports a mass of froth or spray which on most trays (including the most widely used sieve trays) is not in any way controlled. The two important results of the gas/ liquid interaction are the tray efficiency and the tray throughput or capacity. After many years of practical experience, both may be predicted by empirical correlations, despite the lack of understanding. It is known that the tray efficiency is in part determined by the liquid flow pattern and the throughput by the liquid froth height which in turn depends on the liquid hold-up and vapour velocity.

This thesis describes experimental work on sieve trays in an air-water simulator, 2.44 m in diameter. The liquid flow pattern, for flow rates similar to those used in commercial scale distillation, was observed experimentally by direct observation ; by water-cooling, to simulate mass transfer ; use of potassium permanganate dye to observe areas of longer residence time ; and by height of clear liquid measurements across the tray and in the downcomer using manometers. This work presents experiments designed to evaluate flow control devices proposed to improve the gas liquid interaction and hence improve the tray efficiency and throughput. These are (a) the use of intermediate weirs to redirect liquid to the sides of the tray so as to remove slow moving/ stagnant liquid and (b) the use of vapour-directing slots designed to use the vapour to cause liquid to be directed towards the outlet weir thus reducing the liquid hold-up at a given rate i.e. increased throughput. This method also has the advantage of removing slow moving/ stagnant liquid.

In the experiments using intermediate weirs, which were placed in the centre of the tray, it was found that in general the effect of an intermediate weir depends on the depth of liquid downstream of the weir. If the weir is deeper than the downstream depth it will cause the upstream liquid to be deeper than the downstream liquid. If the weir is not as deep as deep as the downstream depth it may have little or no effect on the upstream depth. An intermediate weir placed at an angle to the direction of flow of liquid increases the liquid towards the sides of the tray without causing an increase in liquid hold-up/ froth height. The maximum proportion of liquid caused to flow sideways by the weir is between 5 % and 10 %.

Experimental work using vapour-directing slots on a rectangular sieve tray has shown that the horizontal momentum that is imparted to the liquid is dependent upon the size of the slot. If too much momentum is transferred to the liquid it causes hydraulic jumps to occur at the mouth of the slot coupled with liquid being entrained. The use of slots also helps to eliminate the hydraulic gradient across sieve trays and provides a more uniform froth height on the tray. By comparing the results obtained of the tray and point efficiencies, it is shown that a slotted tray reduces both values by approximately 10 %. This reduction is due to the fact that with a slotted tray the liquid has a reduced residence time on the tray coupled also with the fact that large size bubbles are passing through the slots. The effectiveness of using vapour-directing slots on a full circular tray was investigated by using dye to completely colour the biphasic. The removal of the dye by clear liquid entering the tray was monitored using an overhead camera. Results obtained show that the slots are successful in their aim of reducing slow moving liquid from the sides of the tray. The net effect of this is an increase in tray efficiency. Measurements of slot vapour-velocity found it to be approximately equal to the hole velocity.

Key Words : DISTILLATION, SIEVE TRAYS, FLOW PATTERNS, TRAY EFFICIENCY, SLOTS.

Acknowledgements

I would like to express my gratitude to the following:

My supervisors, Dr. J.P. Fletcher and Prof. K.E. Porter, for their guidance and stimulating ideas and constant encouragement throughout the course of my research.

The excellent technicians Ian Murkett and Maurizio Santoro for their practical help and assistance. The secretarial staff especially Lynn for their valuable help and advice throughout the programme. Many thanks also to Dr. Eric Smith whose help was invaluable in the submission of this thesis.

The Engineering and Physical Science Research Council (EPSRC) for their financial support and VLE Data Centre (Aston) Co. Ltd. For their funding of the CASE award.

Finally, I would like to thank all members of my family, without whose encouragement and faith in me, this thesis would never have been written.

Dedicated to my beloved parents.

TABLE OF CONTENTS

	Page No.
Thesis Summary	2
Acknowledgements	3
Table of Contents	4
List of Figures	9
List of Tables	15
Nomenclature	16
Chapter 1 Introduction	
1.1 Overview	20
1.2 Outline of Thesis	24
Chapter 2 Literature Review	
2.1 Introduction	26
2.2 Hypothetical Flow Patterns	28
2.2.1 Stagnant Regions Model	28
2.2.2 Retrograde Flow Model	29
2.2.3 Turbulent Two-Dimensional Liquid Phase Flow	30
2.2.4 Conclusions on Hypothetical Flow Patterns	30
2.3 Modelling of Tray Efficiencies	31
2.3.1 Definitions of Point and Tray Efficiencies	31
2.4 Theoretical Modelling of Tray Efficiencies from Liquid Flow Patterns	34
2.4.1 Completely Mixed Tray	34
2.4.2 Plug Flow Tray	35
2.4.3 Series of Mixed Pools	37
2.4.4 Back-mixing Imposed on Plug Flow	38
2.5 Flow Regimes	41
2.5.1 Spray Regime	41
2.5.2 Mixed Froth Regime	42
2.5.3 Emulsion Flow Regime	42
2.6 Previous Work on the 2.4 m Column	44
2.7 Separated or Non-Separated Flow	46
2.8 Effects of Separated Flow on Tray Efficiency	48
2.9 Conventional Procedures for Sieve Tray Design	51
2.10 Downcomer Backup	53
2.11 Hydraulic Gradient	54

2.12	High Throughput Trays	56
2.13	Flow Control Devices for Trays	59
2.13.1	UOP Slotted Sieve Tray	59
2.13.2	FRI Downcomer	60
2.13.3	Step Flow Downcomer	61
2.13.4	Inclined Counter-Current Contact Tray	61
2.13.5	Winged Downcomer	62
2.13.6	Kuhni Slit Tray	62
2.13.7	BOC Double Expanded Metal Tray	63
2.13.8	Conclusion on Flow Control Devices	64
2.14	Conclusion on Literature Review	65
Chapter 3	Approach to the Problem	66
Chapter 4	Description of the Apparatus, Measurement and Operational Procedures	
4.1	Introduction	69
4.2	Overall Test Facility	69
4.2.1	Air Supply	74
4.2.2	Water Supply	74
4.2.3	Heating Supply	75
4.2.3.1	Gas Fired Boilers	76
4.2.3.2	Steam Supply	76
4.2.3.3	Double Heat Exchanger	77
4.3	The 2.4 m Diameter Simulator Column	78
4.3.1	Air Distribution Shell	78
4.3.2	The Test Column	80
4.3.3	Exhaust Section	81
4.4	Measurement of Operating and System Variables	81
4.4.1	Maximum Air and Water Flow Rate Specifications	82
4.4.2	Measurement Specifications of the Instrumentation by Error Analysis	82
4.4.3	Measurement of Air Flow rates	86
4.4.4	Measurement of Water Flow rates	86
4.5	Operation of the Air-Water Simulator	88
4.5.1	Start-Up Procedure	88
4.5.2	Normal Operation	89
4.5.3	Shut Down Procedure	89
Chapter 5	The Effect of Intermediate Weirs on the Flow Pattern Across a Rectangular Sieve Tray	
5.1	Introduction	90
5.2	Measurement of Clear Liquid Hold-Up	93

	5.3	Measurement Technique Using Manometers	93
	5.4	Experimental Procedure	94
	5.5	Results and Discussions	97
	5.5.1	Critical Flow In An Open Channel	97
	5.5.2	No Intermediate Weir	99
	5.5.3	10 mm Intermediate Weir	100
	5.5.4	50 mm Intermediate Weir	101
	5.6	Conclusions	127
Chapter 6		Flow Directing Weir Placed At An Angle to the Direction of Flow	
	6.1	Introduction	128
	6.2	Measurement Technique	129
	6.3	Calibration	129
	6.4	Experimental Procedure	131
	6.5	Results and Discussion	133
	6.6	Conclusions	138
	6.7	Future Work Using Intermediate Weirs On a Full Circular Tray	139
Chapter 7		The Use of Vapour-Directing Slots to Improve The Throughput of a Rectangular Sieve Tray	
	7.1	Introduction	141
	7.1.1	Vapour-Directing Slots	144
	7.2	The Design and Testing of Different Size Vapour-Directing Slots	145
	7.2.1	Experimental Procedure	145
	7.2.2	Results and Discussion	150
	7.3	Experimental Work Using Vapour-Directing Slots Placed Across a Rectangular Sieve Tray	153
	7.4	Results and Discussion	156
	7.4.1	Downcomer Backup	156
	7.4.2	Height of Clear Liquid	159
	7.5	Conclusions	165
Chapter 8		The Effect of the Vapour-Directing Slots on the Point and Tray Efficiency of a Rectangular Sieve Tray	
	8.1	Introduction	166
	8.2	The Water-Cooling Experiment	167
	8.2.1	Resistance Thermometer Detectors and Data Logger	167
	8.2.2	Calibration of Platinum Resistance Thermometers	170

	8.2.3	Temperature Positions on the Rectangular Tray	173
	8.3	Experimental Procedure	174
	8.3.2	Data Treatment and Presentation of Temperature Profiles	174
	8.3.3	Efficiency Calculations	176
	8.4	Results and Discussion	178
	8.4.1	Temperature Contours over the Tray	179
	8.4.2	Efficiency Results	189
	8.5	Conclusions	195
Chapter 9		The Use of Vapour-Directing Slots on a Circular Tray to Remove Stagnant or Circulating Regions and Increase Throughput	
	9.1	Introduction	196
	9.2	Camera Recording of Coloured Dye	197
	9.3	Vapour-Directing Slot Layout Across Circular Tray	199
	9.4	Experimental Procedure	201
	9.5	Results and Discussion	203
	9.5.1	Dye Injection Results	203
	9.5.2	Downcomer Back-Up Results	210
	9.5.3	Tray Efficiency Results	214
	9.6	Conclusions	217
Chapter 10		Experiment to Measure the Velocity of Air Through a Single Vapour-Directing Slot	
	10.1	Introduction	218
	10.2	Experimental Procedure and Programme	219
	10.3	Measurement Technique and Calibration	221
	10.4	Results and Discussion	222
	10.5	Conclusions	226
Chapter 11		CONCLUSIONS	226
		Recommendations For Future Work	
		References	
Appendix 1A		Height of Clear Liquid Measurements (mm), No Intermediate Weir, Rectangular Sieve Tray	236
Appendix 1B		Height of Clear Liq. Measurements (mm), 10 mm Intermediate Weir, Rectangular Sieve Tray	243

Appendix 1C	Height of Clear Liq. Measurements (mm), 50 mm Intermediate Weir, Rectangular Sieve Tray	250
Appendix 2	Flow Over the Outlet Weir Measurements	256
Appendix 3	Height of Clear Liquid Measurements in Downcomer Rectangular Tray	259
Appendix 4	Height of Clear Liquid Measurements in Downcomer Full Circular Tray	262
Appendix 5	Video Recording of Dye Injection Experiments (Attached to Thesis)	

LIST OF FIGURES

		Page No
Fig. 2.1	Hypothetical Flow Pattern- Stagnant Regions Model	28
Fig. 2.2	Hypothetical Flow Pattern- Retrograde Flow Model	29
Fig. 2.3	Hypothetical Flow Pattern- Turb.2-Dim. Model	30
Fig. 2.4	Schematic diagram of the relationship between the point tray and overall column efficiencies (simplified)	31
Fig. 2.5	Schematic diagram of the concentration profile of vapour and liquid streams entering and leaving the tray.	32
Fig. 2.6	Schematic diagram of Flows on Consecutive Trays for the Lewis Model	37
Fig. 2.7	Structure of the two-phase dispersions in the different flow regimes	42
Fig. 2.8	The two-phase flow regime map suggested by Hofhuis and Zuiderweg	44
Fig. 2.9	Schematic diagram of the onset of Flow Separation	47
Fig. 2.10	Direct-observation of the liquid flow pattern using flow pointers indicating uniform forward flow across the tray	49
Fig. 2.11	Direct-observation of the liquid flow pattern using flow pointers indicating inlet liquid circulation	49
Fig. 2.12	Water-Only flow pattern- 20% circulation	50
Fig. 2.13	Water-Only flow pattern- 30% circulation	50
Fig. 2.14	Hydraulic Gradient Profile on a Sieve Tray	55
Fig. 2.15	Schematic diagrams of High Throughput Trays	57
Fig. 2.16	Schematic diagram of a single slot as used on sieve trays	60
Fig. 2.17	Schematic diagram of an Inclined Counter-Current contact Tray	61
Fig. 2.18	Schematic diagram of a Winged Downcomer	62

Fig. 4.1	Schematic diagram of the air-water distillation test plant	71
Fig. 4.2	Photograph of the air-water simulator	72
Fig. 4.3	Schematic diagram of the air-water distillation simulator with modified air distributor	79
Fig. 4.4	Tray Flooding Curve, 12.7 mm hole sieve tray, 8% free area and 0.6 m tray spacing	83
Fig. 5.0	Intermediate weir placed in the centre of rectangular sieve tray	92
Fig. 5.1	Schematic diagram of a manometer for measuring the height of clear liquid	93
Fig. 5.2	A Pressure diagram for the calculation of the height of clear liquid	94
Fig. 5.3	Position of the manometer tappings across the 1 mm tray	95
Fig. 5.4 a,b,c	Surface of Clear Liquid Hold-Up, No Intermediate Weir, IG/OW= 10 mm, Superficial Air Velocity 1.5 m/s, Water Loading (a) 50 (b) 150 © 250 cm ³ /cm.s	101
Fig. 5.5 a,b,c	Surface of Clear Liquid Hold-Up, No Intermediate Weir, IG/OW= 10 mm, Superficial Air Velocity 2.5 m/s, Water Loading (a) 50 (b) 150 © 250 cm ³ /cm.s	102
Fig. 5.6 a,b,c	Surface of Clear Liquid Hold-Up, No Intermediate Weir, IG/OW= 20 mm, Superficial Air Velocity 1.5 m/s, Water Loading (a) 50 (b) 150 © 250 cm ³ /cm.s	104
Fig. 5.7 a,b,c	Surface of Clear Liquid Hold-Up, No Intermediate Weir, IG/OW= 20 mm, Superficial Air Velocity 2.5 m/s, Water Loading (a) 50 (b) 150 © 250 cm ³ /cm.s	105
Fig. 5.8 a,b,c	Surface of Clear Liquid Hold-Up, No Intermediate Weir, IG/OW= 50 mm, Superficial Air Velocity 1.5 m/s, Water Loading (a) 50 (b) 150 © 250 cm ³ /cm.s	107
Fig. 5.9 a,b,c	Surface of Clear Liquid Hold-Up, No Intermediate Weir, IG/OW= 50 mm, Superficial Air Velocity 2.5 m/s. Water Loading (a) 50 (b) 150 © 250 cm ³ /cm.s	108
Fig. 5.10 a,b,c	Surface of Clear Liquid Hold-Up, 10 mm Interm. Weir, IG/OW= 10 mm, Superficial Air Velocity 1.5 m/s, Water Loading (a) 50 (b) 150 © 250 cm ³ /cm.s	110

Fig. 5.11 a,b,c	Surface of Clear Liquid Hold-Up, 10 mm Interm. Weir, IG/OW= 10 mm, Superficial Air Velocity 2.5 m/s, Water Loading (a) 50 (b) 150 © 250 cm ³ /cm.s	111
Fig. 5.12 a,b,c	Surface of Clear Liquid Hold-Up, 10 mm Interm. Weir, IG/OW= 20 mm, Superficial Air Velocity 1.5 m/s, Water Loading (a) 50 (b) 150 © 250 cm ³ /cm.s	113
Fig. 5.13 a,b,c	Surface of Clear Liquid Hold-Up, 10 mm Interm. Weir, IG/OW= 20 mm, Superficial Air Velocity 2.5 m/s, Water Loading (a) 50 (b) 150 © 250 cm ³ /cm.s	114
Fig. 5.14 a,b,c	Surface of Clear Liquid Hold-Up, 10 mm Interm. Weir, IG/OW= 50 mm, Superficial Air Velocity 1.5 m/s, Water Loading (a) 50 (b) 150 © 250 cm ³ /cm.s	115
Fig. 5.15 a,b,c	Surface of Clear Liquid Hold-Up, 10 mm Interm. Weir, IG/OW= 50 mm, Superficial Air Velocity 2.5 m/s, Water Loading (a) 50 (b) 150 © 250 cm ³ /cm.s	116
Fig. 5.16 a,b,c	Surface of Clear Liquid Hold-Up, 50 mm Interm. Weir, IG/OW= 10 mm, Superficial Air Velocity 1.5 m/s, Water Loading (a) 50 (b) 150 © 250 cm ³ /cm.s	118
Fig. 5.17 a,b,c	Surface of Clear Liquid Hold-Up, 50 mm Interm. Weir, IG/OW= 10 mm, Superficial Air Velocity 2.5 m/s, Water Loading (a) 50 (b) 150 © 250 cm ³ /cm.s	119
Fig. 5.18 a,b,c	Surface of Clear Liquid Hold-Up, 50 mm Interm. Weir, IG/OW= 20 mm, Superficial Air Velocity 1.5 m/s, Water Loading (a) 50 (b) 150 © 250 cm ³ /cm.s	121
Fig. 5.19 a,b,c	Surface of Clear Liquid Hold-Up, 50 mm Interm. Weir, IG/OW= 20 mm, Superficial Air Velocity 2.5 m/s, Water Loading (a) 50 (b) 150 © 250 cm ³ /cm.s	122
Fig. 5.20 a,b,c	Surface of Clear Liquid Hold-Up, 50 mm Interm. Weir, IG/OW= 50 mm, Superficial Air Velocity 1.5 m/s, Water Loading (a) 50 (b) 150 © 250 cm ³ /cm.s	124
Fig. 5.21 a,b,c	Surface of Clear Liquid Hold-Up, 50 mm Interm. Weir, IG/OW= 50 mm, Superficial Air Velocity 2.5 m/s, Water Loading (a) 50 (b) 150 © 250 cm ³ /cm.s	125
Fig. 6.1	Calibration of liquid flowrate against recorded height	130
Fig. 6.2	Diagram of angled weir on rectangular sieve tray	132
Fig. 6.3	Graph of weir load against weir length, IG/OW =50 mm, Air Velocity = 0.7 m/s, Weir Load = 25 cm ³ /cms	134

Fig. 6.4	Graph of weir load against weir length, IG/OW =50 mm, Air Velocity = 0.9 m/s, Weir Load = 35 cm ³ /cms	135
Fig. 6.5	Graph of weir load against weir length, IG/OW =50 mm, Air Velocity = 0.7 m/s, Weir Load = 55 cm ³ /cms	136
Fig. 6.6	Graph of weir load against weir length, IG/OW =50 mm, Air Velocity = 1.2 m/s, Weir Load = 110 cm ³ /cms	137
Fig. 6.7	Graph of weir load against weir length, IG/OW =50 mm, Air Velocity = 1.5 m/s, Weir Load = 110 cm ³ /cms	138
Fig.6.8	Future Expts. Using IW's on a Full Circular Tray	139
Fig. 6.9	Future Expts. Using IW's on a Full Circular Tray	140
Fig. 7.1	Schematic diagram of the detrimental effect of stagnant regions on tray efficiency	142
Fig. 7.2	Side-View of Vapour-Directing Slot	146
Fig. 7.3	Side-View of Vapour-Directing Tray	146
Fig. 7.4 a,b,c	Photographs of Vapour-Directing Slots	147
Fig. 7.5	Hydraulic Gradient due to vapour-directing slot	151
Fig. 7.6	Side view of vapour-directing tray	154
Fig. 7.7	Photograph of slotted rectangular sieve tray	155
Fig. 7.8	Graph of Downcomer Hydraulics, Rectangular Tray, IG/OW = 50 mm, Air Velocity = 1.5 m/s	157
Fig. 7.9	Graph of Downcomer Hydraulics, Rectangular Tray, IG/OW = 50 mm, Air Velocity = 2.0 m/s	158
Fig. 7.10a	Surface of Clear Liquid Hold-Up, Superficial Air Velocity 1.5 m/s, IG/OW= 50 mm, Water Loading 50 cm ³ /cm.s, UNSLOTTED TRAY	160
Fig 7.10b	Surface of Clear Liquid Hold-Up, Superficial Air Velocity 1.5 m/s, IG/OW= 50 mm, Water Loading 50 cm ³ /cm.s, SLOTTED TRAY	160

Fig. 7.11a	Surface of Clear Liquid Hold-Up, Superficial Air Velocity 1.5 m/s, IG/OW= 50 mm, Water Loading 100 cm ³ /cm.s, UNSLOTTED TRAY	161
Fig. 7.11b	Surface of Clear Liquid Hold-Up, Superficial Air Velocity 1.5 m/s, IG/OW= 50 mm, Water Loading 100 cm ³ /cm.s, SLOTTED TRAY	161
Fig. 7.12a	Surface of Clear Liquid Hold-Up, Superficial Air Velocity 1.5 m/s, IG/OW= 50 mm, Water Loading 150 cm ³ /cm.s, UNSLOTTED TRAY	162
Fig. 7.12b	Surface of Clear Liquid Hold-Up, Superficial Air Velocity 1.5 m/s, IG/OW= 50 mm, Water Loading 150 cm ³ /cm.s, SLOTTED TRAY	163
Fig. 7.13a	Surface of Clear Liquid Hold-Up, Superficial Air Velocity 1.5 m/s, IG/OW= 50 mm, Water Loading 200 cm ³ /cm.s, UNSLOTTED TRAY	163
Fig. 7.13b	Surface of Clear Liquid Hold-Up, Superficial Air Velocity 1.5 m/s, IG/OW= 50 mm, Water Loading 200 cm ³ /cm.s, SLOTTED TRAY	163
Fig. 7.14a	Surface of Clear Liquid Hold-Up, Superficial Air Velocity 1.5 m/s, IG/OW= 50 mm, Water Loading 250 cm ³ /cm.s, UNSLOTTED TRAY	164
Fig. 7.14b	Surface of Clear Liquid Hold-Up, Superficial Air Velocity 1.5 m/s, IG/OW= 50 mm, Water Loading 250 cm ³ /cm.s, SLOTTED TRAY	164
Fig 8.1	Schematic diagram of resistance thermometer and water shroud attachment to the test tray	168

Fig. 8.2	Photograph of resistance thermometer and water shroud	169
Fig. 8.3	Photograph of microlink data logger and PC	170
Fig. 8.4	Schematic diagram of the positions of PRT's across a rectangular sieve tray	171
Fig. 8.5	Schematic diagram of an operating tray	176
Fig. 8.6 a,b,c,d,e	Two Dimensional Reduced Temperature Contour Plot, Superficial Air Velocity 1.5 m/s, Water Weir Loading (a) 50 (b) 100 (c) 150 (d) 200 (e) 250 cm ³ /cms, SLOTS	179
Fig. 8.7 a,b,c,d,	Two Dimensional Reduced Temperature Contour Plot, Superficial Air Velocity 2.0 m/s, Water Weir Loading (a) 50 (b) 100 (c) 150 (d) 200 , SLOTS	181
Fig. 8.8 a,b,c,	Two Dimensional Reduced Temperature Contour Plot, Superficial Air Velocity 2.5 m/s, Water Weir Loading (a) 50 (b) 100 (c) 150 , SLOTS	183
Fig. 8.9 a,b,c,d,e	Two Dimensional Reduced Temperature Contour Plot, Superficial Air Velocity 1.5 m/s, Water Weir Loading (a) 50 (b) 100 (c) 150 (d) 200 (e) 250 cm ³ /cms, NO SLOTS	185
Fig. 8.10 a,b,c,d,	Two Dimensional Reduced Temperature Contour Plot, Superficial Air Velocity 2.0 m/s, Water Weir Loading (a) 50 (b) 100 (c) 150 (d) 200 , NO SLOTS	187
Fig. 8.11 a,b,c,	Two Dimensional Reduced Temperature Contour Plot, Superficial Air Velocity 2.5 m/s, Water Weir Loading (a) 50 (b) 100 (c) 150 , NO SLOTS	189
Fig. 8.12	Graph of Measured Tray Efficiency Against Weir Load	193
Fig. 8.13	Graph of Measured Point Efficiency Against Weir Load	194
Fig. 9.1	Schematic diagram showing the dye injection apparatus	198
Fig. 9.2	Diagram showing the residence time/ flow path length across a circular tray	200
Fig. 9.3	Diagram showing the 24 vapour-directing slots positioned over the 2.44 m circular tray	202
Fig. 9.4a	Still photograph of an Unslotted Tray, Sup. Air Vel. 0.75 m/s, Water Weir Load 25 cm ³ /cms	204
Fig. 9.5a	Still photograph of an Slotted Tray, Sup. Air Vel. 0.75 m/s, Water Weir Load 25 cm ³ /cms	205

Fig. 9.5 a	Still photograph of an Unslotted Tray, Sup. Air Vel. 1.0 m/s, Water Weir Load 75 cm ³ /cms	206
Fig. 9.5 b	Still photograph of an Slotted Tray, Sup. Air Vel. 1.0 m/s, Water Weir Load 75 cm ³ /cms	207
Fig. 9.6a	Still photograph of an Unslotted Tray, Sup. Air Vel. 1.5 m/s, Water Weir Load 100 cm ³ /cms	208
Fig. 9.6 b	Still photograph of an Slotted Tray, Sup. Air Vel. 1.5 m/s, Water Weir Load 100 cm ³ /cms	209
Fig. 9.7	Graph of Downcomer Hydraulics, Full Tray, IG/OW = 50 mm, Sup. Air Vel. = 1.0 m/s.	211
Fig. 9.8	Graph of Downcomer Hydraulics, Full Tray, IG/OW = 50 mm, Sup. Air Vel. = 1.5 m/s.	212
Fig. 9.9	Graph of Downcomer Hydraulics, Full Tray, IG/OW = 50 mm, Sup. Air Vel. = 2.0 m/s.	213
Fig. 9.10	Murphree Tray Efficiency Against Weir Load, Superficial Air Velocity = 1m/s	215
Fig. 9.11	Murphree Tray Efficiency Against Weir Load, Superficial Air Velocity = 2m/s	216
Fig. 10.1	Calibration Curve of Air-Flow Against Pressure Drop	220
Fig. 10.2	Graph of Superficial Air Velocity Against Corresponding Slot Velocity	223

LIST OF TABLES

		Page No.
4.1	Summary of the design specifications of all the peripheral equipment.	72
4.2	Summary of the tray design specifications and experimental variables	73
4.3	Accuracy of Murphree Tray Efficiency with associated errors of the measured variables	85
8.1	Measured Murphree Efficiency data- Slotted Tray, IG/OW= 50 mm.	192
8.2	Measured Murphree Efficiency data- Normal Tray, IG/OW= 50 mm	192
10.1	Superficial Air Velocity and Corresponding Slot Velocity	222

NOMENCLATURE

a	Interfacial area per volume of two-phase mixture	(m^2/m^3)
A	Effective transfer area	(m^2)
A_B	Active area of tray	(m^2)
A_D	Downcomer area	(m^2)
A_T	Column cross-sectional area	(m^2)
C_{air}	Specific heat capacity of air	$(\text{kJ}/\text{kg K})$
C_{wat}	Specific heat of water vapour	$(\text{kJ}/\text{kg K})$
C_p	Specific Heat Capacity	$(\text{kJ}/\text{kg K})$
C_{SB}	Bubbling area capacity factor	(m/s)
C_s	Load Factor	(m^2/s)
D	Tray Diameter	(m)
D	Kinematic viscosity (Eddy viscosity)	(m^2/s)
D_e	Eddy diffusion coefficient	(m^2/s)
d_h	Diameter of tray perforations	(m)
d_i	Diameter of the distributor tray	(m)
d_o	Hole Diameter	(m)
E_{ml}	Murphree tray efficiency, based on liquid phase	$(-)$
E_{mv}	Murphree tray efficiency, based on vapour phase	$(-)$
E_o	Overall column efficiency	$(-)$
E_{og}	Murphree point efficiency, based on overall vapour phase resistance	$(-)$
E_{ol}	Murphree point efficiency, based on the overall liquid phase resistance	$(-)$
F	Flooding factor in tray design	$(-)$

f_a	Free area on the active area of the tray	(m^2 / m^2)
f_w	Flow Parameter	(-)
G	Total air (vapour) mass flowrate	(kg/s)
h_{cl}	Height of clear liquid	(mm)
h_{DT}	Dry tray pressure drop	(mm)
h_f	Froth Height	(mm)
h_R	Residual pressure drop	(mm)
h_{ow}	Height of Outlet Weir	(m)
h_{wt}	Wet tray pressure drop	(m of H ₂ O)
$H_{\Delta i}$	Outlet enthalpy of air from position i on a tray	(kJ/kg)
H_m	Average inlet enthalpy of air	(kJ/kg)
H_{Ti}	Enthalpy of air in equilibrium with water at temp. T_i	(kJ/kg)
$H_{T_{out}}$	Enthalpy of air in equilibrium with water at temp. T_{out}	(kJ/kg)
$H_{i, (db, wb)}$	Humidity of air under dry/wet bulb conditions	(kg moisture/ kg dry air)
$H_{(out)}$	Humidity of air at average outlet water temperature	(kg moisture/ kg dry air)
IG	Height of gap under the inlet downcomer	(m)
k	Turbulent kinematic energy	(J)
k_G	Mass transfer coefficient in the gas (vapour) phase	(m/s)
k_L	Mass transfer coefficient in the liquid phase	(m/s)
k_T	Heat Transfer coefficient in the gas (vapour) phase	(kJ/ m ² .s.k)
L	Total liquid mass flowrate	(kg/s)
Le	Lewis number (Sc / Pr)	(-)
L_w	Liquid flowrate per unit weir length	(m ³ / m.s)
m	Gradient of equilibrium line in mass transfer	(-)
N	Number of passes in tray design	(-)

N_{OG}	Number of overall transfer units in the gas phase	(-)
N_{pe}	Peclet Number	(-)
OW	Outlet Weir Height	(m)
P	Pressure	(N/m ²)
P_e	Peclet Number	(-)
Q_G	Vapour volumetric flowrate	(m ³ /s)
Q_L	Liquid volumetric flowrate	(m ³ /s)
S	Foam or 'ignorance derating' factor in tray design	(-)
t	Time	(s)
t_L	Average liquid contact time	(s)
t_G	Mean residence time of gas in dispersion	(s)
t_w	Water temperature	(K)
T_{db}	Air dry bulb temperature	(K)
T_i	Temperature of water at position i on a tray	(K)
T_r	Reduced temperature driving force	(-)
T_{wb}	Air wet bulb temperature	(K)
u	Mean component velocity in x direction	(m/s)
U_{DF}	Downcomer velocity of vapour-liquid mixture	(m/s)
u_H	Hole gas velocity through tray	(m/s)
u_S	Superficial Velocity	(m/s)
u_{SB}	Superficial velocity based on tray bubbling area	(m/s)
V	Volumetric vapour flow rate	(m ³ /s)
v_A	Gas velocity through the tray	(m/s)
W	Weir Length	(m)
W_G	Total air (vapour) mass flowrate	(kg/s)
W_L	Total water (liquid) mass flowrate	(kg/s)
x	Liquid concentration	(Mol. Frac)

x_n	Composition of liquid leaving stage n	(Mol. Frac)
x_{n+1}	Average composition of liquid leaving n+1	(Mol. Frac)
x_n	Composition of liquid in equilibrium with vapour composition y_n	(Mol. Frac)
y_n	Composition of vapour leaving stage n	(Mol. Frac)
y_{n-1}	Composition of vapour leaving stage n-1	(Mol. Frac)
y_{n-1}	Average composition of vapour leaving stage n-1	(Mol. Frac)
y_n	Composition of vapour in equilibrium with liquid composition x_n	(Mol. Frac)
z	Flow Path Length	(m)
ρ_g	Vapour Density	(kg/m ³)
ρ_l	Liquid Density	(kg/m ³)
θ	Contact Time	(s)
λ	Ratio of operating line to equilibrium line	(-)
ϕ	Point to plate efficiency enhancement	(-)
ΔT	Temperature Difference	(k)
μ	Viscosity	(kg/m s)
α	Relative Volatility	(-)

1. INTRODUCTION

1.1 OVERVIEW

Distillation is a mature business, which like the motor industry, is constantly being driven by market forces and is often led by research and design, Porter 1992. Thus the assertion that distillation is a fully mature technology and lacking the potential for further improvement can be countered by the fact that it is the most frequently used process for separating fluid mixtures and that more sophisticated distillation technology is continually being developed.

The one main drawback of distillation is that it consumes large quantities of energy. In 1976, it was estimated that distillation accounted for 3 % of world energy demand. Mix 1980. There are around 1700 distillation columns in operation throughout the UK ; the energy usage in these columns amounts to around 160 PJ/year, of which 100 PJ/year is used in oil refining. There is still, however, the potential to save around 7 PJ/year through improving tray efficiency in the process industries. In 1980, Rush demonstrated that for most cases, it would be economically viable to use an alternative method of separation. Furthermore, he stated that there was a need to design distillation columns 'leaner and harder', at a time when energy conservation and power savings were top priority. Due to the high operating costs associated with distillation, any incremental improvements in efficiency, however small, may produce substantial rewards in energy and financial savings.

In order to keep distillation competitive in the fluid separation field, both capital and operating costs must be kept to a minimum. Capital costs can be reduced by making the contacting devices, be they trays or packings, as efficient as possible and operating costs can be reduced by the better integration of distillation equipment into the whole process. If designs are to be made tighter to reduce both capital and operating costs, then the degree of risk associated with the column not performing to the design specification must increase.

To reduce this risk requires a thorough understanding of the distillation process and in the case of distillation trays, this means understanding the liquid flow patterns. The long term objective for distillation tray research must therefore be to develop the appropriate theories of two-phase flow, such that for any tray design and fluid system the flow pattern may be predicted.

Originally, the use of trays was favoured over packings since trays were less expensive to manufacture and there was considerable uncertainty in the performance of scaled-up packed columns. These problems were later overcome through the better design of liquid and vapour distribution systems. Hence, the use of packings as contacting devices is becoming more widespread in distillation. Nevertheless, trays remain a popular column internal device for use in new plants because of the reduced initial cost. Hence there are still many tray distillation columns in industrial use and there is the possibility of developing new trays with increased throughput and high operating efficiency.

The importance of liquid flow patterns on distillation trays was recognised as far back as the 1930's (Kirschbaum, 1934), when it was discovered that the assumption of completely mixed liquid on a tray was erroneous. Since this period, many theoretical models have been proposed (Lewis, 1936 ; Kirschbaum, 1948 ; Gautreaux and O'Connell, 1955 ; Diener, 1967 ; Porter et al., 1972 ; Bell and Solari, 1974 ; Yu et al., 1990), which account for the flow and mass transfer interactions over distillation trays. These models are based on the concepts of well mixed pools of liquid with liquid flow between them, the plug (unmixed) flow of liquid with backmixing, or diffusional mixing within the liquid flow across circular trays. These theories assume that predicted liquid changes only occur in the direction of liquid flow whilst remaining constant perpendicular to the direction of flow. This can be described as one dimensional modelling.

During the 1970's theoretical models which accounted for non-uniform liquid flow and mixing on a tray, Porter et al., 1972, were proposed on the basis of limited amount of experimental observations. These models in particular that based on liquid channelling associated with stagnant regions at the sides of the tray predict loss in tray efficiency and account for scale up failures on large trays. The results of this work have prompted developments of more complex models as well as highlighting the need for experimental data on trays of a commercially significant size. The most recent example of the modern approach to modelling is the three dimensional non-equilibrium pool model, Yu et al., 1991, which predicts concentration changes and inter-diffusional mixing in two dimensions, in both the liquid and vapour mixing pools. Current research is directed towards the identification of the physical principles which are valid in a new branch of fluid mechanics, recently defined by Porter (1992) as 'Open Channel Two-Phase Flow'.

With this in mind, a research program commenced at Aston University in the late 70's, with the intention of gaining an in depth understanding of the phenomena which affect flows on industrial scale distillation trays. A 2.44 m diameter single tray air-water simulator was constructed (Hine 1990) which simulated distillation by forcing air (vapour) through a liquid (water) flowing on a commercial size tray where the ratio of the froth depth to flow path length is typical of that found in practice. This apparatus has been used by a succession of workers (Hine 1990, Chambers 1993, Fenwick 1996) in order to build up a comprehensive bank of data, including height of clear liquid measurements, tray efficiencies and information about flow patterns over a range of operating conditions designed to simulate a wide range of distillation conditions. The experimental results collected from this and other research programmes will be incorporated in an open-channel two-phase flow theoretical model during the next stage of tray research. This will be used to describe the controlling phenomena for any test system and tray configuration which is necessary for the more scientific approach to the design of new trays. By predicting column efficiency more accurately it will be possible to reduce the number of trays added to allow for uncertainty.

Although it is clearly important to be able to model trays which have been built and which are probably even now are operating under conditions of non-ideal flow, it is also necessary to consider ways of straightening and improving the liquid flow pattern on trays that will be installed in the future i.e. to introduce corrective measures for controlling the liquid flow at the inlet downcomer and dispersing the vapour-liquid flow into the stagnant or circulating regions. According to Biddulph and Lavin (1990) 'The hydraulic flow problems should be corrected rather than rigorously modelled. There seems to be little point in developing ever more sophisticated models of trays which are operated badly. Modified tray designs are needed to correct the flow problems'. In order to do this flow control devices need to be tested and their performance evaluated.

The first question that needs to be answered is ' Is it possible to design a flow directing device which is able to reduce the circulating/ slow moving liquid and also increase the throughput of sieve trays ?'. If this is possible then ' What are the parameters which influence the successful operation of the device ?'. Tray suppliers have already perceived an opportunity for High Throughput Trays which are necessary for the tray business to compete with large diameter, structured packing columns Porter (1996).

1.2 OUTLINE OF THESIS

The aim of the experimental work described in this thesis is to improve the flow patterns on large diameter trays and hence the tray efficiency and throughput. In order to do this, new flow control straightener devices have been developed and tested. A brief literature review is presented in Chapter 2, chosen for evidence of the existence and effect of the liquid flow pattern on tray and column performance and to illustrate the continuous development of flow control devices. This is followed in Chapter 3 by an outline of the approach to the research programme.

Chapter 4 describes the air-water simulator column, which incorporates an air supply from an industrial scale fan and a water heating facility for heat transfer experiments to measure tray efficiency.

Chapter 5 presents work concerned with straightening the flow pattern by using different size intermediate weirs. A broad range of water flowrates was investigated, for various settings of inlet gap and outlet weir. An attempt was made to relate any change in the height of clear liquid directly to the size of the intermediate weir.

Chapter 6 describes work involving intermediate weirs placed at an angle to the direction of flow. The aim was to investigate whether liquid would be able to be deflected to the areas of stagnant/ slow moving liquid hence provide a uniform flow pattern. Any deflection of liquid was detected by the use of a liquid collection box placed in the outlet downcomer.

In Chapter 7 and 8, the use of vapour-directing slots is investigated by comparing a normal sieve tray with a slotted tray. The slots were pop-riveted to the tray floor across a rectangular tray. Data was collected and compared using manometers to measure the height of clear liquid across the tray and in the inlet downcomers : the water-cooling technique was used to quantify the effect of the slots on the point and tray efficiencies.

Chapter 9 describes work involving the use of vapour-directing slots placed evenly across a circular tray to compare with the results obtained on a rectangular slotted tray. In order to assess their effectiveness with regard to removal of stagnant or circulating regions, a dye injection technique was used which was monitored by an overhead camera. Tray efficiencies of the slotted tray were measured using the water cooling technique and were compared with the tray efficiencies of a normal tray.

Chapter 10 describes work involving the measuring of the slot vapour-velocity and also investigating the slot hydraulics in terms of any liquid under the slotted section of the tray.

For each investigation the objectives of each experiment are stated along with a discussion of the results at the end of each section. Results of all the experiments are collected and discussed. Finally all the major findings from the work are summarised in the main conclusions followed by recommendations for future work.

CHAPTER 2

LITERATURE REVIEW

2.1 INTRODUCTION

The origins of distillation date back several hundred years, to the small scale production of crude liquors by ancient civilisations, but the development of distillation as a scientific technology has only been around for 70 years, coinciding with the establishment of the petrochemical industry. The main problem to upgrade tray technology in order to meet increasing demands of the consumer was the enormous difficulty in testing full scale distillation columns such that negligible plant data was published over a period of many years.

Initial research was confined to defining stable operating conditions on small laboratory scale distillation trays, and mathematical models were formulated to predict the effect of liquid flow on mass transfer efficiency. In addition tray design was, and still is, based on empirical (trial and error) correlations and past experience.

The theoretical origins of many of these empirical correlations and simple models for tray design were incorrect, Porter and Jenkins (1979), and raised the question of whether tray performance would have been greatly enhanced through a better understanding of the controlling phenomena. It was through the rapid increase in the scale of trayed columns, brought about by the economic pressures and the need for cost effective design, that serious discrepancies were revealed between the simple tray theories and what was happening in reality. Since the 1970's experimental work on commercial scale trays and a new generation of theoretical models have given a better insight into the complex vapour-liquid behaviour on trays and its effect on performance. However, a considerable amount of work remains to be done for a complete understanding of tray hydraulics and flow patterns in order to improve current tray design procedures and column performance.

This literature review is intended to put the research presented in this thesis into perspective and to explain why it was carried out.

2.2 Hypothetical Flow Patterns on Trays

Liquid flow across a tray consists of an underlying bulk velocity profile onto which the random movement of liquid flow by gas bubbling is superimposed. This determines the liquid residence time distribution (RTD) on a tray. If the liquid distribution was equal at all points on the tray, the RTD profiles would be straight and parallel to the tray downcomers. This would produce the same vapour-liquid residence time over the whole tray and thus yield an optimum mass transfer efficiency Lockett (1976).

Through experimental investigation of the liquid flow pattern on circular distillation trays, several hypothetical liquid flow patterns have been proposed. These hypothetical liquid flow patterns have been used as input parameters to mathematical tray models, which can then determine the effect of a given flow pattern on tray efficiency.

The following flow patterns are described:

- (1) The Stagnant Regions Model
- (2) The Retrograde Flow Model
- (3) Turbulent Two-Dimensional Liquid Phase Flow

2.2.1 Stagnant Regions Model

The stagnant regions model was proposed by Porter et al. (1972) and is presented in Figure 2.1 below.

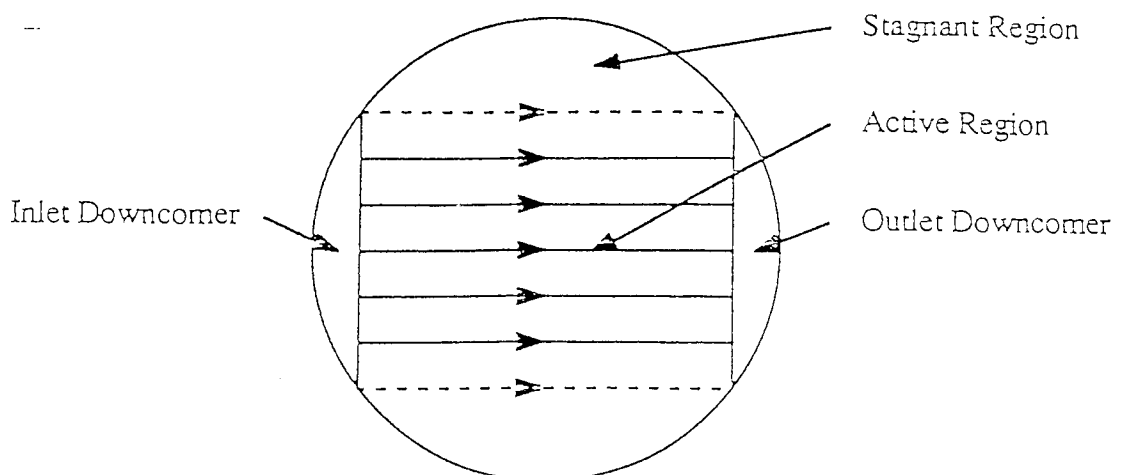


[Fig. 2.1] Hypothetical Flow Pattern: Stagnant Regions Model.

This model of the liquid flow pattern came about by the experimental observation of the way in which water flowed across a 1.2 m diameter tray section, which was inserted in a water flume. The water entered the tray section and flowed straight across to the outlet of the section with a uniform bulk velocity. As the tray is a diverging/converging open channel, there is very little tendency to flow sideways across the longer liquid flow path around the column walls. This leaves two stagnant regions, at the sides of the tray, in which liquid is in between slow forward moving or reverse flow.

2.2.2 Retrograde Flow Model

The retrograde flow model was proposed by Bell (1972b) and is presented in Figure 2.2.

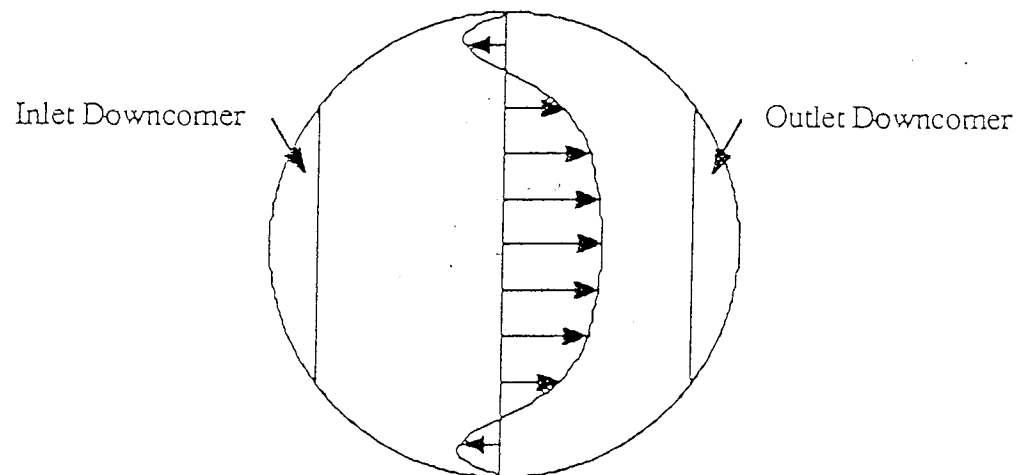


Fig. 2.2 .Hypothetical Flow Pattern: Retrograde Flow Model.

This model was based upon the experimental findings of a fibre-optic technique, carried out on a 2.44m diameter test tray. Although data were not gathered adjacent to the tray wall, extrapolated data revealed the presence of closed lines of constant residence time. The explanation of the closed lines was for reverse or retrograde flow to be occurring at the sides of the tray, with high speed flow down the centre of the tray between the two weirs.

2.2.3 Turbulent Two-Dimensional Liquid Phase Flow

Since direct measurement of liquid velocity is very difficult it would be advantageous to predict liquid velocity profiles and RTD by computational fluid dynamics. Some progress has been made in this area (Yu and Zhang, 1991; Yu, 1992; Porter et al., 1992) with the development of a liquid flow mathematical model in which the rising vapour provides a resisting force to liquid flow. To simulate two-dimensional flow on a large diameter tray, relationships, which are valid for single phase turbulent flow, were applied to a situation where turbulence and mixing is produced by a continuous vapour stream passing through the liquid (ie., treat the biphase as a homogenous fluid). Development of the model is outlined by Chambers (1993). Three regions are described over the tray area. A main flow region exists between the inlet and outlet weirs, on which a non-uniform velocity distribution is superimposed. At the side of the tray two regions exist, one a slowly forward flow region positioned towards the outlet weir and the other a backward flow region positioned towards the inlet weir, see figure 2.3.

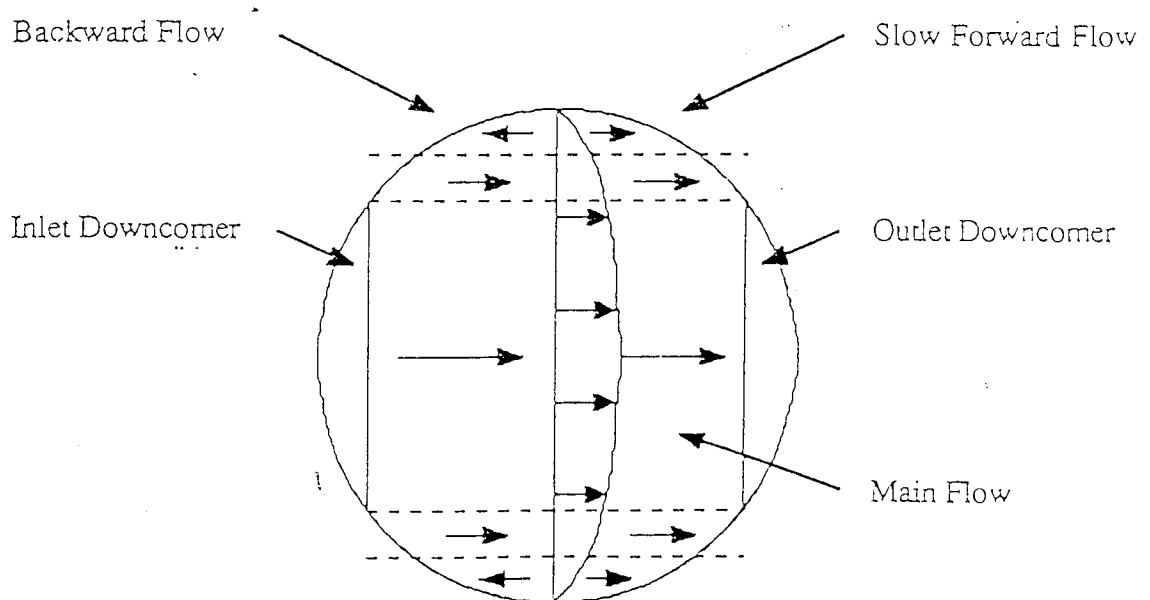


Fig. 2.3 : Turbulent Two-Dimensional Liquid Phase Model

2.2.4 Conclusions on Hypothetical Flow Patterns

The hypothetical models of the liquid flow patterns on distillation trays are in agreement with some form of liquid channelling between the two downcomers. However, between the channelling liquid and the sides of the column exist regions which could be stagnant, circulating or slowly moving forward.

2.3 Modelling of Tray Efficiency

Distillation column design based on the flow rates and vapour-liquid equilibrium data assumes that the column consists of a series of equilibrium stages, the vapour and liquid leaving each stage in equilibrium with each other. In reality, equilibrium stages are replaced by column hardware such as cross-flow contact trays (sieve, valve and bubble-cap), and usually a fractional approach to equilibrium is achieved. The number of actual trays is related to the number of calculated theoretical trays by the tray efficiency. With the establishment of non-uniform liquid flow on circular trays, both theoretically and by experiment, the next section assesses these effects on tray efficiency.

2.3.1 Definitions of Point and Tray Efficiencies

The term efficiency is a measure of the rate of mass transfer in tray design, and is dependent on several factors such as liquid film and gas film resistances. For the prediction of overall column efficiency, use is made of point and tray efficiencies as shown in Figure 2.4. There are a number of tray efficiency definitions, the most common being that defined by Murphree (1925), since it is the most widely comprehended parameter and is relatively easy to calculate.

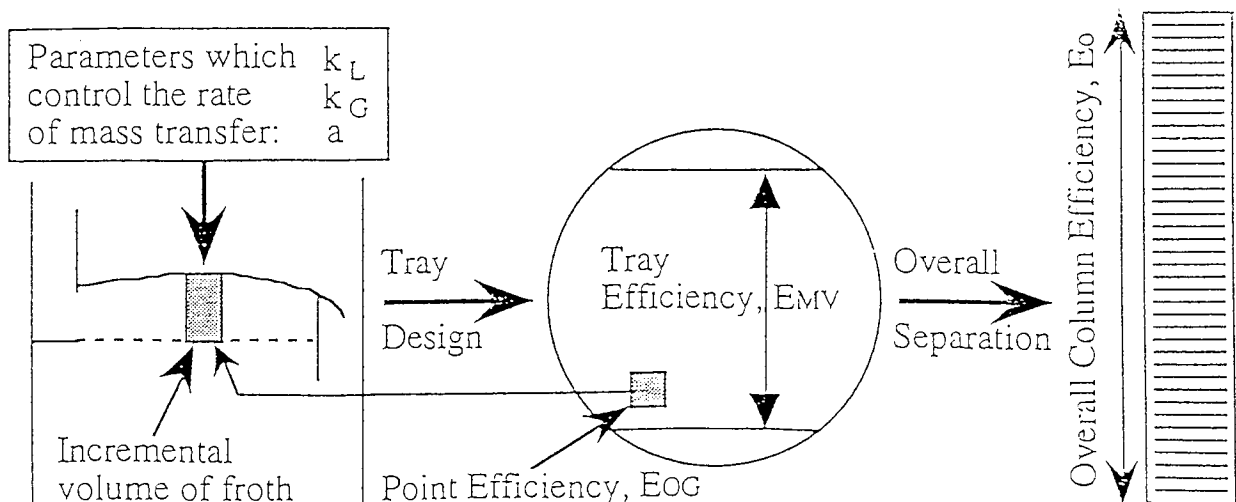


Figure 2.4: Schematic Diagram of the Relation Between Point, Tray and Overall Column Efficiency

The definition of point and tray efficiencies are best explained by means of a vapour-liquid composition diagram, see Figure 2.5. For a binary system, efficiencies can be defined in terms of either the least or most volatile component. It is more convenient to define efficiencies in terms of the least volatile component (lvc), since the concentration of the lvc in the liquid, x , increases as it crosses the tray.

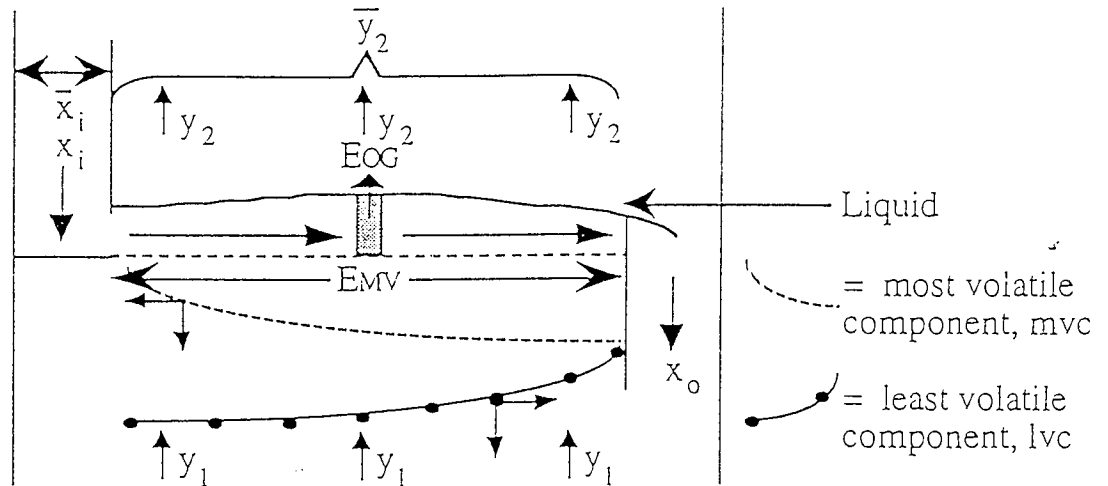


Figure 2.5: Schematic Diagram of the Concentration Profile of Vapour and Liquid Streams Entering and Leaving the Tray

From Figure 2.5, the Murphree Point Efficiency, E_{OG} , is defined in terms of the mole fraction of the vapour and liquid streams entering and leaving the tray. The compositions of the vapour entering and leaving the tray are y_1 and y_2 respectively. Similarly, the liquid phase enters the tray from that above it with a composition x_i and leaves the tray with a composition x_0 . In an ideal situation, the composition of the vapour, y^* , is assumed to be in equilibrium with the liquid composition at a point being considered on the tray. However, in reality, this is not the case and the non-equilibrium froth element on the tray can be described in terms of a local or point efficiency. Thus the fractional approach to equilibrium is given by,

$$E_{og} = \frac{y_1 - y_2}{y_1 - y^*}$$

where y_1 is assumed to be of uniform composition when entering the tray. The term E_{og} indicates that point efficiency has been defined in terms of the overall resistances to mass transfer based on vapour phase driving forces. The same argument applies to the less commonly used E_{ol} which is based on the liquid driving forces. That is,

$$E_{ol} = \frac{x_0 - x_1}{x^* - x_1}$$

where x^* is the liquid composition in equilibrium with the vapour composition, y_2 , leaving the tray at the point being considered.

To define the Murphree tray efficiency, the overall composition of the vapour entering and leaving the tray in question, are y_1 and y_2 respectively, whereas the overall liquid phase composition entering and leaving the tray can be defined as x_1 and x_0 respectively. The composition of the vapour, y_0^* , is in equilibrium with the liquid leaving the tray for an ideal situation.

$$E_{mv} = \frac{y_1 - y_2}{y_0^* - y_2}$$

The subscript mv indicates the Murphree efficiency for the whole tray on the basis of the vapour concentrations. In contrast the less commonly used E_{ml} is based on the liquid concentrations such that,

$$E_{ml} = \frac{x_0 - x_1}{x_0 - x_1^*}$$

where x_1^* is the equilibrium liquid concentration with the overall vapour composition y_2 . The above definitions of point and tray efficiency are used in theoretical models for binary systems described in the next section.

2.4 THEORETICAL MODELLING OF TRAY EFFICIENCY FROM LIQUID FLOW PATTERNS

Development of theoretical analyses to predict tray efficiency became necessary since the availability of full scale column data was scarce. Tray efficiency concepts have been proposed and used as bases for the development of tray models :

- (1) Completely mixed tray
- (2) Plug flow tray
- (3) Tray modelled by mixed pools
- (4) Backmixing imposed on the plug flow of liquid
- (5) Multi-region tray model with backmixing

2.4.1 Completely Mixed Tray

Up to the 1920's it was customary to believe that the action of the rising vapour passing through the froth on a distillation tray was sufficient to mix completely the froth on the tray. On a completely mixed tray, the liquid composition at any point is equal to the outlet composition of the liquid, and if the assumption is made that the inlet vapour composition is completely mixed also, then the vapour leaving all points of the tray must also be equal. These conditions of a completely mixed tray lead to the tray efficiency being equal to the point efficiency, i.e.

$$E_{mv} = E_{og}$$

Kirschbaum (1935), however, found considerable liquid concentration gradients across a tray of only a few inches in diameter, even at high superficial vapour velocities. This observation was to lead Kirschbaum and others to develop hypothetical models for the way in which the liquid crossed an operating tray.

2.4.2 Plug Flow Tray

Lewis (1936) proposed that the liquid crossed the tray in a plug flow fashion across a rectangular tray and developed equations to account for this. Three analyses were carried out, but it must be noted that the analyses were all performed for a tray within a section of trays. He continues by making the following assumptions:

- (1) No mixing of liquid across the tray
- (2) Rectangular liquid flow path, no segmental regions
- (3) Constant liquid and vapour flowrates
- (4) Constant point efficiency

Lewis Case 1

Lewis case 1 describes the tray efficiency where the vapour entering the tray of interest is completely mixed and the direction of liquid is of no consequence, the result obtained is:

$$E_{mv} = \frac{1}{\lambda} \left[\exp(\lambda E_{og}) - 1 \right]$$

where λ = ratio of operating line to equilibrium line.

Lewis Case 2

Case 2 describes the tray efficiency where no vapour mixing occurs and the liquid flows in the same direction on successive trays, giving:

$$E_{mv} = \frac{\alpha - 1}{\lambda - 1} \text{Lew}$$

where $\lambda = \left[\frac{1}{E_{og}} - \frac{1}{\alpha - 1} \right] \ln \alpha$

Here α is the relative volatility.

Lewis Case 3

Lewis Case 3 describes the tray efficiency where again no vapour mixing occurs but the liquid flows in alternate directions on successive trays, giving the result:

$$E_{mv} = \frac{\alpha - 1}{\lambda - 1}$$

where, if $\alpha < 1$,

$$\lambda = \left[\frac{\alpha^2 - (1 - E_{og})^2}{E_{og}^2 (1 + \alpha)(1 - \alpha)} \right]^{0.5} \cos^{-1} \left[1 - \frac{(1 - \alpha)(\alpha - 1 + E_{og})}{\alpha(2 - E_{og})} \right]$$

and, if $\alpha > 1$,

$$\lambda = \left[\frac{\alpha^2 - (1 - E_{og})^2}{E_{og}^2 (\alpha + 1)(\alpha - 1)} \right]^{0.5} \cos^{-1} \left[1 - \frac{(1 - \alpha)(\alpha - 1 + E_{og})}{\alpha(2 - E_{og})} \right]$$

The main contribution of Lewis was to show the difference between parallel flow of liquid, where the liquid flow on successive trays is in the same direction, and non-parallel flow of liquid, where the liquid flows in different directions on successive trays. For example the point to plate efficiency enhancement can be increased from 1.40 to 1.57 by using parallel flow trays rather than cross flow trays at a typical condition where the point efficiency is 70 % and $m V/L$ is 1.0. This 12 % increase in efficiency is gained without sacrifice of tray capacity or pressure drop and is achieved solely by a structural change in the tray design.

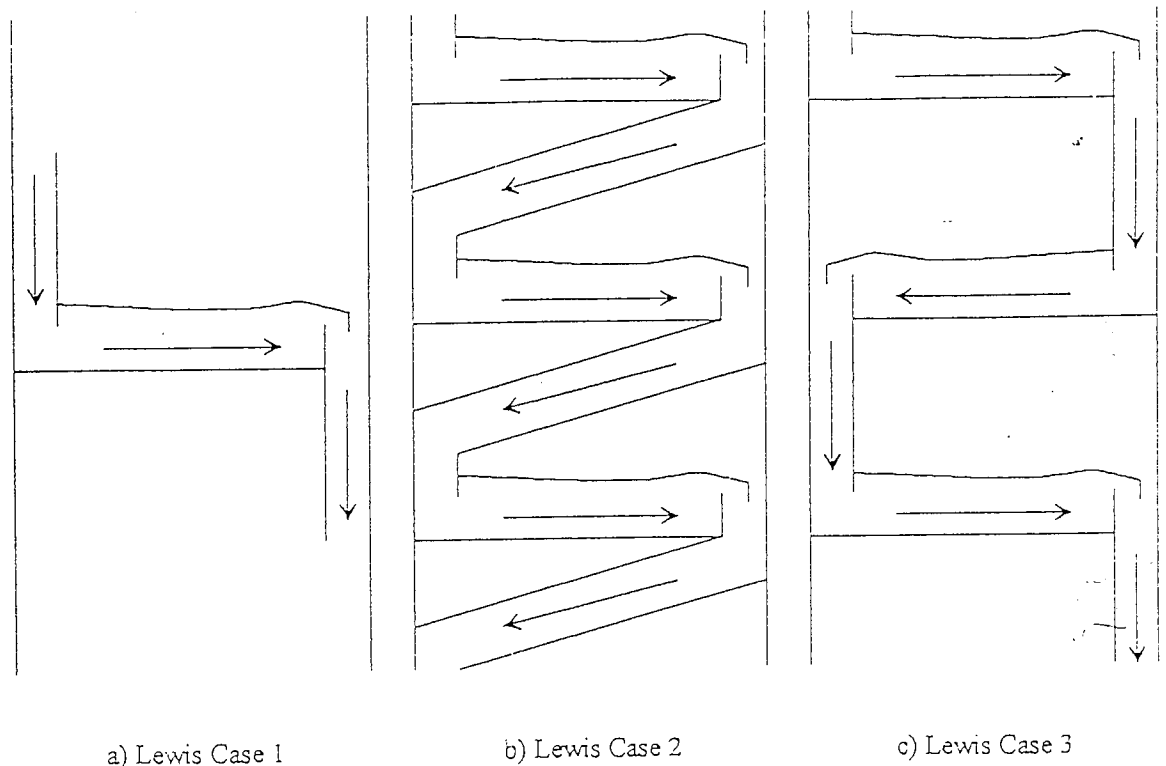


Fig 2.6: Flows on consecutive trays for the Lewis Model

2.4.3 Series of Mixed Pools

Kirschbaum (1934) working at the same time as Lewis, divided the liquid on the tray into a number of well mixed pools which were in series. The liquid moved from pool to pool changing composition as it crossed the tray. This idea of a series of mixed pools was extended by Gautreaux and O'Connell (1955) who derived an expression for the tray efficiency. The main difficulty in using this technique is determining the number of mixed pools. Bruin and Freize (1974) later proposed a two-dimensional model using the same series of mixed pools approach.

2.4.4 Backmixing Imposed on Plug Flow

Gerster et al. (1958), working on the AIChE research program, were the first worker to use an eddy diffusion model to represent the liquid mixing on a tray, which was carried out for a one-dimensional, rectangular tray. The eddy diffusion model assumes the rate of mixing of a component is proportional to the local concentration gradient of that component. Gerster's method was the basis for the well documented AIChE method of estimating tray efficiency (AIChE, 1958).

In the AIChE method the mass transfer is modelled on a twin resistance concept, one resistance in the liquid phase and the other in the gas phase. The method involves fixing a tray design and calculating, or fixing, the operating and system variables. The following empirical equations give a guide to the efficiency calculation procedure.

Step 1: Calculate the superficial gas velocity, u_s (ft/s),

$$u_s = \frac{Q_v}{A}$$

Step 2: Calculate the F-factor, F (lb/ft s²)^{0.5}

$$F = U_s (\rho_g)^{0.5}$$

Step 3: Calculate the height of clear liquid on the tray, h_{cl}

$$h_{cl} = 103 \pm 11.8 h_{ov} \mp 40.5F \pm 1.25 \frac{Q_l}{W} \div \rho_l$$

Step 4: Calculate the average liquid contact time on the tray,

$$\theta_l = \frac{37.4 h_{cl} A}{Q_l}$$

Step 5: Calculate the resistance to mass transfer in the liquid phase, N_l

$$N_l = 103 (D_l)^{0.5} (0.26F + 0.15) \theta_l$$

Step 6: Calculate the resistance to mass transfer in the gas phase, N_g

$$N_g = \frac{\rho_g D_g}{\mu_g} (0.776 + 0.116h_w - 0.290F + 0.0217 Q_l/W + 0.200\Delta)$$

Step 7: The calculated vapour and liquid resistances are combined to obtain the overall resistance to mass transfer, N_{og}

$$\frac{1}{N_{og}} = \frac{1}{N_g} + \frac{\lambda}{N_l}$$

Step 8: The point efficiency, E_{og} , is calculated from the overall mass transfer resistance,

$$E_{og} = 1 - \exp(-N_{og})$$

Step 9: The eddy diffusivity coefficient, D_e , is calculated,

$$D_e = (1 + 0.044)(d_c - 3)^2 \left[0.0124 + 0.015h_w + 0.017U_s + 0.0025 \frac{Q}{w} \right]^2$$

Step 10: The Peclet number, Pe , is calculated,

$$Pe = \frac{Z_1^2}{D_e \theta} \quad \text{where } \theta = \text{contact time}$$

Step 11: The enhancement of the Murphree point efficiency, or Murphree tray efficiency can be found graphically knowing values of λE_{og} and Pe .

Some of the deficiencies in the AIChE method for predicting point efficiency are as follows:

- (1) The correlations for N_g and N_l were developed from absorption and stripping systems where the resistance to mass transfer was confined entirely to either the vapour or the liquid phase.
- (2) The method takes no account of interphase heat transfer which occurs in distillation.
- (3) The correlations for N_g and N_l ignore the flow regime on the tray (e.g. Froth or spray). It is likely that better correlations could be achieved for each regime separately because of the quite difference in hydrodynamics of each regime.
- (4) The bulk of the work was concerned with bubble caps and a comparable body of work for other trays has not been published in the open literature.

2.5 Flow Regimes On Sieve Trays

When a gas is mixed with a liquid at sufficient high flowrates of the gas and liquid, a mass motion of gas bubbles is produced, which in turn, gives rise to an intensive mixing of the liquid. Depending on the flow rates of the gas and liquid in the mixture, different hydrodynamic regimes arise and consequently changes in the structure of the mixture occur. The aim of this section is to describe each flow regime and identify the operating conditions in which they exist.

There are three main reasons why flow regimes are of importance. Firstly, the hydrodynamic behaviour on the tray depends upon the flow regime. For instance, different correlations in each regime, such as dispersion density, are required to examine the effect of dispersion density on entrainment or weeping, since this will affect column throughputs. The second reason is that some flow regimes need to be avoided. For example, foaming is aggravated in the emulsion flow regime and entrainment rapidly increases in the spray regime. The final reason is that there is some evidence of improvements in tray efficiency which can be achieved by designing the tray to operate in a particular regime, Porter et al., 1975 and 1977; Raper et al., 1984.

2.5.1 SPRAY REGIME

Spray regime is a gas phase-continuous dispersion and is produced at high gas flow rates and low liquid rates. The liquid phase is 'atomised' by the gas emerging with a high velocity from the perforations, into a fluidised bed of small liquid droplets of various sizes. The dispersion has no observable upper surface. In simple terms the spray regime is associated with large diameter holes, large hole gas velocities and low clear liquid heights. Note this regime is not suitable for vapour-directing slots as it is difficult to control the liquid, see figure 2.7.

2.5.2 MIXED FROTH REGIME

This is an intermediate regime between the spray and bubbling regimes in which the dispersion close to the tray deck is predominately a bubbly regime while at the top, the dispersion moves towards the spray regime. Gas passes through the liquid as jets and bubbles, the shape of which are ill-defined and undergo continuous changes in size. The irregular bubbles subsequently burst into a large shower of liquid fragments and coarse spray droplets.

2.5.3 EMULSION FLOW REGIME

This regime is a predominant feature of high pressure distillation where the reduced difference between the physical properties of the gas and liquid phases leads to small buoyancy forces. This flow dispersion consists of a large number of small bubbles (1 to 3 mm) which are 'emulsified' in the liquid phase, and can be described as a gas continuous gas-in-liquid flow. It is thought that these bubbles formed are sheared off in the direction of flow by a horizontal liquid shear force which is favoured by a high horizontal liquid momentum compared with the vertical gas momentum.

Other flow regimes, such as the free bubbling regime and the foaming regime, may occur depending on the system properties and flow conditions, but these are not usually met in industrial columns and so are not considered here. In the case of the foaming

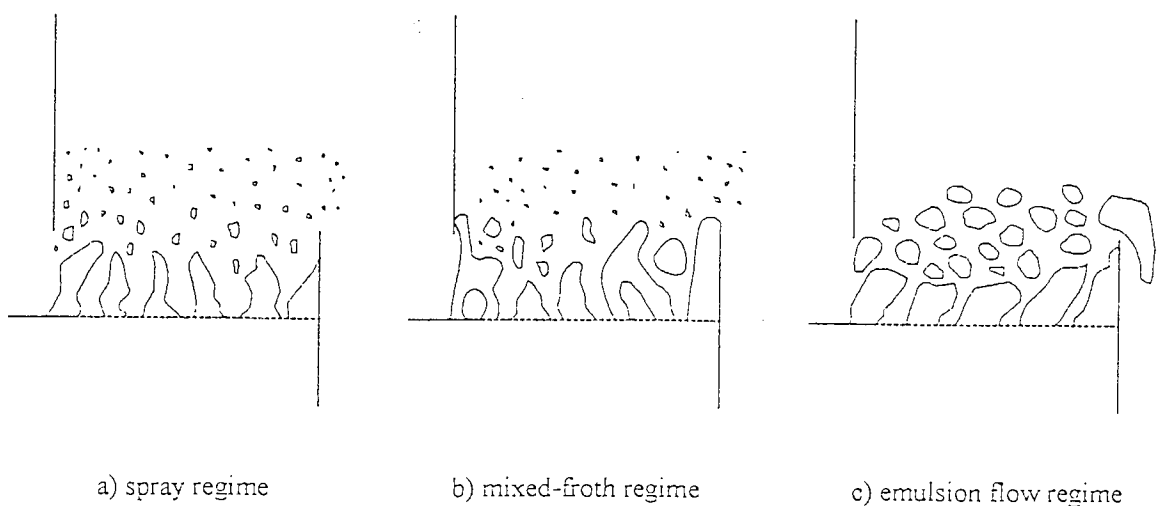


Fig. 2.7 : Structure of the Two-Phase Dispersions in the Different Flow Regimes

The transition between the spray and mixed-froth regimes has been widely studied in order to both gain an insight into the mechanism of liquid transport and to predict under what conditions this transition occurs. This is a difficult process as the definition of the upper limit of the spray regime is vague. Figure 2.8 shows the flow regime map as proposed by Hofhuis and Zuiderweg (1979). The flow conditions are described in terms of the capacity factor, CF, and the flow parameter, FP. The capacity factor is an indication of the effect of the vapour, whereas the flow parameter gives an indication of the liquid/ vapour ratio.

$$CF = u_v \left\{ \frac{\rho_v}{\rho_l - \rho_v} \right\}^{0.5}$$

$$FP = \frac{L}{G} \left[\frac{\rho_v}{\rho_l} \right]^{0.5}$$

As can be seen from Figure 2.8, the practical operating conditions for a tray are bounded by a flooding limit and a weeping limit. The first of these defines the conditions under which, for various reasons, the liquid cannot exit the tray at a sufficiently high rate, and so liquid accumulates. This is known as flooding. The second of the limits mentioned here is the weeping limit. This describes the conditions where a relatively low vapour flow-rate cannot support the liquid on the tray. The liquid pressure therefore forces liquid through the perforations on the tray. The liquid effectively by-passes the tray and as a result does not fully contact the vapour.

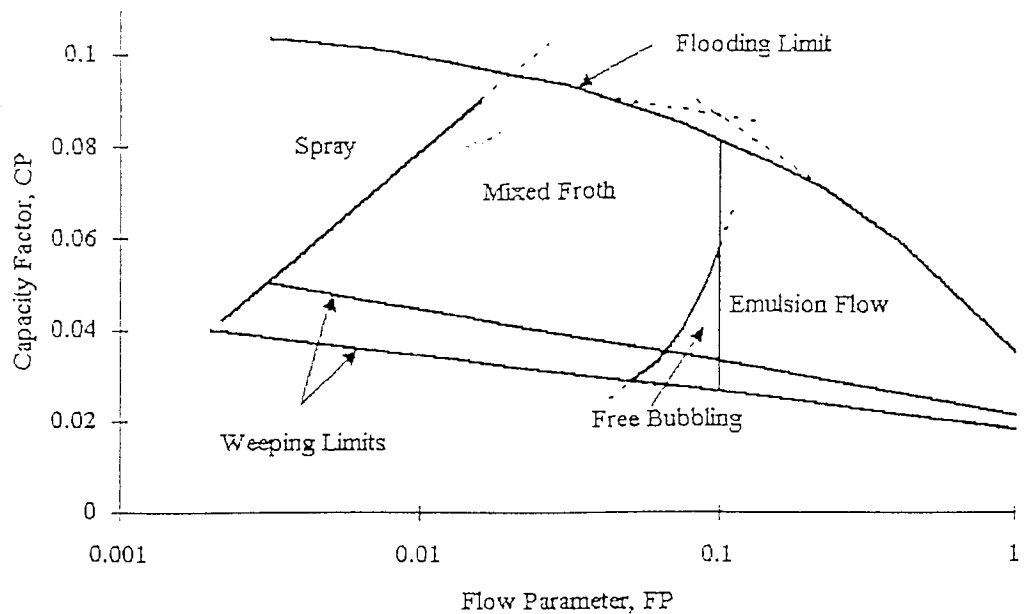


Fig. 2.8: The two-phase flow regime map suggested by Hofhuis and Zuiderweg

2.6 Previous Work on the 2.4 m Column

The large tray test rig incorporating a 2.44 m diameter column, a 150 HP air fan and a 1.2 MW water heating facility had been constructed by Hine (1990). This unique facility is equipped for the experimental observation of liquid flow patterns, and can also be used for the evaluation of the effect of the liquid flow pattern on mass transfer by cooling water with a cross-flow of air.

Single pass sieve trays perforated with 1 mm, 6.35 mm and 12 mm diameter holes have been extensively tested by Hine (1990), Chambers (1993) and Fenwick (1996) respectively. Liquid channelling associated with liquid circulation at the sides of the tray had been observed on the tray by Hine. Temperature profiles, revealed by the water cooling technique, have confirmed that the driving force for heat transfer is reduced in the circulating regions. In water-only experiments, with the exception of extremely low weir loads, the flow separated at the ends of the inlet downcomer forming circulating regions at the sides of the tray, these regions with a small increase in weir load increased to completely fill the sides of the tray outside of the downcomers. The liquid flow patterns on the 1 mm diameter hole sieve tray were similar to those observed in the water-only experiments. The effect of the air flow is to delay the onset of separation and circulation, which occurs at higher weir loads than in the water-only experiments. Hine concluded the size of the circulating regions formed on the 1 mm diameter hole sieve tray depended upon the velocity of the water entering the tray and hence on the setting of the gap beneath the inlet downcomer as well as on the weir load.

Chambers continued studies on the commercial scale sieve tray with 6.35 mm diameter hole sizes. Initial gas-liquid contacting experiments showed that under certain conditions, the gas flow pattern beneath the test tray, can have significant effect on the tray liquid flow pattern such that gas driven circulation was produced. These non-uniform gas flow effects were removed by modification of the gas distribution system.

By eliminating gas circulation effects, the effect of the gas flow on the separation of liquid flow was similar to that obtained on the 1.0 mm tray. Studies into gas-liquid interactions on two trays, set at a spacing of 300 mm, showed that the gas flow did not change the direction of liquid flow on the second tray in the same way as that observed on the one tray. Furthermore the flow patterns on the second tray were, on the whole, superior to that produced on the one tray in that the size and velocity of reverse or circulating flow was less compared to those on the one tray. Chambers concludes by stating that in a real tray column, gas influenced liquid flow patterns may only occur on the first tray above the vapour feed inlet, but at higher tray spacings the above phenomena might be observed.

2.7 Separated or Non-Separated Flow

As liquid flows in a straight pipe of constant diameter, all the liquid moves in the forward direction, all be it with an imposed velocity distribution as determined by the flow regime. This is an example of non-separated flow.

As liquid flows in a straight open channel of constant width and flow depth, provided the flow is not critical at any point all the liquid moves in the forward direction, again with an imposed velocity distribution. This is another example of non-separated flow.

However, when the physical flow boundary changes greatly over a short distance, such as in the case in a rapidly diverging channel, the pressure of the fluid varies in the direction of flow and the behaviour of the fluid may greatly be affected. As the fluid flows along the flat surface the pressure gradient in the x-direction is, as expected, negative and the net pressure force on an element in the boundary layer is in the forward direction. Such a pressure gradient is said to be favourable and it counteracts to some extent the 'slowing down' effect of the boundary on the fluid. However, as the physical flow boundary moves away from the direction of flow, the velocity must decrease. (The Bernoulli equation requires that as the velocity term decreases the pressure term must increase accordingly, if all the other items are kept constant). Thus the net pressure force on an element in the boundary layer opposes the forward flow. Although the pressure gradient has practically the same value throughout the cross-section of the boundary layer, its most significant effect is on the fluid closest to the physical flow boundary. This is because the fluid there has less momentum and so when its momentum is reduced further by the adverse pressure gradient, the fluid near the physical flow boundary is soon brought to standstill. The velocity gradient at the physical flow boundary is then zero, which becomes the point of separation.

Separation is caused by the reduction of the velocity in the boundary layer, combined with an adverse pressure gradient; and it can only take place when an adverse pressure gradient exists. The line of zero velocity dividing the forward and reverse flow leaves the physical flow boundary at the separation, and is known as separation streamline. The result of the reverse flow is the formation of an eddy in which energy is dissipated leaving the pressure downstream similar to that at the point of separation. Separation having occurred, the fluid flow is guided by the separation streamline or flow boundary as opposed to the physical flow boundary, see figure 2.9.

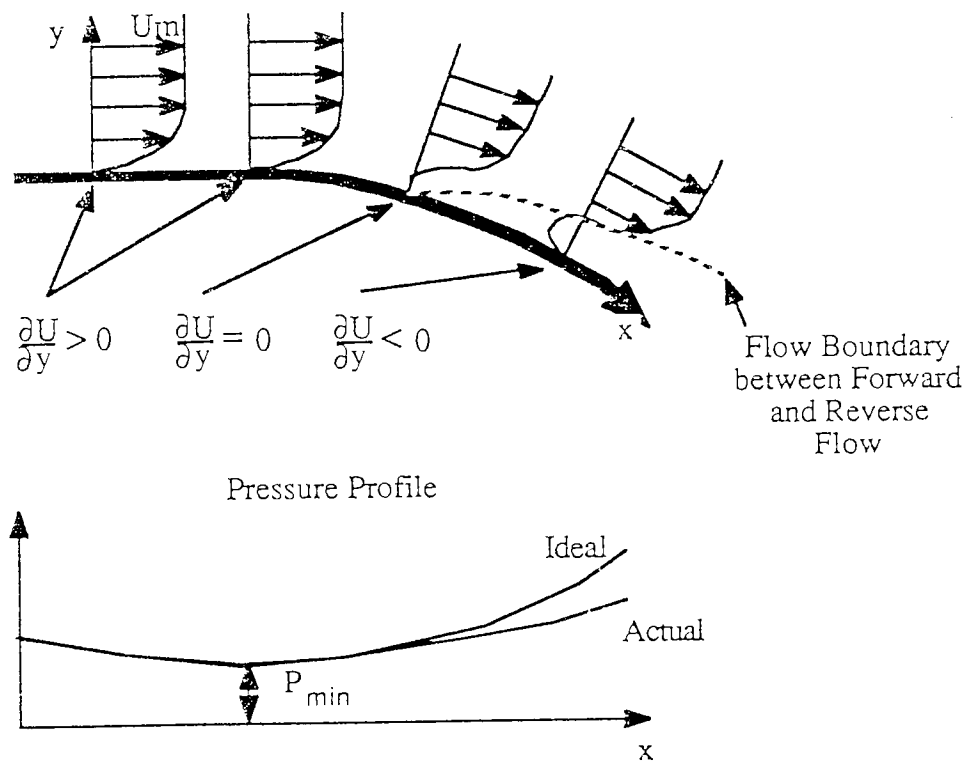


Fig. 2.9 : Onset of Separation

It appears that circulation zones can only exist if an adverse pressure gradient exists. The pressure gradient is caused by the difference between water velocity through the inlet gap and the water immediately on the tray area. If the hold-up on the tray is large, the entering water must slow down thereby causing an adverse pressure gradient and the possibility of separation. Therefore any factor which increases the depth of water or flow on the tray has a chance of causing separation ie. increasing the water flowrate.

2.8 The Effects Of Separated Flow On Tray Efficiency

As the liquid flows onto a single-pass tray from the downcomer, it enters a diverging channel. It has little tendency to move sideways to follow the curved walls. Instead it tends to channel preferentially down the central part of the tray taking the shortest route from downcomer to downcomer. This leaves the slow-moving/ stagnant or even re-circulating liquid at the sides of the tray.

Since there is no bulk flow of liquid through the stagnant regions, they quickly reach equilibrium with the vapour flowing through them. Subsequent vapour passing through the stagnant regions undergoes no composition change i.e. reduction in tray efficiency. Although stagnant regions are not replenished by bulk liquid flow, they do receive fresh liquid from the active region by transverse liquid mixing. However, mixing acts only over a limited distance estimated to be about 0.5 m by Porter et al (1974).

This has very important consequences for scale-up. When the maximum width of the stagnant zone is less than 0.5 m transverse mixing is sufficient to overcome the adverse effect on the tray efficiency. On the other hand, as tray diameter and size of the stagnant regions increases, transverse mixing is inadequate and tray efficiency suffers. The reduction in efficiency is even more severe when we consider a large diameter column having a single pass tray with stagnant regions stacked one above the other. This causes a far bigger reduction in tray and overall efficiency than if a single tray is considered in isolation. Figures 2.10 to 2.13 present a sequence of the flow patterns as the water flowrate is increased. Hine (1990). The percentage of the total tray area taken up by the circulating regions is also expressed below each figure.

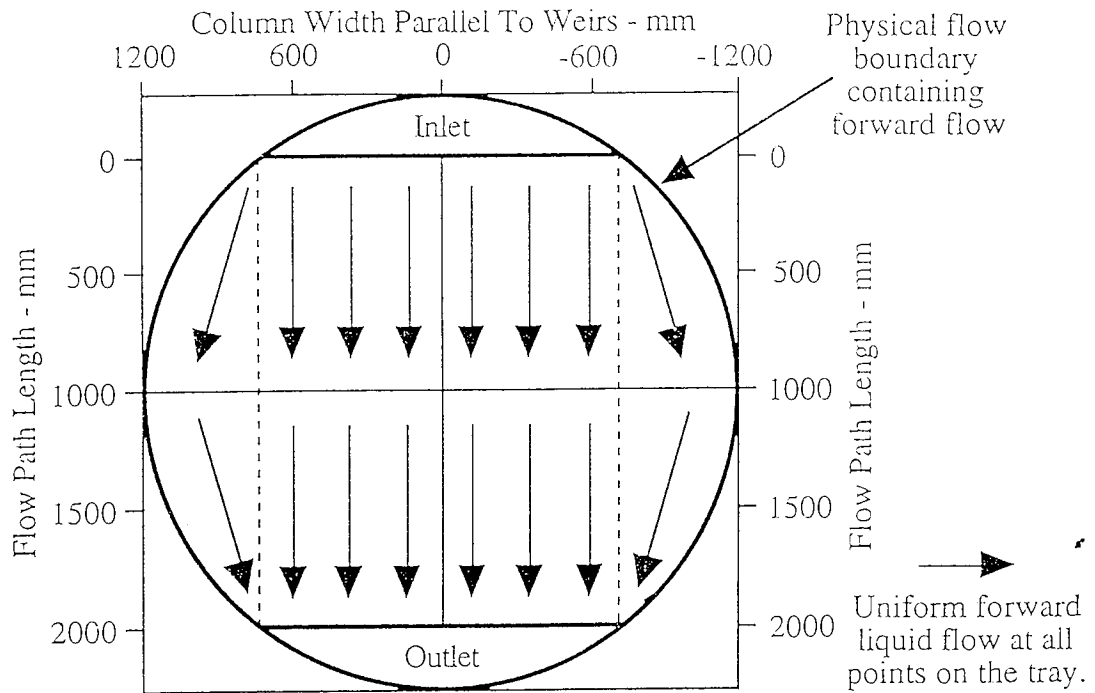


Fig. 2.10 Direct-observation of the liquid flow pattern using flow pointers indicating uniform forward flow across the tray.

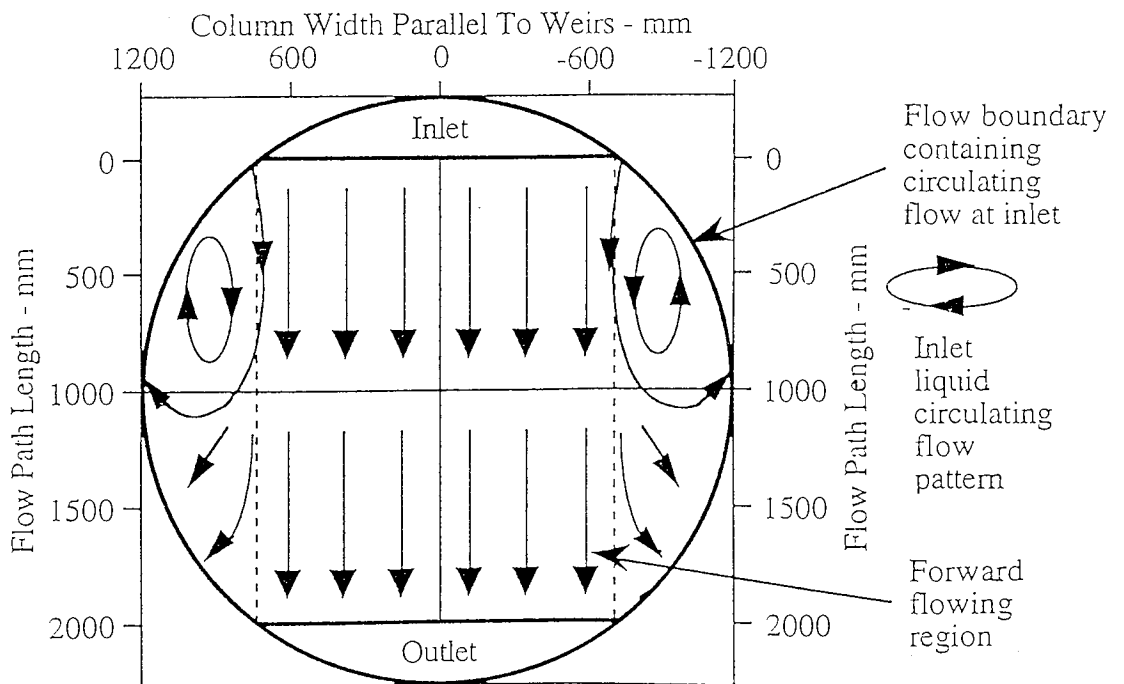


Fig. 2.11 Direct-observation of the liquid flow pattern using flow pointers indicating inlet liquid circulation.

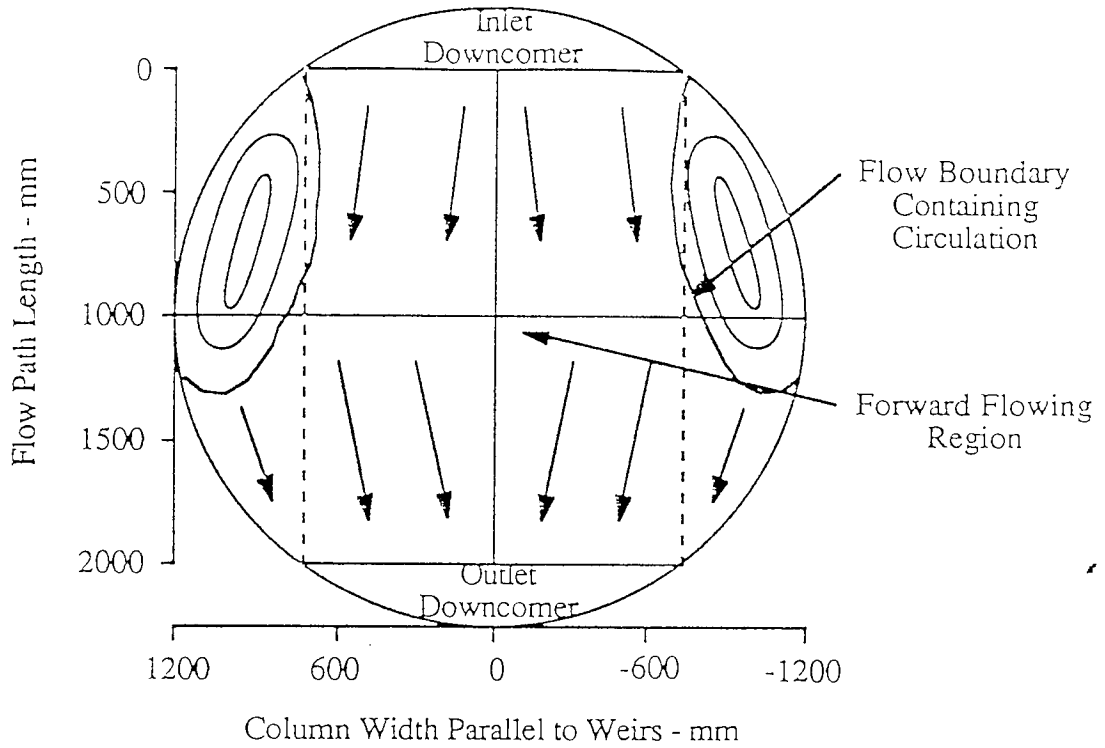


Fig. 2.12 Water-Only Flow Pattern - 20% Circulation.

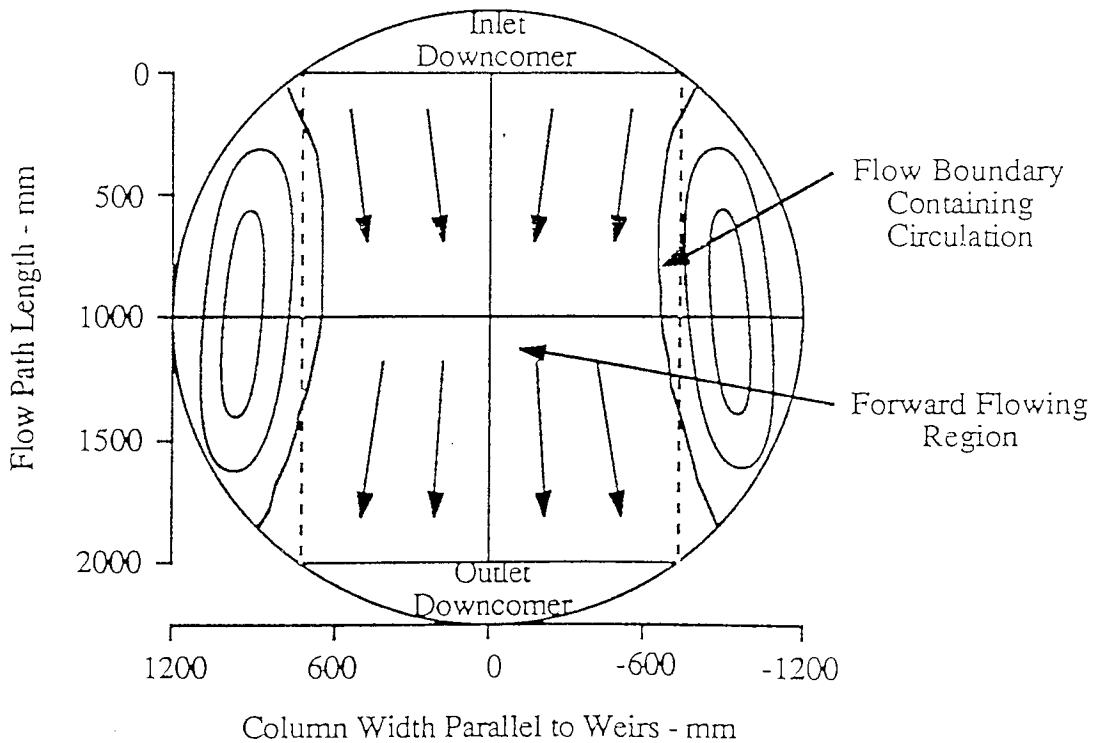


Fig. 2.13 Water-Only Flow Pattern - 30% Circulation.

2.9 Conventional Procedures for Sieve Tray Design

A complete distillation column design must satisfy two requirements. These are the ability to perform the separation task safely at the specified throughputs, and that the design must be economically viable such that the whole process can be operated profitably. Set out below are the essentially empirical methods used in tray design.

In the design of sieve trays, the main objective is to calculate tray bubbling area, downcomer area, and the number of passes on a tray in order to minimise the column diameter (and hence costs) for a given separation duty. The usual strategy is to design the sieve tray at 80 % of total flooding so as to force the maximum vapour and liquid throughputs through the smallest possible distillation column, in terms of diameter and height. Furthermore, based on the engineering judgement of the tray designer, the material costs of fabricating the column must be kept at a minimum whilst at the same time, a minimum safety factor needs to be incorporated into the overall design.

The information required for the design of a tray, are the vapour and liquid mass flow rate specifications, and the vapour and liquid phase density ratio. Note that the densities of vapour and liquid are determined by the operating pressure (and so the temperature), while the liquid and vapour flowrates are determined by the throughput and reflux ratio for the column duty.

Calculation Procedure for Tray Design

The procedures for a typical tray design are as follows :

a) Estimate the column diameter from either the flooding correlation based on entrainment (Fair 1963), or the total flows chart based on an 80 % flood single pass sieve tray at a spacing of 600 mm, and of hole diameter 12.5 mm (Porter and Jenkins, 1979). In this review the method of Porter and Jenkins will be considered.

The method involves the calculations of the total volumetric vapour and liquid flow rates which are then used to look up column diameter and the number of passes required for the tray at 80 % flood using the above mentioned total flow charts. That is,

$$D = 2 (\Lambda_T \div \pi)^{0.5}$$

b) Calculate the downcomer area, $A_D = 0.05 (A_T)$, in order to evaluate the downcomer velocity, U_{DF} , at 80 % flood.

$$U_{DF} = 0.17$$

$$U_{DF} = 0.007 (\rho_l - \rho_v)^{0.5}$$

$$U_{DF} = 0.008 \left[TS(\rho_l - \rho_v)^{0.5} \right] \text{ where } TS = \text{Tray Spacing}$$

Calculate the tray bubbling area, $A_B = (A_T - A_D)$, and the bubbling area load factor, C_{SB} , where

$$C_{SB} = u_{SB} \left(\frac{\rho_v}{\rho_l - \rho_v} \right)^{0.5} \text{ where } u_{SB} = \text{superficial velocity in bubbling area}$$

The design procedure is slightly complicated because C_{SB} depends on the weir loading, that is, on the volumetric flow of liquid per unit length of weir.

$$\text{Weir Load} = \frac{q}{b} \text{ m}^3/\text{m.s}, \text{ with } b = \text{weir length and } q = \text{liquid flow over weir}$$

it is usual practice that b is not less than $0.6 D_T$, since this prevents severe channelling and loss of efficiency.

c) Identify C_{SB} at the weir load and calculate the vapour fractional flood.

d) Alter the design to produce the same fraction of flood for the bubbling area and downcomer. Compare this fraction of flood with that specified, and readjust the design until the specification is satisfied.

The overall aim at this stage is to achieve a balanced design by adjusting A_D and b in order to modify A_B so as to produce the same percent flood both in the downcomer and on the tray bubbling area. If necessary alter the column diameter and repeat the above steps until a balanced design is achieved.

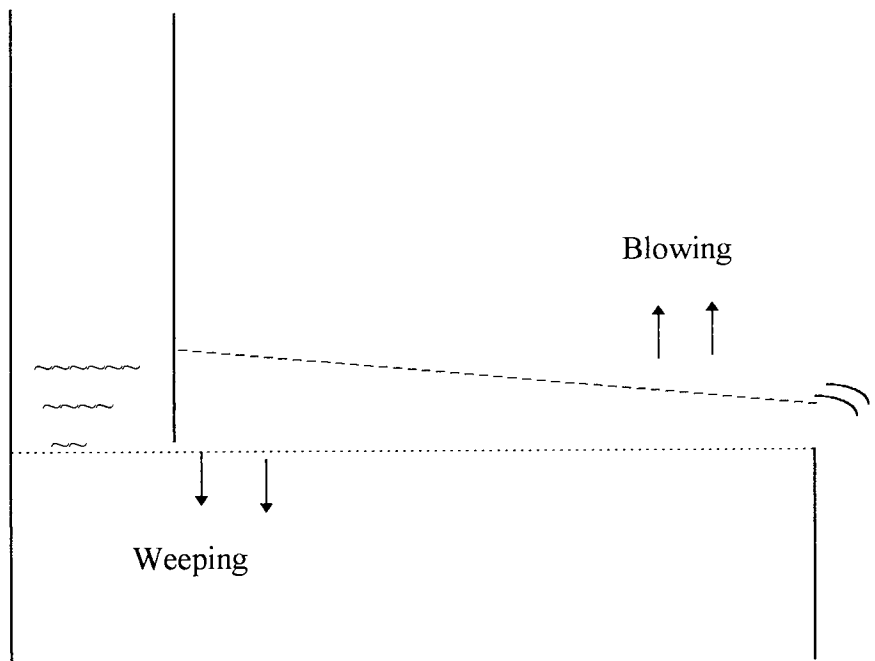
2.10 Downcomer Backup

Liquid is conveyed through the downcomer from a lower to a higher pressure and consequently liquid backs up in the downcomer to overcome the pressure difference. The primary requirement of a downcomer is that its height must be sufficient to accommodate this backup to avoid flooding. When a large liquid flowrate has to pass through the mouth of the downcomer, the latter can act as a restriction to flow and so require an increase in froth height on the tray in order to achieve the liquid flowrate. The mouth of the downcomer becomes choked and normal weir flow is prevented. The froth in the downcomer backs up over the weir to the tray above leading to flooding.

2.11 HYDRAULIC GRADIENT

Hydraulic gradient exists on sieve trays because a motive force must be provided to overcome the various losses accompanying liquid movement, see figure 2.14. This difference in hydrostatic head provides the required motive force for the liquid flow. The difference in hydrostatic head between tray inlet and tray outlet also causes a dry tray pressure difference between inlet and outlet because the total pressure drop must be the same at all locations on the tray surface. This causes the vapour to flow preferentially through that part of the tray where the hydrostatic head is low (tray outlet) causing a corresponding increase in dry tray pressure drop. The situation is reversed at the tray outlet. Note that when we speak of a gradient, it is not the froth height gradient which is important, but the hydrostatic head or clear liquid head gradient. This explains why observations of froth height gradients are often deceptive- there may actually be little visible froth height gradient on a tray whereas the corresponding hydrostatic measurements will show a very definite hydrostatic head gradient over a long flow path length.

The conventional way to achieve more uniform contact in the presence of a hydraulic gradient is to increase the dry tray pressure drop by reducing the perforated area of the tray. This increases stability everywhere on the tray and thereby lessens the percentage variation in stability across the tray floor. The drawback, however, is an unwanted increase in tray pressure drop. As the hydraulic gradient, which plays the main role in fixing the liquid flow rate on the plate, is eliminated, it can handle higher liquid rates without weeping or dumping.



HYDRAULIC GRADIENT PROFILE ON A SIEVE TRAY

Fig. 2.14

2.12 HIGH THROUGHPUT TRAYS

As stated in Chapter 1, distillation is an energy intensive separation process and there is a need to design distillation columns 'leaner and harder' and any improvements in efficiency, however small, may produce substantial rewards in energy and financial savings. One of the aims of this research work is to develop new distillation trays which have a better flow pattern than existing trays i.e. due to the elimination of stagnant zones and also to try to improve the throughput of the distillation column as a whole. It is important to note that it is necessary to strike a compromise between factors promoting a high throughput and factors promoting tray efficiency. It is of little use to develop a high throughput tray which lowers the tray efficiency.

The tray suppliers have already perceived an opportunity for High Throughput trays; some of those on offer or are being developed can be seen in Figure 2.15. Before 1985 tray users were unwilling to install packed columns of a large diameter to replace trays due to the many scale up failures. Once this problem was solved by installing improved distributors, packing dominated the column internals market, particularly the new structured packings. At present column internals are chosen on the conventional basis of costs. Robinson (1997) has published results of calculations which show that the total cost of a column containing structured packings is always less than that of a column containing trays. If this becomes accepted practice then the use of trays would be restricted to special situations. Hence the direction of research for trays is to increase the throughput if the tray business is to survive.

Robinson's claim for the universal cost advantages of structured packing is not accepted by everyone, nevertheless, we can accept that packings will always be the economic choice for vacuum distillation because of the much lower pressure drop per theoretical plate of packing compared to trays. In general approximate terms, we may assume trays will be used for all distillations above atmospheric pressure. Thus, in general, High Throughput trays should be developed for pressures of atmospheric or above and if possible have a low pressure drop relative to the other trays. Small diameter holes, low pressure drop trays are those likely to produce a spray regime. It is thus unlikely that

Some High Throughput Trays

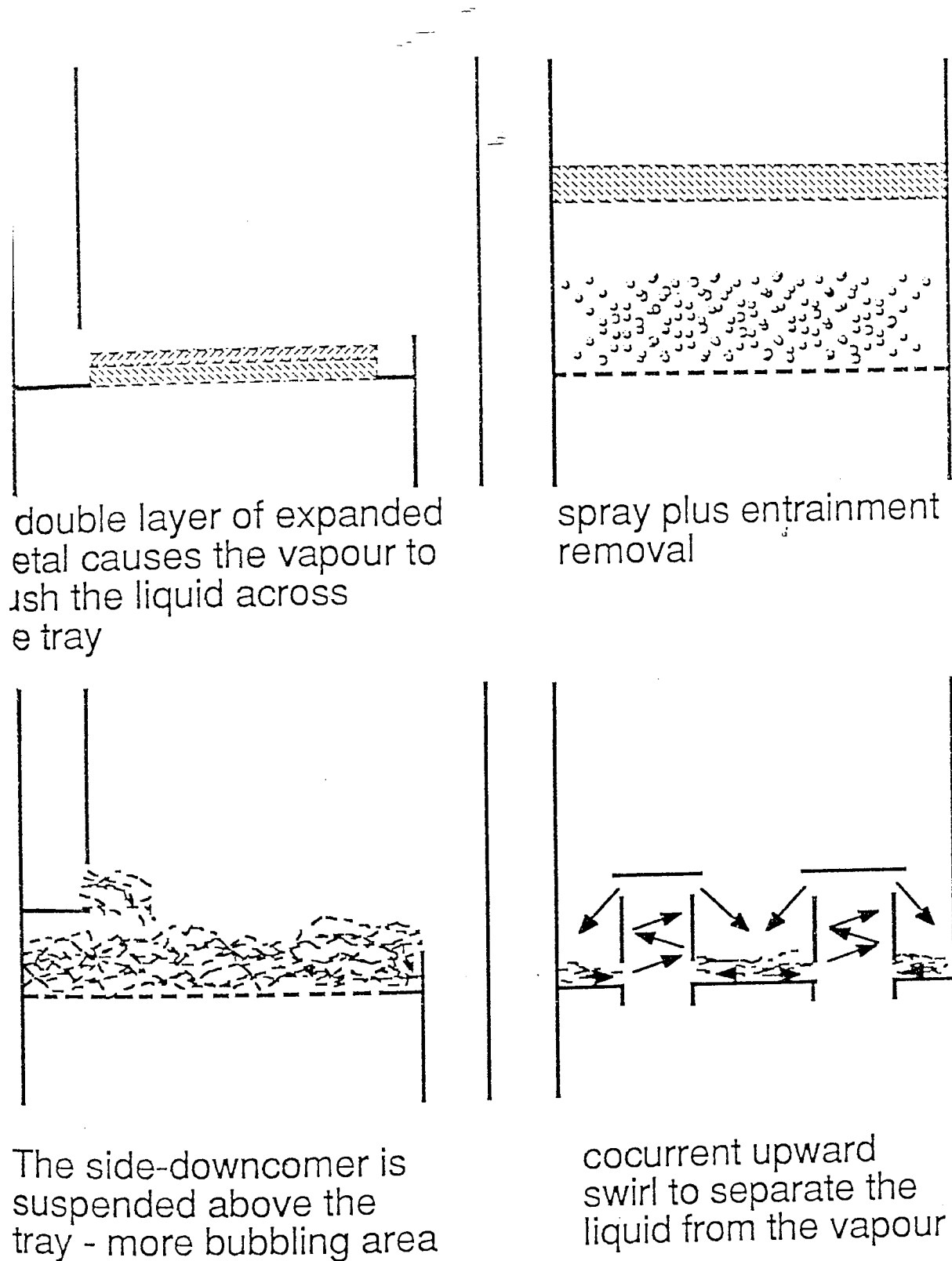


Fig. 2.15 Schematic Diagram of High Throughput Trays

spray regime studies will have a continuing importance. It then follows that High Throughput trays should be designed to replace conventional trays working in the mixed or emulsified flow regimes which occur at high weir loads. It should be noted that trays operating with high weir loads, in normal operation, lead to large froth heights and the need therefore to use excessive tray spacings.

2.13 Flow Control Devices For Trays

Liquid channelling was thought to be the major contributor to the decrease in tray efficiency as column diameters increased. This fact was reported by Smith and Delnicki (1975) when a large diameter column failed to achieve separation. A series of papers by Porter et al. (1972); Lockett et al., Lim et al., (1974) predicted that the width of the mixing zone was approximately 0.3 m by 0.5 m and that on trays above 1.50 m diameter, the liquid channelling would be detrimental to tray efficiency. Research was and is being carried out into how the liquid flow pattern could be controlled or with a view to restoring the expected tray efficiency.

Many tray and downcomer developments to control the liquid flow have been invented and patented with a view to eliminating the flow non-uniformities, each claiming that the tray efficiency is improved due to the more uniform liquid flow although they are not widely used at present. Presented below are examples of such corrective flow pattern devices :

2.13.1 UOP Slotted Sieve Tray

The use of slots to overcome the non-uniform liquid flow on large sieve trays was developed by UOP (formely Union Carbide) as patented by Williams and Yendall (1963 and 1968), Matsch (1973) and Kirkpatrick and Weiler (1978). Directional slots are punched into a sieve plate through which vapour preferentially passes, imparting some horizontal momentum to the liquid in the direction that the slot faces. A typical design of the slot is shown in Figure 2.16. The slot density and alignment are controlled over the tray area so that a more uniform liquid flow can be achieved. Weiler et al. (1971 and 1973) have tested the slotted trays and found that the liquid flow is near to uniform.

The advantages of slotted trays over conventional sieve trays claimed by UOP are:-

- (1) Non-uniform liquid flow and unbalanced vapour-liquid contacting are minimised by the horizontal liquid propulsion mechanism from the tray slots.
- (2) Control of the liquid residence time to give maximum efficiency is achieved.
- (3) Complete vapour-liquid agitation over the tray bubbling area is produced by an inlet bubble promoter, and that single or two pass versions are available depending upon the weir load.
- (4) High tray efficiencies are reported in which parallel flow trays achieve a high efficiency followed by cross flow trays. Note there is no claim that this type of slotted tray increases the throughput of the tray.

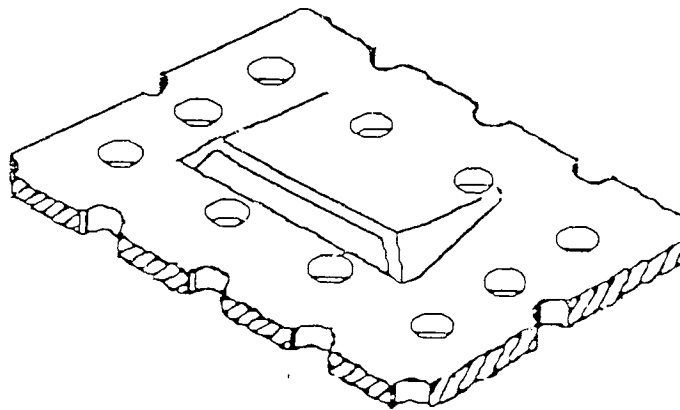


Fig. 2.16 Single Slot as used on Sieve Trays.

2.13.2 The FRI Downcomer

Bell (1974) has suggested that an important cause of the severe flow non-uniformities which he observed was non-uniform flow of liquid issuing from the downcomer.

Fractionation Research Incorporated (FRI) have patented modifications to the inlet downcomer and the outlet weir (Keller, 1973). The modification at the inlet was that the downcomer clearance could be independently varied along the length of the inlet weir. This was accommodated by the downcomer apron being made from numerous vertical

strips of metal. The technique seemed to increase the gap size at the ends of the inlet weir and to decrease the gap at the centre of the downcomer. The draw-back of this modification would seem that the inlet arrangement was tuned for a particular liquid flowrate and that the performance would deteriorate for non-design flowrates. The modifications to the outlet weir consisted of notches in the outlet weir to allow the preferential flow of liquid off the tray at certain positions along its length.

2.13.3 The Step Flow Downcomer

The Step Flow Downcomer is a modification to the inlet downcomer of a tray (Porter, 1972). The top of the downcomer is, in general, of a conventional arrangement as it is meant to fit the outlet downcomer of the tray immediately above. The bottom part is half a cylindrical tube with the circular part facing the active area of the tray. If, as is held by several authors, flow uniformities originate from the uneven momentum flux of the liquid issuing from a straight downcomer, then liquid redistribution forced by the shape of the downcomer is expected to make the liquid flow more even.

2.13.4 Inclined Counter-Current Contact Tray

Monovyan and Gaivanskii (1980) reported that the non-uniformity of the liquid flow pattern can be eliminated by the slanting of the tray deck towards the downcomer leaving the tray. However, the use of an inclined tray of this type, reduces the residence time of liquid in the bubbling zone.

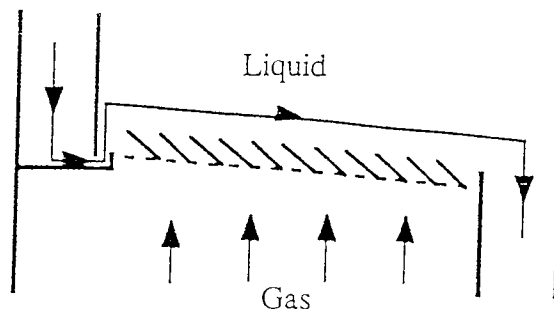


Fig. 2.17 Sketch of Inclined Counter-Current Contact Tray.

2.13.5 Winged Downcomer

The British Oxygen Group (BOC) have patented a downcomer development whereby the length of the inlet weir is greatly increased Lavin. (1986). This design seems to serve two purposes. The effective weir length to diameter ratio is much increased serving to minimise the size of any stagnant regions, and, the flow path length from all positions along the inlet weir seems to be much more uniform. Lavin (1986) also suggests that the hole density over the active tray should be varied to compensate for the different froth velocities in different parts of the tray.

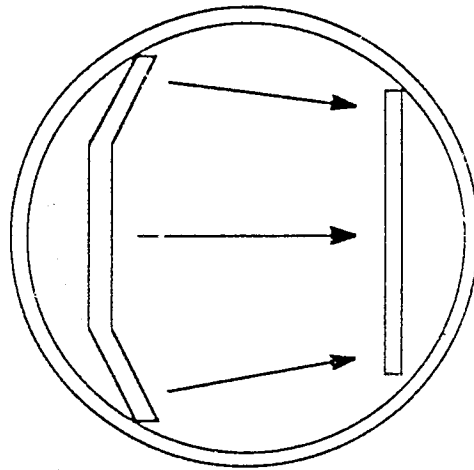


Fig. 2.18 Winged Downcomer.

2.13.6 Kuhni Slit Tray

The column-internals vendors Kuhni developed a slit tray which operates on the principle that liquid flow is in the same direction on all trays. This is achieved by a central downcomer combined with a liquid distribution network of radial pipes to direct liquid to the outer edge of the tray below. The tray bubbling area consists of slits rather than sieve tray perforations which produces a horizontal distribution of vapour into the liquid flow thus providing the biphasic with a flat trajectory for reducing the levels of entrainment. In addition the tray design permits intensive vapour-liquid mixing as well as long contact times.

Advantages of the slit tray claimed by Kuhni are :-

- (1) Vapour passes through the parallel flow of liquid on successive trays (Lewis Case II) yields a high number of theoretical stages per metre of trayed height.
- (2) A high efficiency and a low pressure drop is achieved over a wide operating range at very low tray spacings of between 200 and 400 mm.
- (3) The turndown range is greater than that for conventional sieve trays.

2.13.7 Double Expanded Metal (BOC) Tray

The flow control tray consists of a fine expanded metal mesh to support the biphase, and a course grid attached on top. This was designed for cryogenic distillation of air (BOC Cryoplants Ltd., Biddulph, 1990), which requires a low tray spacing and pressure drop.

Operation of the tray involves vapour issuing through fine slots of the bottom metal mesh, by a slot alignment away from the inlet downcomer, to assist liquid cross flow from the inlet to the outlet. The course grid permits long vapour-liquid contact times for mass transfer by maintaining a uniform height of clear liquid across the tray. The Flow Control tray, like the UOP slotted tray was designed to overcome non-uniform liquid flow and thus high efficiencies were claimed at a low pressure drop over a wide operating range Urua et al., 1992.

2.13.8 Conclusion on Flow Control Devices

Many flow control devices already exist and more are currently being invented which suggests that commercial research and development into distillation hardware is still a very active field and due to the number of new flow control devices invented, the liquid flow pattern is of great importance to optimum tray performance. However, results reported in the literature on controlled-flow trays are in apparent contradiction. While Yanagi and Scott (1973) reported that tray efficiency was almost unaffected by straightened-flow devices, Smith and Delnicki (1975) and Winter and Uitti (1976) found that tray performance could be significantly improved by using bubbling promoters and slotting as flow-control devices in large diameter, low pressure fractionators. These facts raise the question of whether flow control devices should be restricted to some specific services, or be widely used as it is unclear how well these methods work under different regimes as well as controlling the flow patterns developed over a range of throughputs. So far, the information available in the open literature is not enough to provide a definite answer, despite the fact that controlled flow plates represent a higher investment. There is a clear need for investigations to establish sufficient understanding of flow patterns such that it allows the process engineer to predict the type of flow pattern of a given tray for a specific service and its relationship to tray efficiency so he can decide if flow-control devices are actually justified Kafarov et al. (1979).

2.14 CONCLUSION ON THE LITERATURE REVIEW

Sufficient practical experience and theoretical analysis exist to demonstrate the importance of the liquid flow pattern in determining tray and column efficiency. In general, a non-uniform flow of liquid frequently occurs over operating distillation trays and this reduces the tray and column efficiency. The most obvious method of overcoming these effects is the improvement of the liquid velocity profile itself. A number of methods have been devised to improve the liquid flow pattern and restore the expected tray efficiency by incorporating corrective measures which may only work for a particular operating condition. It is also important, however, that due to competition from new structured packings if the tray business is to survive the direction of research for trays is also to look at ways of improving the throughput.

The next section explains the approach to designing the experiments described in this thesis.

CHAPTER 3

APPROACH TO THE PROBLEM

It was shown in the literature survey that the formation of slow-moving, stagnant or circulating liquid at the sides of the tray lead to a decrease in the tray efficiency. This reduction in efficiency is even more severe when a large diameter column is considered.

The continuous development of flow control devices suggest that improving the liquid flow pattern is of considerable importance in optimising tray and column performance, although they are not widely used at present. It is unclear how well these methods work under different flow regimes as well as controlling the flow patterns developed over a range of throughputs.

Thus the approach taken was to test different flow control devices and to observe their effect on the liquid flow pattern. Most of what is described is concerned with comparing a normal sieve tray with a flow control tray in terms of eliminating stagnant zones, and improving point/tray efficiencies and throughput. The research programme was pursued using the 2.44 m diameter test facility for the study of air-water flow patterns using a range of experimental techniques.

The research plan was drawn up with the following objectives in mind:-

The Use of Intermediate Weirs to Direct Liquid to the Sides of the Tray

The aim of this work was concerned with straightening the flow pattern by using different size (10 mm, 50 mm) intermediate weirs. The purpose of the weirs was to deflect some of the liquid towards the sides of the circular tray hence providing a constant flow of liquid and reducing the formation of stagnant or slow moving liquid. A broad range of water flowrates was investigated for various settings of the inlet gap and outlet weir. An attempt was made to relate any changes in the height of clear liquid directly to the size of the intermediate weir.

The Use of Vapour-Directing Slots to Improve the Throughput of Distillation Trays

The vapour-directing slots used were constructed from aluminium and pop-riveted to the tray floor (previous work on slots involved them being incorporated into the tray). In total 16 slots were evenly distributed across a rectangular sieve tray. Information was obtained by measurement of the height of clear liquid both on the tray and in the downcomer and, qualitatively, by direct observation.

Questions that needed to be answered were 'How does the design and size of the slots affect the amount of momentum transferred to the liquid?' and 'Is the placing of the slots critical in removing the hydraulic gradient and stagnant zones?'

The Effect of the Vapour-Directing Slots on the Point and Tray Efficiencies of a Rectangular Sieve Tray

In the design and operation of any separation device it is necessary to strike a balance between factors promoting a high capacity, on the one hand, and factors promoting the tray efficiency, on the other. It is of little use to develop a High Throughput Tray which lowers the tray efficiency. Use was made of the water-cooling technique to try and quantify the effect of the slots on the point and tray efficiencies. In order to do this 70 platinum resistance thermometers were used and placed over the rectangular tray area.

The Use of Vapour-Directing Slots on a Circular Sieve Tray to Remove Stagnant or Circulating Regions and Increase Throughput

The objective of this work was to compare the tray and point efficiencies of a circular slotted tray with those obtained on a slotted rectangular tray. The slots were positioned across the circular tray in proportion to the flow path length. In order to assess their effectiveness with regard to removal of stagnant or circulating regions the dye injection technique was used and changes monitored by an overhead camera. The study was performed for inlet gap and outlet gap combination of 50 mm. For the slotted circular tray 24 vapour-directing slots were used.

Measurement of the Velocity of Air Through a Single Vapour-Directing Slot

The hydraulics of a slotted tray are mainly controlled by the slot vapour-velocity, slot vapour-pressure and the liquid flow rate on the sieve tray. Knowledge of the process of momentum transfer from the vapour to the liquid is important in understanding how these trays function. The aim of this work was to measure the slot vapour velocity (and hence momentum) and to relate it to the reduction in liquid depth.

Complete details of the programme of experiments, including the objectives of each investigation along with a discussion of the results, are contained in subsequent chapters. A description of the apparatus is contained in the next section.

CHAPTER 4

DESCRIPTION OF THE APPARATUS

4.1 INTRODUCTION

This chapter is concerned with describing the air-water simulator column, which incorporates an air supply from an industrial scale fan and a water heating facility for heat transfer experiments to measure tray efficiency. Details of the air, water and heating circuits; the associated instrumentation for measuring flowrates; and the level of accuracy of measured variables are presented.

4.2 Overall Test Facility

The industrial scale distillation test plant incorporates a 2.44m diameter simulator column; a 150 HP air fan; and a 1.2 MW water heating supply in the form of two gas fired process boilers and a steam top up facility. The test facility is equipped for the direct-observation of liquid flow patterns; the investigation into the effect of liquid flow patterns on mass transfer by the heat transfer water-cooling technique; and the use of manometers to measure the liquid head variation on the test tray. A schematic diagram of the overall distillation test plant is shown in Figure 4.1 and 4.2.

The procedures used in the design and construction of the 2.44m diameter distillation simulator are detailed elsewhere (Hine,1990), a summary of the tray design specifications and experimental variables together with a summary of all peripheral equipment can be seen in Table 4.1 and 4.2. A brief description of the air, water and heating supply facilities is in the following subsections.

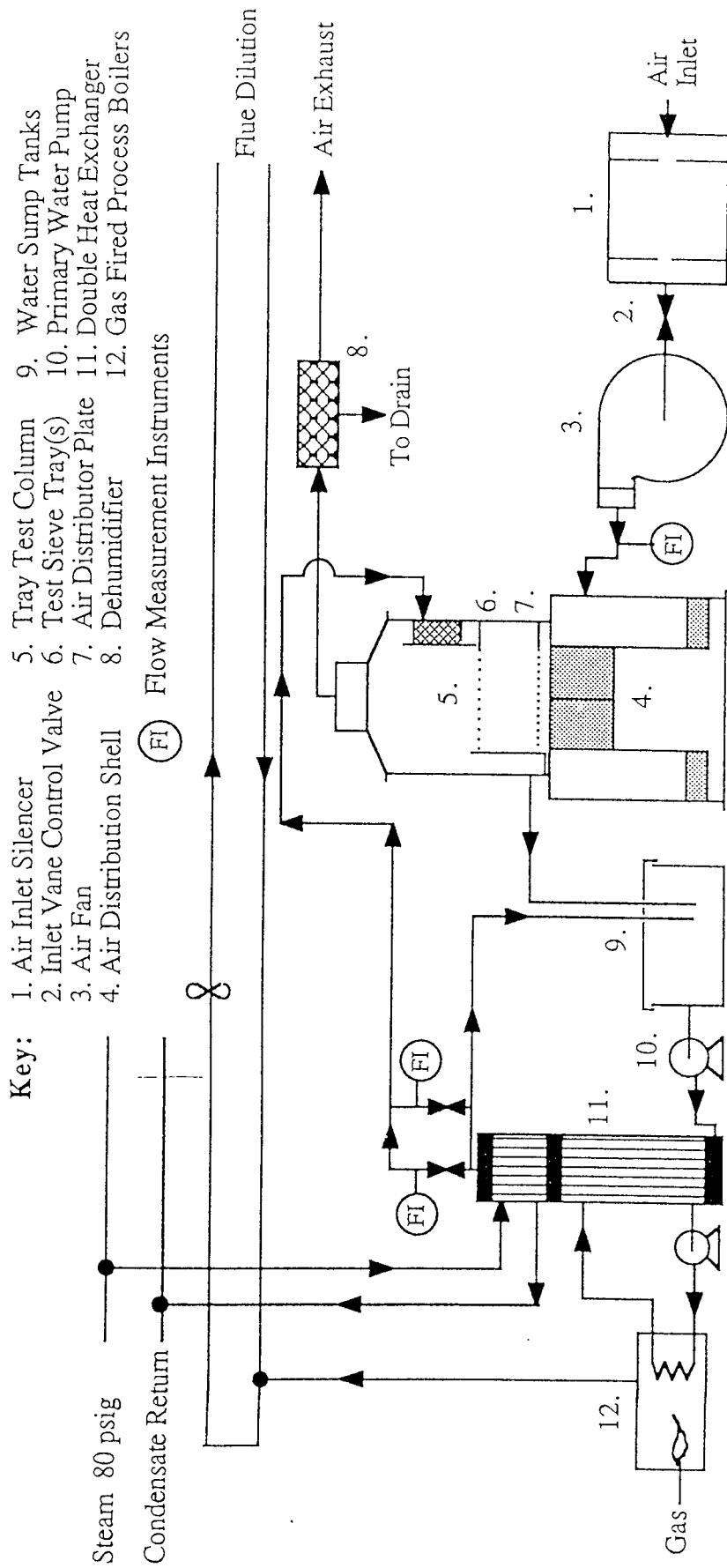


Figure 4.1 Schematic diagram of the air-water distillation test plant



Fig. 4.2 Photograph of the air water simulator

Ancillary Units		Design Specifications		
Air Equipment	Number 48 "Mistral Backward Inclined" Air Fan Air Inlet Ducting	Max. Air Flowrate - m ³ /s	14.38	
		Pressure Head - mH ₂ O	0.51	
		Electric Motor - HP	150.0	
		Dimensions - m ²	0.978 × 0.622	
Water Equipment	Two Sump Tanks	Total Capacity - m ³	5.448	
	Main Centrifugal Water Pump	Max. Water Flowrate - m ³ /s	0.055	
		Pressure Head - mH ₂ O	12.75	
		Electric Motor - kW	15.00	
Heating Equipment	Double Water Heat Exchanger	Top Exchanger	Heat Transfer Area - m ²	3.37
			Hydraulic Resistance - mH ₂ O	3.21 - through tubes section
		Bottom Exchanger	Heat Transfer Area - m ²	10.22
			Hydraulic Resistance - mH ₂ O	2.79 - on shell side
	Gas - Fired Process Boilers	Nominal Burner Rating for each boiler - kW	500	
		Heating Efficiency of each boiler - kW	400 (ie 80% of total rating)	
		Water Flow Rate from each boiler - 10 ³ .m/s	8.66	
		Hydraulic Resistance of each boiler - mH ₂ O	0.26	
	Steam top - up supply	Steam Pressure - psig	80.0	
		Corresponding Temperature - °C	162.0	

Table 4.1 Summary of the design specifications of all the peripheral equipment.

COLUMN

Diameter = 2.44 m

Weir Length = 1.5 m

Flow Path Length = 1.925 m

Material = Aluminium

TRAY

Free Area = 10 %

Hole Sizes = 1 mm, 6.35 mm, 12.7 mm

Thickness = 1 mm

AREAS

Downcomer Area = 0.243 m²

Active Area = 4.189 m²

Free Area = 0.419 m²

Experimental

Inlet Gap = 10, 20 and 50 mm

Variables

Outlet Weir = 0, 10, 20 and 50 mm

Superficial Air Velocities = 1.0, 1.25, 1.5, 2.0 and 2.5 m/s

Water Weir Loads = 25, 50, 100, 150, 200, 250 cm³/cm s

Table 4.2 : Summary of the Tray Design Specifications and Experimental Variables

4.2.1 Air Supply

Unsaturated ambient air, outside the pilot plant, is drawn through a protective grill, at floor level, into the test plant system. On route to the inlet of the fan, air is passed through a silencer, to reduce excessive noise levels, and a vane control valve, used to preset the superficial column velocity. The air is fed to the inlet of the air-water simulator via a rotary impeller blade unit, driven by an electric motor and fan belt system, and a short section of rectangular ducting. This contains an array of fifteen pitot tube pressure sensors which are linked to an air flow meter. The air, on passing through the liquid cross flow on the test tray becomes saturated and leaves the simulator column through the top exhaust duct, positioned approximately 8m above ground level. Excess water is removed from the exiting air stream, using a demister, prior to being vented from the pilot plant to the atmosphere.

4.2.2 Water Supply

The water circuit consists of two water storage tanks, a double heat exchanger, a mainline centrifugal pump, and a grey PVC pipe network. The PVC pipe is able to withstand high water temperatures of up to 75°C when used in the heat transfer experiments. For the direct-observation experiments, cold water is pumped, from the sump tanks through the heat exchanger and into the water bypass circuit, using the 15 kW centrifugal pump, from which it is returned to the sump tanks. Once a uniform flow of water has been achieved in the circuit, the desired water flow rate is preset using one of the two flow meters, according to whether a high or low water loading is required in the column. Water is subsequently delivered to the inlet downcomer of the simulator, directly, from which it is discharged onto the test tray where it is contacted with vertically rising air. The aerated water is removed from the column by flowing over the

outlet weir and into the outlet downcomer, from where it is discharged to the sump tanks through an exit-return pipe.

The same principle was applied to the heat transfer experiments by water cooling, with the exception that water is heated in two sections of a double heat exchanger prior to delivery to the simulator. In the first exchanger, the water is preheated by hot water delivered from the process boilers. Water is immediately transferred to the second heat exchanger where it undergoes additional heating by condensing steam from the departmental utilities generator. The warm water on leaving the heat exchanger, is subsequently delivered to one of two flow meters and undergoes the same process as that described above. A water top-up line supplied fresh water to the sump tanks in order to replenish water lost through evaporation in the simulator column.

4.2.3 Heating Supply

The heat transfer process by water-cooling, involves the removal of heat from water in the main water circuit. Under steady state conditions, this must be equivalent to the heat input supplied from the hot water closed-loop cycle. Since the experimental investigations, involve the use of various air and water throughputs, ranging from very low to very high flow rates, the heating duty was designed to be variable. Hence the heat load would vary from a small temperature drop across the tray, with a large water flow rate, to a large temperature drop across the tray, with a low water flow rate, for a given air throughput.

From the work of Ani (1988) and Hine (1990), it was shown that the heat removed from the water on the tray, for any given air flow rate, was greatest at high weir loads. The heat required for a maximum water loading on the 2.44 m diameter column was, therefore, calculated to be 1.2 MW. Thus a flexible heat source of two 0.50 MW gas fired process boilers and the steam top-up supply was used to supply the simulator column with the required heat load.

4.2.3.1 Gas Fired Boilers

In the majority of heat transfer experiments, the two gas fired boilers provided the primary source of heat to the water flow prior to entering the column. Hot water circulating in a closed loop cycle between the boilers and the bottom water-water heat exchanger preheats water in the main circuit before being delivered to the top steam-water exchanger. One or both process boilers can be operated on line according to the heating duty required for water-cooling. Flue gases, produced from the process boilers, are diluted with fresh ambient air, using a flue pipe and extractor fan system, and discharged to the atmosphere from the test plant at a height of 8 metres above ground level.

4.2.3.2 Steam Supply

Steam at a pressure of 80 psig, is delivered to the top steam-water section of the double heat exchanger from the utilities generator through a 100 mm I.D. lagged steam line. A condensate line from the exchanger returns condensed steam for recycle in the generator. The purpose of the steam is to provide a high grade top-up heat source in order to obtain a rapid but efficient fine tuning of the water inlet temperature to the test tray. All the steam supply could be used if the maximum heat load is required. Steam injection into the steam

the steam-water stage of the heat exchanger is controlled using a perforated copper tube spring valve of length 0.5 m and diameter 25 mm.

4.2.3.2 Double Heat Exchanger

The function of the heat exchanger is to transfer heat from the process boilers and the steam line to the main water circuit prior to entering the simulator. When pumped through the bottom water-water heat exchanger stage, the water is heated by a counter current flow of hot water supplied from the process boilers in the closed loop cycle. Since the primary heating load is produced in the process boilers, the heat transfer area in the water-water exchanger is much greater than that in the steam-water exchanger.

When the main water flow is discharged to the top steam-water exchanger, further heating takes place using condensed steam from the utilities generator.

4.3 The 2.44 m Diameter Simulator Column

The air-water simulator column comprises of three principle units: a 3.05 m diameter air inlet and distribution shell, the middle 2.44 m diameter tray column shell, and the top air exhaust ducting system. A schematic diagram of the simulator column is presented in Figure 4.3.

4.3.1 Air Distribution Shell

Air enters the 3.048 m diameter gas distributor from a section of ducting, after leaving the air fan and passing through a flow meter. The air swirls inside an annulus, between the outer and inner shells, until it reaches the 32 radial baffles, which are 0.3m deep. The radial baffles remove most of the tangential swirl and cause a downward vertical flow of air to the base of the distributor. The air escapes from the annulus under the inner shell into the central body of the distributor where four more radial baffles, 0.978m deep, continue to remove any tangential swirl. The distributor was designed using methods based on work by Ali (1984), who showed that for an inlet tangential feed, a system of internal cross and radial baffles, in an internal cylinder, minimised high velocity swirling and large pressure differentials, thus producing a more uniform gas distribution with negligible pressure drop. The shells of the distributor were constructed of mild steel, 0.005 m thick, and the baffles being non-weight bearing were fabricated of thinner steel.

The original air riser (chimney) distributor plate, situated immediately above the cross baffles and annulus was replaced with a 1.80 mm hole diameter perforated tray. This improved the gas flow pattern in the region between the distributor plate and the test tray.

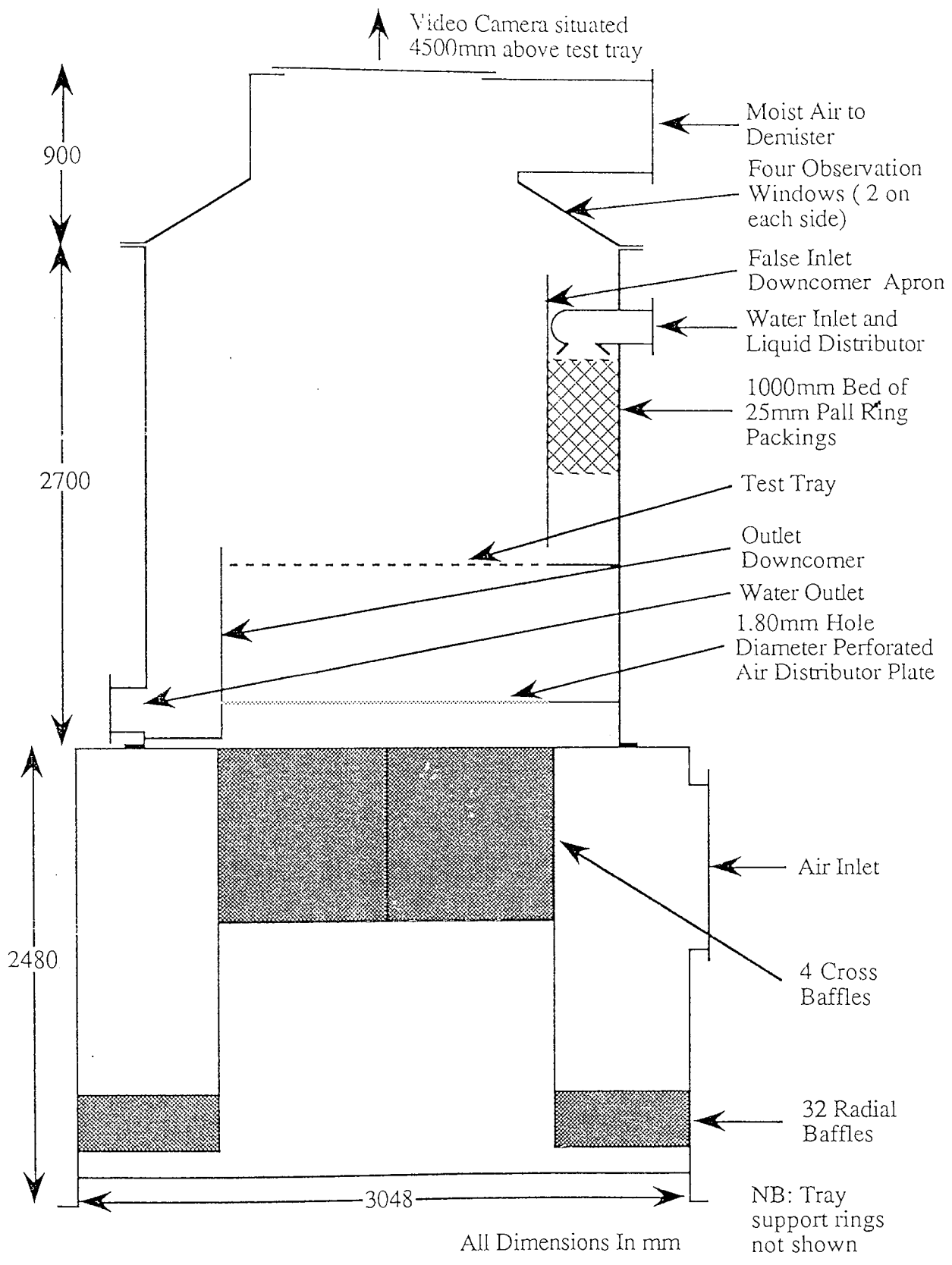


Figure 4.3 Schematic diagram of the 2.44m diameter air - water distillation simulator with modified air distributor.

The whole gas distribution system ideally works on a dry basis in order to prevent the accumulation of moisture by the rising air, and thus change its properties. Hence four drainage pipes were installed in each quadrant of the perforated distributor tray such that any weeped liquid was collected and discharged from the column.

4.3.2 The Test Column

The 2.44 m diameter test section is mounted directly on to the air distribution shell. The air travels 850 mm before encountering the tray support on which the test trays are mounted. The tray support is integral and connects to the outlet downcomer. After the air leaves the tray it flows up and into the exhaust ducting system where it is subsequently vented to the atmosphere.

The water distribution in the tray column shell consists of the water inlet and a sparge pipe, from which water is discharged onto a 1.0 m packed bed of 25 mm Pall Rings in the inlet downcomer. The packing is held at a clearance height of 600 mm above the under downflow plate. This method, developed by Enjugu (1986), is used to ensure a uniform distribution of water across the inlet downcomer before entering the test tray. The water on crossing the active bubbling area of the test tray is contacted with a cross flow of air before flowing over the outlet weir and leaving the outlet downcomer through an exit pipe.

At the bottom of the inlet downcomer apron is a moveable aluminium face plate, in which the inlet gap clearance can be set, using PVC spacers, at heights of between 10 and 50 mm. The outlet weir height can be varied between heights of 0 and 50 mm using specially made angled aluminium strips.

4.3.3 The Exhaust Section

At the top of the column, there is a reducing section which links the tray column shell to the exhaust ducting system. The cross section is reduced from 2.44 m to 1.50 m and the exhaust air leaves from the sides. The reducing section consists of four windows for direct-observation of liquid flow patterns. A video camera, supported on a platform 4.5 m above the test tray, permits flow patterns to be recorded or displayed on a monitor at ground level.

4.4 Measurement of Operating and System Variables

The important variables used in the direct-observation, heat transfer and measurement of liquid head profile experiments can be separated into two categories. The air and water flow rates can be classified as the operating variables while air enthalpy, air humidity and water temperature can be categorised as system variables. The assumption was made that other physical properties of the air-water system, such as density and viscosity did not undergo significant changes for all the experimental operating conditions used in the research programme.

4.4.1 Maximum Air and Water Flow Rate Specifications

The air and water flow rate specifications required for delivery to the simulator by the flow instruments, were obtained from a tray loading diagram similar to that shown in Figure 4.4, in which the capacity factor, based on the superficial air vapour velocity, is plotted against weir load. Hine 1990. This diagram contains a jet flooding curve and a weep limit for a 12.7 mm hole tray, set at a spacing of 600 mm and free area 8.0 % , which indicates the range of operation between the maximum and minimum throughputs (Note : jet flooding refers to flooding of the trays which is caused by entrainment of liquid droplets to the tray above).

The calculation of the maximum air and water flow rates was based on the operating condition of 80 % of total flooding from which data was extracted and substituted into the appropriate equations in order to compute the maximum flow rate specifications. The maximum air flowrate, Q_v , (max), was calculated to be 14.38 m³/s and the optimum water flow rate of 0.045 m³/s. In addition to the maximum air flow rate to be delivered by the air fan, the total pressure head resistance specification against the direction of flow was calculated to be 0.51 m of water. A complete description of how the above operating variables were calculated, is given by Hine, 1990.

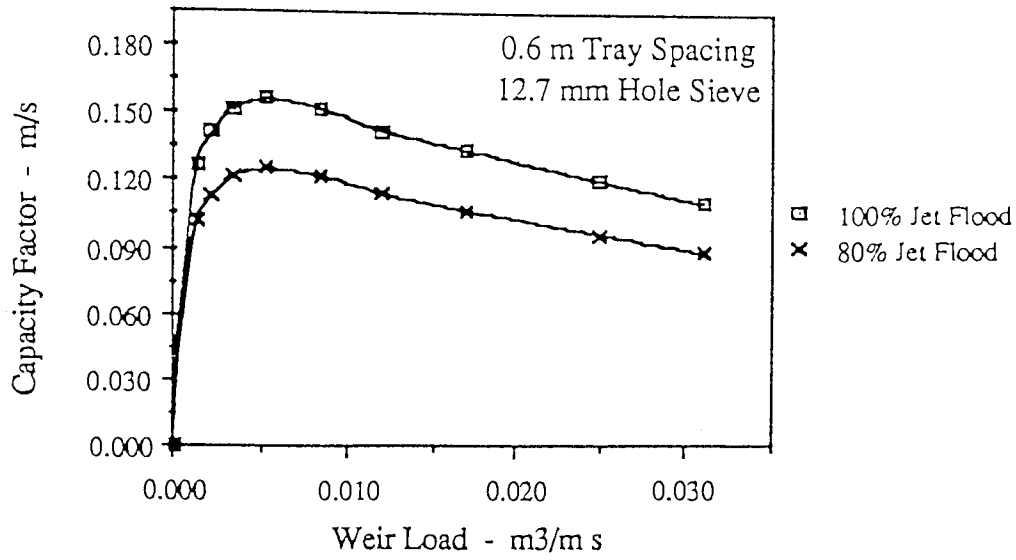


Fig. 4.4 Tray Flooding Curve- 12.7 mm hole sieve, 8% free area and 0.6 m tray spacing

4.4.2 Measurement Specifications of the Instrumentation by Error Analysis

The aim of this task is to determine the accuracy of a given experimental quantity by considering the range of error permitted for each of the measured operating and system variables required to calculate the value of this quantity. If a large error specification of the measured variables associated with the experimental quantity was permitted, this would seriously undermine the value of this quantity when used in results for publication.

If, however, a very low error specification of the measured variables, such that the accuracy of the experimental quantity was very high, would prove counter productive owing to the high costs of purchasing the appropriate instrumentation. Hence a compromise must be achieved in order to obtain a satisfactory balance between the two extreme situations. The objective, outlined above, was thus achieved by Hine (1990) in which an error analysis was carried out whereby the selected experimental quantity was Murphree tray efficiency. This was calculated from air enthalpy driving forces which are obtained from temperature measurements during the heat transfer experiments by water-cooling. The accuracy of the tray efficiency was determined by the error range permitted during the measurement of the operating and system variables such that suitable instrumentation could be incorporated into the test facility. The analysis was based upon the 'Principle of Superposition of Errors' in which the error associated with the calculated tray efficiency is caused by the cumulative effect of the errors for each of the operating variables, ie., air and water mass flow rates, and the system variables, ie T_{in} , T_{out} , T_{db} , and T_{wb} .

The magnitude of the error range for tray efficiency, obtained by iterative calculation using a consecutive set of error values for each measured variable, was greatest for the system variables (i.e., air and water temperatures) and least for the operating variables (i.e., air and water flow rates). Thus from the error range of the calculated tray efficiency together with the known errors for each variable, which are summarised in Table 4.3, the following error specifications for the operating and system variables were selected:

Air Flow Rate	2.0%
Liquid Flow Rate	0.5%
Air Temperatures	0.5C
Water Temperatures	0.02C

These permitted specifications yielded a Murphree tray efficiency that was within an error range of 2.1%. This was acceptable considering the scale of the apparatus being used.

Measured Variable	Error	Error	Error	Error
Air Flow Rate	4.0%	2.0%	1.0%	1.0%
Water Flow Rate	4.0%	2.0%	1.0%	0.5%
In/Out Water Temp	0.1C	0.05C	0.02C	0.02C
Dry/Wet Bulb Temp	1.0C	1.0C	0.5C	0.5C
Of Inlet Air				
Calculated	6.6%	3.8%	1.9%	1.6%
Murphree Tray				
Efficiency (86.7%)				

With the minimum error specification for each variable established, and the maximum air and water flowrates known, a description of the flow measurement instruments used is presented below.

4.4.3 Measurement of Air Flow Rates

The air flow meter is directly linked to a high and low pressure tapping on the rectangular section of ducting at the air inlet to the simulator column. The device measures the differential pressure produced from an integrated network of fifteen impact and static pitot pressure sensors located in the ducting. According to the Bernoulli principle, a differential pressure, proportional to flow, is generated across the uniformly distributed network of pressure sensors, spread over the whole cross section of ducting. Each pressure sensor is of equal area, and is contained within an integrated network, in order to obtain an average differential pressure. The pressure sensors, required for the full air flow operating range, was designed and purchased from Tekflo Limited, who supplied the flow grid sensors and a calibration certificate to meet the desired flow rate specifications. The differential pressure range of 3.19 up to 57.92 mm of manometric fluid is measured using a mechanical micromanometer (purchased from Perflow Instruments) with an accuracy of ± 0.005 mm of manometric fluid. The differential pressure range corresponds to superficial air (empty column) velocities of between 0.70 and 3.00 m/s.

4.4.4 Measurement of Water Flow Rates

Since a wide range of flow rates are used in the experiments, two flow meters were incorporated into the water flow circuit. An orifice plate flowmeter is used for low water loadings, of upto $0.009 \text{ m}^3/\text{s}$, and is controlled using a mechanical gate valve. The error specification for this device was approximately 2.0%. For high water loadings, in the

range 0.009-0.090m³/s, an electromagnetic flow meter, supplied from Combustion Engineering together with a calibration certificate to meet the required water flow rate specification and with an accuracy of less than 0.5%, is used. This 10cm unit contains no moving parts, thus creating no disturbance to the liquid flow. The flow meter is a compact, volumetric liquid flow rate device in which a transducing method is employed, such that the conduction properties of the liquid are used to produce an induced voltage on passing through a magnetic field. The amplitude of the generated voltage is directly proportional to the average flow velocity of the liquid. The output of the water flow rates was calibrated in milliamps, and for a given flow rate, the corresponding current output is shown on a digital display unit located above the electromagnetic flow meter.

4.5 Operation of the Air-Water Simulator

Set below are the start-up, normal operation and shut down procedures used for the safe operation of the distillation simulator. The steps presented are those used during heat transfer experiments by water-cooling since it involves the use of the whole apparatus.

4.5.1 Start-Up Procedure

1. Switch on the main electricity isolator and open the manual gas valves to the gas fired process boilers.
2. Start the circulation water pump, in the primary heating circuit, and the flue dilution fan
3. Start the main water pump, in the secondary water circuit, to circulate water through the double heat exchanger and bypass network from where it is returned to the water sump tanks.
4. Switch on the electrical supply to the gas shut-off valve.
5. Start one or both of the gas fired boilers. This is the primary heating source to the main water circuit.
6. Open the steam valve. This the secondary heating source which is used as a heat top-up supply. A spring valve is used to fine tune the inlet water temperature to the simulator prior to entering the test tray.
7. When the water, in the sump tanks, approaches 40°C start the air fan and set the desired air flowrate using the mechanical micromanometer.
8. Once the water temperature reaches 45°C, set the desired water flowrate to the tray simulator, then make any small adjustments to the air flowrate.
9. Adjust the steam and gas fired boiler heating flowrates, by manual control, until a steady water temperature is reached.

10. After about ten minutes of steady operation has elapsed, initiate temperature data collection. During most of the test runs, height of clear liquid measurements are recorded from the manometer pressure tapings attached to the tray.

4.5.2 Normal Operation

11. Set the new air and water flowrates and return to instruction 8.

4.5.3 Shut-Down Procedure

12. Once the last temperature data collection is complete, close the steam valve and switch off the gas fired boilers, leaving the simulator in operation.

13. Switch off all the electrical equipment, apart from the two water pumps and the air fan, and close the manual gas valves.

14. When the water in the sump tanks has cooled down to a temperature of about 20°C and both sections of the heat exchanger are cool, the water pumps can be shut down.

15. Five minutes after stopping the water pumps the air fan can be shut down.

CHAPTER 5

The Effect of Intermediate Weirs on the Flow Pattern Across a Rectangular Sieve Tray

5.1 Introduction

It is well known that non-ideal flow causes a loss of efficiency on scale-up in many distillation trays. The term non-ideal flow includes fluid channelling and recycling, the presence of stagnant regions and non-uniform fluid velocity profiles. Until recently theories for predicting distillation plate efficiency took no account for non-ideal flow. The theories predicted that for large single-pass cross-flow distillation trays very high plate efficiencies should be obtained, but in practice such high efficiencies are not observed. The cause of the loss of efficiency has been suspected to be non-ideal liquid flow on the plate and a number of workers have sought to measure the extent of the non-ideality which occurs.

Although it is clearly important to be able to model plates which have been built and which are probably even now are operating under conditions of non-ideal flow, it is also necessary to consider ways of straightening and improving the liquid flow pattern on plates that will be installed in the future. Straight flow patterns represent an approach to the ideal plug flow and thus enhance tray efficiency over point efficiency. Distillation is a significant business area and the industry is always looking for more cost effective equipment. Rush (1979) investigated the economics of replacing distillation by other competing technologies. He concluded that although distillation was heavily energy intensive, in many cases, it was still the best way to achieve a given separation by an industrial scale, though improvements could be made to optimise the processes and run them 'harder and leaner'. Even small improvements in efficiency were found to be economically viable.

The aim of the research described in this Chapter is concerned with straightening the flow pattern on the 2.44 m diameter sieve tray by using intermediate weirs. The question that needs to be asked is 'Is it possible to use intermediate weirs to deflect some of the liquid towards the sides of the circular tray hence providing a more uniform distribution of liquid and hence reduce or eliminate the formation of stagnant or slow moving liquid'. This would increase the efficiency of the column and it is hoped that this can be used in the design of new columns so as to reduce capital costs or can be fitted into existing columns. The ultimate choice of a flow directing device to remove flow non-uniformities is both an economic consideration and a practical one. Before experimental work could be started a few questions about the weirs needed to be answered :

1. How long and how high do the weirs need to be ? The weirs should not interfere with the flow pattern across the rest of the tray i.e. act as a barrier which will obviously reduce the throughput of the tray . They should be of a practical design which can be easily installed into existing distillation columns and can be walked on (or over) by those people installing trays.
2. In what position do they need to be placed (i.e. what angle) with respect to the inlet gap in order to be most effective.
3. Is it more efficient to use one long weir or use several smaller weirs.

The first part of this work is concerned with establishing the flow patterns that occur on the tray with no intermediate weir placed on the tray. This could then act as a reference for the next part of the experimental work. The second part of this work is concerned with the effect of intermediate weirs of different heights placed in the centre of the tray to try and observe what factors affect the performance of the weirs i.e. different inlet gap and outlet weir combinations, the effect of superficial air velocities and water flowrates. The heights of the intermediate weirs that were tested were 10 mm and 50 mm ; they were constructed of Aluminium, each being 1.25 m long and placed in the centre of the tray, see Figure 5.0. In order to measure the effect, if any, on the flow pattern clear liquid height measurements were collected and 3D Surface of Clear Liquid Hold-Up diagrams plotted.

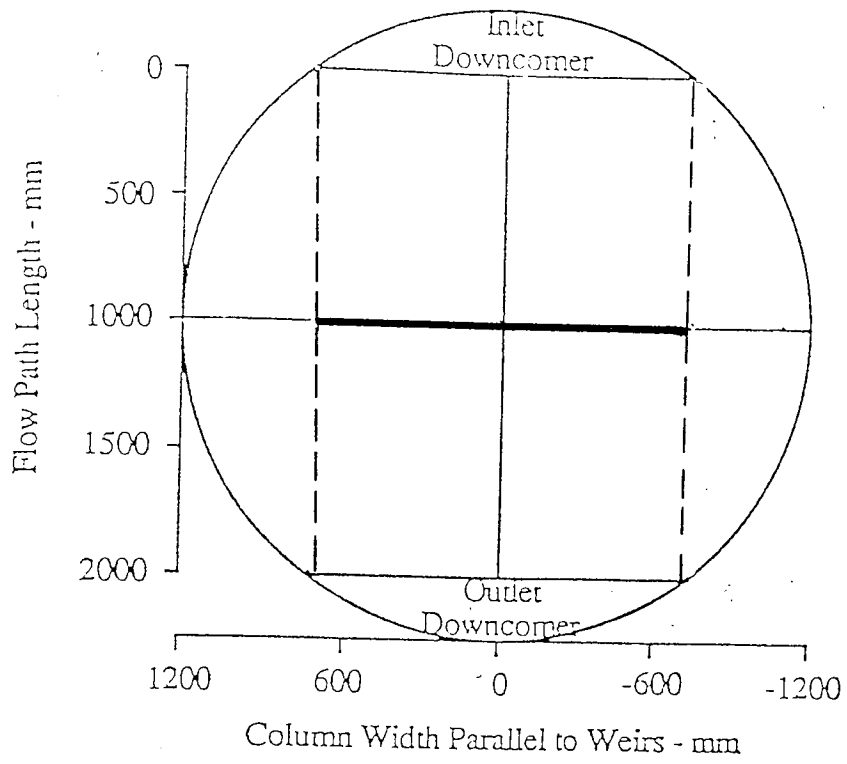


Fig. 5.0 Intermediate weir placed in centre of rectangular sieve tray

5.2 Measurement of Clear Liquid Hold-Up

The flow pattern can be considered to be made up of three components:

Flow Direction

Flow Velocity

Flow Depth

Each of the components combine to give the overall flow pattern. Text books assume all the flow to be in a uniform direction and that the froth height decreases from the liquid inlet to the liquid outlet of the tray.

The froth height is a difficult parameter to measure, due to the mobile froth surface. However, the pressure drop through the froth, which is proportional to the froth height, can be determined by the measurement of the effective froth height or the liquid hold-up. The liquid hold-up on a tray is defined as the height of the clear liquid on the tray when the vapour supply is cut off to eliminate the foaming vapour and liquid droplets above it.

5.3 Measurement Technique using Manometers

One standard method of measuring the clear liquid height on an air-water test tray is to connect a manometer, filled with water, to a pressure tapping mounted flush on the tray floor, see Figure 5.1.

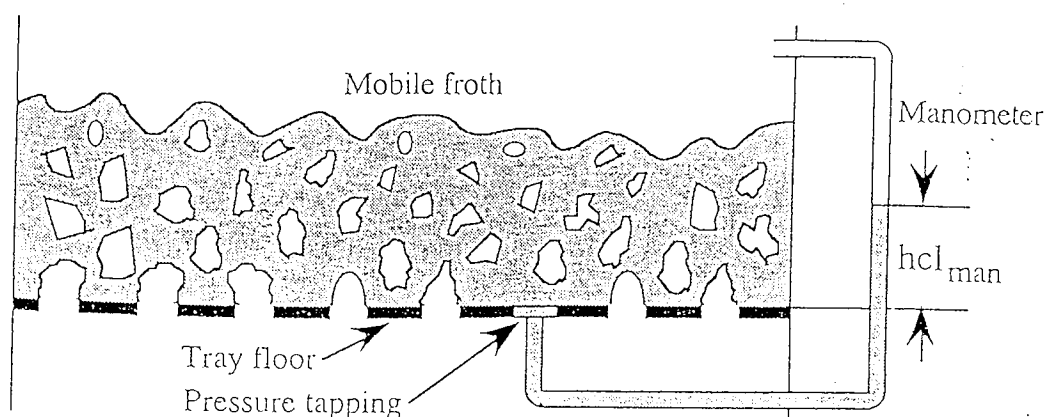


Figure 5.1 Schematic diagram of a manometer for measuring the height of clear liquid.

Lockett (1986) points out that corrections to the measured value must be made to account for capillary rise and gas momentum. These corrections were overcome by relating all the manometer readings to a datum level, which was generated by operation with air flow but no liquid hold-up. Then the datum level was subtracted from the actual reading with the liquid hold-up. This technique also allowed the account to be taken of tray deflection, which is more significant on large diameter trays.

5.4 Experimental Procedure

Height of clear liquid measurements are obtained from thirty six manometer pressure tappings spread evenly across the test tray as shown in Figure 5.2. Manometers are connected to sample points on the tray using PVC tubing which is filled with water and purged of any air bubbles trapped in the water lines using water under pressure. For a particular air flowrate the datum manometer levels were recorded without any water flowrate, and thus zero liquid hold-up. The water flowrate was then set and after a period to allow for steady state to be achieved all the manometer levels were recorded. The water hold-up was then calculated by subtracting the datum manometer levels from the actual levels.

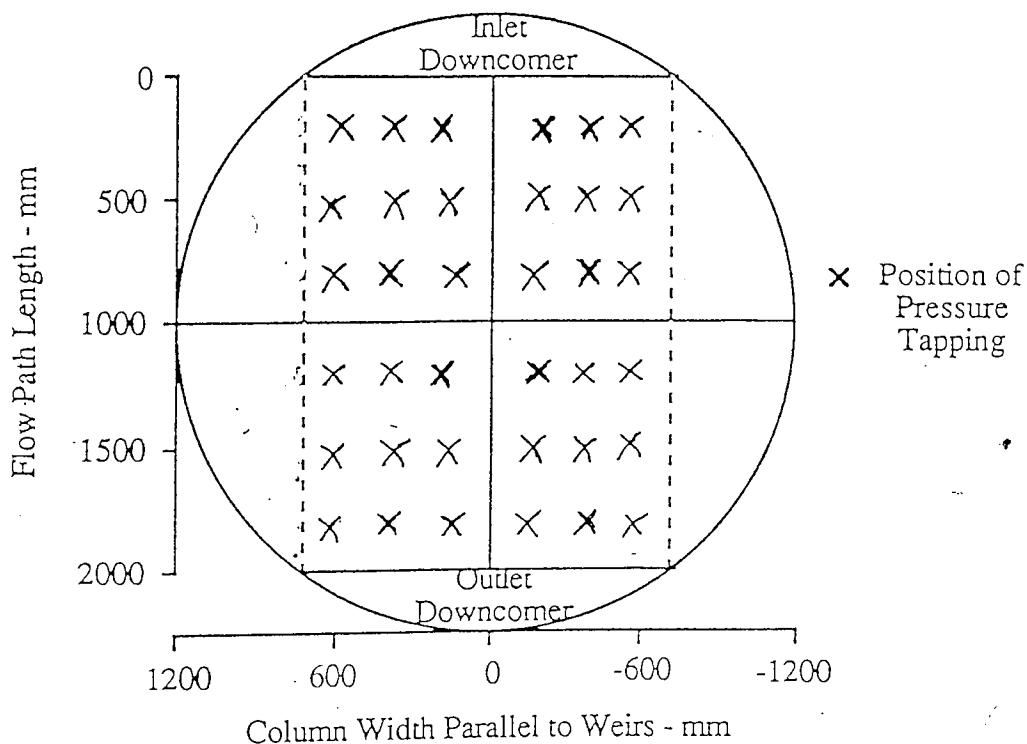
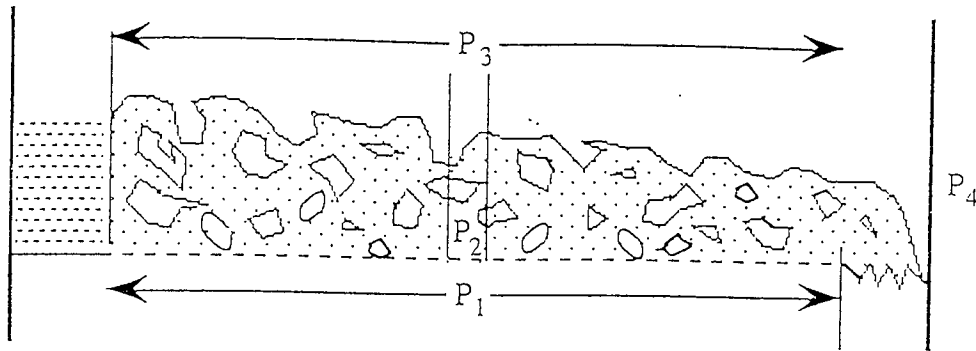


Fig. 5.2 Positions of the Pressure Tappings over the Tray Area.

The results are computer processed to produce three-dimensional liquid surface diagrams and point height of clear liquid readings. Figure 5.3 shows how the height of clear liquid is calculated for a given point on the tray. The total pressure drop from below the tray to the space above the froth on the tray was measured using a U-tube manometer such that $\Delta P_{TOTAL} = P_1 - P_3$, (see figure 5.3).



P_1 - Pressure below test tray

$$\Delta P_{TOTAL} = P_1 - P_3$$

P_2 - Pressure above test tray

$$\Delta P_{CORR} = P_3 - P_4$$

P_3 - Pressure above froth

$$\Delta P_{CORR} = P_1 - P_2$$

P_4 - Atmospheric pressure

Figure 5.3 : A Pressure Diagram For The Calculation Of Height Of Clear Liquid

Step 1: Measure the total pressure drop, $\Delta P_{TOTAL} = P_1 - P_3$

Step 2: Measure the corrected pressure drop, $\Delta P_{CORR} = P_3 - P_4$

Step 3: Measure the liquid height from manometer at point I (where $I = 1$ to 32),

$$\Delta P_{FROTH} = P_2 - P_4$$

Step 4: $\Delta P_{FROTH} - \Delta P_{CORR} = (P_2 - P_4) - (P_3 - P_4) = P_2 - P_3 =$ height of clear liquid at point i

The computer coding that generates three-dimensional liquid surface diagrams are included in Hine's PhD Thesis 1990 and the height of clear liquid measurements are listed in Appendix I.

5.5 RESULTS AND DISCUSSION

An open channel is a conduit in which the liquid flows with a free surface subjected to atmospheric pressure. The nature of the liquid flow in a rectangular tray is quite similar to that in open channel. Therefore, some important phenomena in open channel flow are discussed in the following sections for better understanding of plate hydraulics and effect of the intermediate weirs.

5.5.1 Critical Flow In An Open Channel

For a non-uniform and steady state flow in an open horizontal channel with a gradual variation of depth, the specific energy at any point is defined as the sum of the depth of liquid and the velocity head. As the open channel flow is a free surface flow, the velocity head will also be dependent on the liquid depth. Therefore, for a given section and liquid discharge, the specific energy is a function of the liquid depth only. For a given specific energy (E) there are two possible depths (h_1 and h_2) which are the alternate of each other. This condition of minimum specific energy corresponds to the critical state of flow. Thus, at the critical state the two alternate depths become one, which is known as the critical depth (h_c). When the depth of flow is greater than the critical depth, the flow is known as subcritical flow (deep and slow moving liquid) When the depth of flow is less than the critical depth, the flow is supercritical (shallow and fast moving liquid). The above conditions are controlled by the upstream and downstream conditions i.e. inlet gap and outlet weir. Once these values are set then only one flow regime will be possible. A change of state of flow from supercritical to subcritical or vice versa occurs frequently in open channels. Such a change is manifested in a corresponding change in depth of the flow from a low state to a high state and vice versa. When a rapid flowing stream has its velocity reduced to below the critical value, owing to an obstruction in the channel, the result is usually an abrupt rise of the water surface i.e. hydraulic jump. The height of the slow stream after the hydraulic jump will be determined by the resistance of a weir or other obstruction downstream. The hydraulic jump involves a large amount of energy loss through dissipation in the turbulent body of liquid in the jump. Consequently, the energy content in the flow after the jump is appreciably less than that before the jump.

5.5.2 NO INTERMEDIATE WEIR

Inlet Gap/Outlet Weir = 10/10 mm, 20/20 mm

At the superficial air velocity of 1.5m/s and low weir load of 50 cm³/ cm s there was very little variation in the clear liquid height measured, see Figure 5.4 a and 5.6 a. A good biphasic mixture was observed over the tray area and no weeping occurred. At higher weir loads 150/ 250 cm³/ cm s, a hydraulic jump was observed at the inlet gap which increased in height and length as the weir load increased. Low clear liquid hold-ups were measured just after the inlet weir, see Figures 5.4 b - 5.4 c and 5.6 b- 5.6 c. In these cases the liquid seemed to jet from the inlet gap and did not become fully aerated until about 250 mm from the inlet weir.

Hydraulic jumps are caused by the tray becoming overactive at the inlet gap whereas the liquid outlet area is relatively inactive. The liquid at the inlet is fluidised and is thrown in a trajectory reaching far down the tray. The bubbling activity at the outlet becomes low leading to weeping which coupled with maldistribution of the fluids reduces tray efficiency, Lockett (1980).

Increasing the superficial air velocity to 2.5 m/s, the above results were observed except for the fact that increasing the vapour rate decreases the clear liquid hold-up on the tray, see Figures 5.5 a to 5.5 c and 5.7 a to 5.7 b.

Inlet Gap/ Outlet Weir = 50/50 mm

Increasing the IG/OW combination increases the clear liquid hold-up as more liquid is retained on the tray. At low weir loads, the biphasic was evenly distributed across the tray floor ie. subcritical flow. Increasing the weir load, however, caused the formation of liquid gradient ie. clear liquid hold-up decreasing with distance from the inlet gap. The gradient was observed to increase as the weir load increased, see Figures 5.8 b and 5.8 c.

It is important to note that when we refer to liquid gradient, it is not the froth height gradient which is of importance, but the hydrostatic head gradient or clear liquid head gradient. This explains why observations of froth height gradients are often deceptive - there may be little visible froth height gradient on the tray whereas the corresponding hydrostatic head measurements will show a very definite hydrostatic head gradient over a long flow path length. The difference in hydrostatic head between tray inlet and tray outlet causes a dry pressure drop difference between inlet and outlet, vapour flows preferentially through the tray outlet where the hydrostatic pressure is low.

5.5.3 10 mm INTERMEDIATE WEIR

Inlet Gap/ Outlet Weir = 10/10 mm, 20/20mm

At superficial air velocities of 1.5 m/s and 2.5 m/s and low weir loads, it is clear from Figures 5.10 a and 5.11 a that the intermediate weir causes an increase in the height of clear liquid. It is very difficult to quantify the increase in the height of clear liquid. Increasing the weir load causes hydraulic jumps, as mentioned earlier, and it is very difficult to establish whether the intermediate weirs are causing an effect on the height of clear liquid. It is felt that the hydraulic jumps are masking the effect of the intermediate weir.

Inlet Gap/ Outlet Weir = 50/50 mm

The results obtained in these set of experiments followed the same pattern as those obtained with no intermediate weir being placed on the tray floor see figures 5.12 to 5.15. No evidence could be found to suggest that the intermediate weirs were causing an effect on the height of clear liquid at this IG/OW combination. This would seem to suggest that the height of the intermediate weir with respect to the IG/OW settings is an important factor in assessing the successful operation of a flow directing weir.

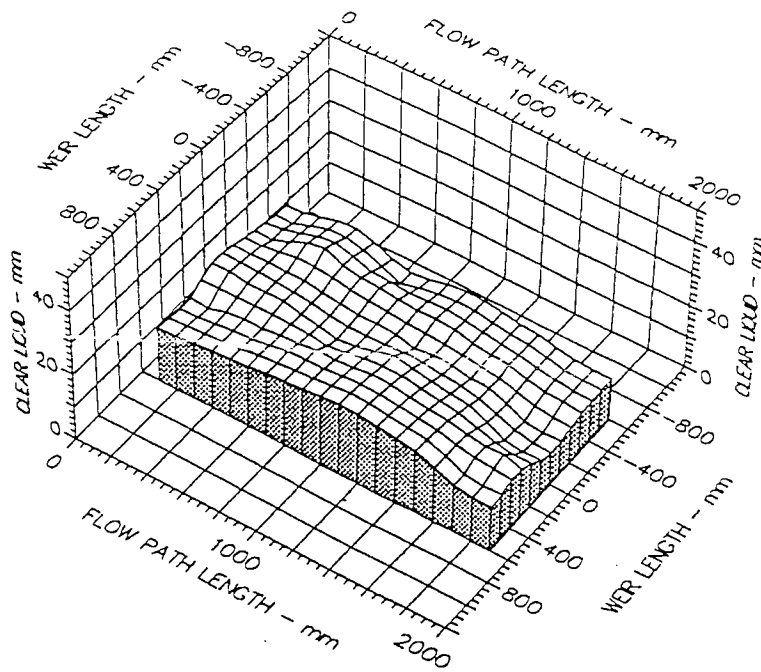
5.5.4 50 mm INTERMEDIATE WEIR

Inlet Gap/ Outlet Weir = 10/10 mm, 20/20 mm

At these inlet and outlet combinations, the intermediate weir acted as a barrier to the flow of liquid due to its size rather, rather than as a flow directing device. This can be seen from figures 5.16 to 5.17 and 5.18 to 5.19. The large intermediate weir causes the tray to operate in two compartments. The first compartment between the inlet gap and intermediate weir the froth is well mixed. In the second compartment, however, there is a reduction in the height of liquid, no bubbling was observed coupled also with weeping.

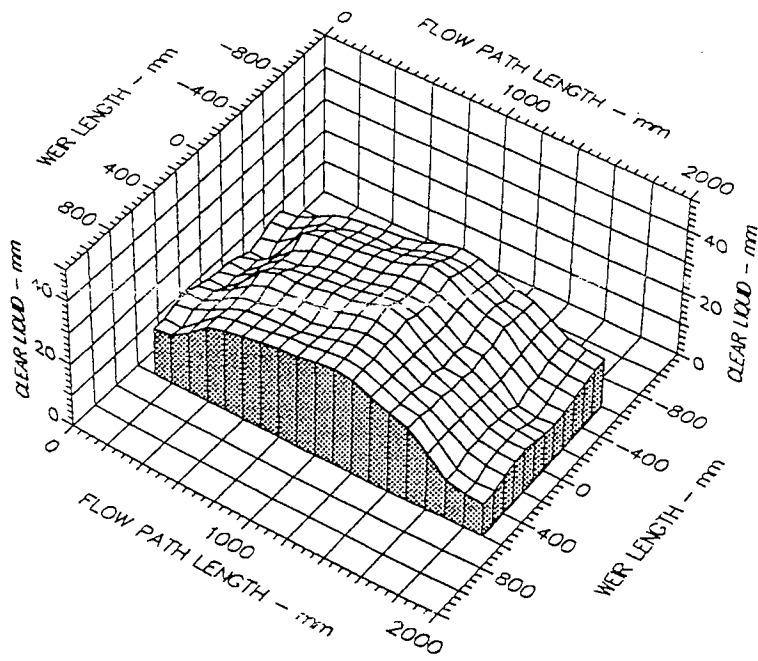
Inlet Gap/ Outlet Weir = 50/50 mm

At low weir loads it is clear from figures 5.20 a and 5.21 a that the intermediate weir is causing an increase in the liquid head across the centre of the tray. By increasing the weir load, however, causes more liquid to be retained on the tray and subsequently masks the effect of the intermediate weir. The above results are repeated at a superficial air velocity of 2.5 m/s.



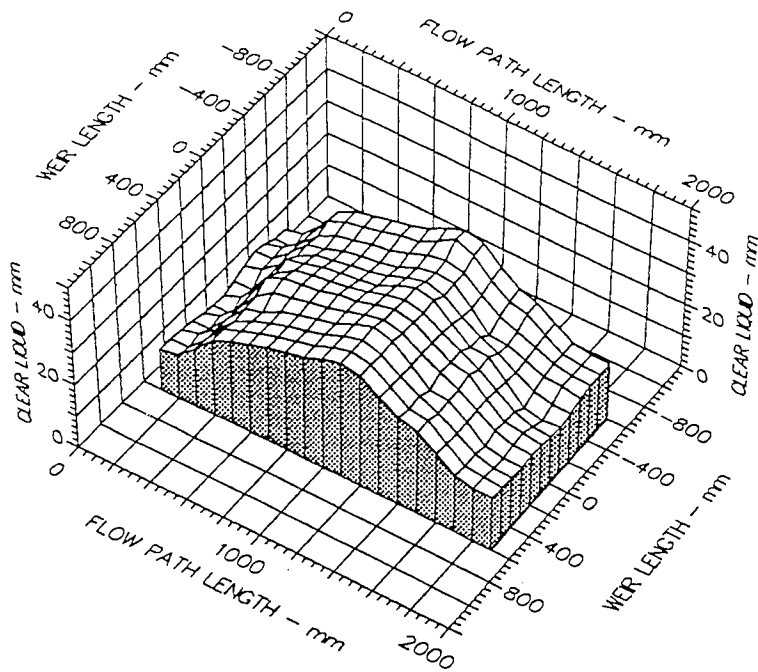
Air Velocity
 1.500 m/s
 Water Loading
 50.0 cm³/cm.s
 Inlet Gap
 0.010 m
 Inlet Weir
 0.000 m
 Outlet Weir
 0.010 m
 Hole Diameter
 0.001 m

Fig. 5.4 a Surface of Clear Liquid Hold-Up, No Intermediate Weir
 IG/OW= 10mm, Water Loading = 50 cm³/cm.s



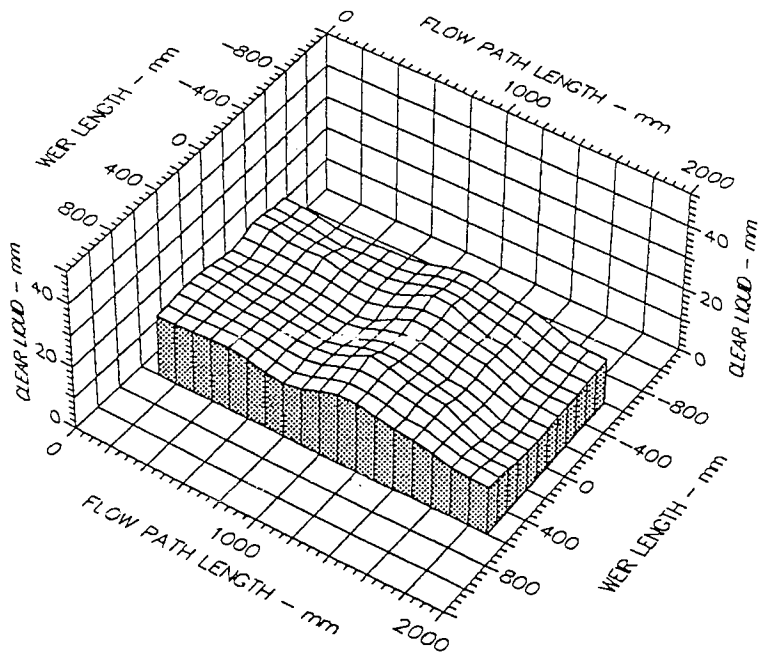
Air Velocity
 1.500 m/s
 Water Loading
 150.0 cm³/cm.s
 Inlet Gap
 0.010 m
 Inlet Weir
 0.000 m
 Outlet Weir
 0.010 m
 Hole Diameter
 0.001 m

Fig. 5.4 b Surface of Clear Liquid Hold-Up, No Intermediate Weir
 IG/OW= 10mm, Water Loading = 150 cm³/cm.s



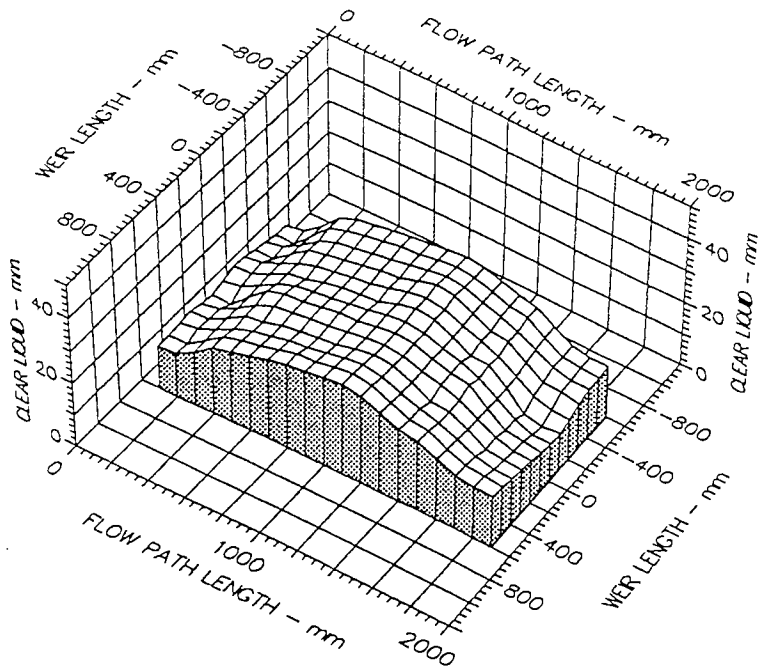
Air Velocity
 1.500 m/s
 Water Loading
 250.0 cm³/cm.s
 Inlet Gap
 0.010 m
 Inlet Weir
 0.000 m
 Outlet Weir
 0.010 m
 Hole Diameter
 0.001 m

Fig. 5.4 c Surface of Clear Liquid Hold-Up, No Intermediate Weir
 IG/OW= 10mm, Water Loading = 250 cm³/cm.s



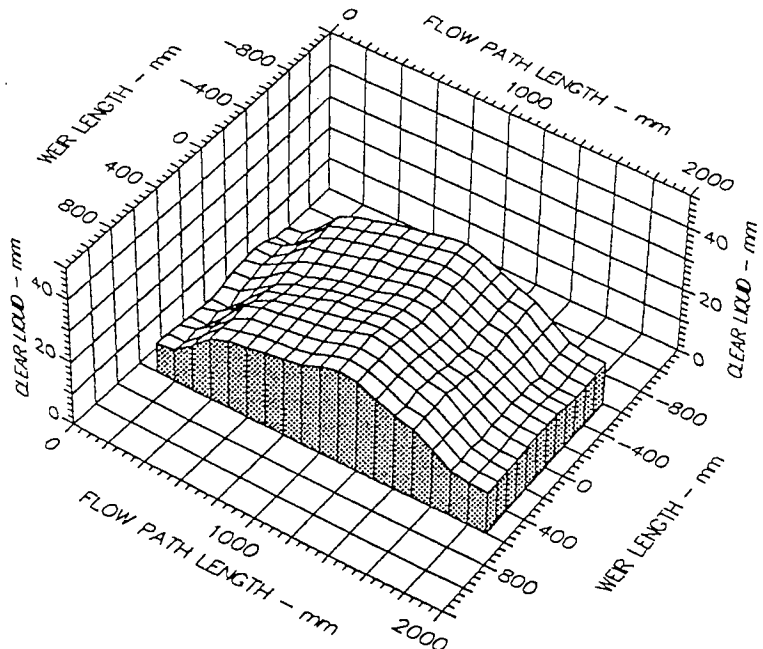
Air Velocity
 2.500 m/s
 Water Loading
 50.0 cm³/cm.s
 Inlet Gap
 0.010 m
 Inlet Weir
 0.000 m
 Outlet Weir
 0.010 m
 Hole Diameter
 0.001 m

Fig. 5.5 a Surface of Clear Liquid Hold-Up, No Intermediate Weir
 IG/OW= 10mm, Water Loading = 50 cm³/cm.s



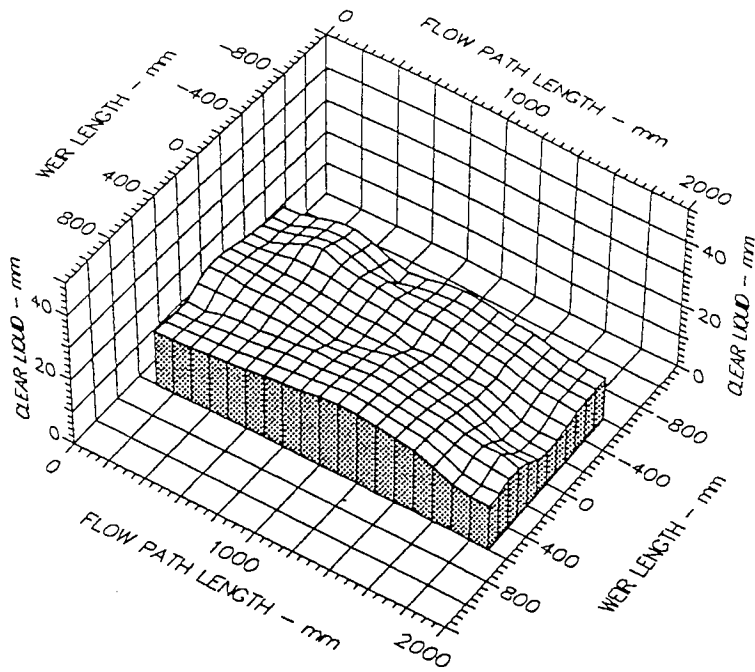
Air Velocity
 2.500 m/s
 Water Loading
 150.0 cm³/cm.s
 Inlet Gap
 0.010 m
 Inlet Weir
 0.000 m
 Outlet Weir
 0.010 m
 Hole Diameter
 0.001 m

Surface of Clear Liquid Hold-Up, No Intermediate Weir
 Fig. 5.5 b IG/OW= 10mm, Water Loading = 150 cm³/cm.s



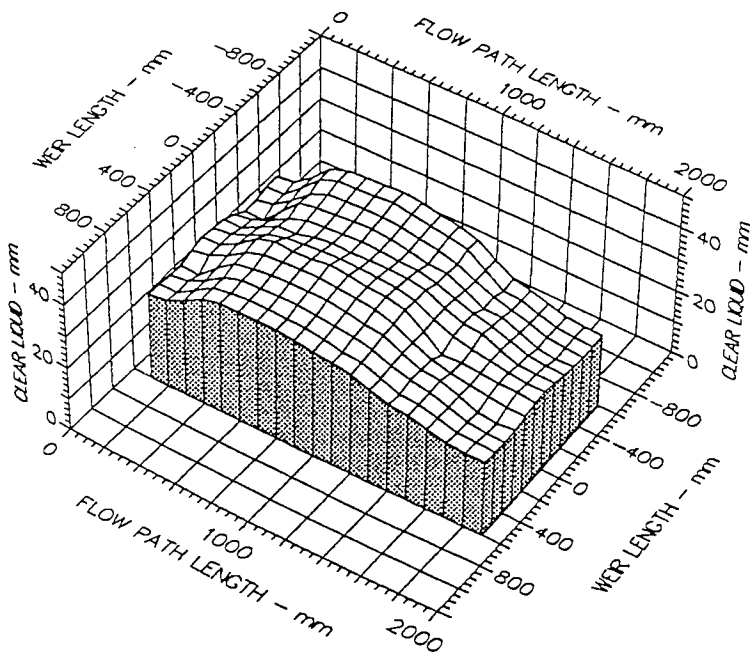
Air Velocity
 2.500 m/s
 Water Loading
 250.0 cm³/cm.s
 Inlet Gap
 0.010 m
 Inlet Weir
 0.000 m
 Outlet Weir
 0.010 m
 Hole Diameter
 0.001 m

Surface of Clear Liquid Hold-Up, No Intermediate Weir
 Fig. 5.5 c IG/OW= 10mm, Water Loading = 250 cm³/cm.s



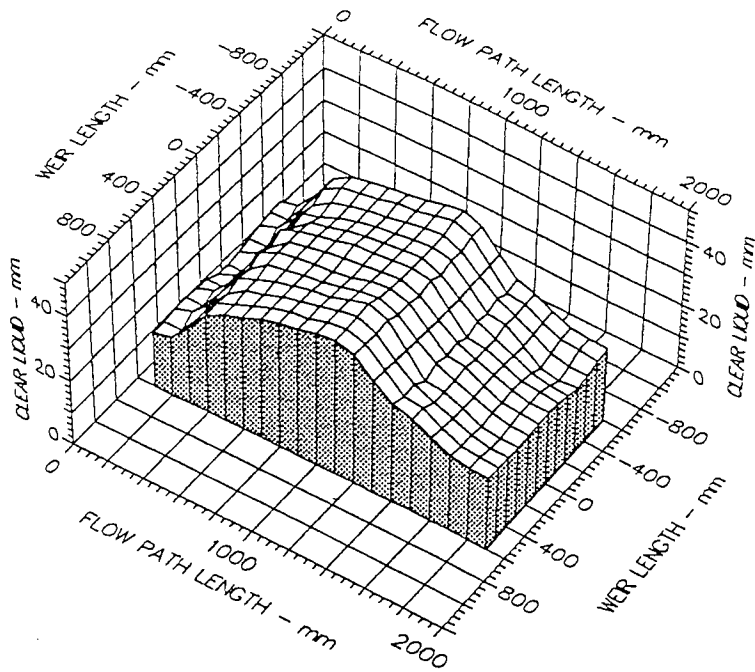
Air Velocity
 1.500 m/s
 Water Loading
 50.0 cm³/cm.s
 Inlet Gap
 0.020 m
 Inlet Weir
 0.000 m
 Outlet Weir
 0.020 m
 Hole Diameter
 0.001 m

Fig. 5.6 a Surface of Clear Liquid Hold-Up, No Intermediate Weir
 IG/OW= 20mm, Water Loading = 50 cm³/cm.s



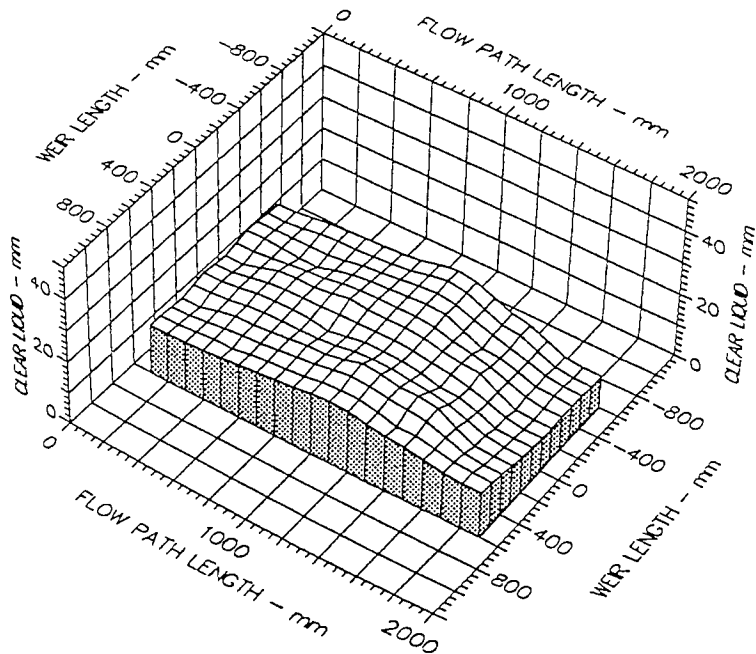
Air Velocity
 1.500 m/s
 Water Loading
 150.0 cm³/cm.s
 Inlet Gap
 0.020 m
 Inlet Weir
 0.000 m
 Outlet Weir
 0.020 m
 Hole Diameter
 0.001 m

Fig. 5.6 b Surface of Clear Liquid Hold-Up, No Intermediate Weir
 IG/OW= 20mm, Water Loading = 150 cm³/cm.s



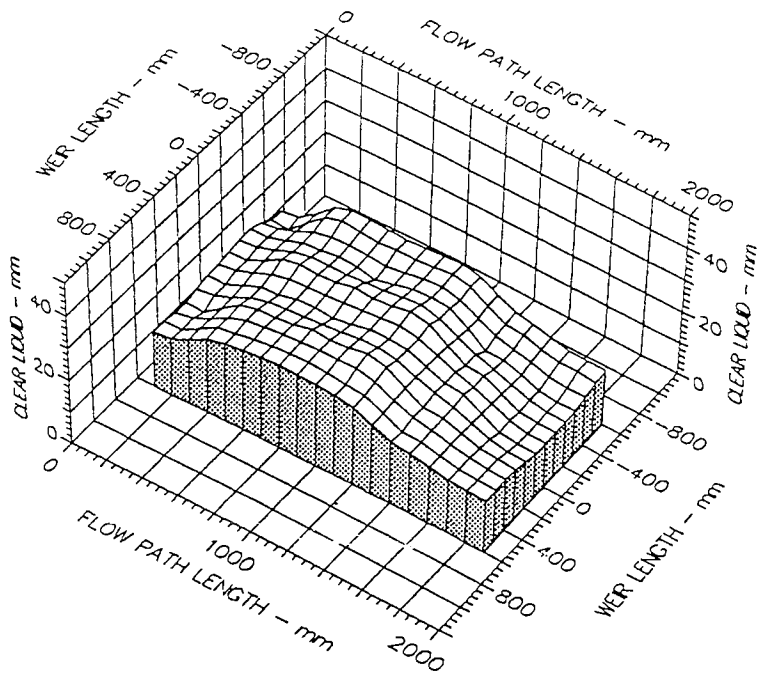
Air Velocity
 1.500 m/s
 Water Loading
 250.0 cm³/cm.s
 Inlet Gap
 0.020 m
 Inlet Weir
 0.000 m
 Outlet Weir
 0.020 m
 Hole Diameter
 0.001 m

Fig. 5.6 c Surface of Clear Liquid Hold-Up, No Intermediate Weir
 IG/OW= 20mm, Water Loading = 250 cm³/cm.s



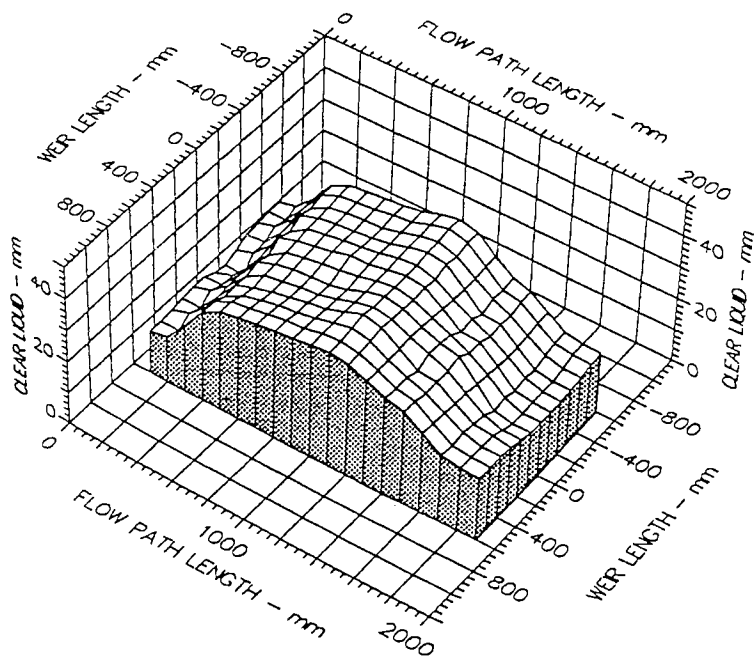
Air Velocity
 2.500 m/s
 Water Loading
 50.0 cm³/cm.s
 Inlet Gap
 0.020 m
 Inlet Weir
 0.000 m
 Outlet Weir
 0.020 m
 Hole Diameter
 0.001 m

Fig. 5.7 a Surface of Clear Liquid Hold-Up, No Intermediate Weir
 IG/OW= 20mm, Water Loading = 50 cm³/cm.s



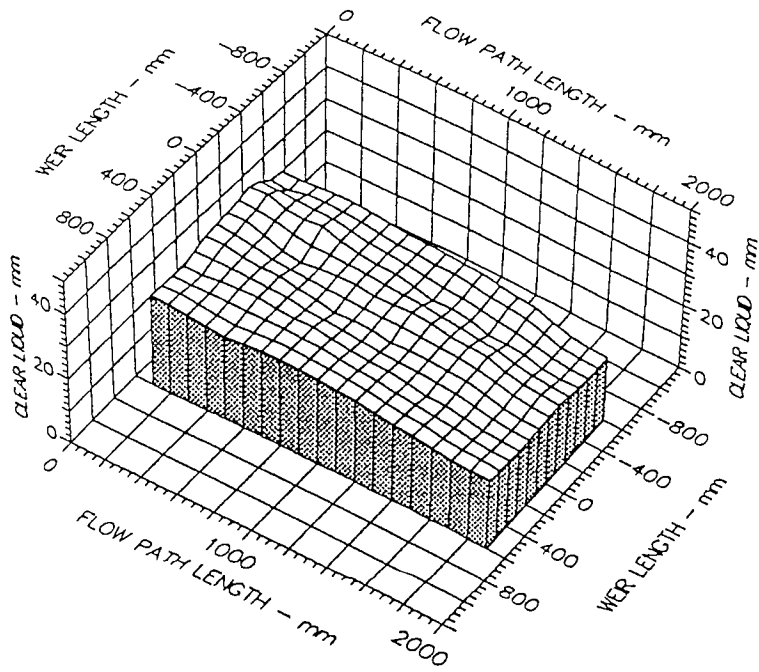
Air Velocity
 2.500 m/s
 Water Loading
 150.0 cm³/cm.s
 Inlet Gap
 0.020 m
 Inlet Weir
 0.000 m
 Outlet Weir
 0.020 m
 Hole Diameter
 0.001 m

Fig. 5.7 b Surface of Clear Liquid Hold-Up, No Intermediate Weir
 IG/OW= 20mm, Water Loading = 150 cm³/cm.s



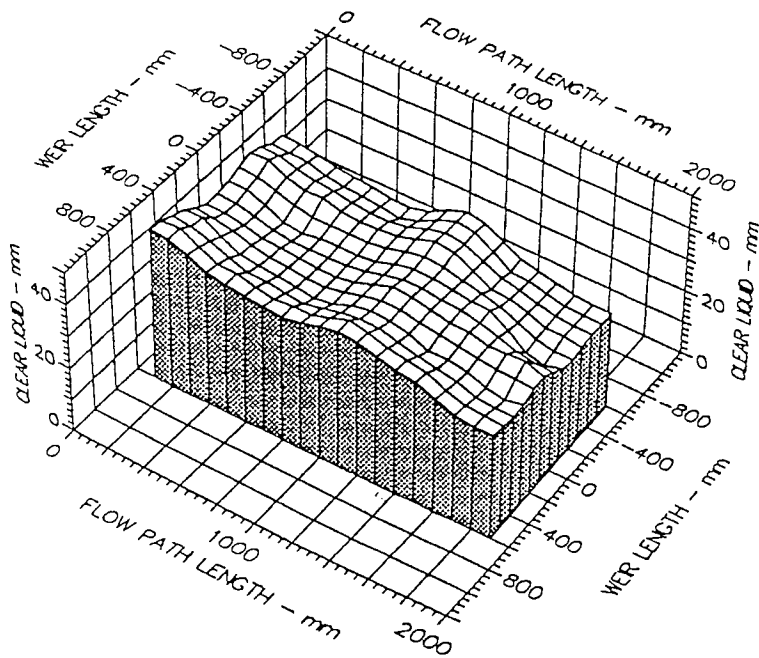
Air Velocity
 2.500 m/s
 Water Loading
 250.0 cm³/cm.s
 Inlet Gap
 0.020 m
 Inlet Weir
 0.000 m
 Outlet Weir
 0.020 m
 Hole Diameter
 0.001 m

Fig. 5.7 c Surface of Clear Liquid Hold-Up, No Intermediate Weir
 IG/OW= 20mm, Water Loading = 250 cm³/cm.s



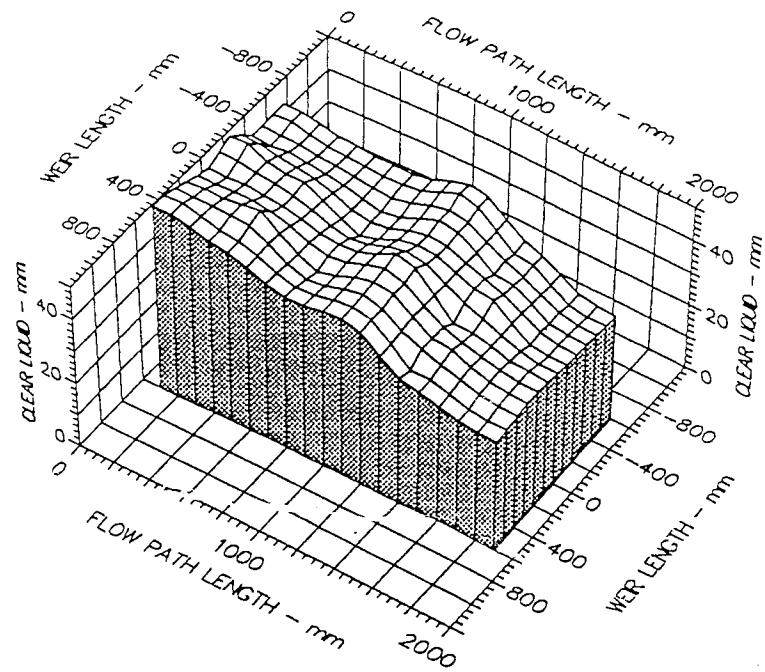
Air Velocity
 1.500 m/s
 Water Loading
 5.0 cm³/cm.s
 Inlet Gap
 0.050 m
 Inlet Weir
 0.000 m
 Outlet Weir
 0.050 m
 Hole Diameter
 0.001 m

Fig. 5.8 a Surface of Clear Liquid Hold-Up, No Intermediate Weir
 IG/OW = 50mm, Water Loading = 50 cm³/cm.s



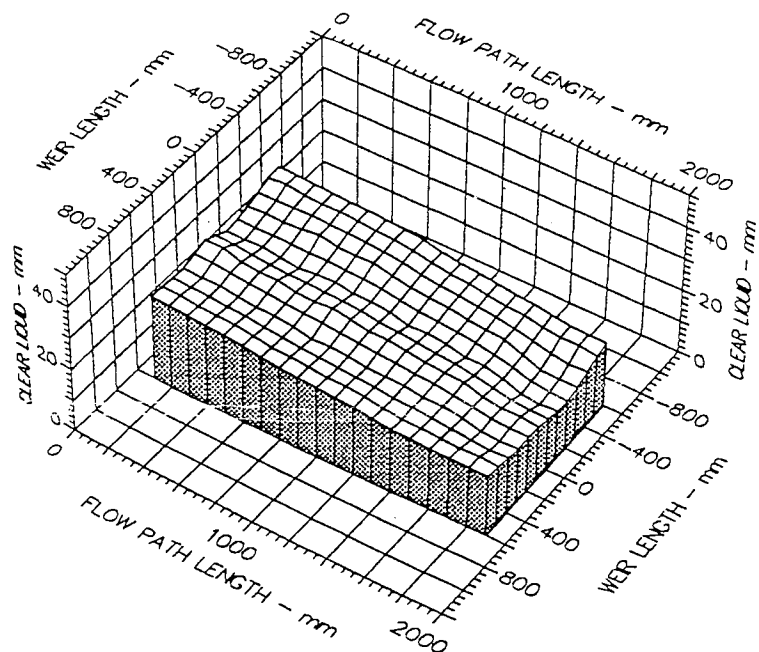
Air Velocity
 1.500 m/s
 Water Loading
 150.0 cm³/cm.s
 Inlet Gap
 0.050 m
 Inlet Weir
 0.000 m
 Outlet Weir
 0.050 m
 Hole Diameter
 0.001 m

Fig. 5.8 b Surface of Clear Liquid Hold-Up, No Intermediate Weir
 IG/OW = 50 mm, Water Loading = 150 cm³/cm.s



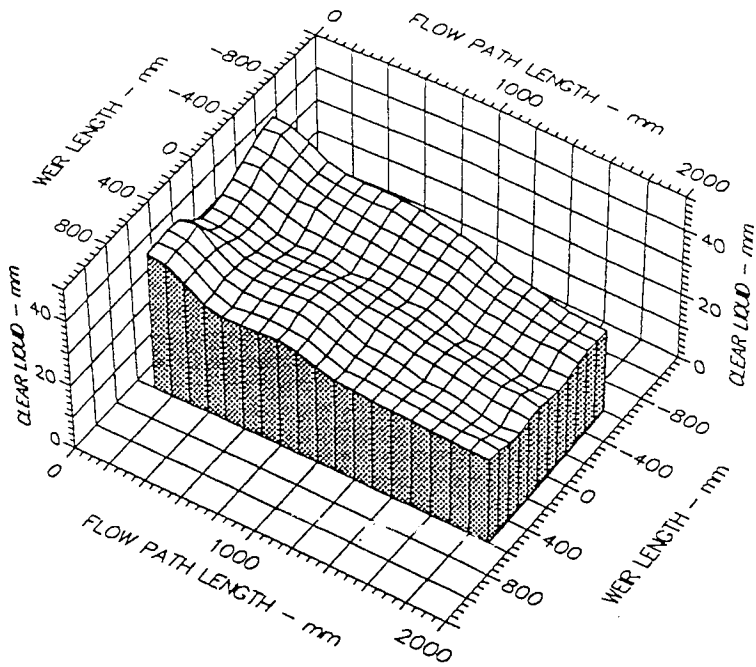
Air Velocity
 1.500 m/s
 Water Loading
 250.0 cm³/cm.s
 Inlet Gap
 0.050 m
 Inlet Weir
 0.000 m
 Outlet Weir
 0.050 m
 Hole Diameter
 0.001 m

Fig. 5.8 c Surface of Clear Liquid Hold-Up, No Intermediate Weir
 IG/OW= 50mm, Water Loading = 250 cm³/cm.s



Air Velocity
 2.500 m/s
 Water Loading
 50.0 cm³/cm.s
 Inlet Gap
 0.050 m
 Inlet Weir
 0.000 m
 Outlet Weir
 0.050 m
 Hole Diameter
 0.001 m

Fig. 5.9 a Surface of Clear Liquid Hold-Up, No Intermediate Weir
 IG/OW= 50mm, Water Loading = 50 cm³/cm.s



Air Velocity
2.500 m/s

Water Loading
150.0 cm³/cm.s

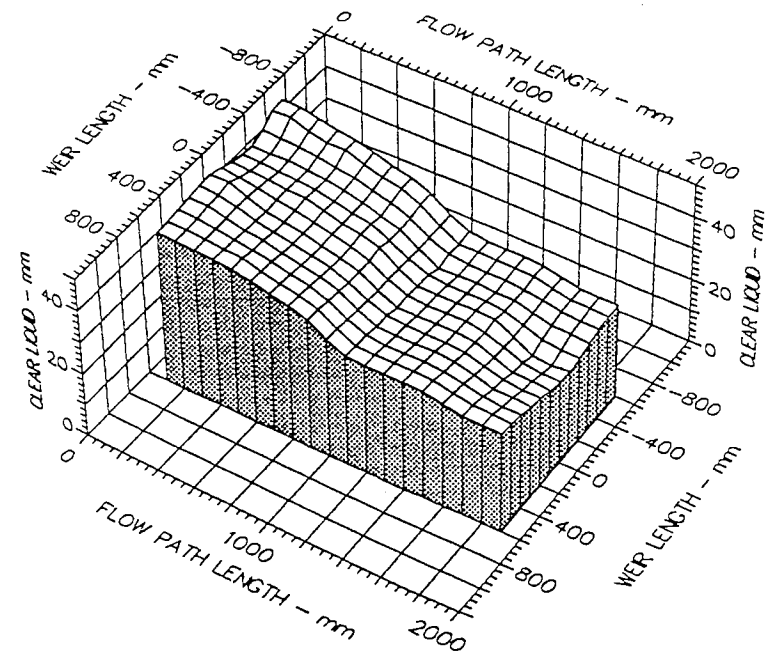
Inlet Gap
0.050 m

Inlet Weir
0.000 m

Outlet Weir
0.050 m

Hole Diameter
0.001 m

Fig. 5.9 b Surface of Clear Liquid Hold-Up, No Intermediate Weir
IG/OW= 50mm, Water Loading = 150 cm³/cm.s



Air Velocity
2.500 m/s

Water Loading
250.0 cm³/cm.s

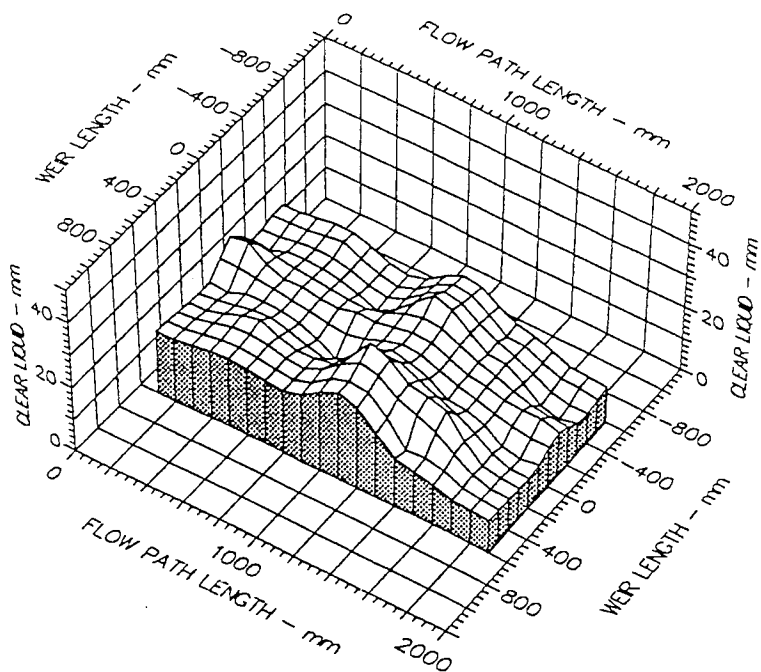
Inlet Gap
0.050 m

Inlet Weir
0.000 m

Outlet Weir
0.050 m

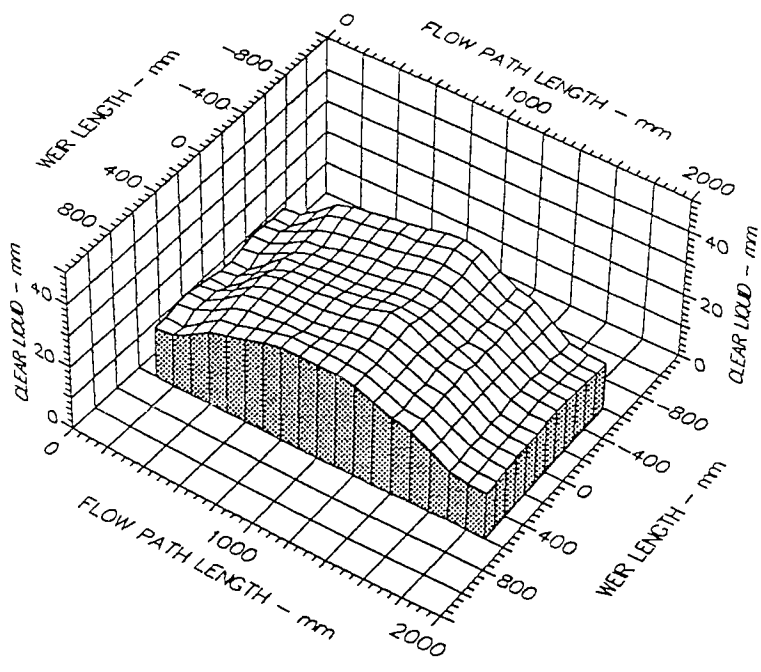
Hole Diameter
0.001 m

Fig. 5.9 c Surface of Clear Liquid Hold-Up, No Intermediate Weir
IG/OW= 50mm, Water Loading = 250 cm³/cm.s



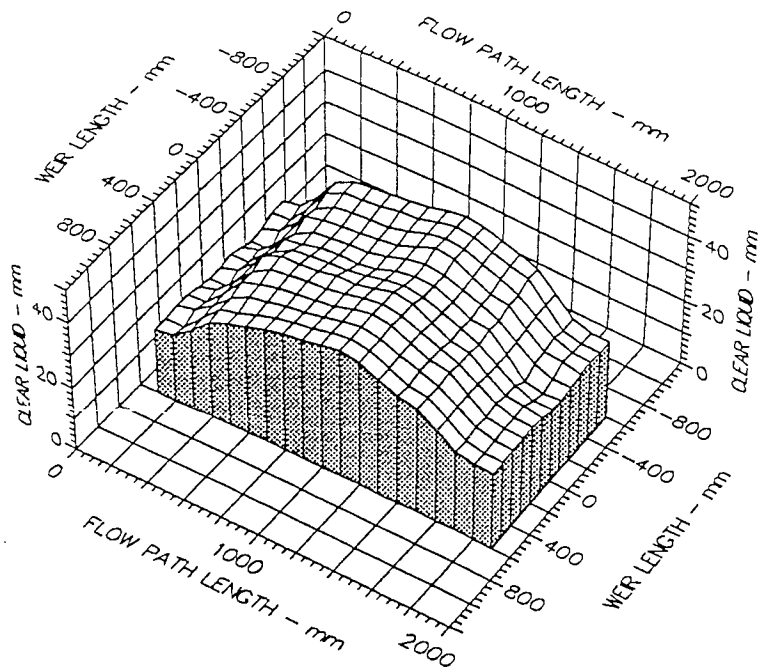
Air Velocity
 1.500 m/s
 Water Loading
 50.0 cm³/cm.s
 Inlet Gap
 0.010 m
 Inlet Weir
 0.000 m
 Outlet Weir
 0.010 m
 Hole Diameter
 0.001 m

Fig. 5.10 a Surface of Clear Liquid Hold-Up, 10mm Intermediate Weir
 IG/OW= 10mm, Water Loading = 50 cm³/cm.s



Air Velocity
 1.500 m/s
 Water Loading
 150.0 cm³/cm.s
 Inlet Gap
 0.010 m
 Inlet Weir
 0.000 m
 Outlet Weir
 0.010 m
 Hole Diameter
 0.001 m

Fig. 5.10 b Surface of Clear Liquid Hold-Up, 10mm Intermediate Weir
 IG/OW= 10mm, Water Loading = 150 cm³/cm.s



Air Velocity

1.500 m/s

Water Loading

250.0 cm³/cm.s

Inlet Gap

0.010 m

Inlet Weir

0.000 m

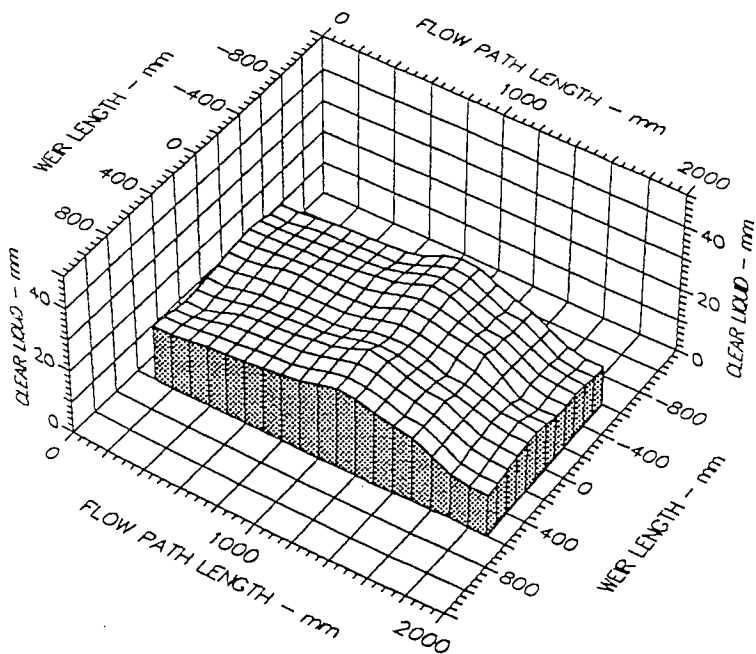
Outlet Weir

0.010 m

Hole Diameter

0.001 m

Fig. 5.10 c Surface of Clear Liquid Hold-Up, 10mm Intermediate Weir
IG/OW= 10mm, Water Loading = 250 cm³/cm.s



Air Velocity

2.500 m/s

Water Loading

50.0 cm³/cm.s

Inlet Gap

0.010 m

Inlet Weir

0.000 m

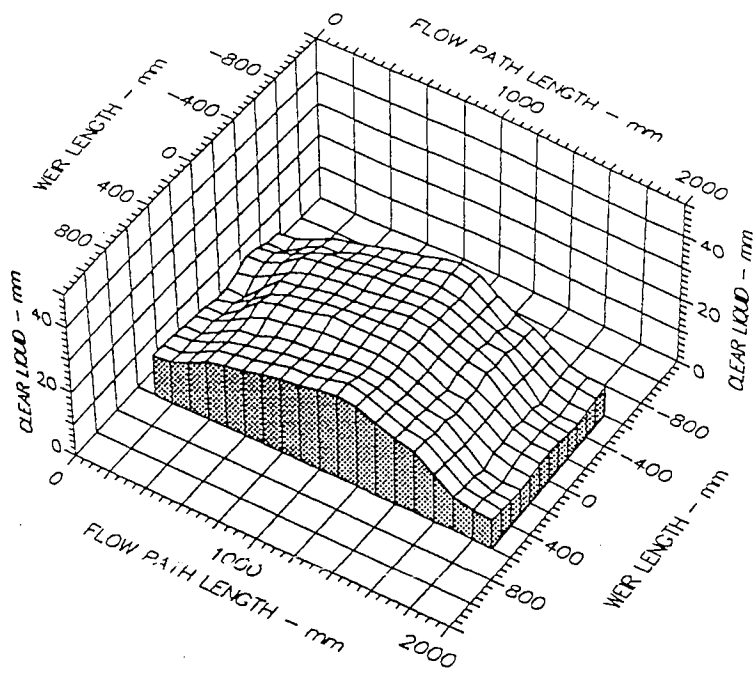
Outlet Weir

0.010 m

Hole Diameter

0.001 m

Fig. 5.11 a Surface of Clear Liquid Hold-Up, 10mm Intermediate Weir
IG/OW= 10mm, Water Loading = 50 cm³/cm.s



Air Velocity
2.500 m/s

Water Loading
150.0 cm³/cm.s

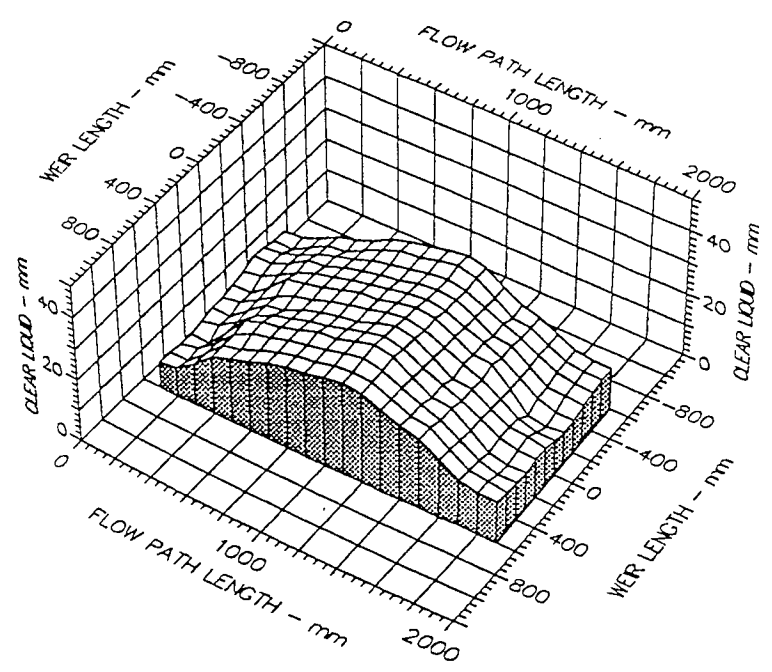
Inlet Gap
0.010 m

Inlet Weir
0.000 m

Outlet Weir
0.010 m

Hole Diameter
0.001 m

Fig. 5.11 b Surface of Clear Liquid Hold-Up, 10mm Intermediate Weir
IG/OW= 10mm, Water Loading = 150 cm³/cm.s



Air Velocity
2.500 m/s

Water Loading
250.0 cm³/cm.s

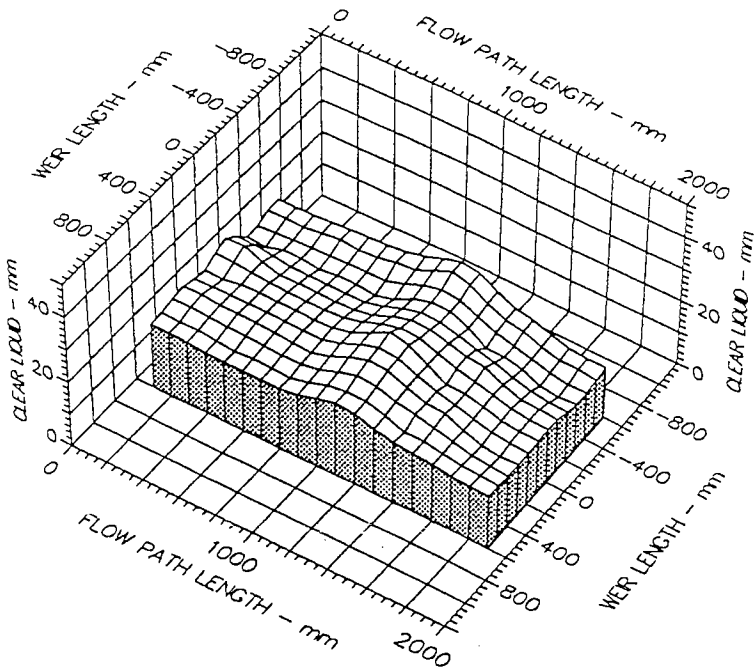
Inlet Gap
0.010 m

Inlet Weir
0.000 m

Outlet Weir
0.010 m

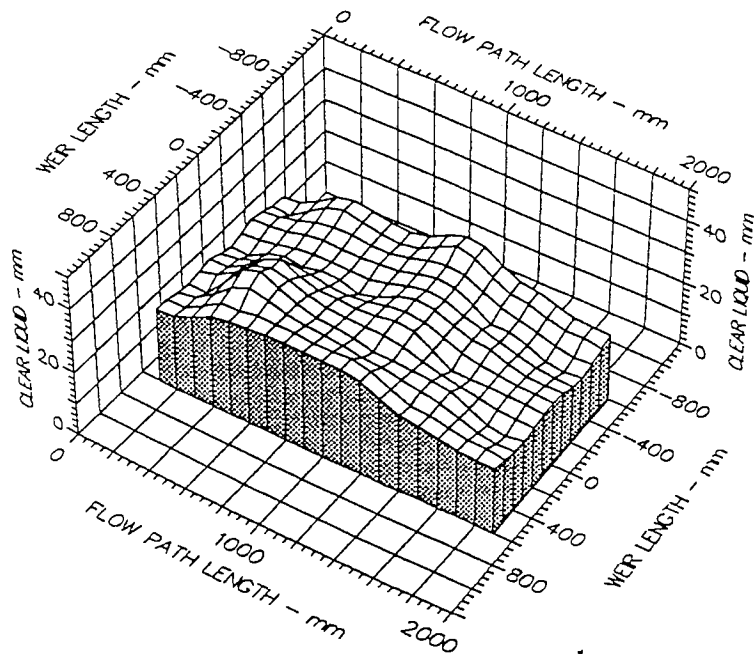
Hole Diameter
0.001 m

Fig. 5.11 c Surface of Clear Liquid Hold-Up, 10mm Intermediate Weir
IG/OW= 10mm, Water Loading = 250 cm³/cm.s



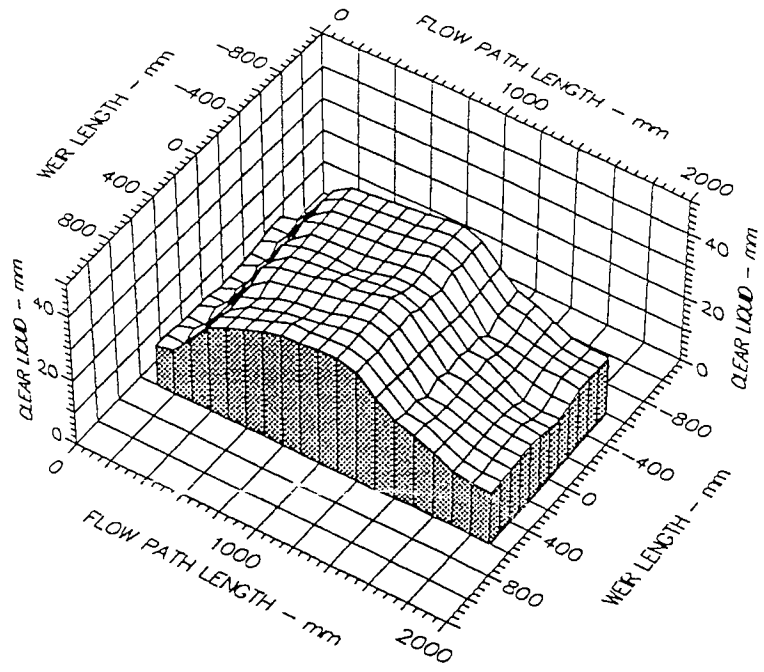
Air Velocity
 1.500 m/s
 Water Loading
 50.0 cm³/cm.s
 Inlet Gap
 0.020 m
 Inlet Weir
 0.000 m
 Outlet Weir
 0.020 m
 Hole Diameter
 0.001 m

Fig. 5.12 a Surface of Clear Liquid Hold-Up, 10mm Intermediate Weir
 IG/OW= 20mm, Water Loading = 50 cm³/cm.s



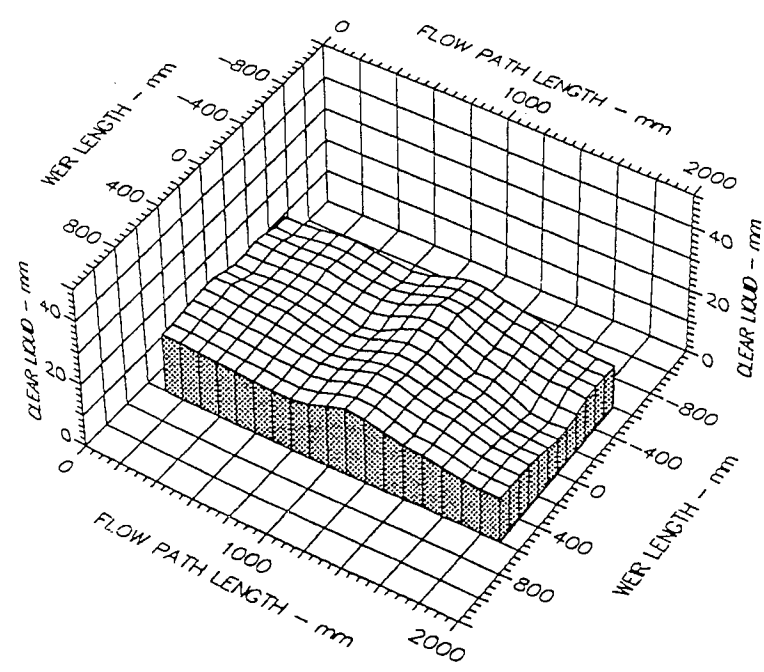
Air Velocity
 1.500 m/s
 Water Loading
 150.0 cm³/cm.s
 Inlet Gap
 0.020 m
 Inlet Weir
 0.000 m
 Outlet Weir
 0.020 m
 Hole Diameter
 0.001 m

Fig. 5.12 b Surface of Clear Liquid Hold-Up, 10mm Intermediate Weir
 IG/OW= 20mm, Water Loading = 150 cm³/cm.s



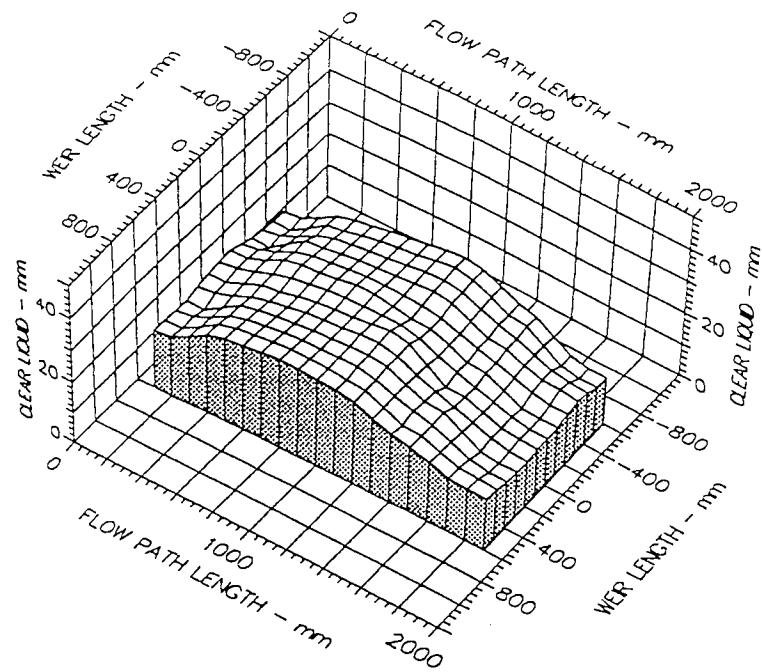
Air Velocity
 1.500 m/s
 Water Loading
 250.0 cm³/cm.s
 Inlet Gap
 0.020 m
 Inlet Weir
 0.000 m
 Outlet Weir
 0.020 m
 Hole Diameter
 0.001 m

Fig. 5.12 c Surface of Clear Liquid Hold-Up, 10mm Intermediate Weir
 IG/OW= 20mm, Water Loading = 250 cm³/cm.s



Air Velocity
 2.500 m/s
 Water Loading
 50.0 cm³/cm.s
 Inlet Gap
 0.020 m
 Inlet Weir
 0.000 m
 Outlet Weir
 0.020 m
 Hole Diameter
 0.001 m

Fig. 5.13 a Surface of Clear Liquid Hold-Up, 10mm Intermediate Weir
 IG/OW= 20mm, Water Loading = 50 cm³/cm.s



Air Velocity
2.500 m/s

Water Loading
150.0 cm³/cm.s

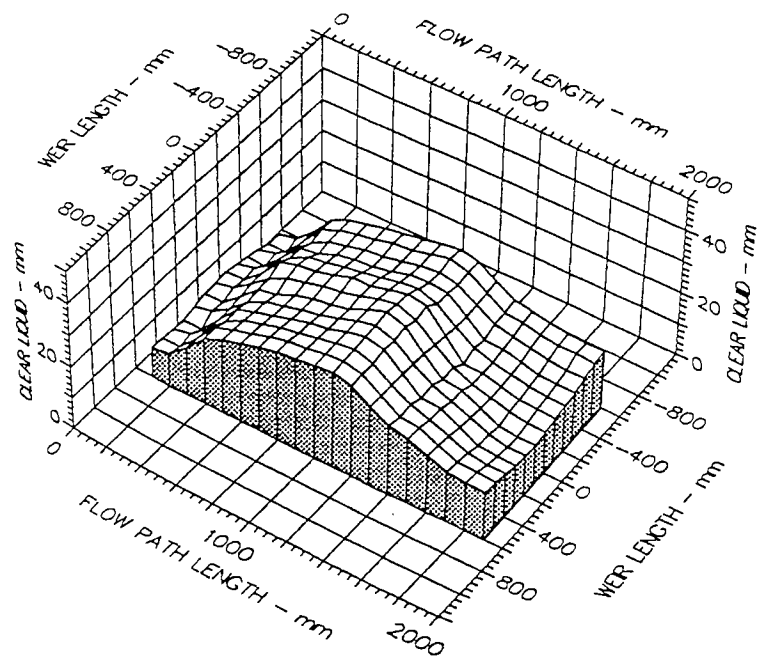
Inlet Gap
0.020 m

Inlet Weir
0.000 m

Outlet Weir
0.020 m

Hole Diameter
0.001 m

Fig. 5.13 b Surface of Clear Liquid Hold-Up, 10mm Intermediate Weir
IG/OW= 20mm, Water Loading = 150 cm³/cm.s



Air Velocity
2.500 m/s

Water Loading
250.0 cm³/cm.s

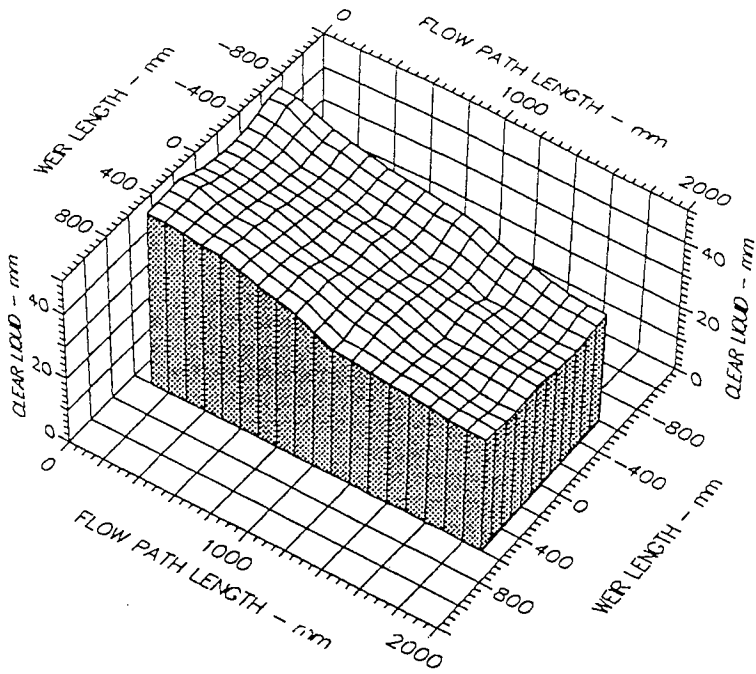
Inlet Gap
0.020 m

Inlet Weir
0.000 m

Outlet Weir
0.020 m

Hole Diameter
0.001 m

Fig. 5.13 c Surface of Clear Liquid Hold-Up, 10mm Intermediate Weir
IG/OW= 20mm, Water Loading = 250 cm³/cm.s



Air Velocity

1.500 m/s

Water Loading

250.0 cm³/cm.s

Inlet Gap

0.050 m

Inlet Weir

0.000 m

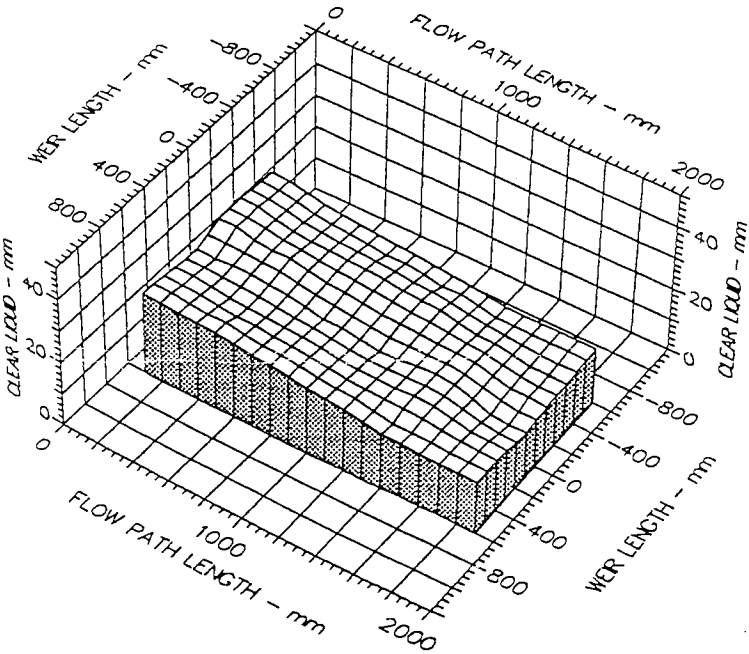
Outlet Weir

0.050 m

Hole Diameter

0.001 m

Fig. 5.14 c Surface of Clear Liquid Hold-Up, 10mm Intermediate Weir
IG/OW= 50mm, Water Loading = 250 cm³/cm.s



Air Velocity

2.500 m/s

Water Loading

50.0 cm³/cm.s

Inlet Gap

0.050 m

Inlet Weir

0.000 m

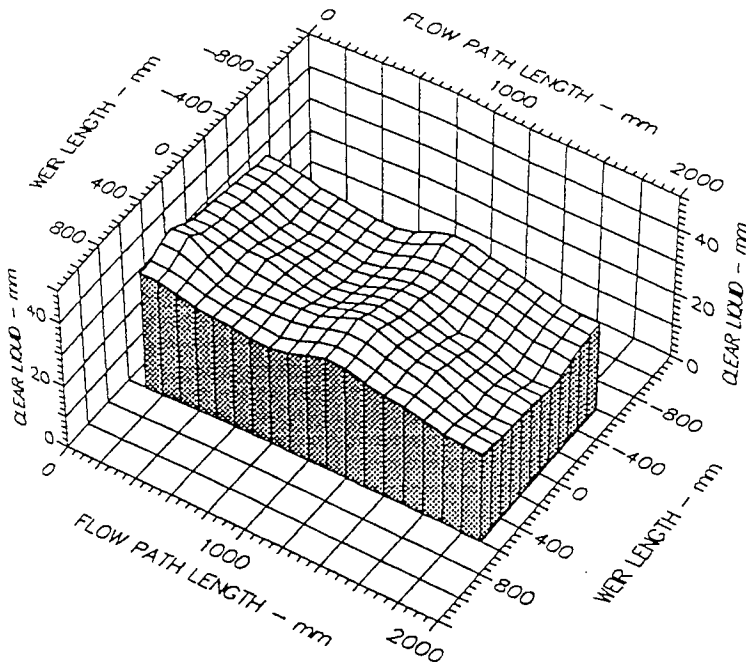
Outlet Weir

0.050 m

Hole Diameter

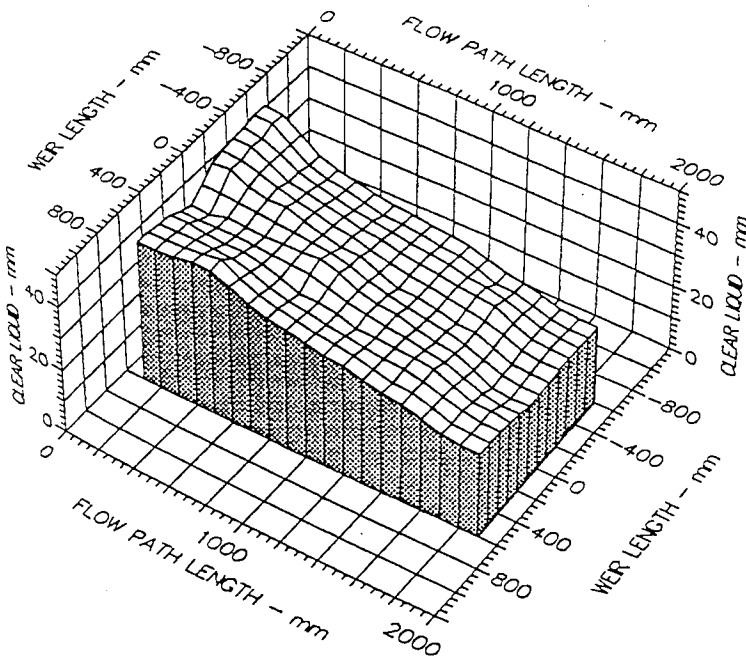
0.001 m

Fig. 5.15 a Surface of Clear Liquid Hold-Up, 10mm Intermediate Weir
IG/OW= 50mm, Water Loading = 50 cm³/cm.s



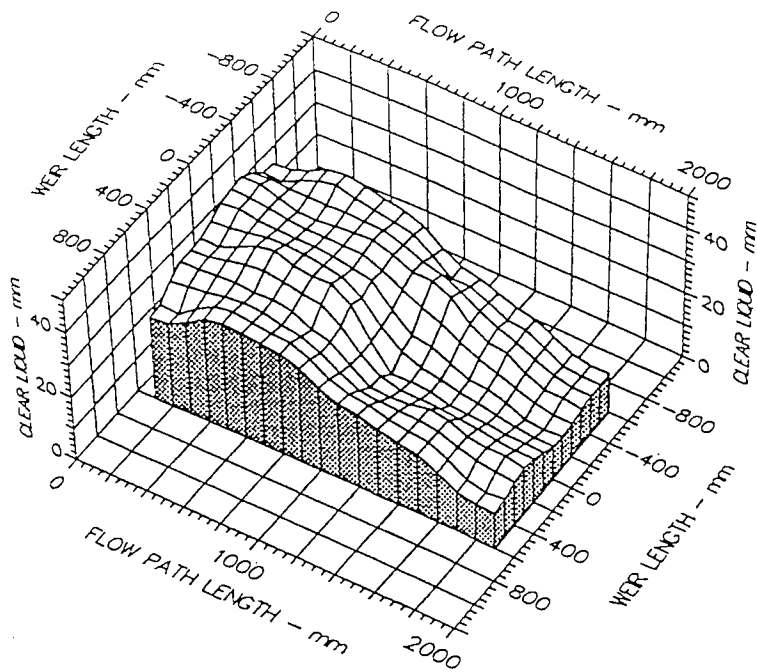
Air Velocity
 2.500 m/s
 Water Loading
 150.0 cm³/cm.s
 Inlet Gap
 0.050 m
 Inlet Weir
 0.000 m
 Outlet Weir
 0.050 m
 Hole Diameter
 0.001 m

Fig. 5.15 b Surface of Clear Liquid Hold-Up, 10mm Intermediate Weir
 IG/OW= 50mm, Water Loading = 150 cm³/cm.s



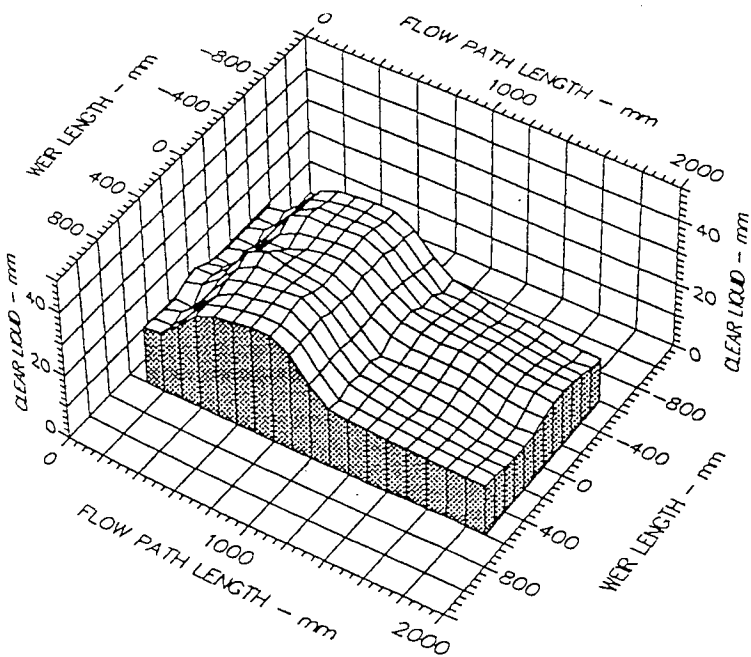
Air Velocity
 2.500 m/s
 Water Loading
 250.0 cm³/cm.s
 Inlet Gap
 0.050 m
 Inlet Weir
 0.000 m
 Outlet Weir
 0.050 m
 Hole Diameter
 0.001 m

Fig. 5.15 c Surface of Clear Liquid Hold-Up, 10mm Intermediate Weir
 IG/OW= 50mm, Water Loading = 250 cm³/cm.s



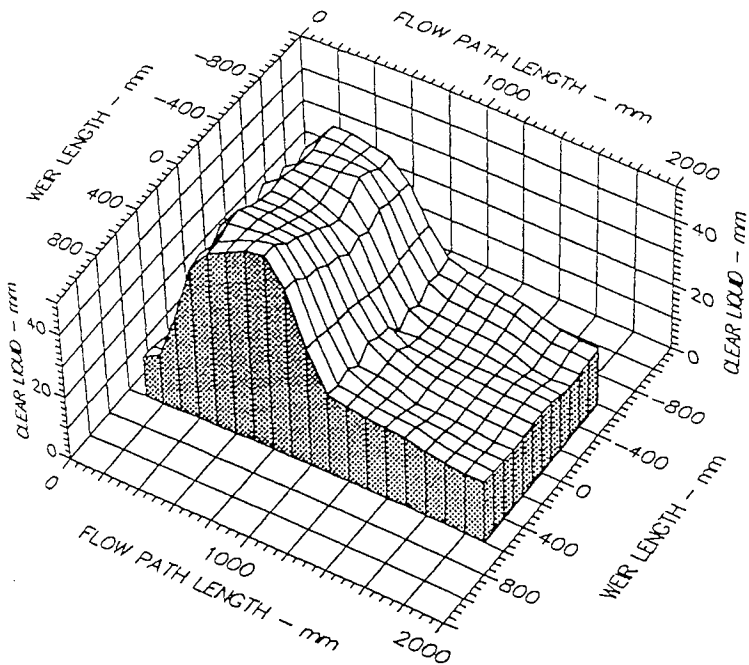
Air Velocity
 1.500 m/s
 Water Loading
 50.0 cm³/cm.s
 Inlet Gap
 0.010 m
 Inlet Weir
 0.000 m
 Outlet Weir
 0.010 m
 Hole Diameter
 0.001 m

Fig. 5.16 a Surface of Clear Liquid Hold-Up, 50mm Intermediate Weir
 IG/OW= 10mm, Water Loading = 50 cm³/cm.s



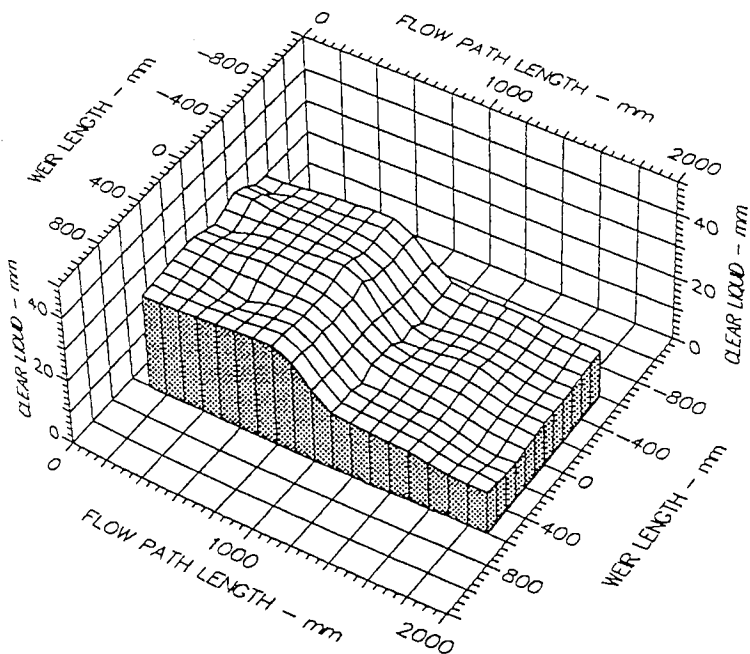
Air Velocity
 1.500 m/s
 Water Loading
 150.0 cm³/cm.s
 Inlet Gap
 0.010 m
 Inlet Weir
 0.000 m
 Outlet Weir
 0.010 m
 Hole Diameter
 0.001 m

Fig. 5.16 b Surface of Clear Liquid Hold-Up, 50mm Intermediate Weir
 IG/OW= 10mm, Water Loading = 150 cm³/cm.s



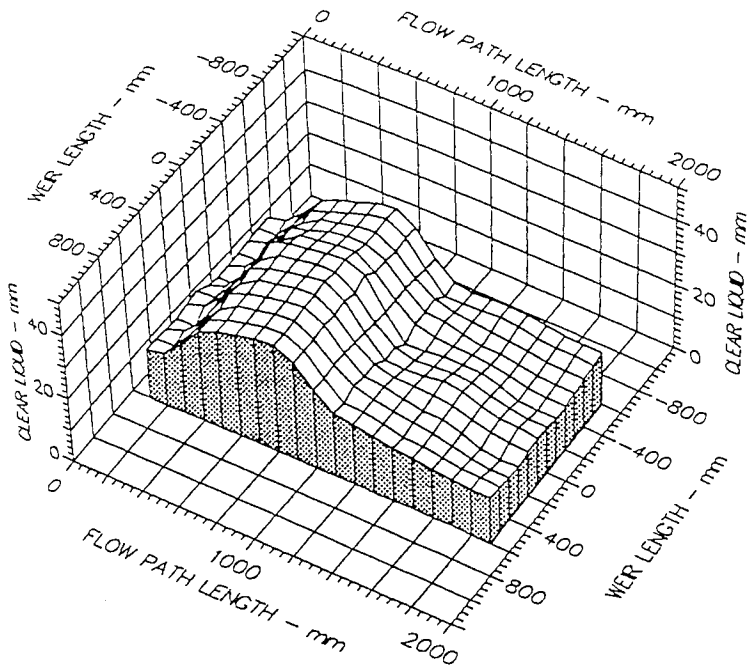
Air Velocity
 1.500 m/s
 Water Loading
 250.0 cm³/cm.s
 Inlet Gap
 0.010 m
 Inlet Weir
 0.000 m
 Outlet Weir
 0.010 m
 Hole Diameter
 0.001 m

Fig. 5.16 c Surface of Clear Liquid Hold-Up, 50mm Intermediate Weir
 IG/OW= 10mm, Water Loading = 250 cm³/cm.s



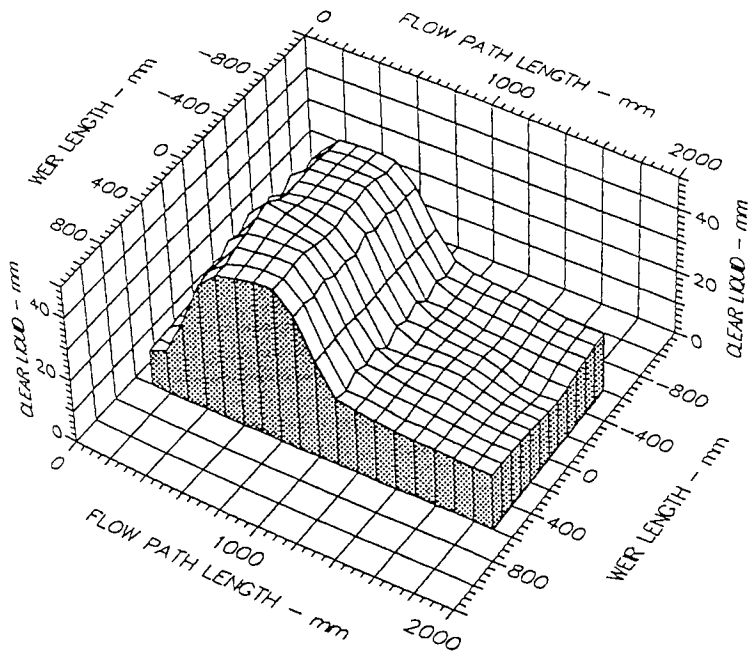
Air Velocity
 2.500 m/s
 Water Loading
 50.0 cm³/cm.s
 Inlet Gap
 0.010 m
 Inlet Weir
 0.000 m
 Outlet Weir
 0.010 m
 Hole Diameter
 0.001 m

Fig. 5.17 a Surface of Clear Liquid Hold-Up, 50mm Intermediate Weir
 IG/OW= 10mm, Water Loading = 50 cm³/cm.s



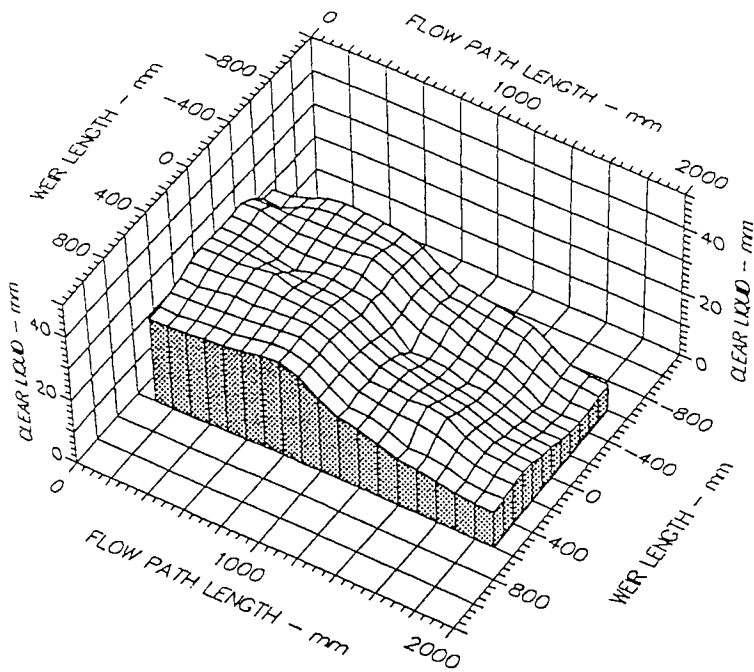
Air Velocity
 2.500 m/s
 Water Loading
 150.0 cm³/cm.s
 Inlet Gap
 0.010 m
 Inlet Weir
 0.000 m
 Outlet Weir
 0.010 m
 Hole Diameter
 0.001 m

Fig. 5.17 b Surface of Clear Liquid Hold-Up, 50mm Intermediate Weir
 IG/OW= 10mm, Water Loading = 150 cm³/cm.s



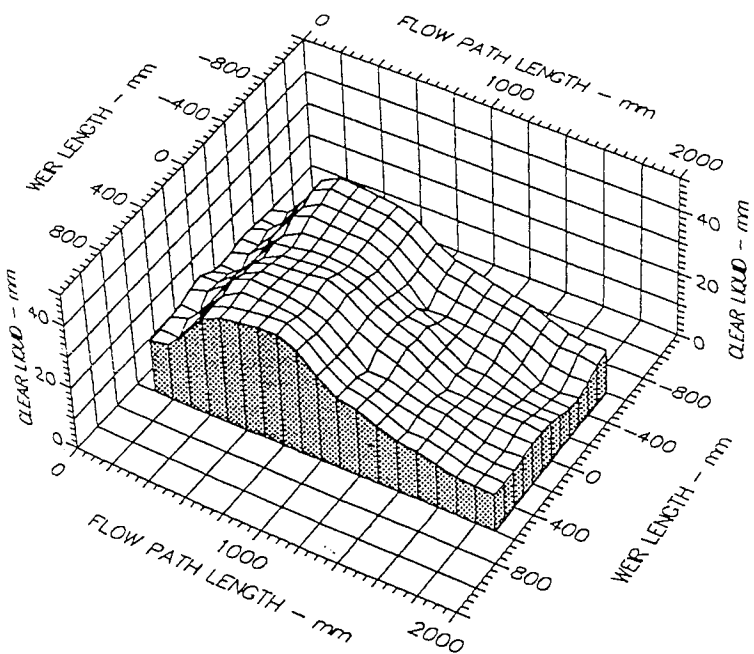
Air Velocity
 2.500 m/s
 Water Loading
 250.0 cm³/cm.s
 Inlet Gap
 0.010 m
 Inlet Weir
 0.000 m
 Outlet Weir
 0.010 m
 Hole Diameter
 0.001 m

Fig. 5.17 c Surface of Clear Liquid Hold-Up, 50mm Intermediate Weir
 IG/OW= 10mm, Water Loading = 250 cm³/cm.s



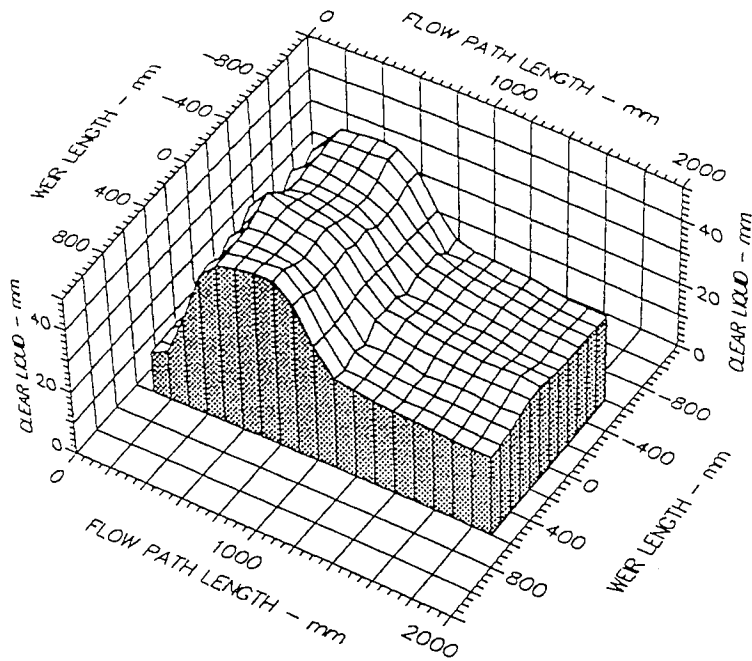
Air Velocity
 1.500 m/s
 Water Loading
 50.0 cm³/cm.s
 Inlet Gap
 0.020 m
 Inlet Weir
 0.000 m
 Outlet Weir
 0.020 m
 Hole Diameter
 0.001 m

Fig. 5.18 a Surface of Clear Liquid Hold-Up, 50mm Intermediate Weir
 IG/OW= 20mm, Water Loading = 50 cm³/cm.s



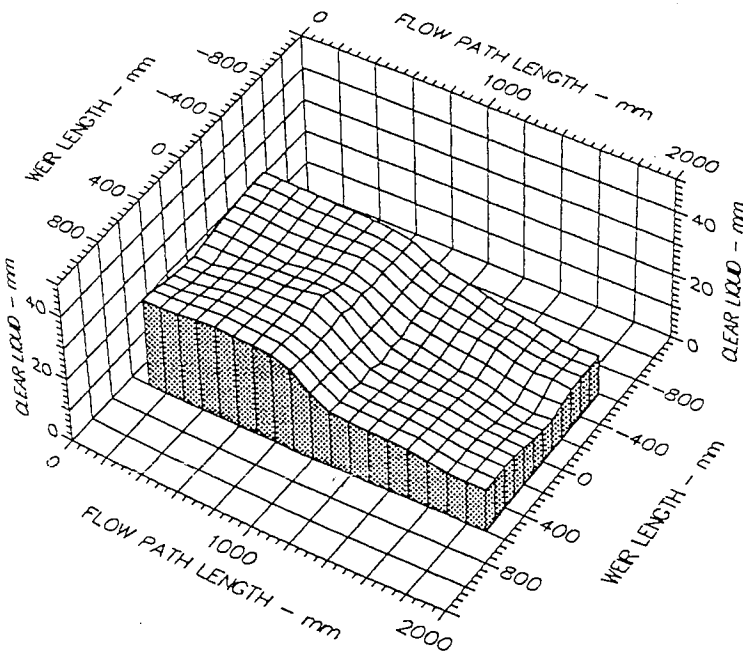
Air Velocity
 1.500 m/s
 Water Loading
 150.0 cm³/cm.s
 Inlet Gap
 0.020 m
 Inlet Weir
 0.000 m
 Outlet Weir
 0.020 m
 Hole Diameter
 0.001 m

Fig. 5.18 b Surface of Clear Liquid Hold-Up, 50mm Intermediate Weir
 IG/OW= 20mm, Water Loading = 150 cm³/cm.s



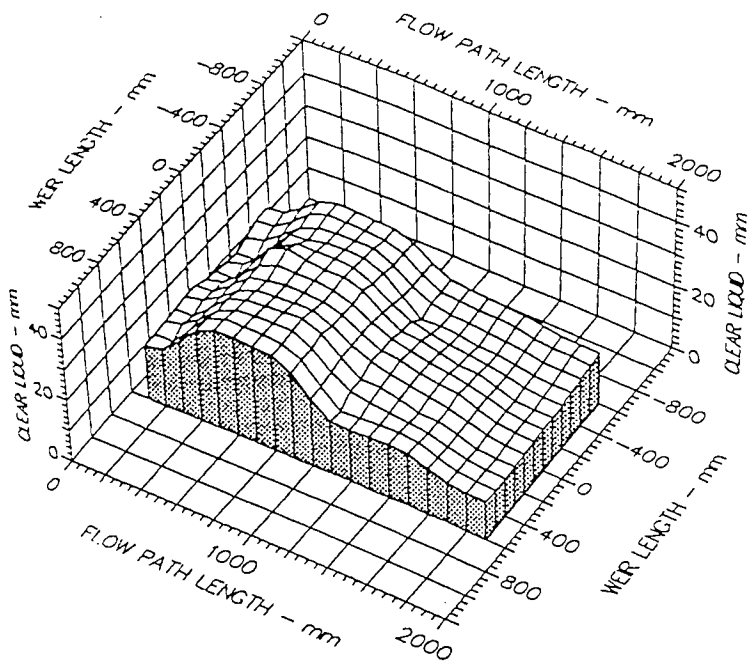
Air Velocity
 1.500 m/s
 Water Loading
 250.0 cm³/cm.s
 Inlet Gap
 0.020 m
 Inlet Weir
 0.000 m
 Outlet Weir
 0.020 m
 Hole Diameter
 0.001 m

Fig. 5.18 c Surface of Clear Liquid Hold-Up, 50mm Intermediate Weir
 IG/OW= 20mm, Water Loading = 250 cm³/cm.s



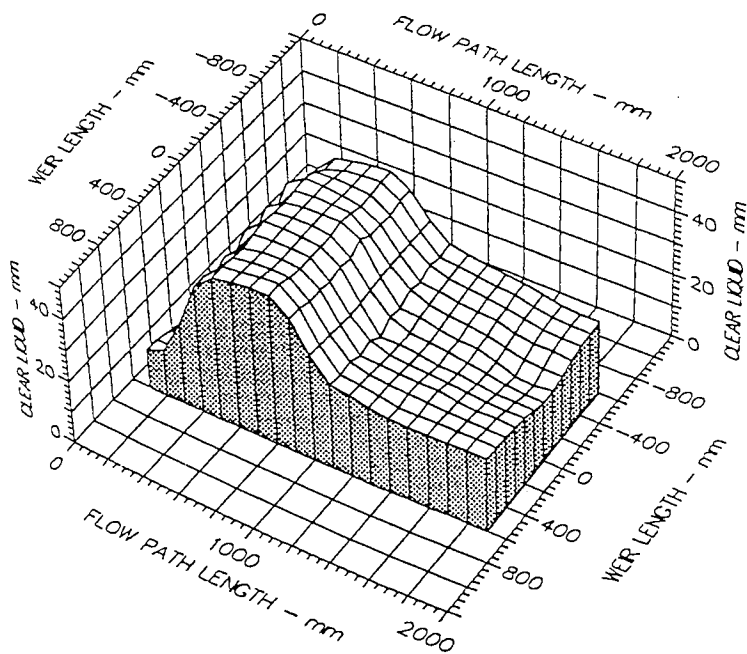
Air Velocity
 2.500 m/s
 Water Loading
 50.0 cm³/cm.s
 Inlet Gap
 0.020 m
 Inlet Weir
 0.000 m
 Outlet Weir
 0.020 m
 Hole Diameter
 0.001 m

Fig. 5.19 a Surface of Clear Liquid Hold-Up, 50mm Intermediate Weir
 IG/OW= 20mm, Water Loading = 50 cm³/cm.s



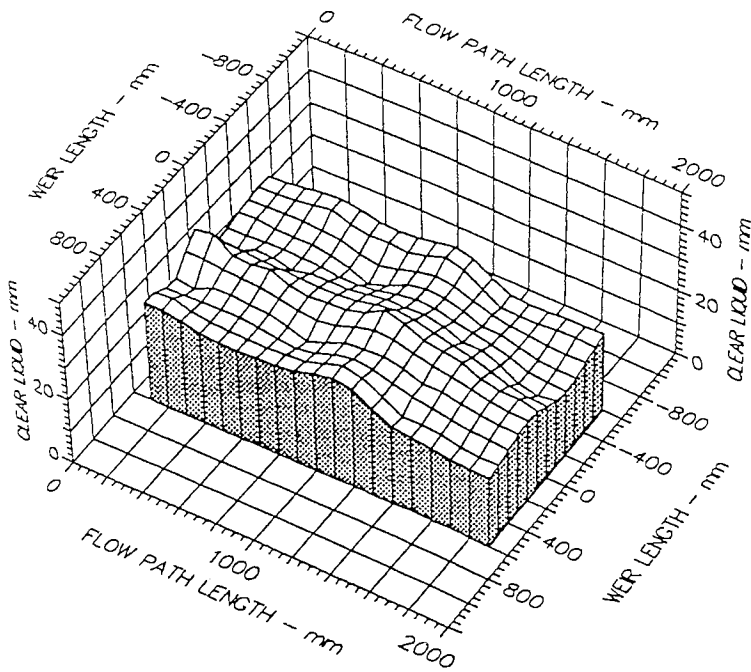
Air Velocity
 2.500 m/s
 Water Loading
 150.0 cm³/cm.s
 Inlet Gap
 0.020 m
 Inlet Weir
 0.000 m
 Outlet Weir
 0.020 m
 Hole Diameter
 0.001 m

Fig. 5.19 b Surface of Clear Liquid Hold-Up, 50mm Intermediate Weir
 IG/OW= 20mm, Water Loading = 150 cm³/cm.s



Air Velocity
 2.500 m/s
 Water Loading
 250.0 cm³/cm.s
 Inlet Gap
 0.020 m
 Inlet Weir
 0.000 m
 Outlet Weir
 0.020 m
 Hole Diameter
 0.001 m

Fig. 5.19 c Surface of Clear Liquid Hold-Up, 50mm Intermediate Weir
 IG/OW= 20mm, Water Loading = 250 cm³/cm.s



Air Velocity
1.500 m/s

Water Loading
50.0 cm³/cm.s

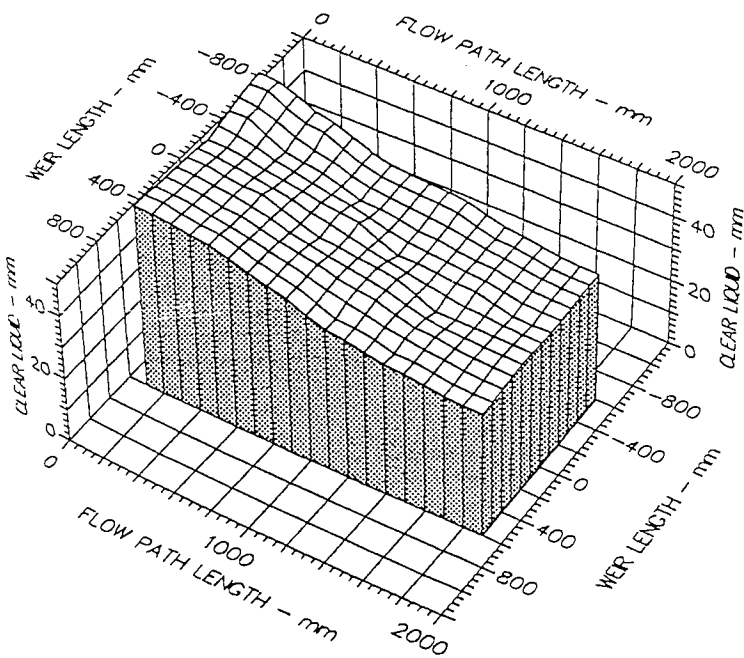
Inlet Gap
0.050 m

Inlet Weir
0.000 m

Outlet Weir
0.050 m

Hole Diameter
0.001 m

Fig. 5.20 a Surface of Clear Liquid Hold-Up, 50mm Intermediate Weir
IG/OW= 50mm, Water Loading = 50 cm³/cm.s



Air Velocity
1.500 m/s

Water Loading
150.0 cm³/cm.s

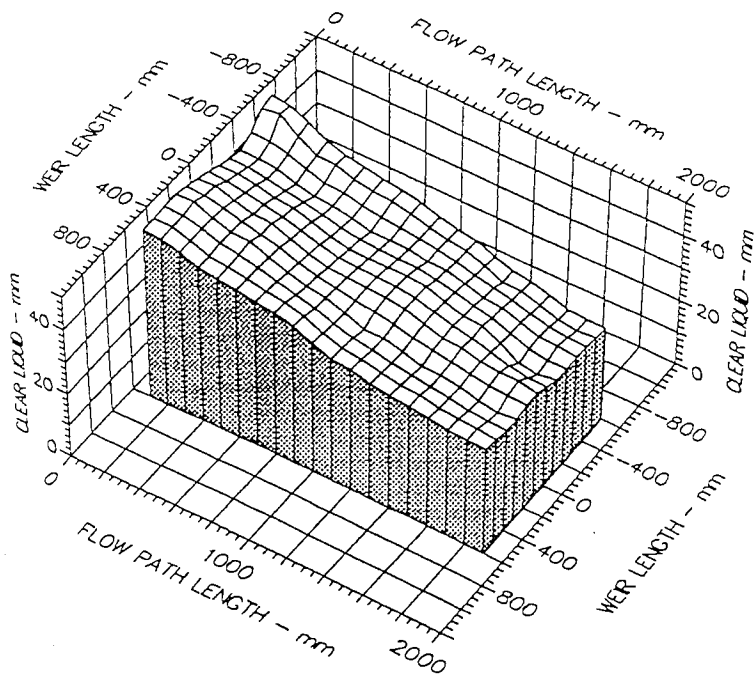
Inlet Gap
0.050 m

Inlet Weir
0.000 m

Outlet Weir
0.050 m

Hole Diameter
0.001 m

Fig. 5.20 b Surface of Clear Liquid Hold-Up, 50mm Intermediate Weir
IG/OW= 50mm, Water Loading = 150 cm³/cm.s



Air Velocity
1.500 m/s

Water Loading
250.0 cm³/cm.s

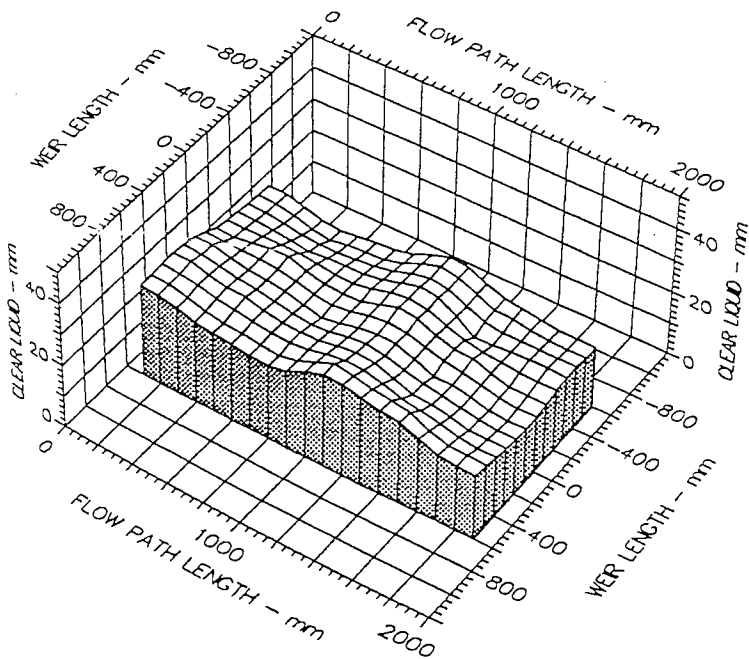
Inlet Gap
0.050 m

Inlet Weir
0.000 m

Outlet Weir
0.050 m

Hole Diameter
0.001 m

Fig. 5.20 c Surface of Clear Liquid Hold-Up, 50mm Intermediate Weir
IG/OW= 50mm, Water Loading = 250 cm³/cm.s



Air Velocity
2.500 m/s

Water Loading
50.0 cm³/cm.s

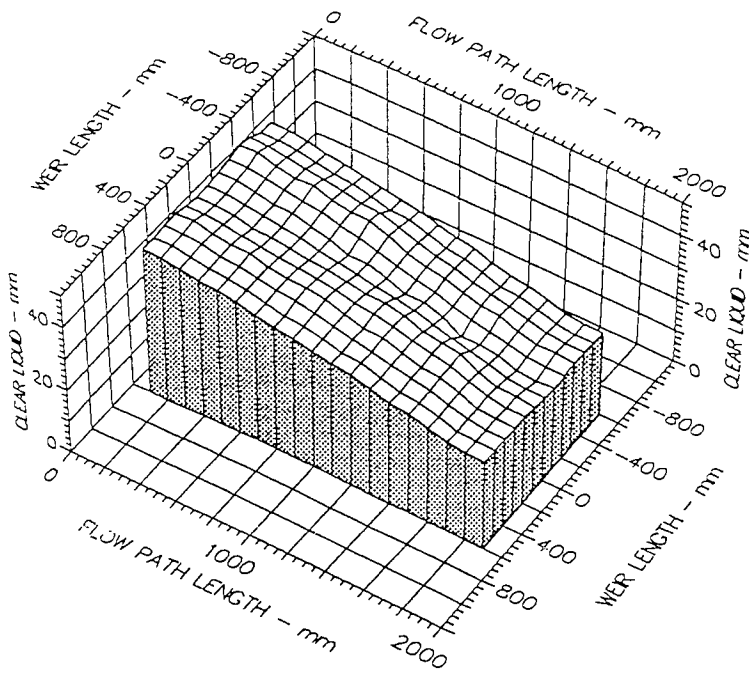
Inlet Gap
0.050 m

Inlet Weir
0.000 m

Outlet Weir
0.050 m

Hole Diameter
0.001 m

Fig. 5.21 a Surface of Clear Liquid Hold-Up, 50mm Intermediate Weir
IG/OW= 50mm, Water Loading = 50 cm³/cm.s



Air Velocity
2.500 m/s

Water Loading
150.0 cm³/cm.s

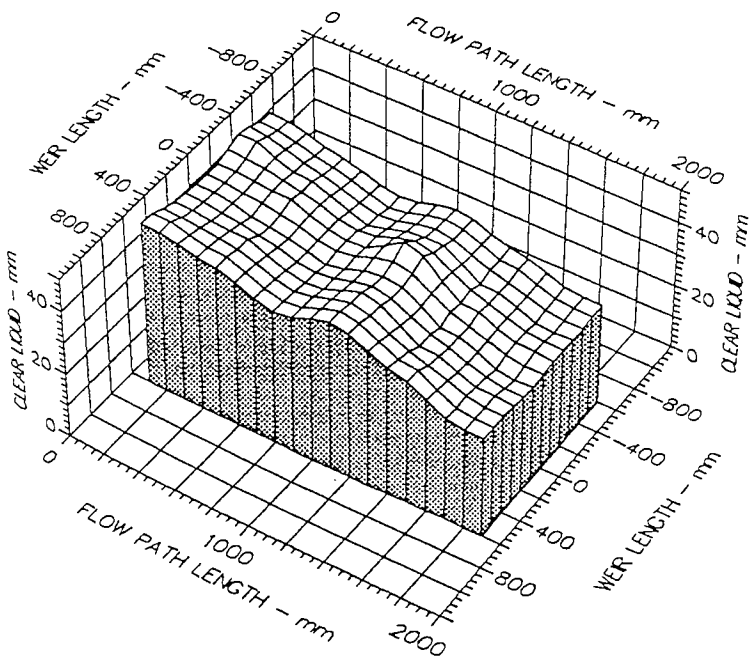
Inlet Gap
0.050 m

Inlet Weir
0.000 m

Outlet Weir
0.050 m

Hole Diameter
0.001 m

Fig. 5.21 b Surface of Clear Liquid Hold-Up, 50mm Intermediate Weir
IG/OW= 50mm, Water Loading = 150 cm³/cm.s



Air Velocity
2.500 m/s

Water Loading
250.0 cm³/cm.s

Inlet Gap
0.050 m

Inlet Weir
0.000 m

Outlet Weir
0.050 m

Hole Diameter
0.001 m

Fig. 5.21 c Surface of Clear Liquid Hold-Up, 50mm Intermediate Weir
IG/OW= 50mm, Water Loading = 250 cm³/cm.s

5.6 CONCLUSIONS

This work has been concerned with developing modifications to sieve trays in order to change the flow pattern and improve their performance. Work has demonstrated that :

- (1) The effect of the intermediate weir on the liquid hold-up depends on the inlet gap and the outlet weir height.
- (2) At high liquid rates hydraulic jumps occur on the tray which interacts with the intermediate weir in an unpredictable way.
- (3) There are some combinations of the inlet gap /outlet weir height where the use of an intermediate weir causes an increase in the liquid hold-up.
- (4) In general the effect of an intermediate weir depends on the depth of liquid/ froth downstream of the weir. If the weir is deeper than the downstream depth it will cause the upstream liquid to be deeper than the downstream liquid. If the weir is not as deep as the downstream depth it may have little or no effect on the upstream depth.
- (5) It should be noted that in some cases the height of clear liquid appears to be less than the outlet weir, see figures 5.4 a and 5.6 a. This occurs mainly at low weir loads and high superficial air velocities and produces the existence of an hydraulic gradient. This causes a low hydrostatic head at the outlet weir leading to vapour to preferentially flow where the hydrostatic head is low which in turn causes an increase in dry tray pressure drop and the entrainment of liquid. This condition needs to be avoided as it leads to a loss in throughput and efficiency.

It may seem likely that, if such a small intermediate weir were placed at an angle to the direction of flow, some redirection of the liquid towards the sides of the tray would occur, but without increasing the froth height and thereby reducing the throughput of the tray. This is the subject of the next Chapter.

CHAPTER 6

FLOW DIRECTING WEIR PLACED AT AN ANGLE TO THE DIRECTION OF FLOW FOR A RECTANGULAR TRAY

6.1 Introduction

As stated in Chapter 1 the aim of this research is to test flow control devices on a full circular tray so that we are able to replenish the slow moving / stagnant liquid areas and hence provide a more uniform flow pattern across the whole of the tray.

This investigation is concerned with the effect on the flow pattern when an intermediate weir is placed at an angle to the direction of flow. The aim is to investigate whether liquid would be able to firstly flow over the intermediate weir but also be deflected to the required area. Any deflection or redistribution of liquid was detected by the use of a liquid collection box placed in the outlet downcomer ie. To detect an increase in liquid head. The questions that needed to be answered were ‘ What is the percent flood liquid which is displaced sideways and is this sufficient displacement to obtain an ideal flow pattern ?’

6.2 MEASUREMENT TECHNIQUE

A liquid collection box was designed and fitted into the outlet downcomer, such that the liquid leaving the tray entered one of six compartments within the collection box. Thus the length of the outlet weir was divided into six equal lengths. Each compartment had an orifice at the base which provided a resistance to the leaving liquid. The result of the resistance to flow was the development of a liquid head within each compartment. At steady state, the head of liquid above the orifice in each compartment was representative of the liquid flow into the compartment. A water manometer connected to the base of the compartment was used to measure the developed head of liquid, from which the compartmental flow was determined using the generated calibration.

6.3 CALIBRATION

The orifice in each compartment was 10 mm in diameter, but as the weir flow measuring device contained varying shapes of collection compartment, due to the column curvature, it was necessary to calibrate each different compartment for the liquid head against flow relationship. Liquid at a known flowrate was passed through each compartment shape using a Rotameter (tube size 65) and the head of liquid in the compartment was recorded. The calibration of liquid flowrate against the recorded height was constructed (\sqrt{H} against weir load) and was then used to determine the actual liquid flowrate in each compartment during the experiment, see Figure 6.1 (Note : the results from the calibration indicated that there was little difference in liquid head in the different compartments, therefore a general calibration curve was used for all compartments).

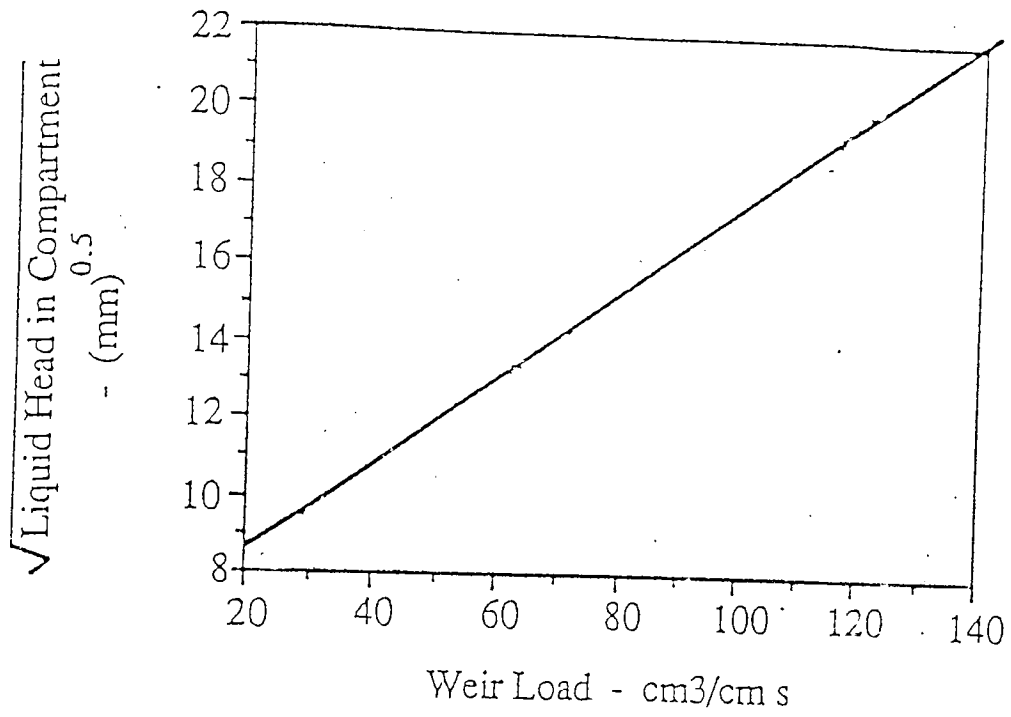


Fig. 6.1 Calibration of liquid flowrate against recorded height

6.4 EXPERIMENTAL PROCEDURE :-

The tray geometry was the same as that used for the previous experiments i.e. 1.9 m by 1.25 m rectangular sieve plate with 1 mm diameter holes. The inlet gap and outlet weir were each set at 10 mm. An intermediate weir of 10 mm was fixed on the centre of the tray at an angle of 30 degrees for each set of experiments, see figure 6.2. Superficial air velocities of 0.7, 0.9, 1.2 and 1.5 m/s, and water flow rates of 25, 35, 55, 75 and 110 cm³/cm s were used in the investigation. It was important to initially test the tray for levelness using an engineering level so that there was no flow distortion due to the tray levelness hence leading to incorrect results. The experiments were repeated with no intermediate weir on the tray.

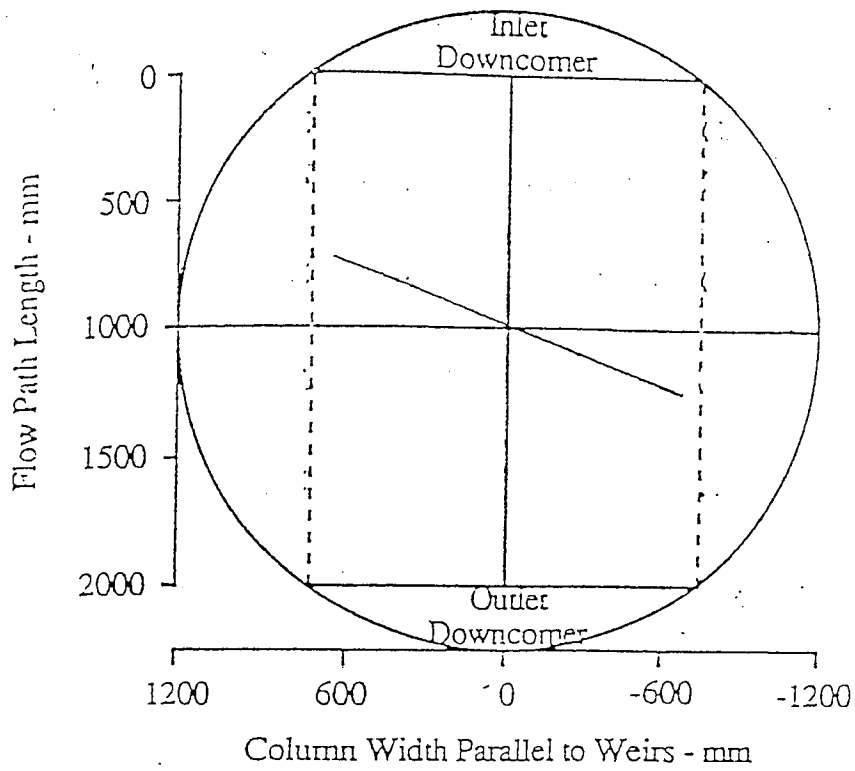


Fig. 6.2 Diagram of angled weir on rectangular sieve tray

6.5 RESULTS AND DISCUSSION:-

The recorded depths of water (cm) in the six compartments for the range of air and water flow rates tested can be seen in Appendix 2. The derived variations in weir loading from the data in Appendix 2 are presented graphically in figures 6.3 to 6.7.

Considering, firstly, the set of experiments in which no intermediate weir was placed on the tray. If we take the low weir load case of $25 \text{ cm}^3/\text{cm s}$ as can be seen from figure 6.3, the flow of liquid over the outlet weir is mainly uniform. At high inlet weir loads the variation of the weir load measured over the outlet weir takes on a different shape and is not as symmetrical as expected. There seemed to be more liquid flowing at the sides of the rectangular tray with a U-shaped profile being formed. From figure 6.4 it can be seen that at a higher weir load the U-shape is more pronounced. A likely cause of unsymmetrical flow over the outlet weir could be due to non-level outlet weir or poor liquid inlet distribution.

By repeating the experiments but with a 10 mm intermediate weir placed at an angle of 30° on the centre of the tray then the shape of the graphs obtained are quite interesting. At low weir load of $25 \text{ cm}^3/\text{cm s}$ the flow of liquid over the outlet weir is similar to that obtained with no intermediate weir i.e. mainly uniform. The positive effect of the intermediate weir can clearly be seen from the results obtained with the higher inlet weir loads of 35, 55.110 $\text{cm}^3/\text{cm s}$. The U-shaped profiles have disappeared and there is more flow of liquid which is weighted rather heavily to the left hand side of the graph (where liquid is being deflected to), this is in contrast to the right hand side of the graph (where liquid is being deflected from) and hence the lower flow of liquid over the outlet weir.

Fig. 6.3

IG/OW = 10 mm, Superficial Air Velocity = 0.7 m/s, Weir Load = 25 cm³/cm s.

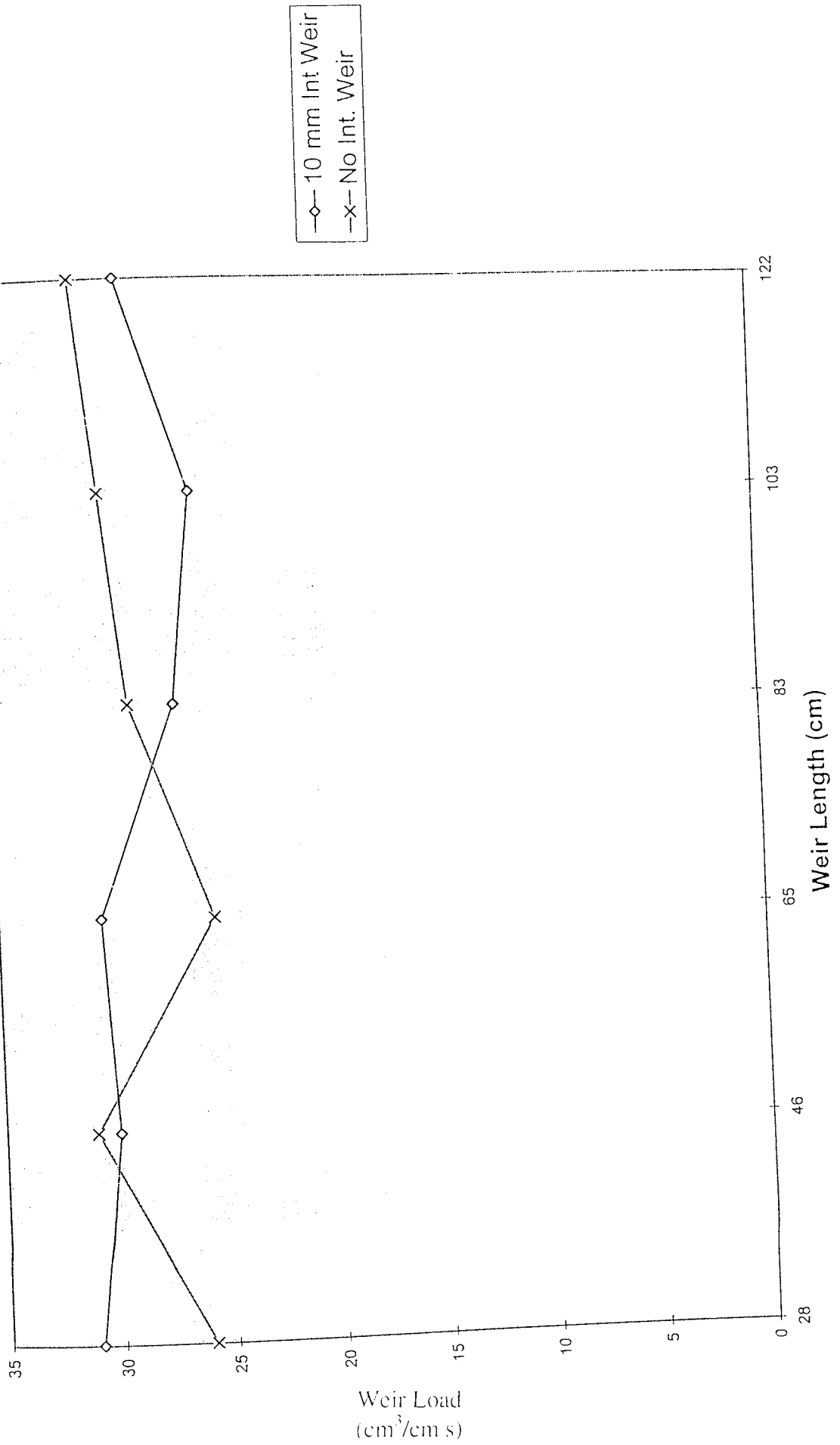


Fig. 6.4

IG/OW = 10 mm, Superficial Air Velocity = 0.7 m/s, Weir Load = 55 cm³/cms

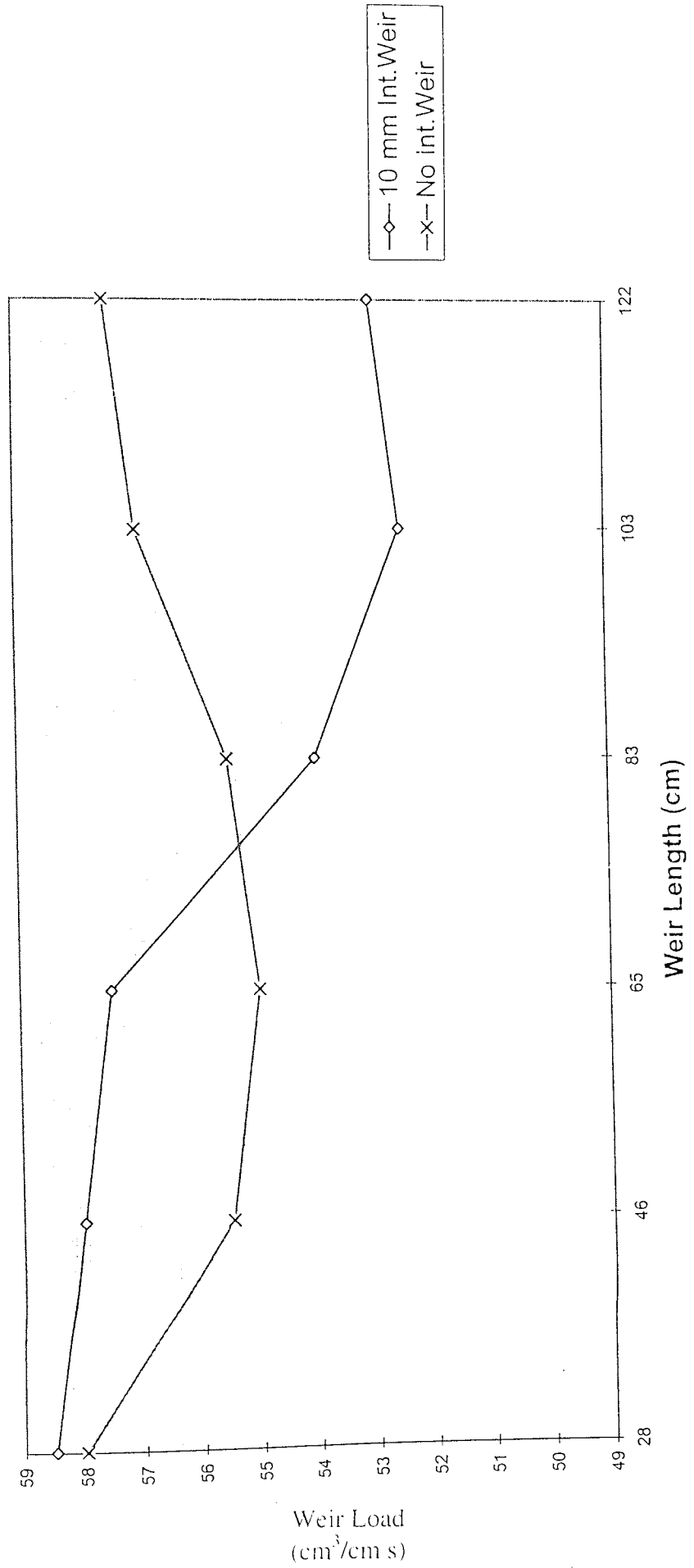


Fig. 6.5

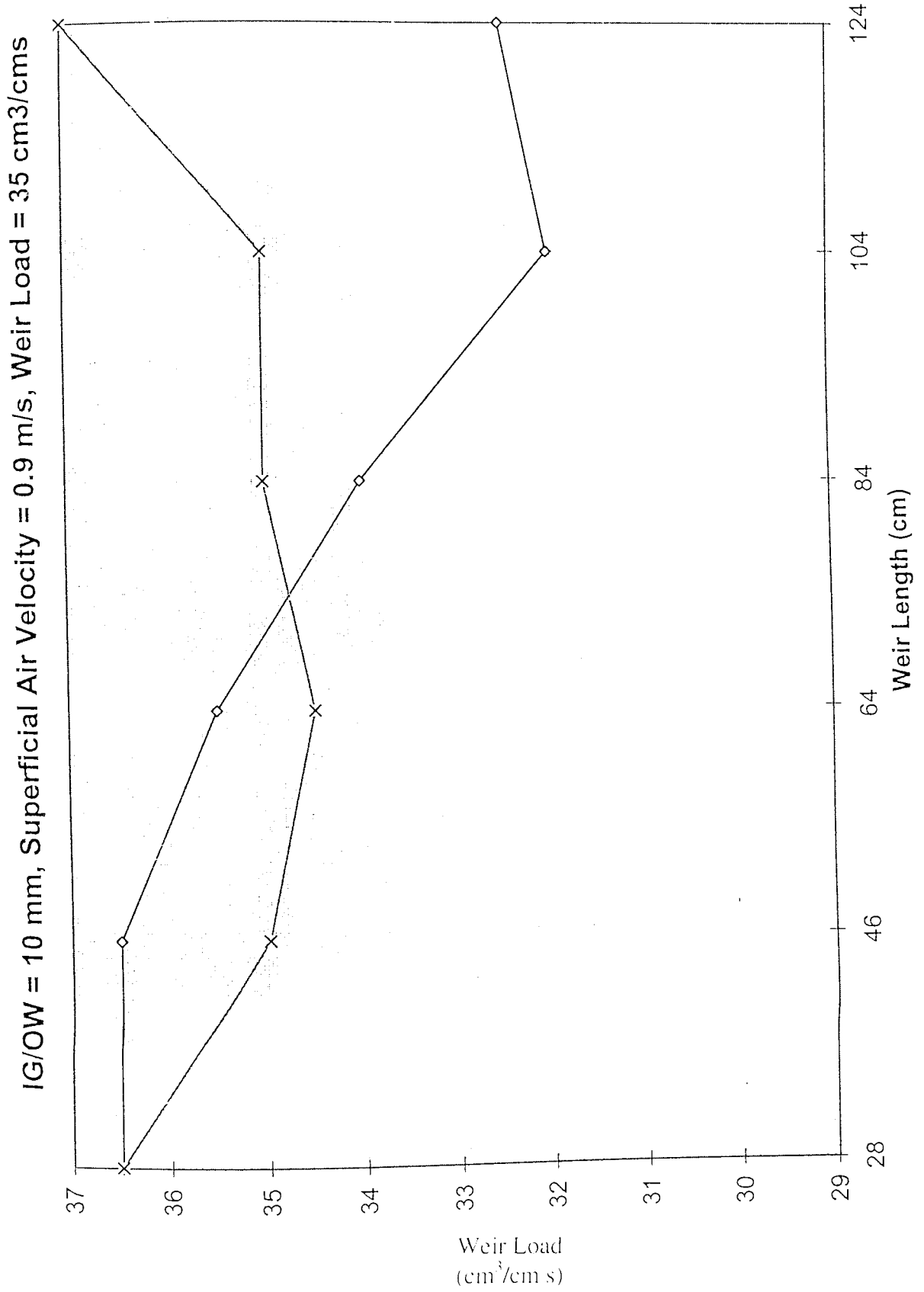


Fig. 6.6

IG/OW = 10 mm, Superficial Air Velocity = 1.2 m/s, Weir Load = 110 cm³/cm s

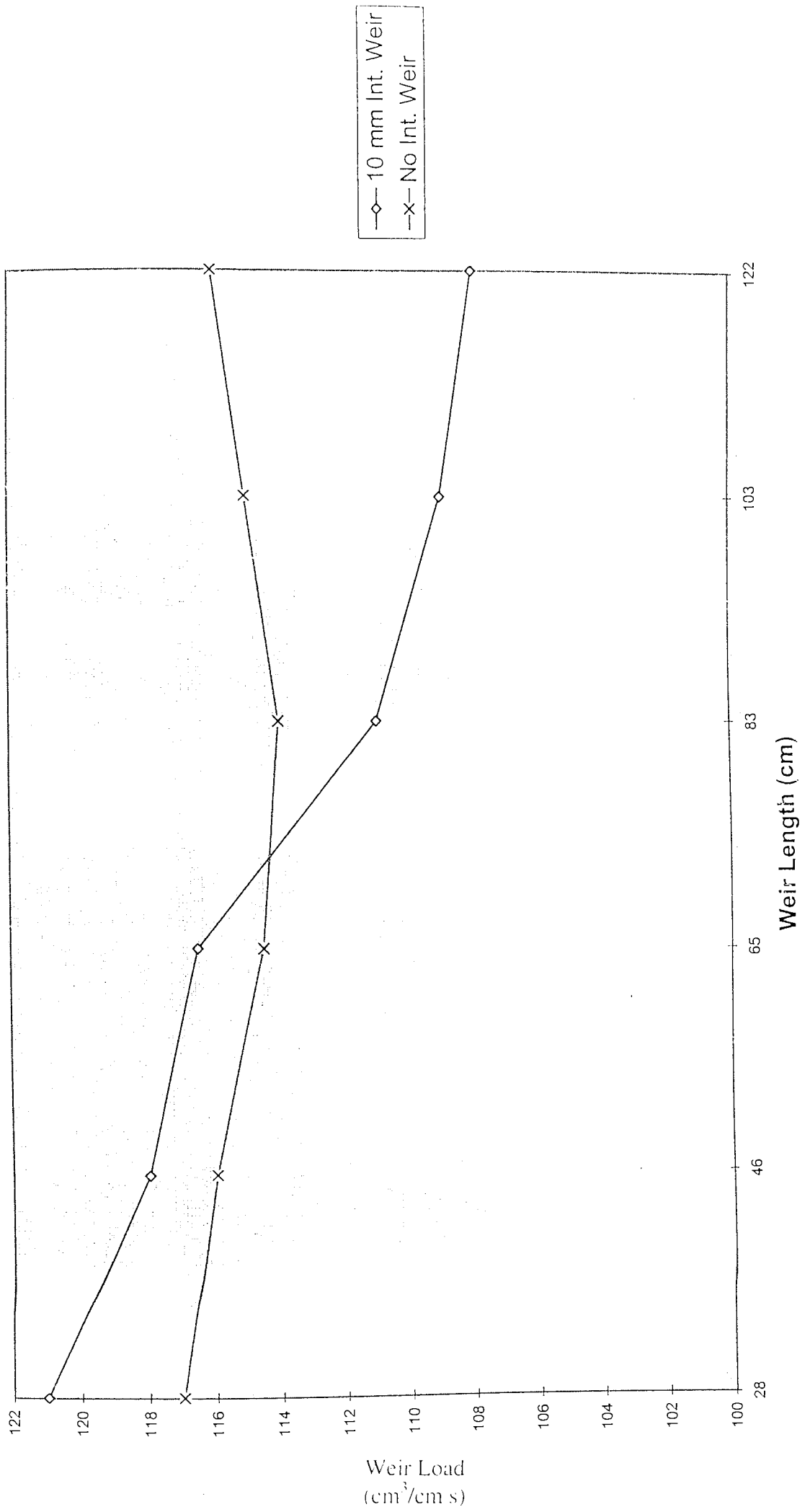
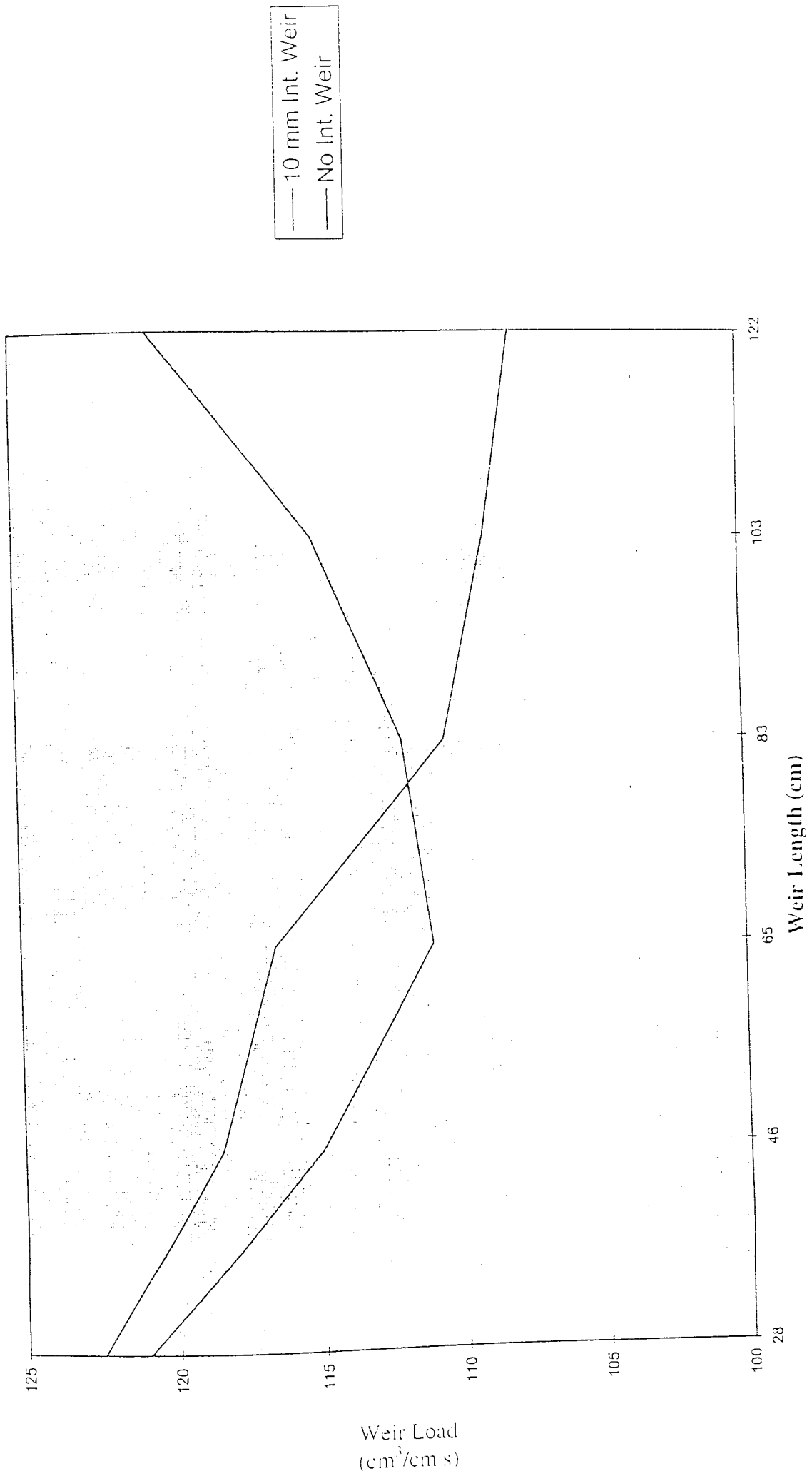


Fig. 6.7

IG/OW = 10 mm, Superficial Air Velocity = 1.5 m/s, Weir Load = 110 cm³/cm s



6.7 Future Work Using Intermediate Weirs on a Full Circular Tray

The work in this Chapter has shown that there is a potential in using intermediate weirs to remove stagnant/ slow moving liquid. Further work, therefore, needs to be carried out on a full circular tray to see how effective intermediate weirs are. It is important to note that in order to obtain equal residence time for the liquid on the tray the liquid in the centre of the tray requires less momentum to travel towards the outlet weir. The liquid travelling at the sides of the circular tray has a longer flow path length and would thus need more momentum in order to obtain equal residence time across the whole of the tray. The following figures outline the likely experiments that need to be carried out with different intermediate weir configurations.:

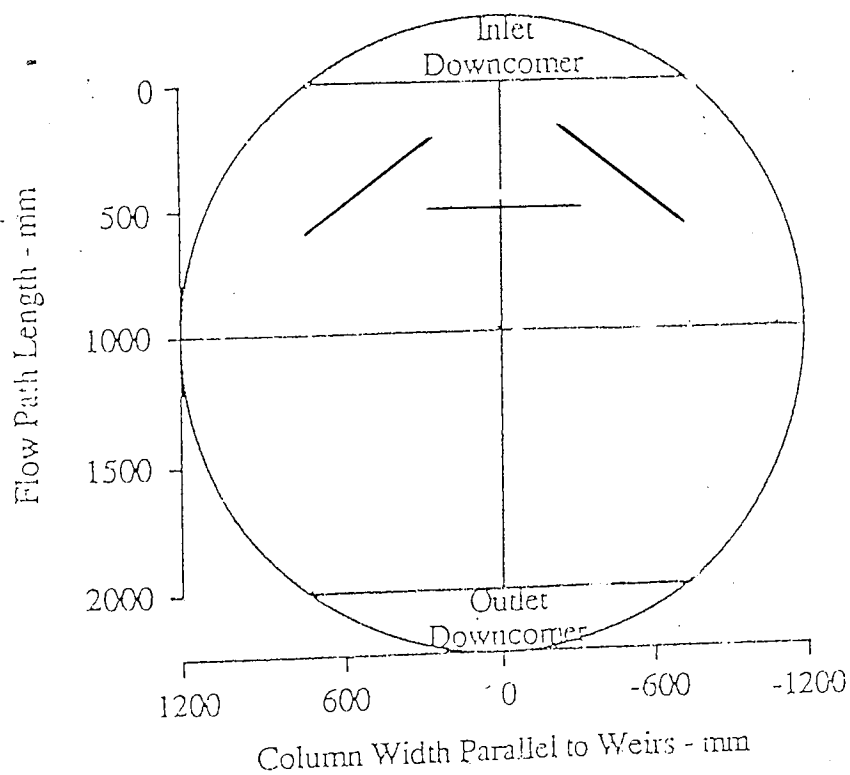


Fig. 6.8 Future Experiments Using Intermediate Weirs on a Full Circular Tray

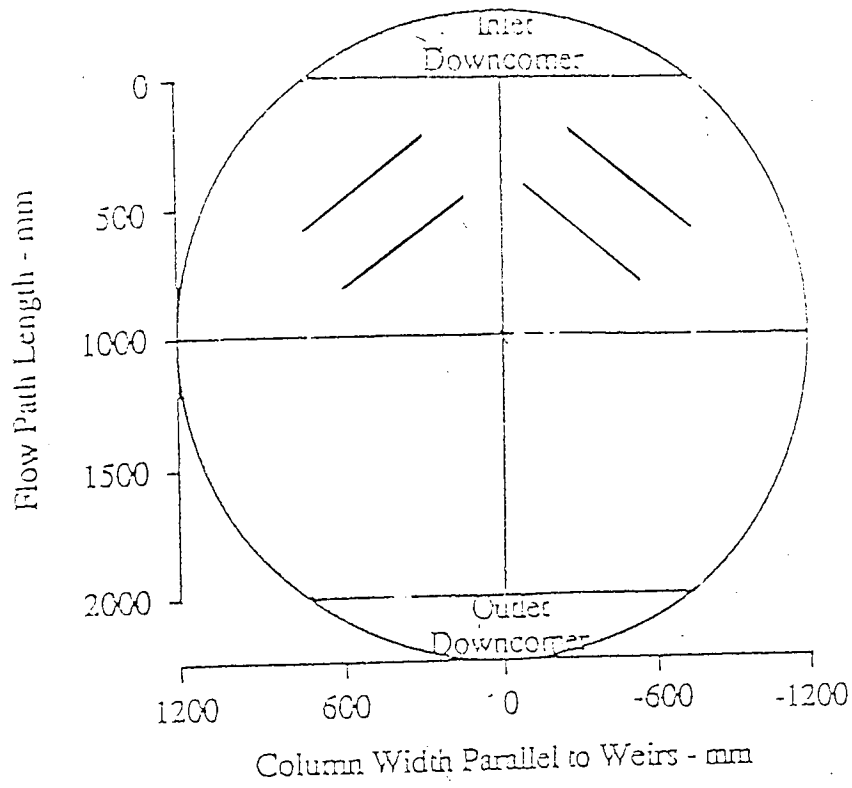


Fig 6.9 Future Experiments Using Intermediate Weirs on a Full Circular Tray

CHAPTER 7

THE USE OF VAPOUR-DIRECTING SLOTS TO INCREASE THE THROUGHPUT OF DISTILLATION TRAYS

7.1 Introduction

The ideal vapour/liquid contacting device is one in which the same degree of bubbling activity is achieved everywhere on the tray. This implies uniform froth depth, uniform froth liquid volume fraction and uniform vapour flow per unit area (dry pressure drop). Under these circumstances, no individual part of the tray surface 'controls' the design.

On large diameter sieve trays uniformity is not achieved due to the formation of stagnant zones which leads to vapour passing through the stagnant regions undergoing no composition change. As the object of the tray is to change the vapour composition, this obviously reduces the tray efficiency. Although stagnant regions are not replenished by the bulk liquid flow, as seen in Figure 7.1. Stagnant regions tend to be depleted of lighter components due to the stripping action of the vapour and mixing from the active region replenishes them in these components. However, mixing acts only over a limited distance, estimated to be about 0.5 m by Porter et al and this distance is independent of tray diameter. This has very important consequences for scale-up. Where the maximum width of the stagnant regions is less than about 0.5 m, transverse mixing is sufficient to overcome the adverse effects on tray efficiency. However, as tray diameter and the size of the stagnant regions increases, transverse mixing is inadequate and tray efficiency suffers.

The reduction in efficiency is even more severe when we consider a large diameter column having single-pass trays with the stagnant regions stacked one above the other. Lockett (1986). In principle, vapour can pass through the stagnant regions of a series of trays without undergoing significant composition change. This causes a far bigger reduction in tray and overall section efficiency than if a single tray is considered in isolation.

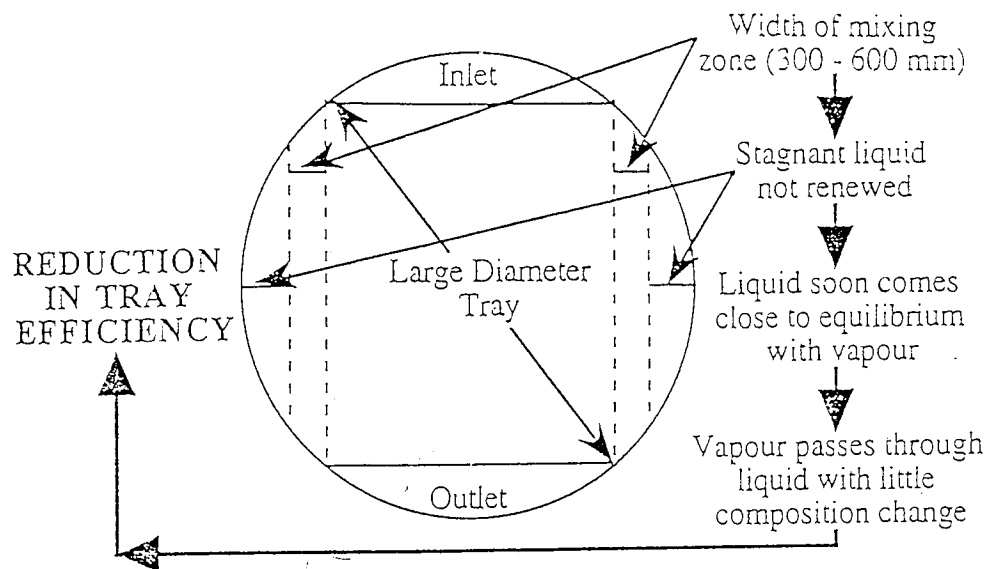


Figure 7.1: Schematic diagram of the detrimental effect of stagnant regions on Tray Efficiency.

As stated in Chapter 1, one of the aims of this research work is to develop new distillation trays which have a better flow pattern than existing trays i.e. due to the elimination of stagnant zones and also try to improve the throughput of the distillation column as a whole. The use of flow directing baffles on conventional sieve trays only addresses the flow pattern problem and does not bring the additional advantage of improved throughput.

The question that needs to be answered is 'Is it possible to design a flow directing device which is able to push the liquid across the tray floor faster i.e. reducing the froth height so that the column can increase its throughput and simultaneously remove stagnant zones'? Note the height of an aerated liquid or froth is a limiting factor in dimensioning the vertical tray spacing and the downcomer size in separation columns.

A reduction in the froth height would also reduce the tray pressure drop and hence the column pressure drop. This would also lead to a reduction in downcomer backup which increases downcomer throughput. Note for bubbly flow conditions the maximum throughput of a tray is expected to occur when the froth height reaches the tray above (assuming that sufficient downcomer area has been provided to avoid downcomer flooding).

This Chapter introduces experimental work firstly testing different designs of vapour-directing slots and secondly choosing the optimum design of slot to test on a rectangular sieve tray with a total of 16 vapour-directing slots evenly distributed across the tray. The experiments were carried out on a 1mm hole sieve tray which was chosen to restrict the experiments to the froth regime.

7.1.1 Vapour-Directing Slots

At present the pressure drop of the vapour passing through the tray is wasted, yet this would seem the most likely source of energy for controlling not only the liquid depth but the overall horizontal liquid flow pattern.

A number of distillation trays have incorporated slots or tabs into the tray deck so that the vapour has a horizontal velocity component as it leaves the tray. Such trays have been variously described as jet trays, directed jet trays and slotted trays. As the vapour passes through the liquid, part of its horizontal momentum is imparted to the liquid. If the slots are arranged to face the outlet weir, the liquid is accelerated and its depth on the tray is reduced. The advantages of such trays are that they largely eliminate hydraulic gradient, give low pressure drop because of the reduced liquid depth on the tray and improve throughput, they have been successfully used in vacuum distillation. Another application has been to move the liquid out of the sides of the tray to eliminate liquid channelling, which otherwise usually occurs and which can reduce tray efficiency Lockett (1986).

A disadvantage which has been reported for these type of trays is that they can work, in a sense too well and at some liquid and vapour rates the liquid can be 'blown off' the tray. It is evident that the process of momentum transfer from the vapour to the liquid is important for understanding how these trays work. Here the questions that need to be asked are 'How does the design and size of the slots affect the amount of momentum transferred to the liquid?' and 'Is the placement of the slots critical in their successful operation with regards removing stagnant zones and hydraulic gradient?' It should be possible to calculate how much of the gas should enter at a specific angle to achieve an optimum depth of liquid.

7.2 The Design and Testing of Different Size Vapour-Directing Slots

The objective of the experimental work is to compare different types of design of slots and subsequently compare a vapour-directing tray (slotted) to an unslotted tray.

7.2.1 Experimental Procedure

This work was carried out on a 1 mm hole rectangular sieve tray of dimensions 1.9 by 1.25 m, which had a single aluminium vapour-directing slot placed on the tray at any one time. The various slot sizes that were tested are shown in Figure 7.2. **Slot (1)** had dimensions $L = 20$ cm, $W = 20$ cm, $\text{Gap} = 2$ cm ; **Slot (2)** had dimensions $L = 10$ cm, $W = 10$ cm, $\text{Gap} = 1$ cm. **Slot (3)** had dimensions $L = 10$ cm, $W = 10$ cm and $\text{Gap} = 1$ cm, see Figure 7.3 and the photographs in Figures 7.4 a to 7.4 c.

The slots were placed on the tray at a distance of 39 cm from the inlet downcomer and 159 cm from the outlet downcomer ; the slots were pop-riveted to the tray floor. It should be noted that previous research into vapour-directing slots have involved the slots being incorporated into the tray rather than placed on the tray. This would lead to an increase in the tray area which in turn would lead to lower hole velocities and hence lower pressure drop. Low hole velocities also lead to weeping and hence low turndown ratio. It is also important to note that the size of the angled slot has to be such that it does not distort the flow pattern.

For a particular superficial air velocity each of the water flowrates were fixed and after allowing for a set period to allow for steady state to be achieved visual observation of the effect of each vapour directing slot on the froth was noted. The superficial air velocity ranged from 1.0 m/s to 2.5 m/s. The inlet gap and outlet weir were both fixed at 50 mm. It is important to note that by reducing the inlet gap a lower liquid hold-up is observed but this leads to higher liquid in the downcomer and eventually to flooding.

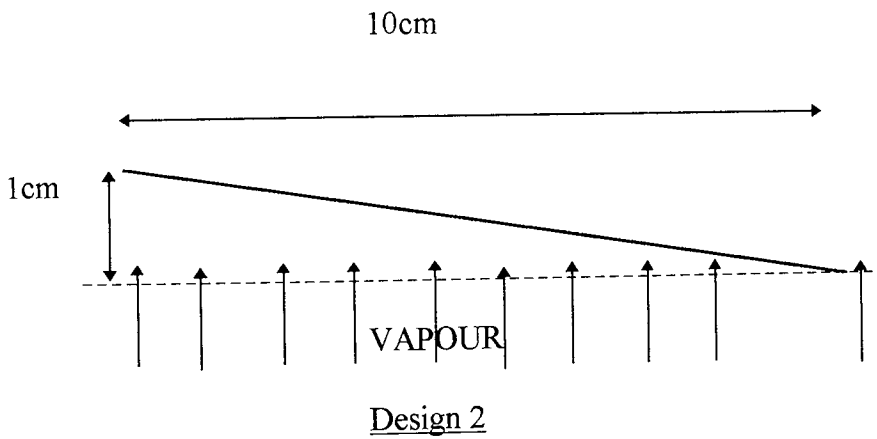
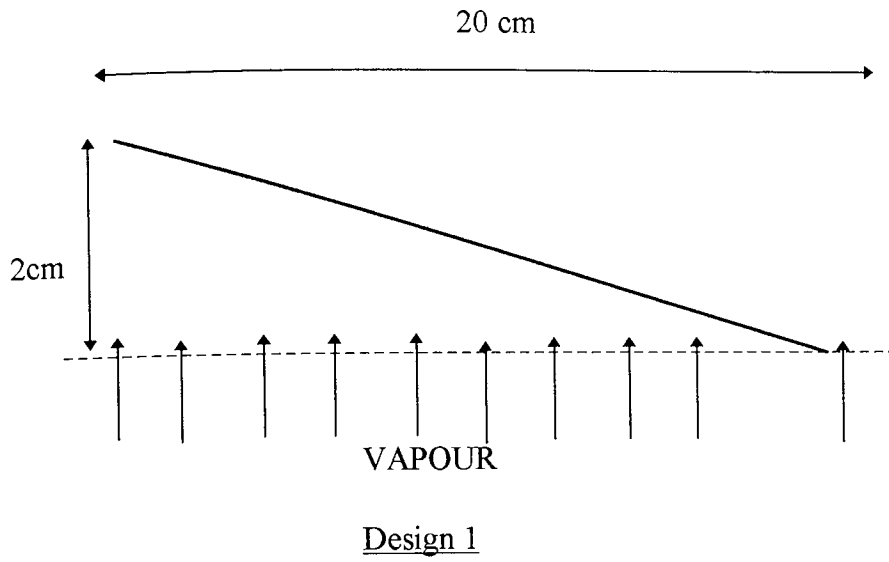


Fig 7.2 Side View of Indined Vapour Directing Slots

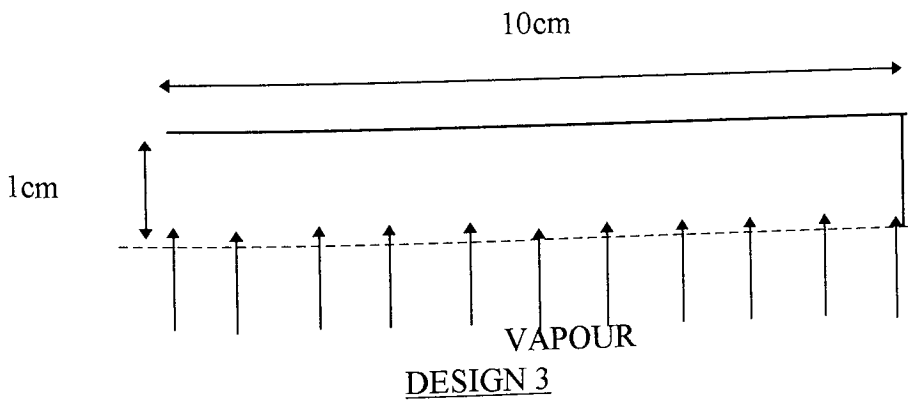


Fig 7.3 Side View of Horizontal Vapour Directing Slot

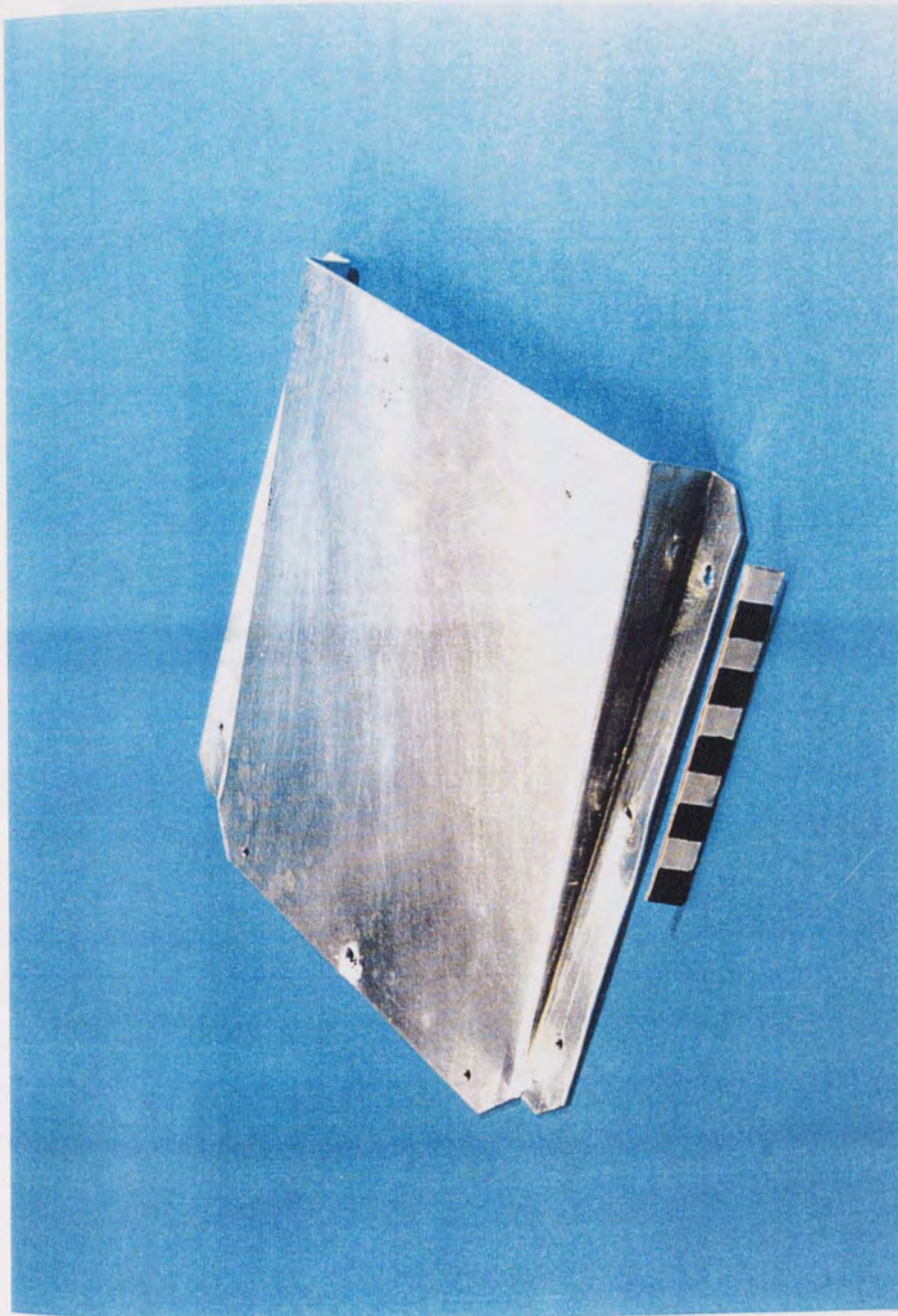


Fig. 7.4 a Photograph of vapour-directing slot, Design 1

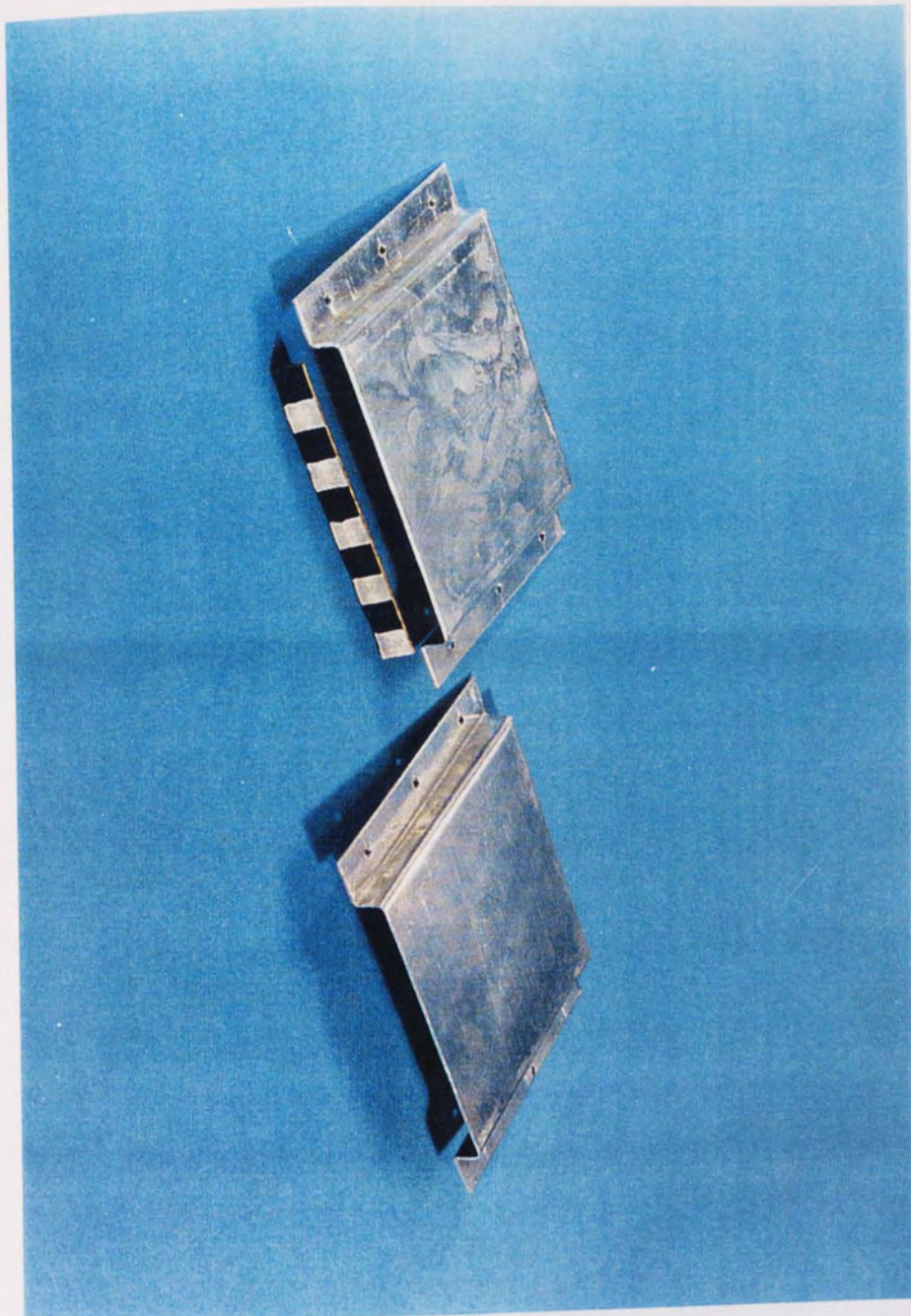


Fig. 7.4 b Photograph of vapour-directing slot, Design 3

7.2.2 Header and Downstream

The channel flow for the design of the vapour-directing slot is shown in Figure 7.4. The channel flow is shown in Figure 7.4. The channel flow is shown in Figure 7.4.

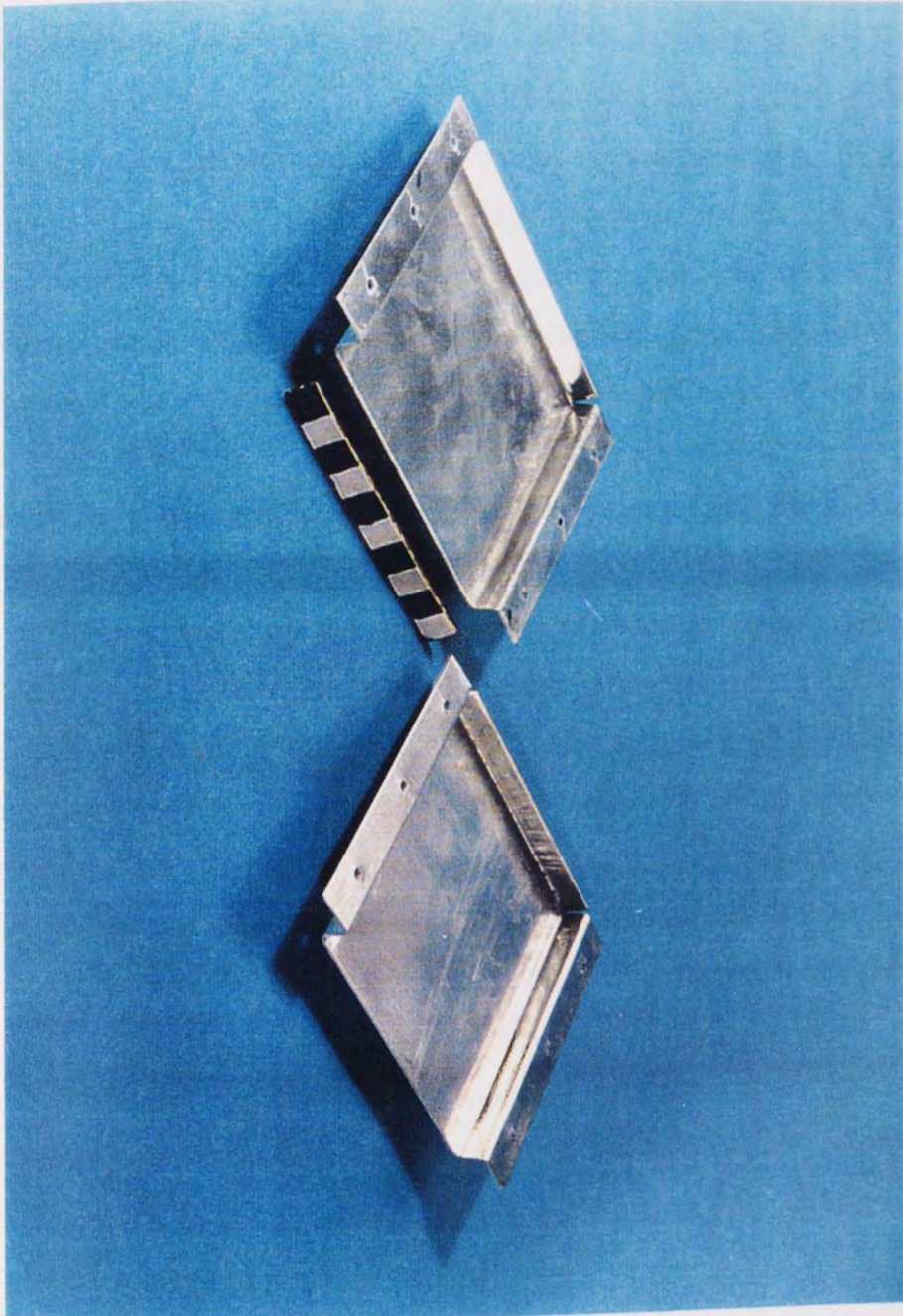


Fig. 7.4 c Photograph of vapour-directing slot, Design 3

7.2.2 Results and Discussion

It was observed from the beginning of the experimental investigation that it was obviously clear that the large vapour directing slot (20cm by 20cm with 2cm outlet) was working too well i.e. the momentum transfer to the liquid was very high and as a result a hydraulic jump by the liquid was observed at a short distance from the outlet of the slot, see Figure 7.5. This was coupled with a reduction in the depth of liquid after the slot and spray droplets rising vertically above the froth height directly above the outlet of the slot. The increase in agitation which occurs upon the tray floor causes erratic and sometimes very powerful horizontal movement of suspended liquid droplets i.e. entrainment. Excessive liquid entrainment can initiate jet flooding occurring at low flow parameters which causes an increase in the tray pressure drop. This, together with the extra liquid load caused by any recycled liquid (which has to leave via the downcomer) contributes to increased backup of froth in the downcomer.

As the air velocity through the slot increased, it caused an increase in the reduction in the depth of liquid after the slot and a higher hydraulic jump, a similar observation was made by Lockett (1986). An increase in the distance the sprayed droplets reached was also observed i.e. distances of 30 cm above the froth height were observed. From the above visual observations it can be concluded that the sideways motion imparted by the vapour was excessive using a slot of 20 cm by 20 cm dimensions and in order to reduce the momentum transfer a smaller size slot needed to be designed and tested.

It should be noted that increasing the weir load reduced the size of the hydraulic jump and the distance of the sprayed droplets. This was noticed at water rates of 75 and 110 $\text{cm}^3/\text{cm s}$, and would seem to suggest that the higher the liquid on the tray floor the less momentum imparted to the liquid.

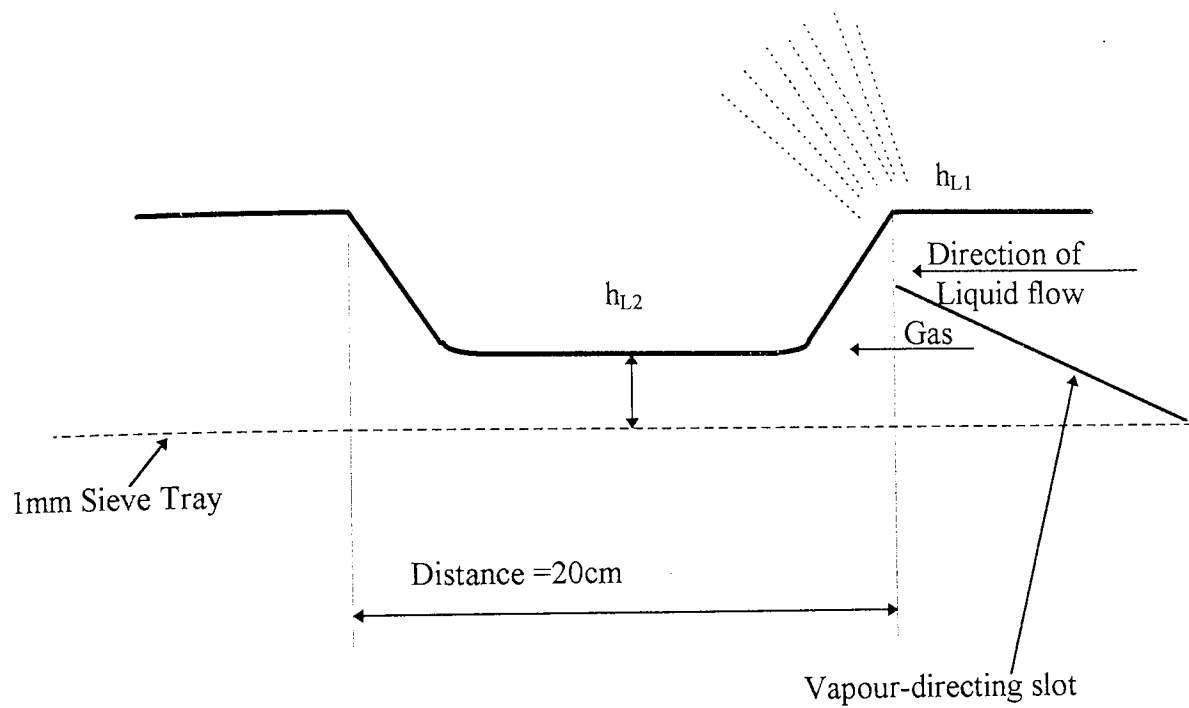


Fig. 7.5 Hydraulic Gradient due to Vapour-Directing Slot

The next part of the experimental work involved the use of a smaller angled slot which had dimension of 10 cm by 10 cm with 1 cm outlet, see figure 7.4 b. It was hoped that by halving the dimensions of the original slot would reduce the momentum transfer to the liquid by approximately 50 % and hence reduce or eliminate the hydraulic jump and sprayed droplets.

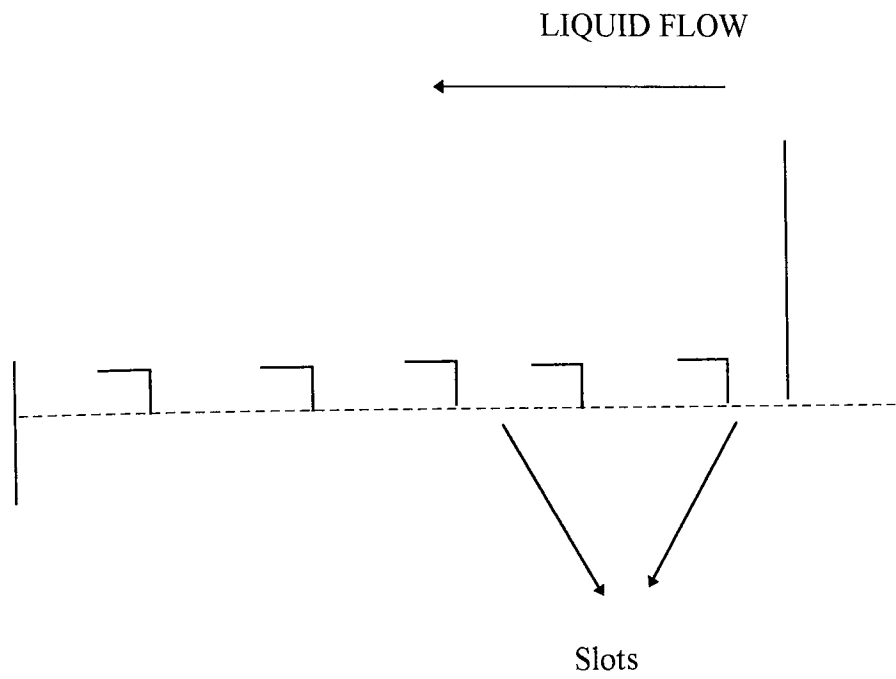
The smaller slot was positioned in the exactly the same position on the tray deck as the larger slot. The effect the smaller slot had on the biphasic flow was the complete removal of the hydraulic jumps that were noted in the above work with the larger slot. A sharp deflection of the vapour as it passed through the tray was observed to be very pronounced and it was felt that this was the required amount to push the liquid across the tray without causing any disruption to the liquid flow pattern. However, sprayed droplets were still observed above the froth height and with this in mind it was decided to change the design of the slot to try and eliminate or reduce the amount and distance of the sprayed liquid droplets i.e. entrainment. It is important to note that entrainment results in the recycling of liquid the wrong way through the column causing a reduction in the driving force for mass transfer between liquid and vapour which lowers the tray efficiency. Kister, Pinzewski and Fell (1981), identified the following factors as being important in determining the rate of entrainment: tray free area, hole diameter, tray spacing and liquid flowrate. Using design 3 the vapour is directed to flow in the horizontal direction i.e. the slot inclination angle is zero. Results obtained show that there was less liquid being entrained by this slot.

7.3 Experimental Work Using Design 3 Vapour-Directing Slots Placed Evenly Across a Rectangular Sieve Tray

Satisfied with the operation of the new design of the vapour-directing slot a total of 16 were positioned along the full length and width of the rectangular tray as shown in Figure 7.6. The distance between each slot was such that it provided an even distribution of the deflected vapour across the tray. The placement of the vapour-directing slots is not believed to be critical as long as the direction of thrust of the vapour rising through the slots imparts a horizontal momentum to the froth and liquid upon the tray in the general direction of the outlet weir. The investigations took the form of (1) general observation of the behaviour of the biphasic (2) measurement of tray pressure drop and downcomer backup with direct comparison with an unslotted sieve tray.

The following superficial air velocities and water flowrates were used:

Water Flowrates (cm ³ /cm s)	Superficial Air Velocity (m/s)
50	1.5
100	
150	2.0
200	
250	2.5



SIDE- VIEW OF VAPOUR-DIRECTING RAY

Fig. 7.6



Fig. 7.7 Photograph of slotted rectangular sieve tray

7.4 RESULTS AND DISCUSSION

7.4.1 Downcomer Backup

The results obtained of the height of clear liquid measurements in the downcomer using the 6 manometers placed in the inlet downcomer can be seen in Appendix 3. The results can be seen in Figures 7.8 to 7.9, where the average downcomer backup is plotted against weir load. At superficial air velocity of 1.5 m/s and at low weir loads, the value of the average downcomer backup for a normal tray is 5.65 cm which steadily increases with increasing weir load values reaching a value of 10.6 cm at a weir load of 250 cm³/cm s. With the slotted tray, however, at low weir loads, the downcomer backup has a value of 4.6 cm (approximately 1 cm less liquid than a normal tray) which rises to a value of 8.9 cm at a weir load of 250 cm³/cm s.

This pattern of results is repeated with increasing superficial air velocities although the difference in downcomer backup between the normal tray and a slotted tray is not as large as with the above. It can be concluded from the data obtained that a slotted tray has approximately 1 cm less liquid in the downcomer than a normal tray indicating that there is the potential for the tray to handle extra throughput. This also confirms the fact that the gas in the vertical flow represents a resistance to flow.

Fig. 7.8 Downcomer Hydraulics Rectangular tray: $lG/Ow = 50 \text{ mm}$, Sup. Air Vel. = 1.5 m/s

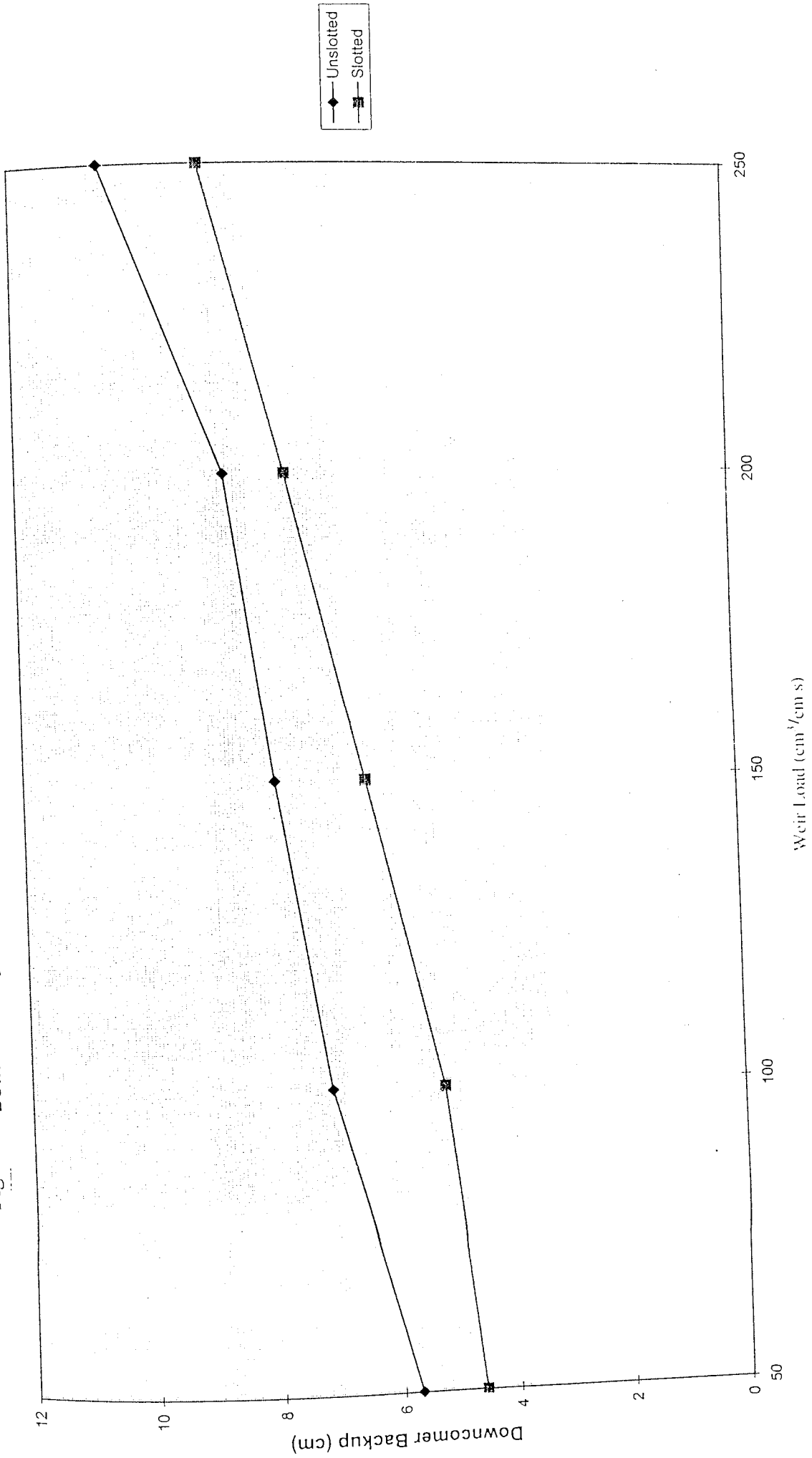
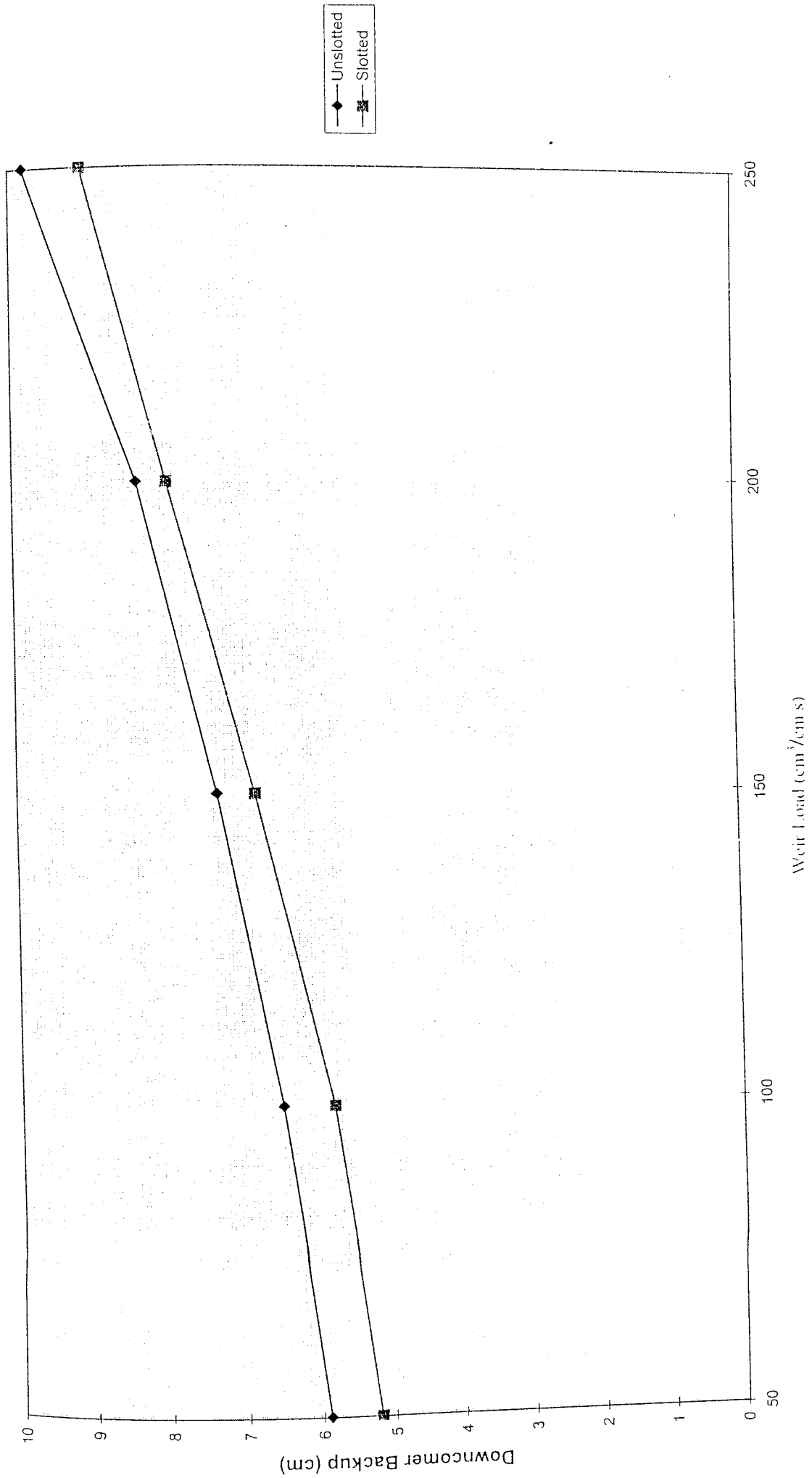


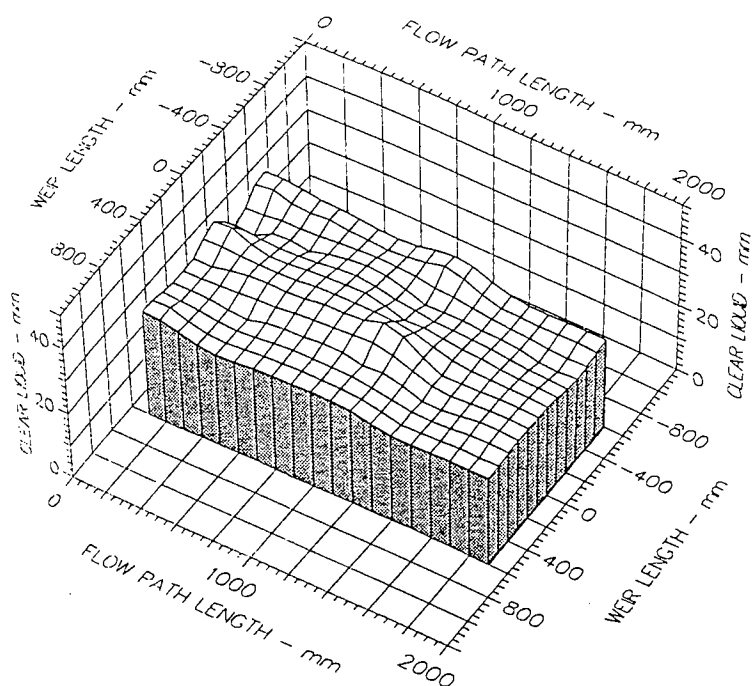
Fig. 7.9 Downcomer Hydraulics Rectangular tray: IG/OW = 50 mm, Sup. Air Vel. = 2.0 m/s



7.4.2 HEIGHT OF CLEAR LIQUID

Figures 7.10 to 7.14 compare the height of clear liquid 3D plots of an unslotted tray with that of a slotted tray. With the superficial air velocity of 1.5 m/s, at low weir loads ($50 \text{ cm}^3/\text{cm s}$) the slotted tray provided slightly too much momentum as some of the liquid was clearly blowing off the tray. At higher weir loads (100 to $250 \text{ cm}^3/\text{cm s}$) the froth height was even across the tray floor, very little liquid was blown off the tray. There was complete mixing of the biphasic with some splashing of the liquid above each angled slot which reached a height of 30cm. The liquid was being pushed quicker across the tray floor in a uniform manner from the inlet to the outlet weir i.e. removal of hydraulic gradient.

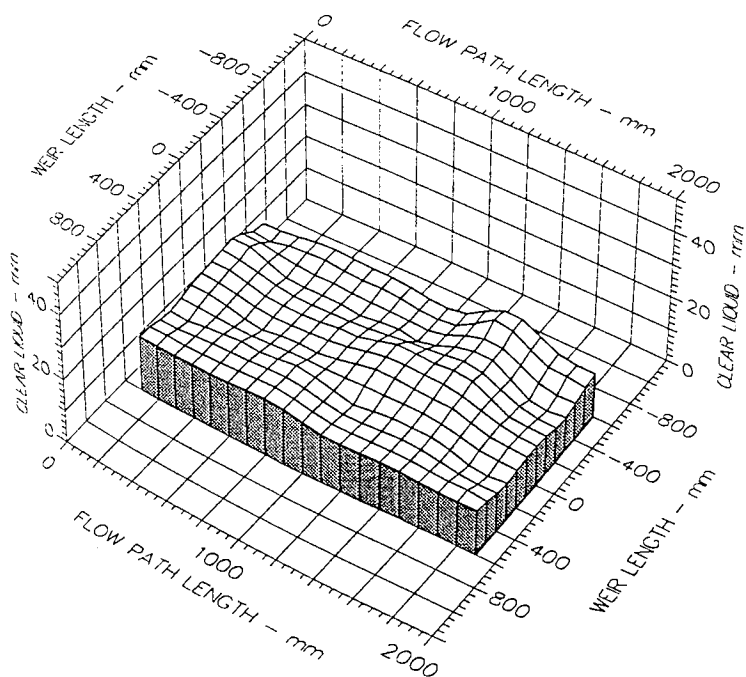
As the vapour rate was increased to 2.0 m/s it was observed that there was an increase in the amount of liquid droplets splashing across the tray. However, the froth still maintained a uniform pattern from a weir load of 100 to $250 \text{ cm}^3/\text{cm s}$. At superficial air velocity of 2.5 m/s the biphasic started to show signs of instability especially at low weir loads. The flow pattern was less rigid and uniform and a higher quantity of entrainment was observed. This observation would seem to suggest that at this flowrate too much momentum is being transferred to the liquid and the turndown ratio is decreasing. The slots tend to cause the droplets to have a flatter (more horizontal) average trajectory and thereby impact with vertically rising droplets sprayed upwards from the slots. This reduces the average height reached by the droplets which have initially a vertical trajectory.



Air Velocity
 1.500 m/s
 Water Loading
 50.0 cm³/cm.s
 Inlet Gap
 0.050 m
 Inlet Weir
 0.000 m
 Outlet Weir
 0.050 m
 Hole Diameter
 0.001 m

Surface of Clear Liquid Hold-Up, Superficial Air Velocity 1.5 m/s
 IG/OW = 50 mm, UNSLOTTED TRAY

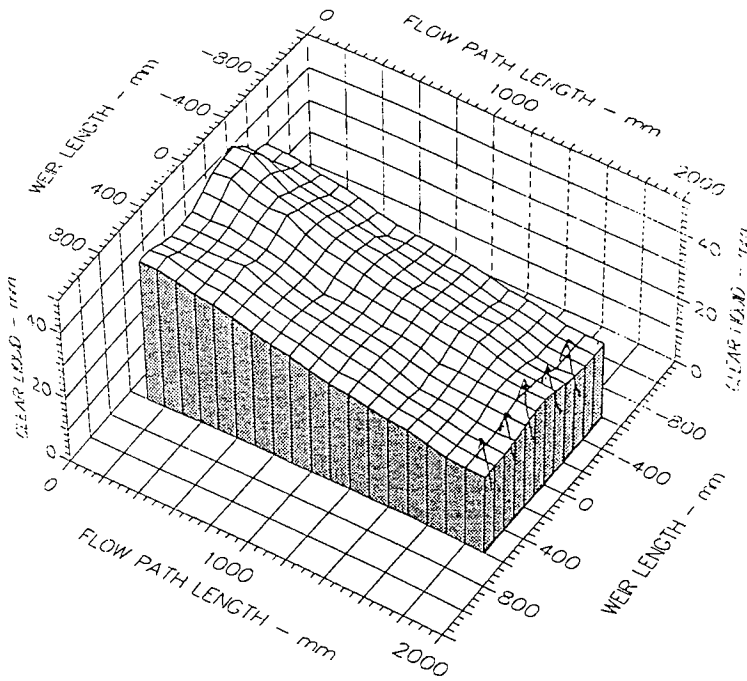
Fig. 7.10 a



Air Velocity
 1.500 m/s
 Water Loading
 50.0 cm³/cm.s
 Inlet Gap
 0.050 m
 Inlet Weir
 0.000 m
 Outlet Weir
 0.050 m
 Hole Diameter
 0.001 m

Surface of Clear Liquid Hold-Up, Superficial Air Velocity 1.5 m/s
 IG/OW = 50 mm, SLOTTED TRAY

Fig. 7.10 b



Air Velocity
1.500 m/s

Water Loading
100.0 cm³/cm.s

Inlet Gap
0.050 m

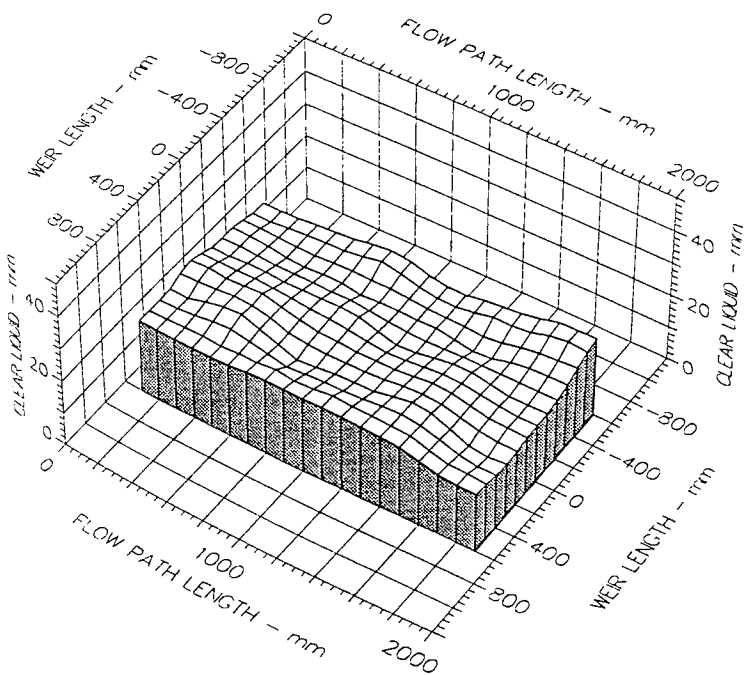
Inlet Weir
0.000 m

Outlet Weir
0.050 m

Hole Diameter
0.001 m

Surface of Clear Liquid Hold-Up, Superficial Air Velocity 1.5 m/s
IG/OW = 50 mm, UNSLOTTED TRAY

Fig. 7.11 a



Air Velocity
1.500 m/s

Water Loading
100.0 cm³/cm.s

Inlet Gap
0.050 m

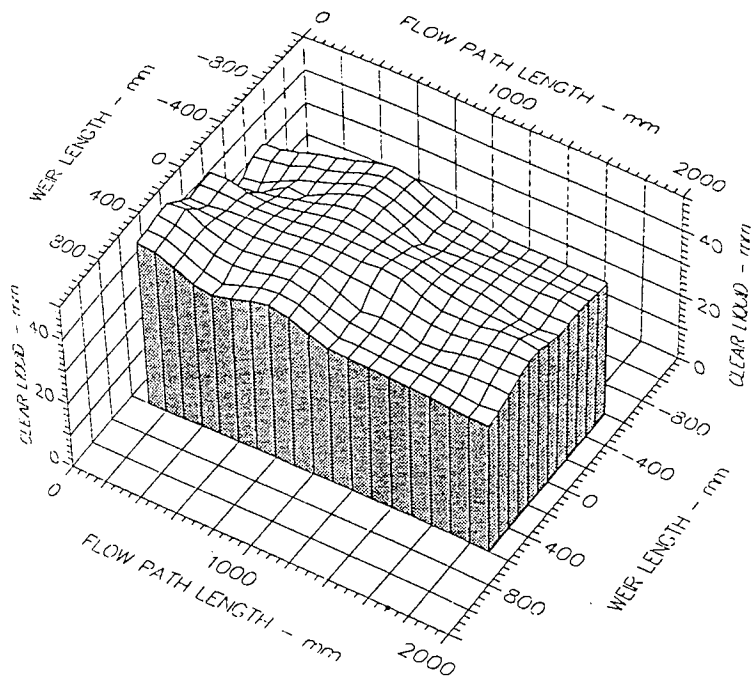
Inlet Weir
0.000 m

Outlet Weir
0.050 m

Hole Diameter
0.001 m

Surface of Clear Liquid Hold-Up, Superficial Air Velocity 1.5 m/s
IG/OW = 50 mm, SLOTTED TRAY

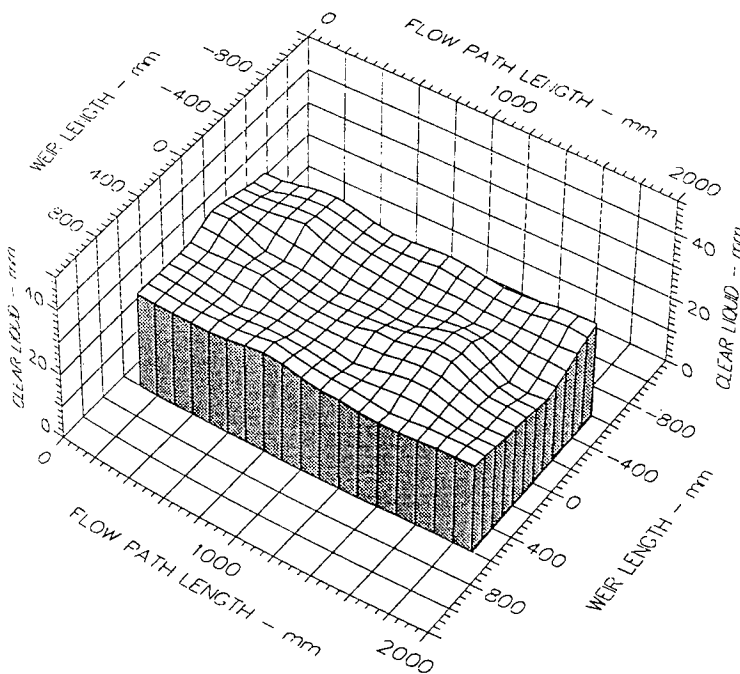
Fig. 7.11 b



Air Velocity
 1.500 m/s
 Water Loading
 150.0 cm³/cm.s
 Inlet Gap
 0.050 m
 Inlet Weir
 0.000 m
 Outlet Weir
 0.050 m
 Hole Diameter
 0.001 m

Surface of Clear Liquid Hold-Up, Superficial Air Velocity 1.5 m/s
 IG/OW = 50 mm, UNSLOTTED TRAY

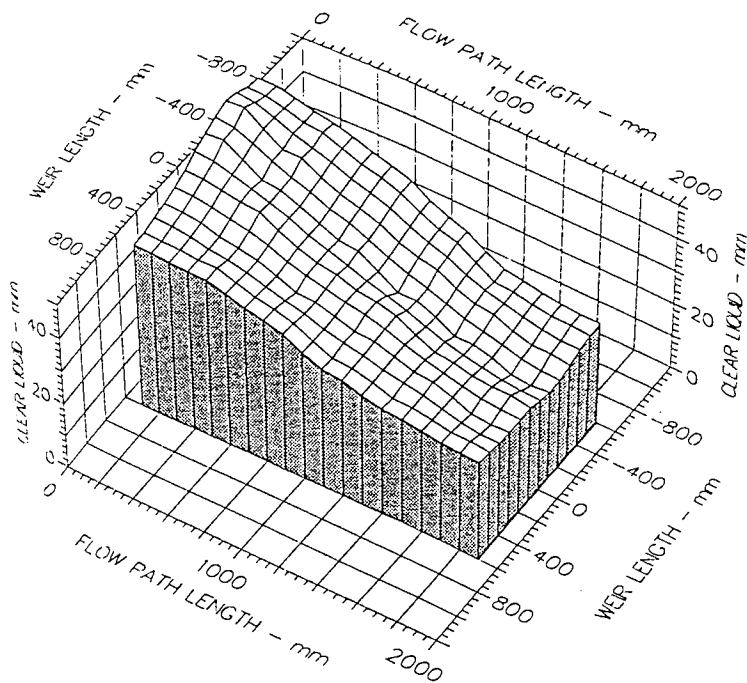
Fig. 7.12 a



Air Velocity
 1.500 m/s
 Water Loading
 150.0 cm³/cm.s
 Inlet Gap
 0.050 m
 Inlet Weir
 0.000 m
 Outlet Weir
 0.050 m
 Hole Diameter
 0.001 m

Surface of Clear Liquid Hold-Up, Superficial Air Velocity 1.5 m/s
 IG/OW = 50 mm, SLOTTED TRAY

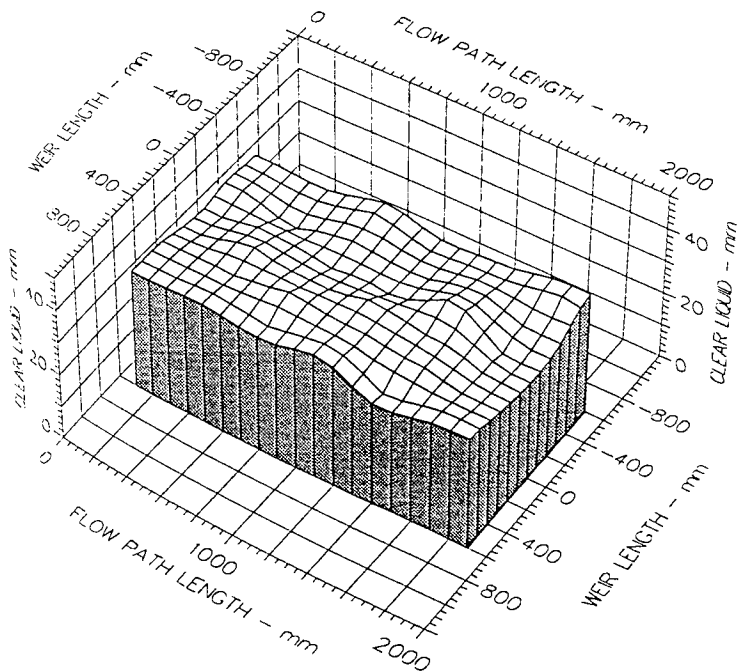
Fig. 7.12 b



Air Velocity
 1.500 m/s
 Water Loading
 200.0 cm³/cm.s
 Inlet Gap
 0.050 m
 Inlet Weir
 0.000 m
 Outlet Weir
 0.050 m
 Hole Diameter
 0.001 m

Surface of Clear Liquid Hold-Up, Superficial Air Velocity 1.5 m/s
 IG/OW = 50 mm, UNSLOTTED TRAY

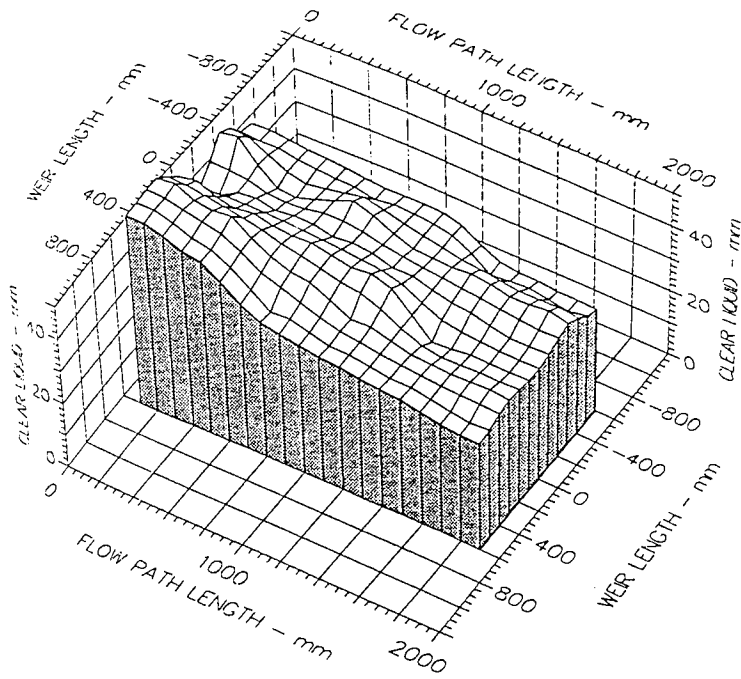
Fig. 7.13 a



Air Velocity
 1.500 m/s
 Water Loading
 200.0 cm³/cm.s
 Inlet Gap
 0.050 m
 Inlet Weir
 0.000 m
 Outlet Weir
 0.050 m
 Hole Diameter
 0.001 m

Surface of Clear Liquid Hold-Up, Superficial Air Velocity 1.5 m/s
 IG/OW = 50 mm, SLOTTED TRAY

Fig. 7.13 b



Air Velocity
1.500 m/s

Water Loading
250.0 cm³/cm.s

Inlet Gap
0.050 m

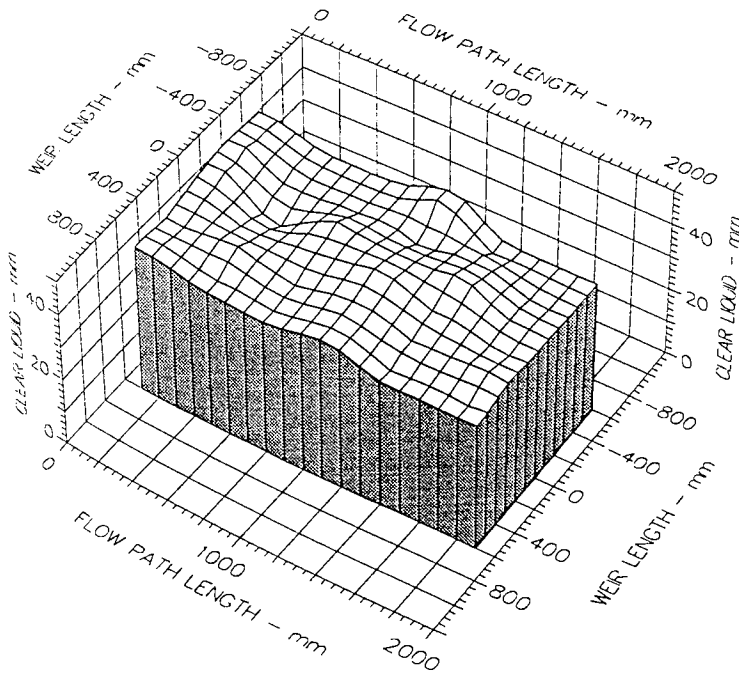
Inlet Weir
0.000 m

Outlet Weir
0.050 m

Hole Diameter
0.001 m

Surface of Clear Liquid Hold-Up, Superficial Air Velocity 1.5 m/s
IG/OW = 50 mm, UNSLOTTED TRAY

Fig. 7.14 a



Air Velocity
1.500 m/s

Water Loading
250.0 cm³/cm.s

Inlet Gap
0.050 m

Inlet Weir
0.000 m

Outlet Weir
0.050 m

Hole Diameter
0.001 m

Surface of Clear Liquid Hold-Up, Superficial Air Velocity 1.5 m/s
IG/OW = 50 mm, SLOTTED TRAY

Fig. 7.14 b

7.5 CONCLUSIONS

The work presented in this Chapter has shown that it is possible to use vapour-directing slots to eliminate the hydraulic gradient across a sieve tray which can otherwise produce vapour-liquid maldistribution. The reduction in froth height brings the advantage of lower pressure drop and increased throughput. The liquid depth on the plate after the slot depends on the slot vapour velocity and liquid flow rate. The amount of momentum that is transferred to the liquid is dependent upon the size of the slot (ie. slot vapour velocity, pressure of the slot) which if too excessive leads to hydraulic jumps occurring after the slots. At high superficial air velocities (and hence slot vapour velocity), some of the liquid can be blown off the tray.

There are still some fundamental questions that need to be answered with respect to using vapour-directing slots on a circular tray eg:

How much momentum is being transferred from the vapour to the liquid and what therefore is the slot vapour-velocity ? It should be possible to calculate how much of the gas should enter at what angle to achieve an optimum depth of liquid.

What is the effect of the slots on the point and tray efficiencies of a sieve tray ?

What is the optimum liquid velocity profile (liquid flow pattern) which is needed to achieve maximum plate efficiency and when is it achieved ? In principle there are an unlimited number of velocity fields which can be imposed on the tray consistent with hydraulic gradient elimination.

CHAPTER 8

THE EFFECT OF THE VAPOUR-DIRECTING SLOTS ON THE POINT/TRAY EFFICIENCY OF A RECTANGULAR SIEVE TRAY

8.1 INTRODUCTION

The previous Chapter has demonstrated that vapour-directing slots can be used to reduce the liquid depth/ froth height on the tray, depending on the operating conditions. In particular at low weir loads the slotted tray provides too much momentum and some of the liquid is blown off the tray. At higher weir loads, however, there is complete mixing of the biphasic with a uniform froth height across the tray. As a result of the elimination of the hydraulic gradient, which plays a major role in fixing the liquid flowrate on the tray, the tray can handle higher liquid rates without weeping.

The next question that needs to be answered is ‘What is the effect of the vapour-directing slots on the point and tray efficiency?’. With this in mind this Chapter describes water-cooling experiments on a rectangular tray with the aim of quantifying the effect of the slots on the point and tray efficiency.

8.2 THE WATER-COOLING TECHNIQUE

The water cooling technique is essentially a steady state technique for investigating flow patterns on an air-water simulator tray. The effect of the liquid flow pattern on mass transfer is investigated by drawing an analogy between heat and mass transfer. Hot water is fed onto the cross-flow test tray and is cooled by the passage of rising air.

During the water-cooling process, water temperature measurements are made over the tray in order to generate temperature profile isotherms. Isotherms permit interpretation of the effect of the biphasic flow on mass transfer when simulating distillation. In addition the temperature isotherms can be interpreted in terms of enthalpy driving forces so as to calculate the thermal point and tray efficiencies. The theory of water-cooling considers both heat and mass transfer from the water surface when contacted with a rising stream of air. It is a well established theory used to design cooling towers; a complete derivation of the water-cooling theory and theoretical analogy between heat and mass transfer can be found in Chamber's PhD Thesis 1993.

8.2.1 RESISTANCE THERMOMETER DETECTORS AND DATA LOGGER SYSTEM

The main criteria for the water-cooling experiment are that the water temperature measurements are made over as many points as possible, and the measurements are made almost instantaneously. To achieve this, platinum resistance thermometers (PRTs) and a computer based data logging system are used.

Resistance thermometry is a high precision technology and is superior to thermocouple technology since PRTs require no cold junction, are less prone to noise, have a better stability and produce a high level of accuracy. In addition, resistance thermometry satisfies the error specification requirement of 0.02 C.

The basic principle involved in PRT technology is that the temperature is determined from the measurement of a comparatively small resistance across a platinum resistor. Since resistance measurements are of a high accuracy, contact resistance of the leads within the PRT becomes significant. To compensate for this, the four-lead arrangement is used since it gives the most accurate measurement. Thus, for a particular temperature, the resistance is measured by applying a measuring current through two leads, while the voltage drop across the PRT is measured with a high impedance device using the other two leads. The measurable resistance range for each PRT corresponds to a temperature range of -10 to 55 C. Each four-wire platinum resistor arrangement was placed inside the tip of a stainless steel probe of length 300mm and width 3mm, the sensor being 15 mm long. The copper lead wires, of length six metres, were enclosed in external PVC coating so as to protect the leads against any moisture. With the exception of the four temperature probes beneath the tray, each PRT was mounted onto the tray deck, from beneath the tray, by means of a rubber grommet and a water shroud as shown in Figure 8.1. Water shrouds were incorporated into the PRT arrangement to prevent premature cooling of the bare probe by the rising air flow since this would have produced erroneous temperature readings. In addition the shroud permitted the capture of a water sample such that it completely surrounds the PRT tip before leaving the shroud to join the biphasic mixture via four water flow outlets.

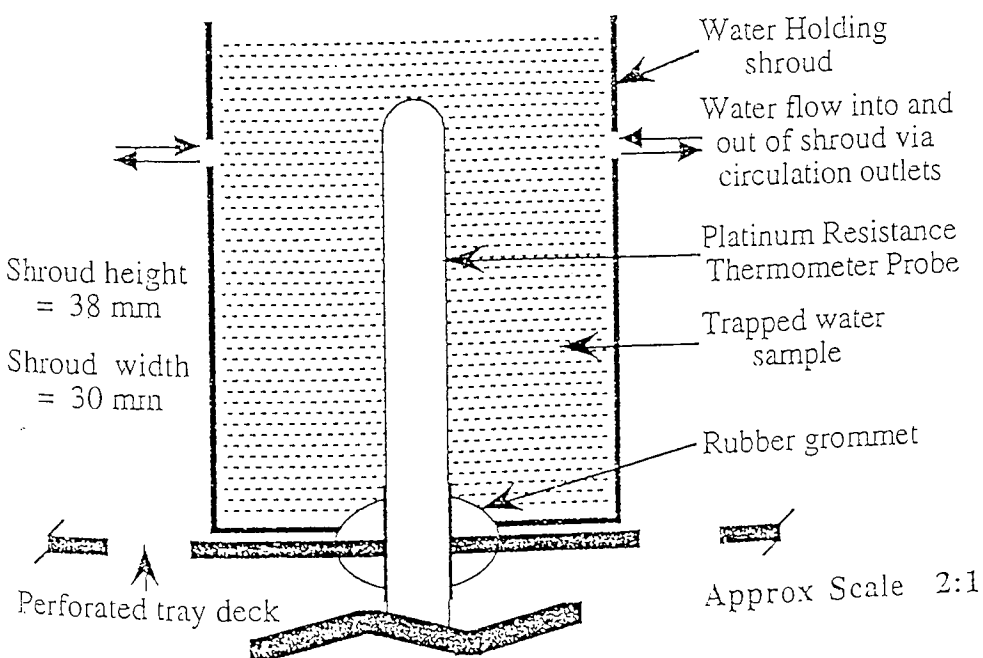


Fig. 8.1 : Schematic Diagram of resistance thermometer and water shroud

Attachment to the test tray

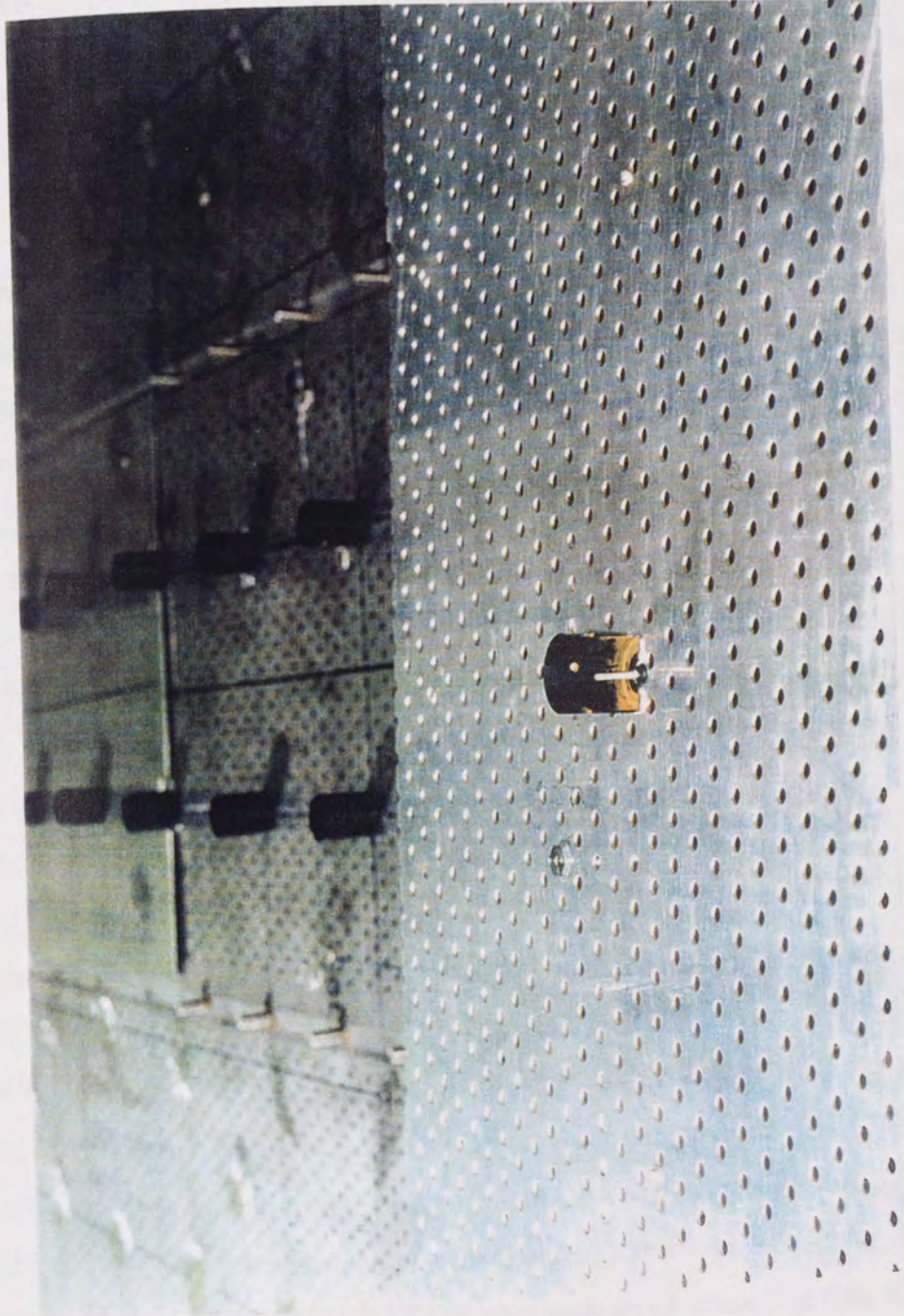


Fig. 8.2 Photograph of resistance thermometer and water shroud

During water-cooling, 'simultaneous' measurements of the tray temperature field were obtained by interfacing the PRTs, attached to the tray, with a MICROLINK data logger which in turn was linked to an on-line personal computer, see Figure 8.3. The data logger unit consisted of eighteen digital cards which comprised of one high speed clock, one analogue to digital (A-D) converter, and sixteen RTD8H D-type connectors. Each RTD8H connector contained eight four-lead PRT's or channels.

8.2.2 CALIBRATION OF THE PLATINUM RESISTANCE THERMOMETERS

The platinum resistance thermometers are a sensitive measuring device and as such are susceptible to damage. From previous work on the column by Fenwick (1996) some erroneous temperatures had been noticed on the temperature plots. Re-calibration of the thermometers was therefore essential.

The method for calibrating the thermometers is to use a standard platinum resistance thermometer, accurate to a hundredth of a degree, and an insulated water bath with a variable heat source. In order to ensure a constant water temperature in the bath the water was circulated by a submerged pump. An effort was made to ensure that all the tips were at the same depth so as to eliminate any effect due to a vertical temperature gradient.

For the calibration the water bath was set to five standard temperatures, 50, 35, 25, 15 and 0^o C (ice was used when necessary). At each temperature the thermometer readings were taken via the datalogger. The datalogger was controlled by a Fortran program called ZEST. This program scanned the thermometers twenty times to collect the temperature readings. The values of these readings were stored in an output file called KEEPCAL.DAT. At each temperature three sets of scans were carried out. This requires the renaming of the KEEPCAL.DAT file after each set of scans. The files were renamed to 1PRT0.DAT, 2PRT0.DAT, 3PRT0.DAT, etc.



Fig. 8.3 Photograph of microlink data logger and PC

When the fifteen data files were collected, a Fortran program called ZEST2 was run. This program took the sets of tree data files for each temperature and averaged them. When the averaging was complete, the program wrote the averaged temperature readings to a file which was used for the actual calibration called CAL.DAT. This was done for all five temperatures.

8.2.3 TEMPERATURE POSITIONS ON THE RECTANGULAR TRAY

Figure 8.4 shows the positioning of the 70 resistance thermometers over the rectangular tray area. The thermometers measuring the temperature of the inlet water, as it enters the tray area, are positioned 50 mm to the rear of the straight chordal inlet downcomer; sixty were placed across the rectangular tray area, four beneath the tray to measure the air inlet temperature and one at the bottom of the outlet downcomer to measure the water outlet temperature.

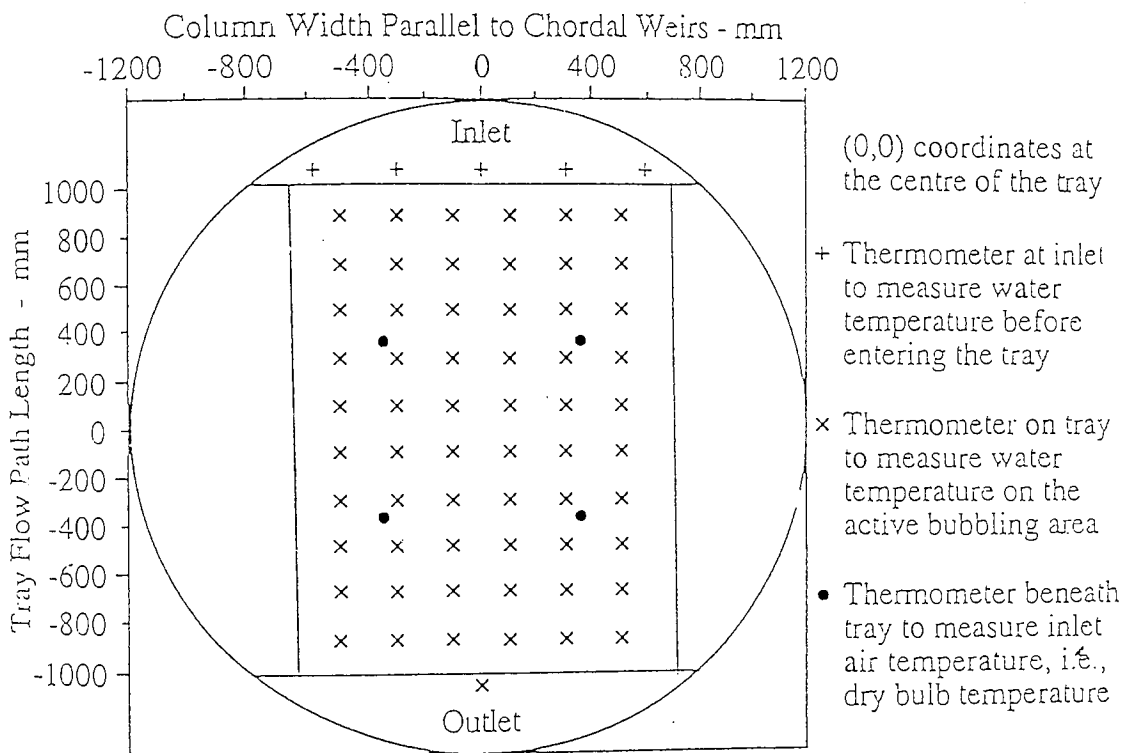


Fig. 8.4 Arrangement of platinum resistance thermometers

8.3 EXPERIMENTAL PROGRAMME AND DATA TREATMENT

8.3.1 EXPERIMENTAL PROGRAMME

During the water-cooling process the water temperatures on the tray were continuously monitored and displayed on a personal computer. When initiated, the temperature data collection software carried out 20 complete scans of all the platinum resistance thermometers, at the end of which the option of recording the collected data was available. The criteria for accepting the collected data was that none of the inlet or outlet resistance thermometers varied by more than 0.1°C.

All the experiments were carried out with 16 vapour-directing slots evenly distributed on the rectangular sieve tray which measured 1.9 m in length and 1.25 m in width. The inlet gap and outlet weir heights were both fixed at 50mm. Superficial air velocities of 1.5, 2.0, 2.5 m/s and water flowrates of 50, 100, 150, 200 and 250 cm³/cm.s were used in the investigation. The experiments were repeated after the removal of the slots from the sieve tray and the results compared.

8.3.2 DATA TREATMENT AND PRESENTATION OF TEMPERATURE PROFILES

The manual control over the heat supply allowed for the inlet water temperature to be held constant during a particular experiment, but it was not possible in the time available to set the inlet water temperature at exactly the same particular value for each experiment. Also the inlet air condition, ie. dry and wet bulb temperatures, varied from day to day. To enable the data from all the experiments to be compared on a like basis, a reduced temperature was calculated and plotted. The reduced temperature, T_r , at a particular point is defined as:

$$T_r = \frac{T - T_{wb}}{T_w - T_{wb}}$$

where T is the measured water temperature at a given point. T_{in} is the water inlet temperature to the tray and T_{wb} is the wet bulb temperature of the entering air. By definition the entering air wet bulb temperature is the minimum temperature that can be exhibited by a simple air-water system. The water entering the tray has a reduced temperature T_r equal to 1.0 and the water leaving the tray has a reduced temperature between 1.0 and 0.0. Experimental results could then be presented in the form of two dimensional contour plots over the tray.

8.3.2.1 EFFICIENCY CALCULATIONS

The air-water test tray while operating can be represented by Figure 8.5.

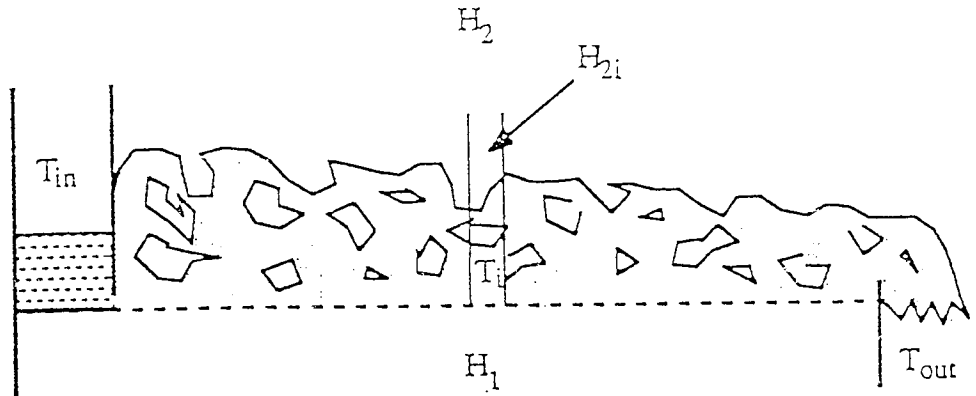


Fig. 8.5 Schematic Diagram of an Operating Tray.

Hot water enters the test tray at a temperature T_{in} and the average temperature of the water leaving the tray is T_{out} . The air enters the tray from below with a uniform enthalpy of H_1 and after passing through the biphase mixture leaves with an enthalpy of H_2 . The Murphree tray efficiency, E_{mv} , based on the enthalpy of the air can thus be defined as:

$$E_{mv} = \frac{H_2 - H_1}{H_{T_{out}}^* - H_1}$$

where $H_{T_{out}}^*$ is the enthalpy of the air in equilibrium with the average temperature of the water leaving the tray. The saturated air enthalpy, in equilibrium with water at a particular temperature, can be calculated from equations given in BS 2520.

The Murphree point efficiency based on the enthalpy of the air can be defined as:

$$E_{og} = \frac{H_{2i} - H_1}{H_{T_i}^* - H_1}$$

where T_i is the local water temperature on the tray and $H_{T_i}^*$ is the enthalpy of the air in equilibrium with the local water temperature and H_{2i} is the enthalpy of the air leaving the biphase mixture.

Using the temperature data collected during the water cooling in the overall heat balance:

$$G (H_2 - H_1) = L C_p (T_{in} - T_{out})$$

yielded the average enthalpy of the leaving air and allowed the calculation of the Murphree point efficiency. The Murphree tray efficiency, averaged over the tray area, was then determined by averaging values of the air enthalpy above each of the 70 temperature measuring devices. A computer program written in Fortran 77 was used to determine the Murphree point and tray efficiencies.

8.4 RESULTS AND DISCUSSION

8.4.1 TEMPERATURE CONTOURS OVER THE TRAY AREA

Figures 8.6 to 8.11 display reduced temperature profiles for the test tray operating with an inlet gap of 50 mm, outlet weir of 50 mm and superficial air velocities ranging from 1.5 m/s to 2.5 m/s. Each diagram shows the water entering the tray having a reduced temperature T_r , equal to 1.0 and the water leaving the tray with a reduced temperature between 1.0 and 0.0.

At the water weir loading of $50 \text{ cm}^3/\text{cm s}$, for the slotted tray, the lines of constant reduced isotherms enter the tray parallel to the inlet downcomer satisfying the condition that at the inlet gap the reduced temperature, T_r , is equal to unity, see figure 8.6 a. The uniform isotherms occupy about a third of the length of the tray before becoming U-shaped. As the temperature profiles move into the outlet half of the tray, the reduced isotherm values become smaller, i.e. decreasing in the direction of the outlet weir. At this weir load, the same effect is seen with a normal tray, see figure 8.9a.

By increasing the weir load to $100 \text{ cm}^3/\text{cm s}$, see figure 8.6 b, the slotted tray differs from the normal tray in that the isotherms are still parallel to the inlet gap i.e. there is plug flow, whereas the normal tray has inverted isotherms, see figure 8.9 b. This is repeated for the higher weir load of $150 \text{ cm}^3/\text{cm s}$, see figures 8.6 c and 8.9 c. A similar pattern of results is observed when the superficial air velocity is increased to 2.0 m/s, see figures 8.7 a to 8.7 d and 8.10 a to 8.10 c.

Comparing the above results with those for the height of clear liquid in the previous Chapter, it is evident that at weir loads between 100 and $200 \text{ cm}^3/\text{cm s}$ the froth height on a slotted tray was even across the tray floor with complete vertical mixing of the biphasic and the removal of the hydraulic gradient. It is also clear that at higher weir loads the slots had less effect on the flow pattern, consequently there was no difference in the temperature contour plots.

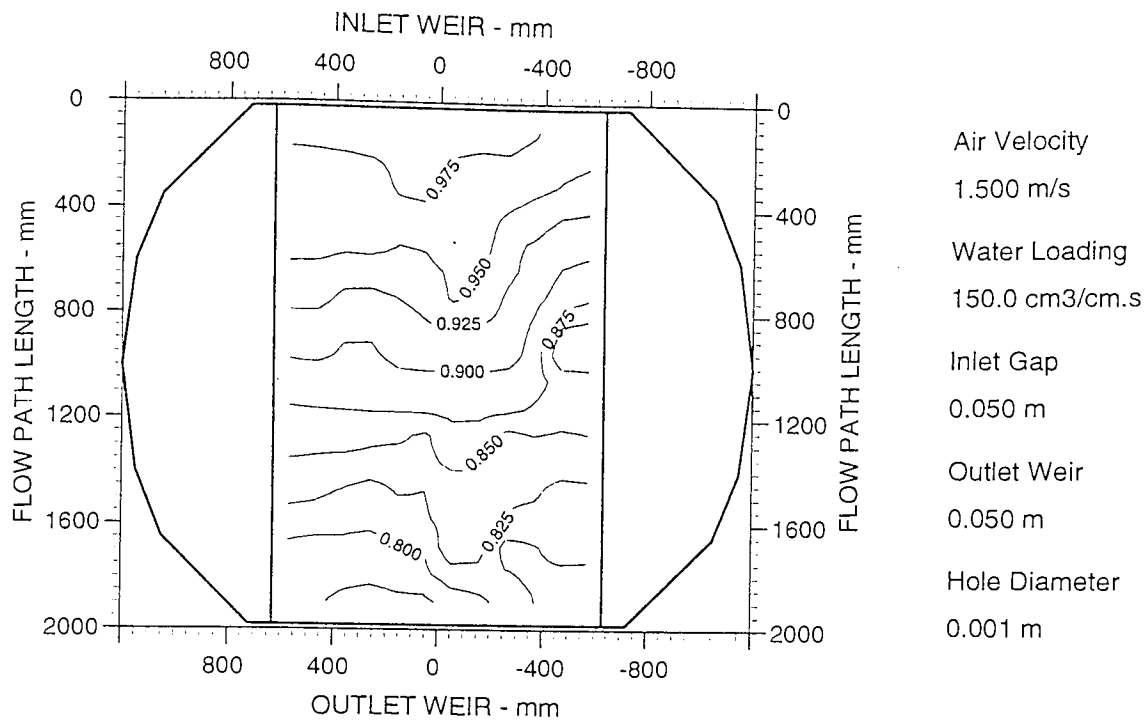


Fig. 8.6 c Two Dimensional Reduced Temperature Contour Plot
Superficial Air Velocity 1.5 m/s, Slots

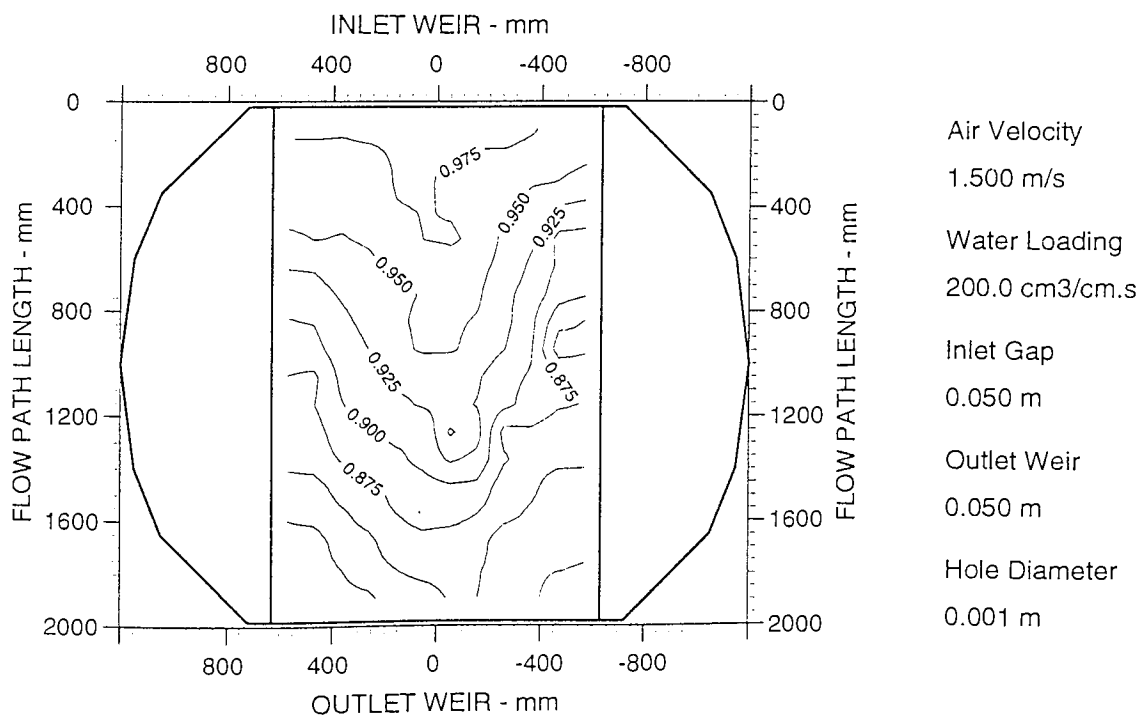


Fig. 8.6 d Two Dimensional Reduced Temperature Contour Plot
Superficial Air Velocity 1.5 m/s, Slots

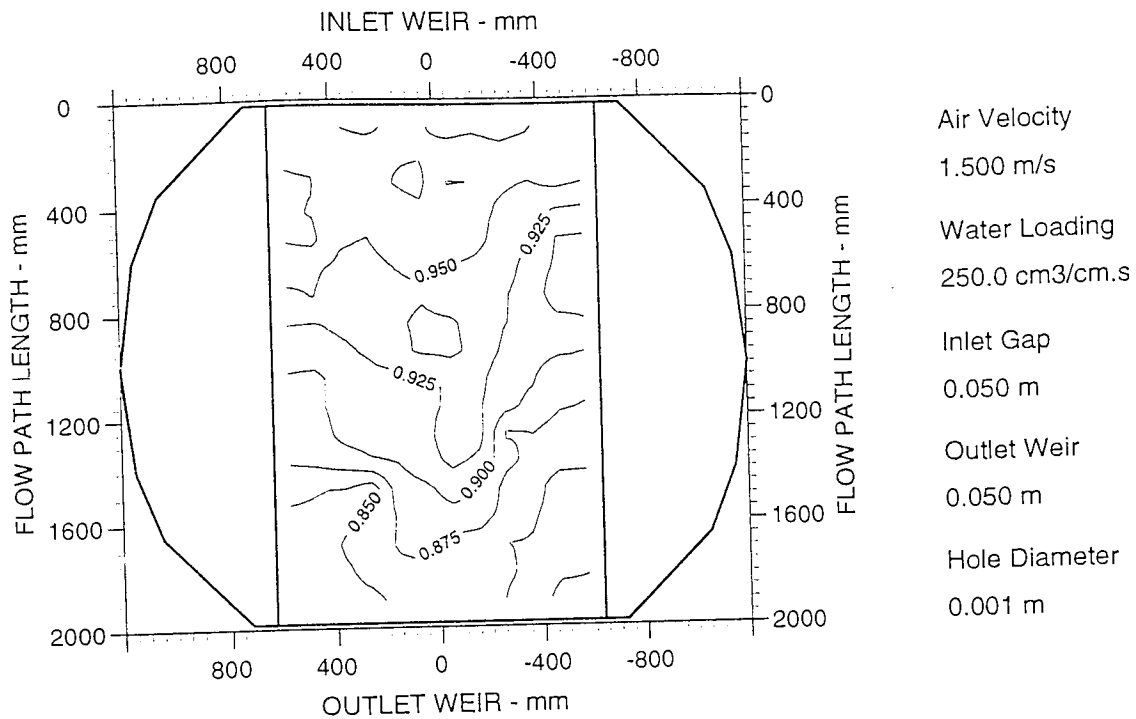


Fig. 8.6 e Two Dimensional Reduced Temperature Contour Plot
Superficial Air Velocity 1.5 m/s, Slots

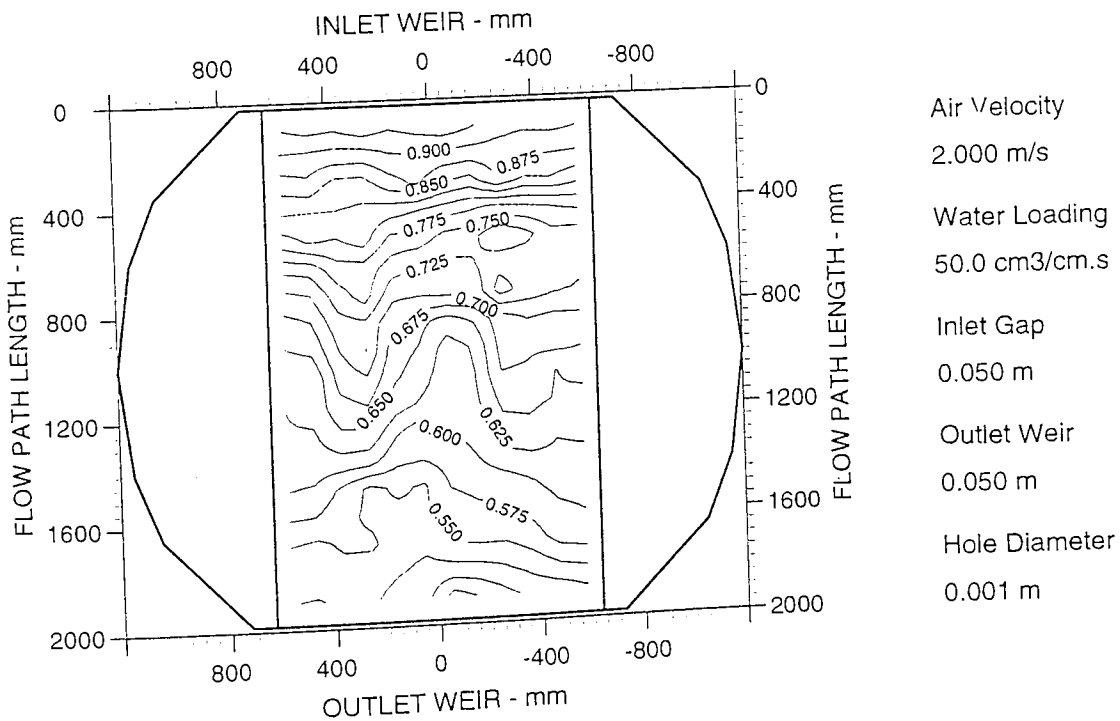
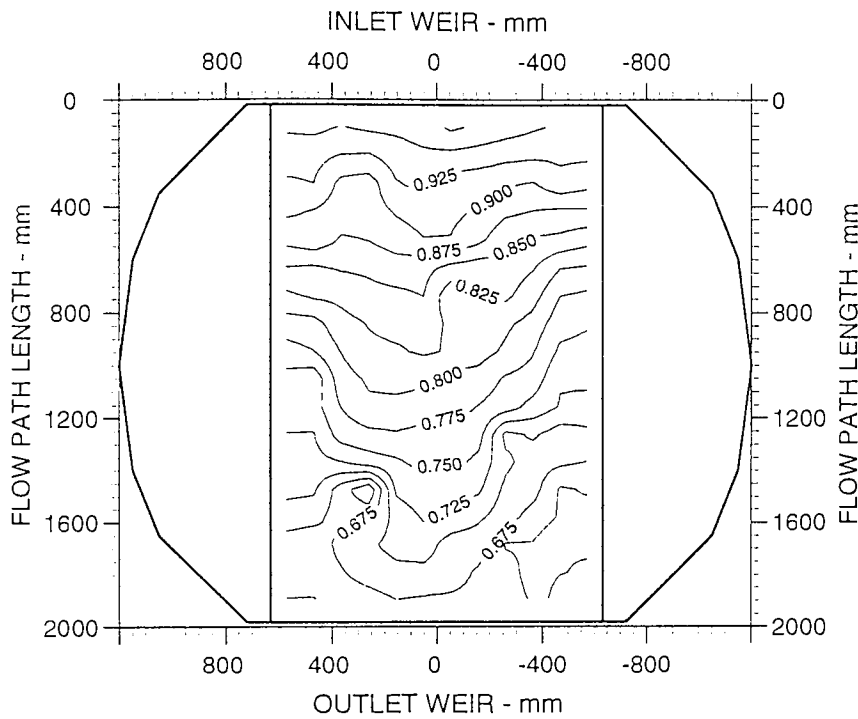


Fig. 8.7 a Two Dimensional Reduced Temperature Contour Plot
Superficial Air Velocity 2.0 m/s, Slots



Air Velocity
2.000 m/s

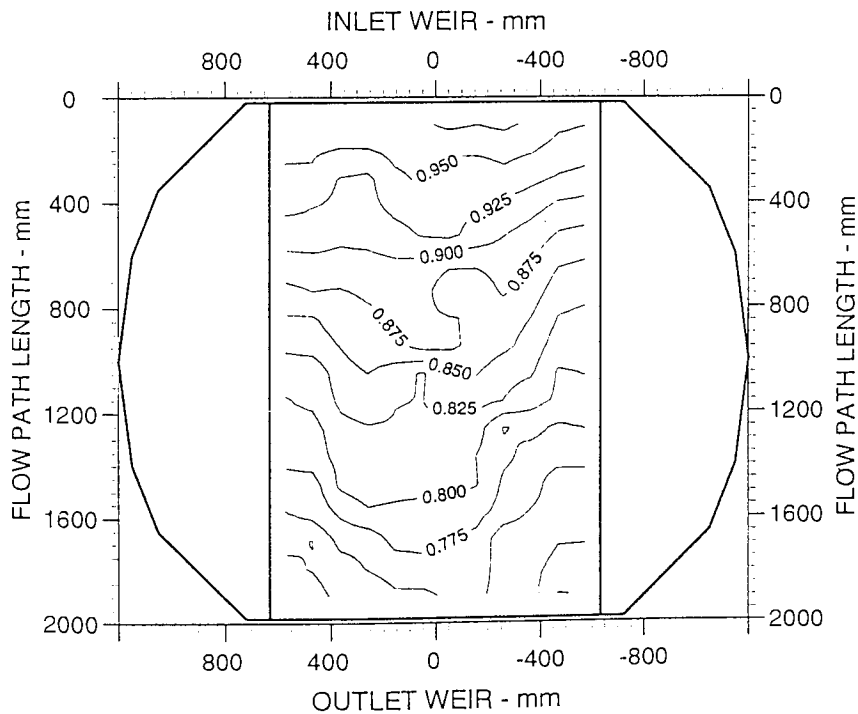
Water Loading
100.0 cm³/cm.s

Inlet Gap
0.050 m

Outlet Weir
0.050 m

Hole Diameter
0.001 m

Two Dimensional Reduced Temperature Contour Plot
Fig. 8.7 b Superficial Air Velocity 2.0 m/s, Slots



Air Velocity
2.000 m/s

Water Loading
150.0 cm³/cm.s

Inlet Gap
0.050 m

Outlet Weir
0.050 m

Hole Diameter
0.001 m

Two Dimensional Reduced Temperature Contour Plot
Fig. 8.7 c Superficial Air Velocity 2.0 m/s, Slots

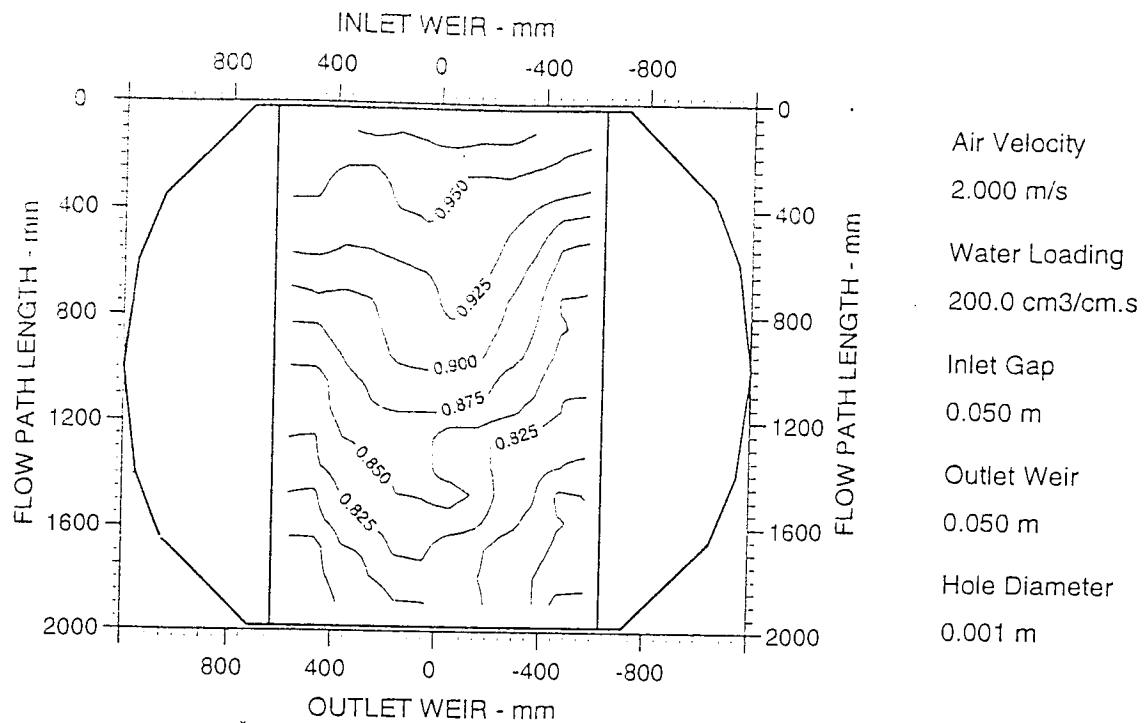


Fig. 8.7 d Two Dimensional Reduced Temperature Contour Plot
Superficial Air Velocity 2.0 m/s, Slots

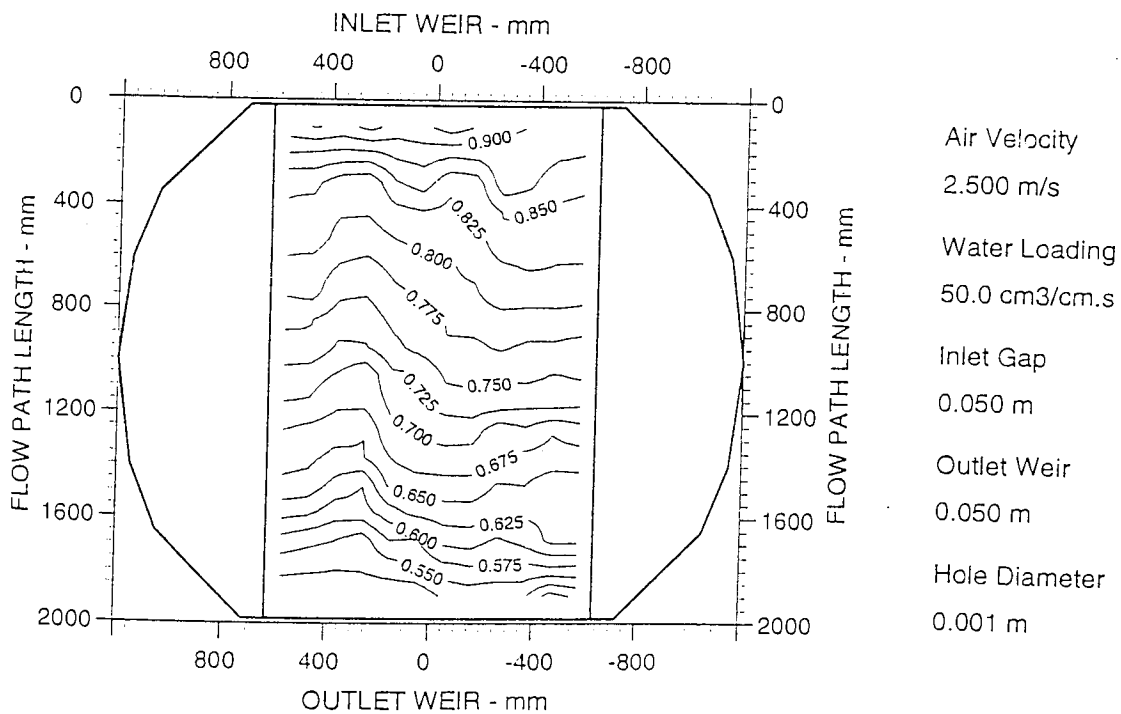


Fig. 8.8 a Two Dimensional Reduced Temperature Contour Plot
Superficial Air Velocity 2.5 m/s, Slots

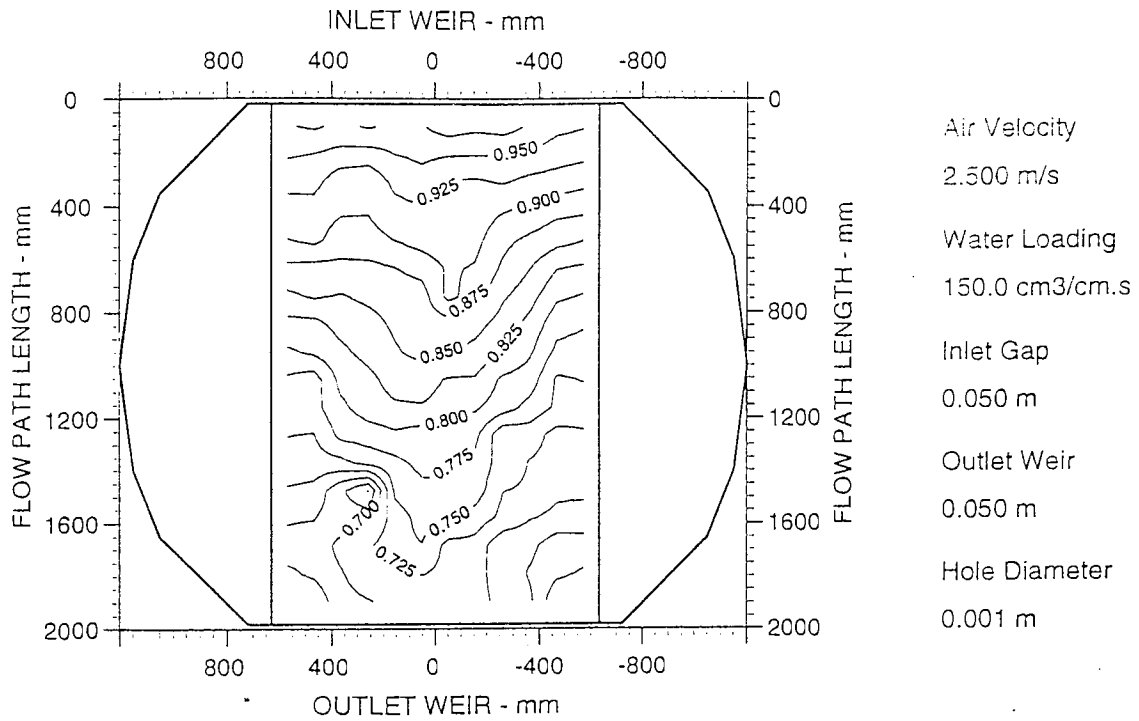


Fig. 8.8 b Two Dimensional Reduced Temperature Contour Plot
 Superficial Air Velocity 2.5 m/s, Slots

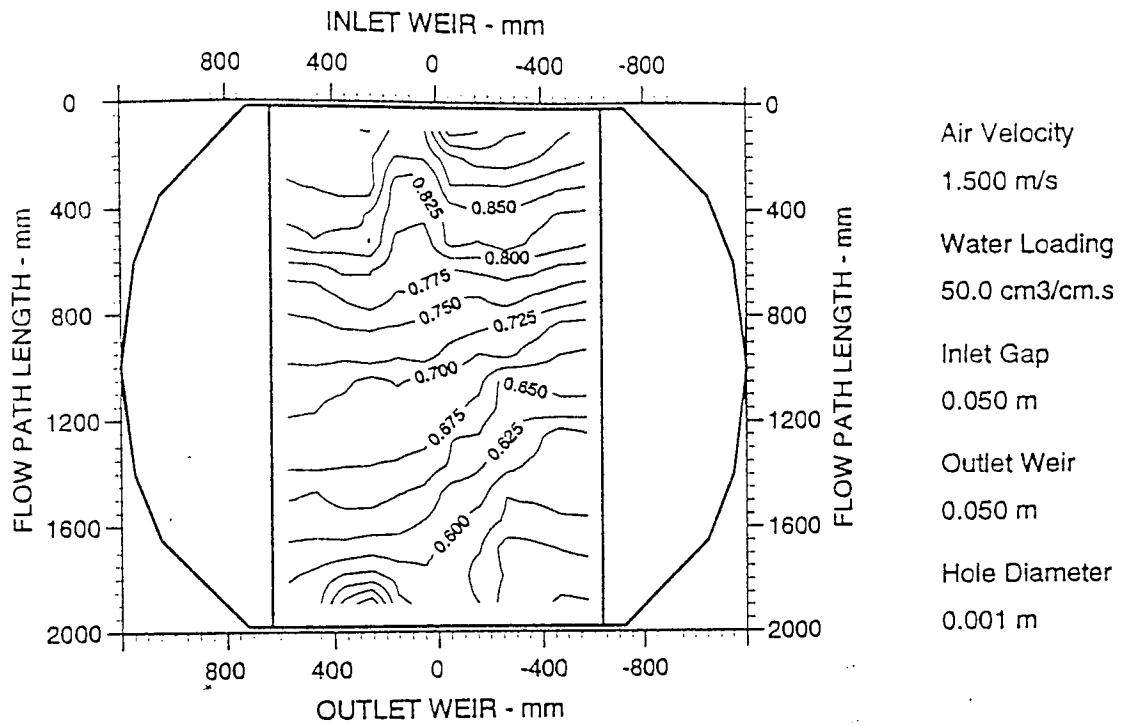


Fig. 8.9 a Two Dimensional Reduced Temperature Contour Plot
Superficial Air Velocity 1.5 m/s, No Slots

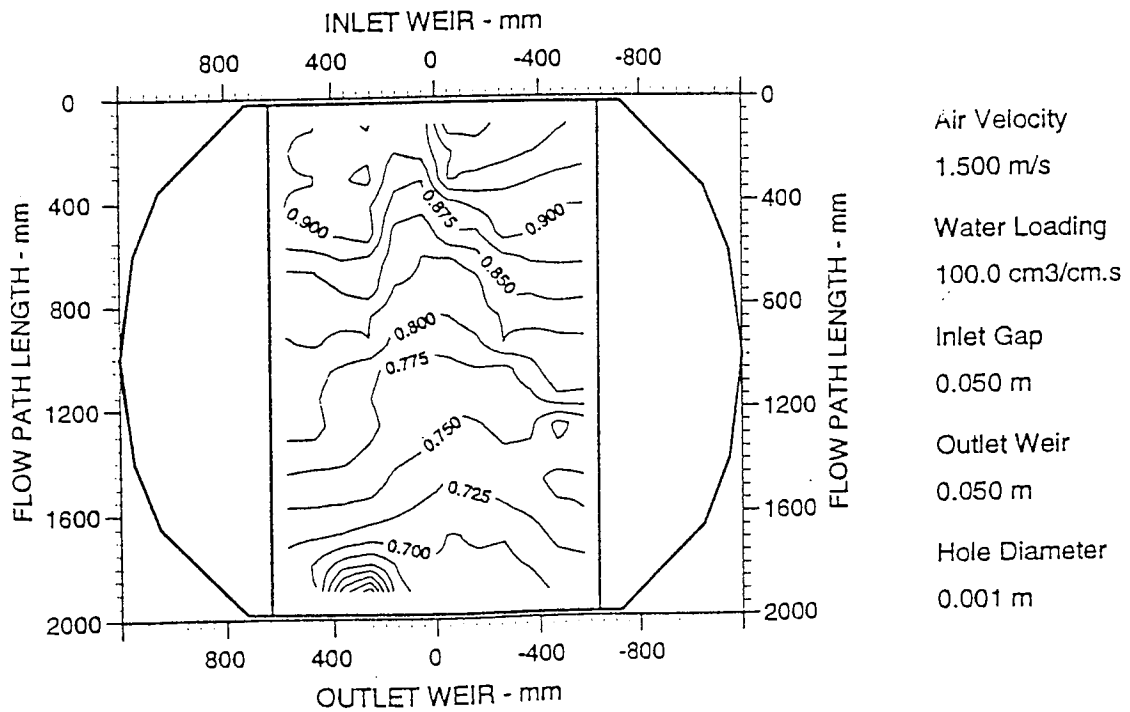


Fig. 8.9 b Two Dimensional Reduced Temperature Contour Plot
Superficial Air Velocity 1.5 m/s, No Slots

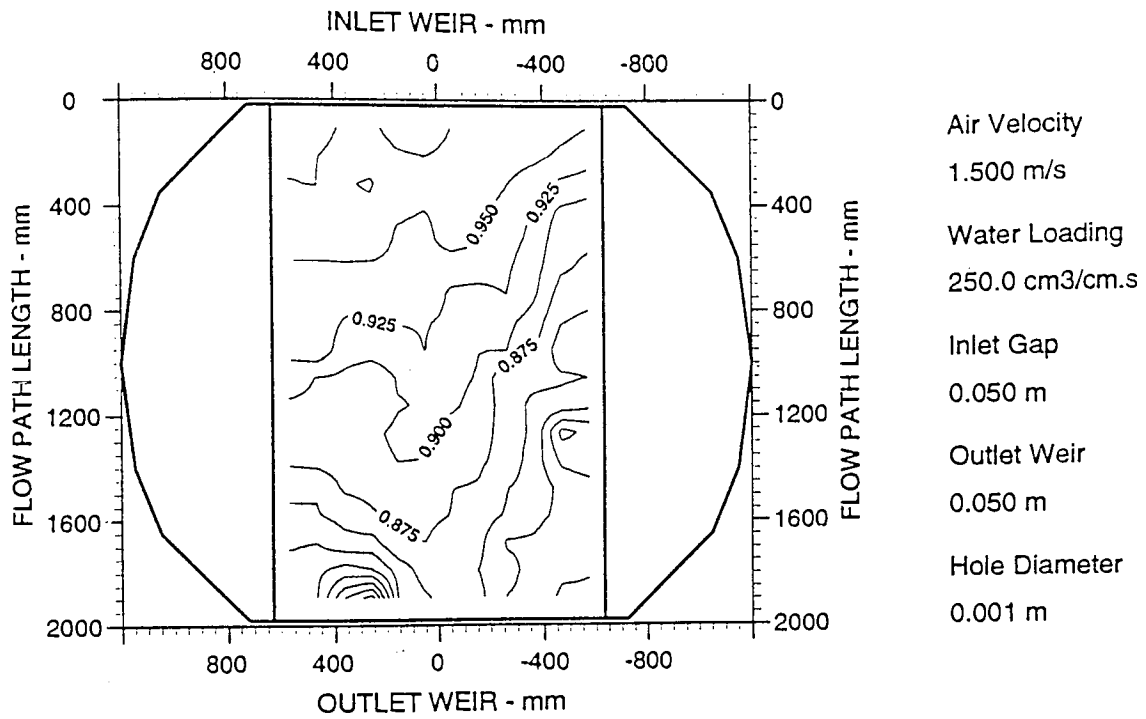


Fig. 8.9 e Two Dimensional Reduced Temperature Contour Plot
Superficial Air Velocity 1.5 m/s, No Slots

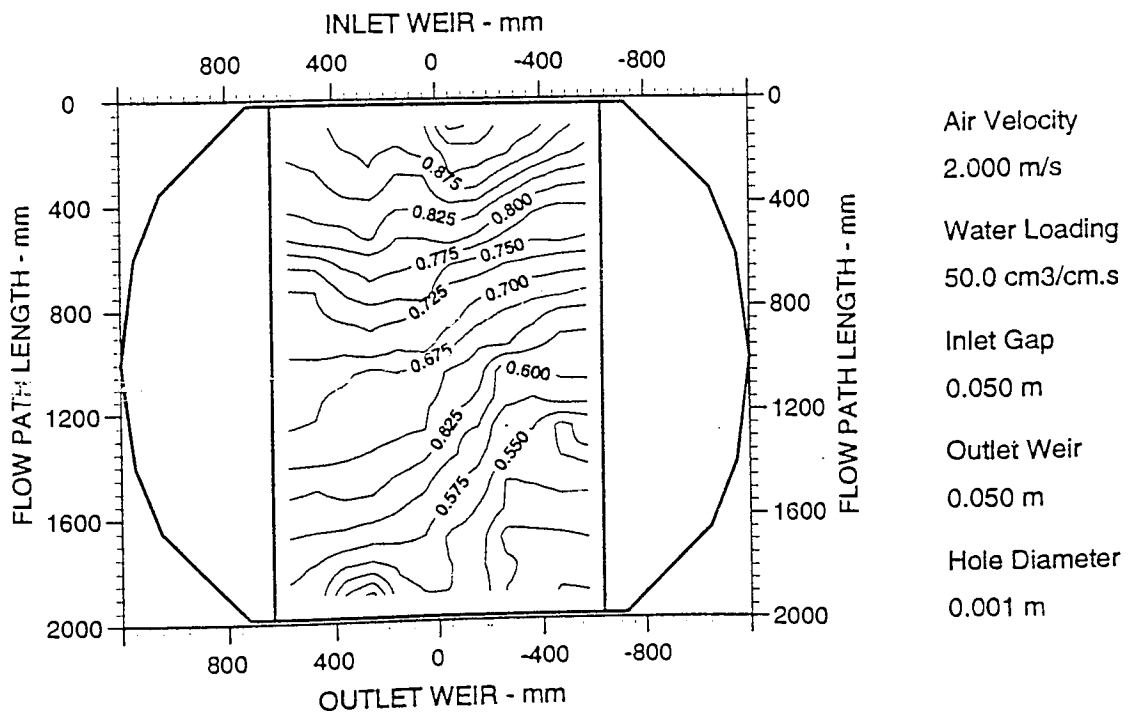


Fig. 8.10 a Two Dimensional Reduced Temperature Contour Plot
Superficial Air Velocity 2.0 m/s, No Slots

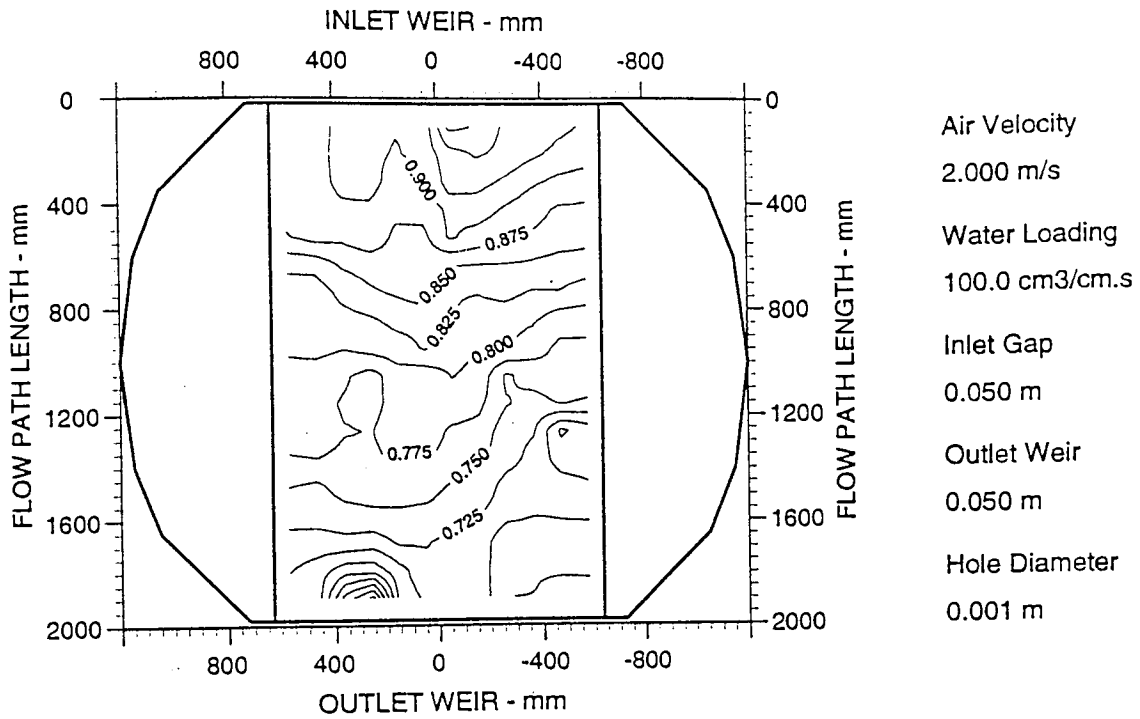


Fig. 8.10 b Two Dimensional Reduced Temperature Contour Plot
Superficial Air Velocity 2.0 m/s, No Slots

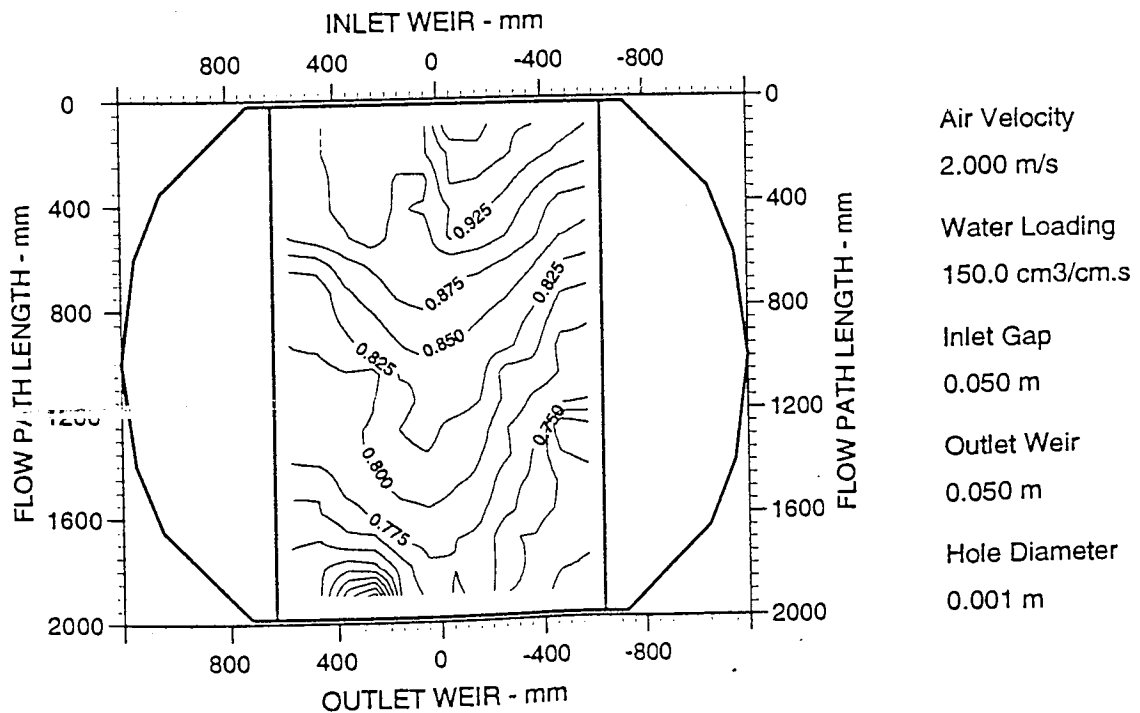
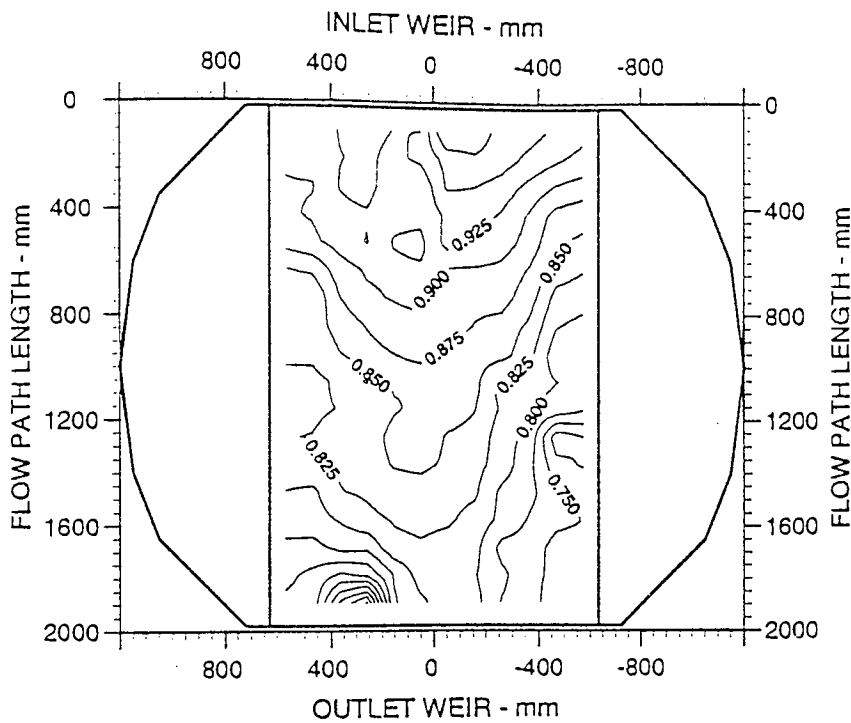


Fig. 8.10 c Two Dimensional Reduced Temperature Contour Plot
Superficial Air Velocity 2.0 m/s, No Slots



Air Velocity
2.000 m/s

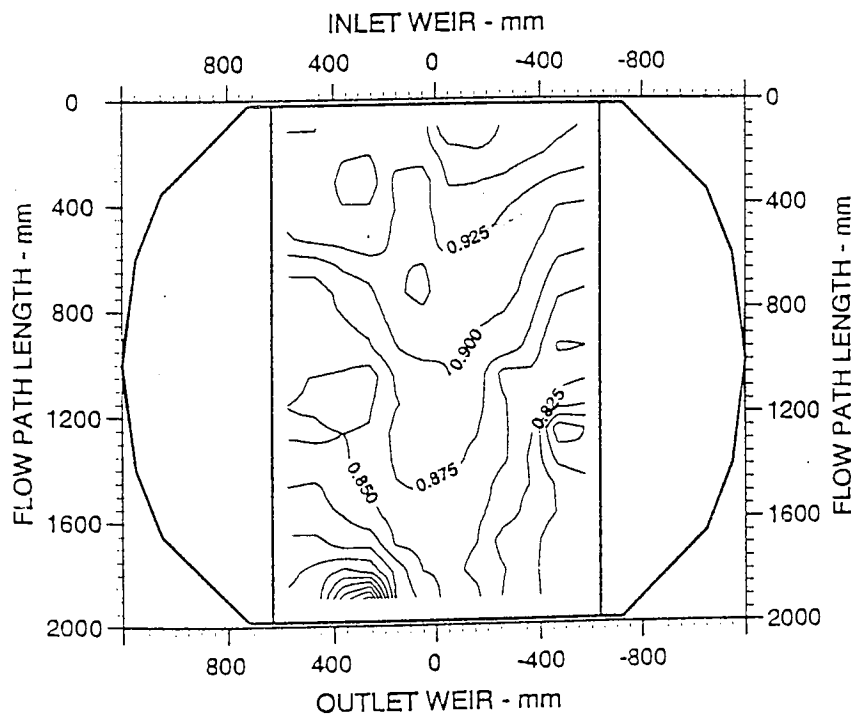
Water Loading
200.0 cm³/cm.s

Inlet Gap
0.050 m

Outlet Weir
0.050 m

Hole Diameter
0.001 m

Fig. 8.10 d Two Dimensional Reduced Temperature Contour Plot
Superficial Air Velocity 2.0 m/s, No Slots



Air Velocity
2.000 m/s

Water Loading
250.0 cm³/cm.s

Inlet Gap
0.050 m

Outlet Weir
0.050 m

Hole Diameter
0.001 m

Fig. 8.10 e Two Dimensional Reduced Temperature Contour Plot
Superficial Air Velocity 2.0 m/s, No Slots

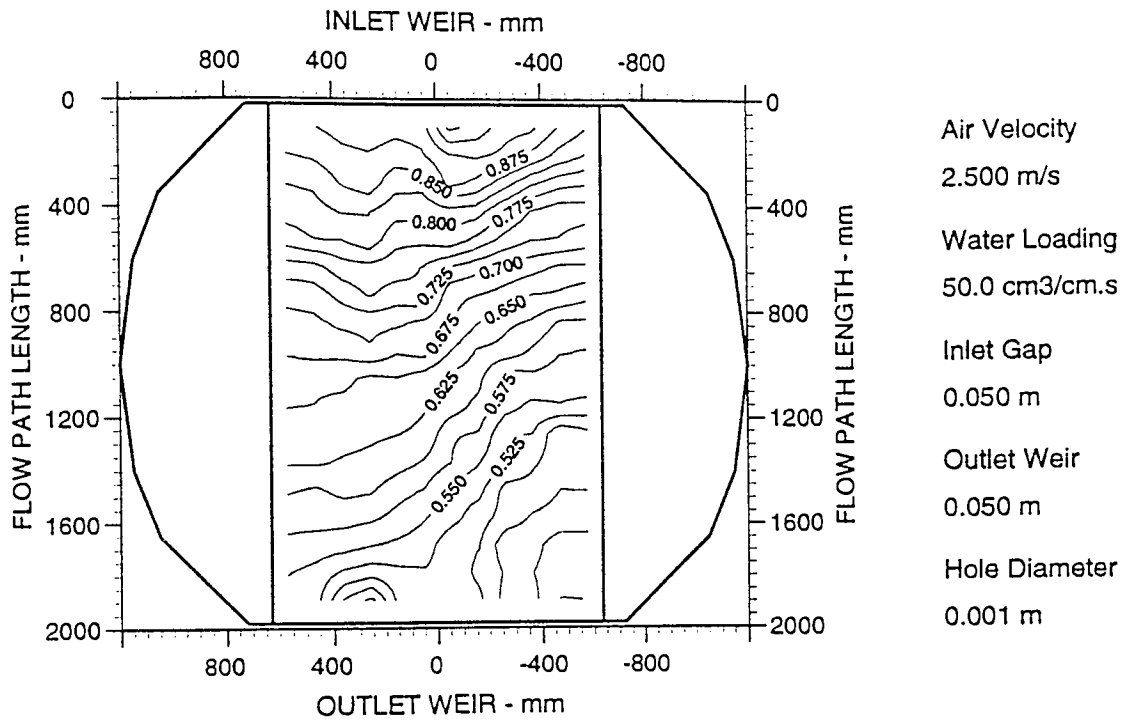


Fig. 8.11 a Two Dimensional Reduced Temperature Contour Plot
Superficial Air Velocity 2.5 m/s, No Slots

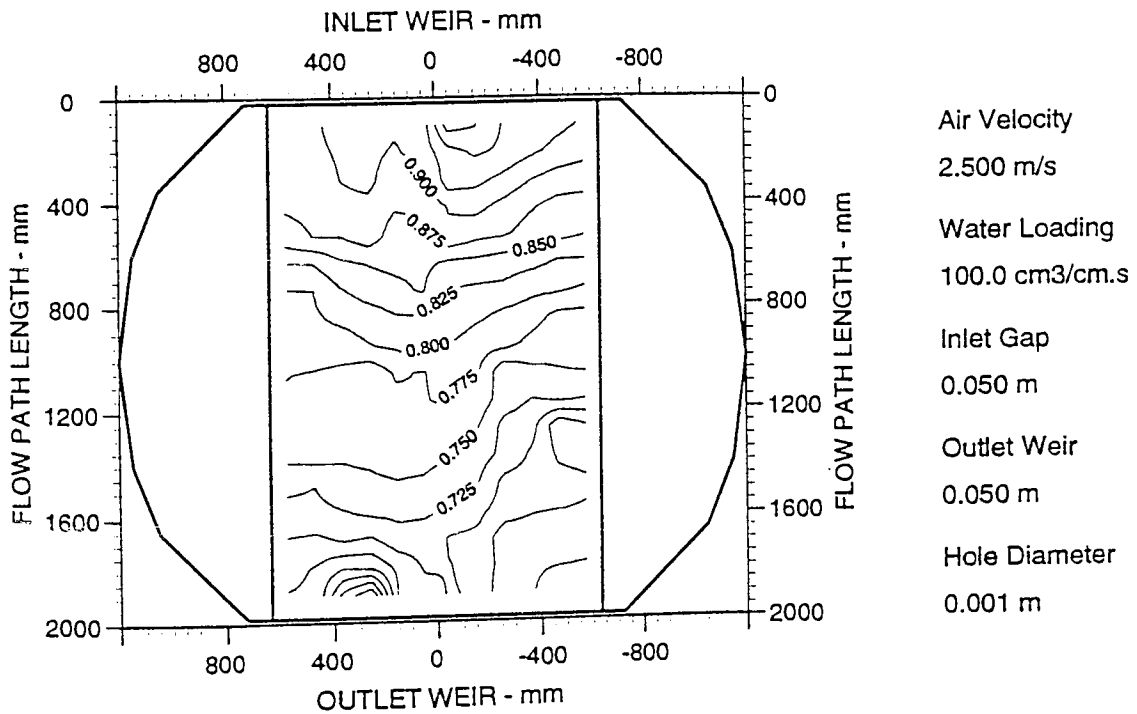


Fig. 8.11 b Two Dimensional Reduced Temperature Contour Plot
Superficial Air Velocity 2.5 m/s, No Slots

8.4.2 EFFICIENCY RESULTS AND DISCUSSION

The measured Murphree Tray and Point Efficiency Data for both the slotted and normal tray can be seen in Tables 8.1 and 8.2.

Figure 8.12 shows how the Murphree tray efficiency averaged for each water weir load, varies with weir load. For the slotted tray, at the low weir loading of $50 \text{ cm}^3/\text{cm s}$, the tray efficiency is found to be 80 % but this value decreases rapidly to 64 % as the weir load increases to $100 \text{ cm}^3/\text{cm s}$. Further increases in the weir load lead to marginal decrease in the efficiency. For an unslotted tray, however, at the low weir loading of $50 \text{ cm}^3/\text{cm s}$ the efficiency was 74 % which slightly decreases as the weir load increases.

Figure 8.13 shows how the Murphree point efficiency averaged for each water weir load, varies with weir load. For the slotted tray the point efficiency at the weir load of $50 \text{ cm}^3/\text{cm s}$ was found to be 49 %. On increasing the weir load to $150 \text{ cm}^3/\text{cm s}$, the point efficiency rises to its maximum value of 62 % and then decreases slightly with further increases in weir load. For the unslotted tray there is consistency in the value of the point efficiency even as the weir load increases from $50 \text{ cm}^3/\text{cm s}$ to $250 \text{ cm}^3/\text{cm s}$.

It is clear from the above results that the use of vapour-directing slots causes a reduction in both the point and tray efficiencies. The question that needs to be asked is 'What is causing these reductions in efficiency?' Using vapour-directing slots to reduce the height of clear liquid on the tray causes an increase in the liquid velocity as it is accelerated towards the outlet weir. This in turn causes a reduction in the liquid residence time which in turn causes a reduction in the tray efficiency. The reduction in the point efficiency can be accounted for by the size of the large bubbles that are passing through each slot.

It should be noted that the reduction in tray efficiency may not be apparent on a circular tray due to the correction of the non-uniform flow pattern. This is confirmed by research by Lockett (1986) who developed a new tray called 'Multiple-Downcomer Fractionation Tray

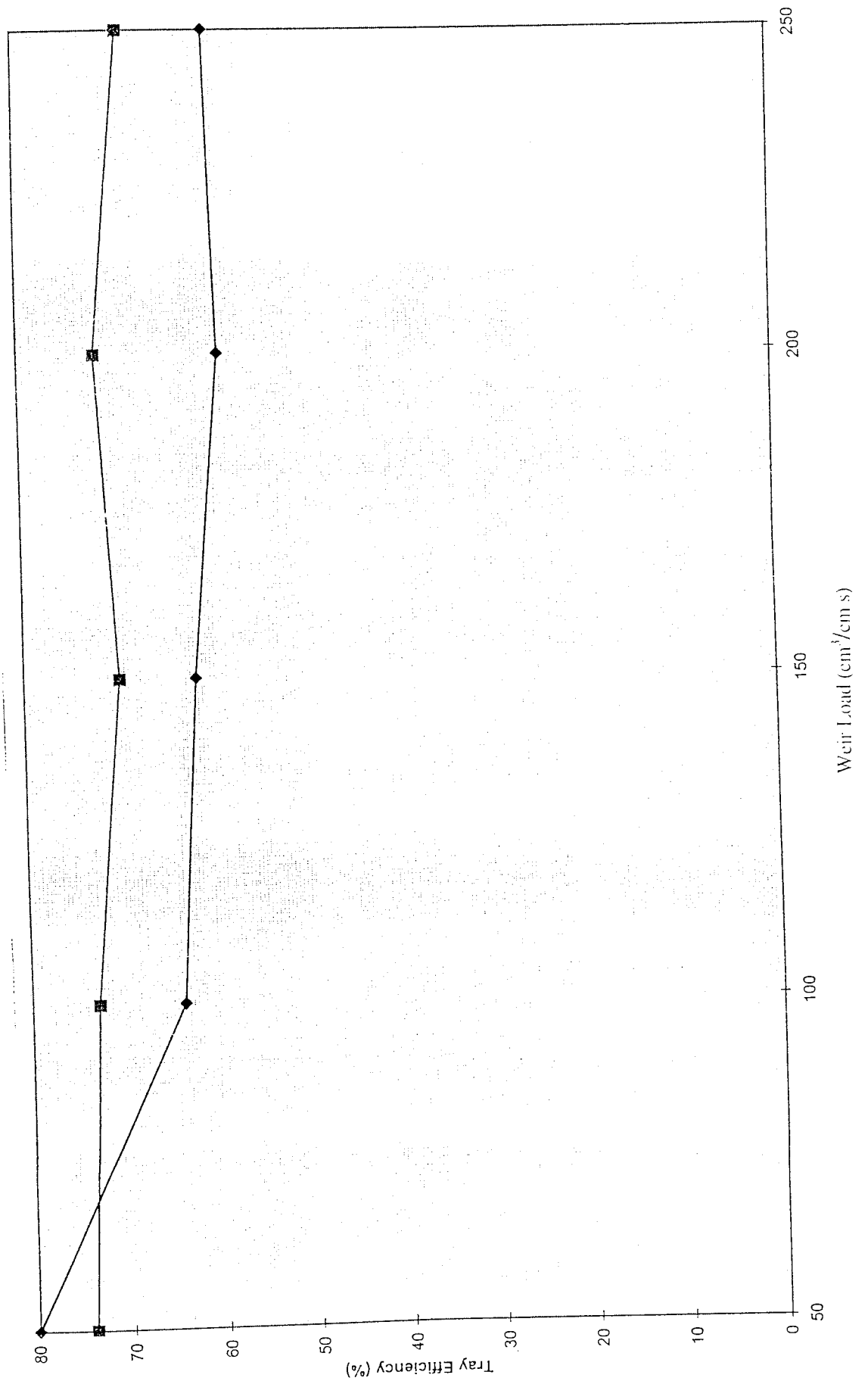
	Weir Load 50 cm ³ /cms	Weir Load 100 cm ³ /cms	Weir Load 150 cm ³ /cms	Weir Load 200 cm ³ /cms	Weir Load 250 cm ³ /cms
Superficial Air	Emv=0.8	Emv=0.63	Emv=0.6	Emv=0.56	Emv=0.58
Velocity 1.5 m/s	Eog=0.5	Eog=0.48	Eog=0.49	Eog=0.49	Eog=0.51
Superficial Air	Emv=0.8	Emv=0.66	Emv=0.64	Emv=0.61	Emv=0.62
Velocity 2.0 m/s	Eog=0.48	Eog=0.5	Eog=0.51	Eog=0.51	Eog=0.54
Superficial Air	Emv=1.01	Emv=0.73	Emv=0.63		
Velocity 2.5 m/s	Eog=0.49	Eog=0.49	Eog=0.48		

Table 8.1 Measured Murphree Efficiency Data- Slotted Tray, IG/OW= 50 mm

	Weir Load 50 cm ³ /cms	Weir Load 100 cm ³ /cms	Weir Load 150 cm ³ /cms	Weir Load 200 cm ³ /cms	Weir Load 250 cm ³ /cms
Superficial Air	Emv=0.77	Emv=0.77	Emv=0.75	Emv=0.75	Emv=0.72
Velocity 1.5 m/s	Eog=0.508	Eog=0.608	Eog=0.64	Eog=0.61	Eog=0.61
Superficial Air	Emv=0.7	Emv=0.69	Emv=0.75	Emv=0.69	Emv=0.65
Velocity 2.0 m/s	Eog=0.48	Eog=0.50	Eog=0.60	Eog=0.58	Eog=0.57
Superficial Air	Emv=0.65	Emv=0.62	Emv=0.65		
Velocity 2.5 m/s	Eog=0.43	Eog=0.48	Eog=0.51		

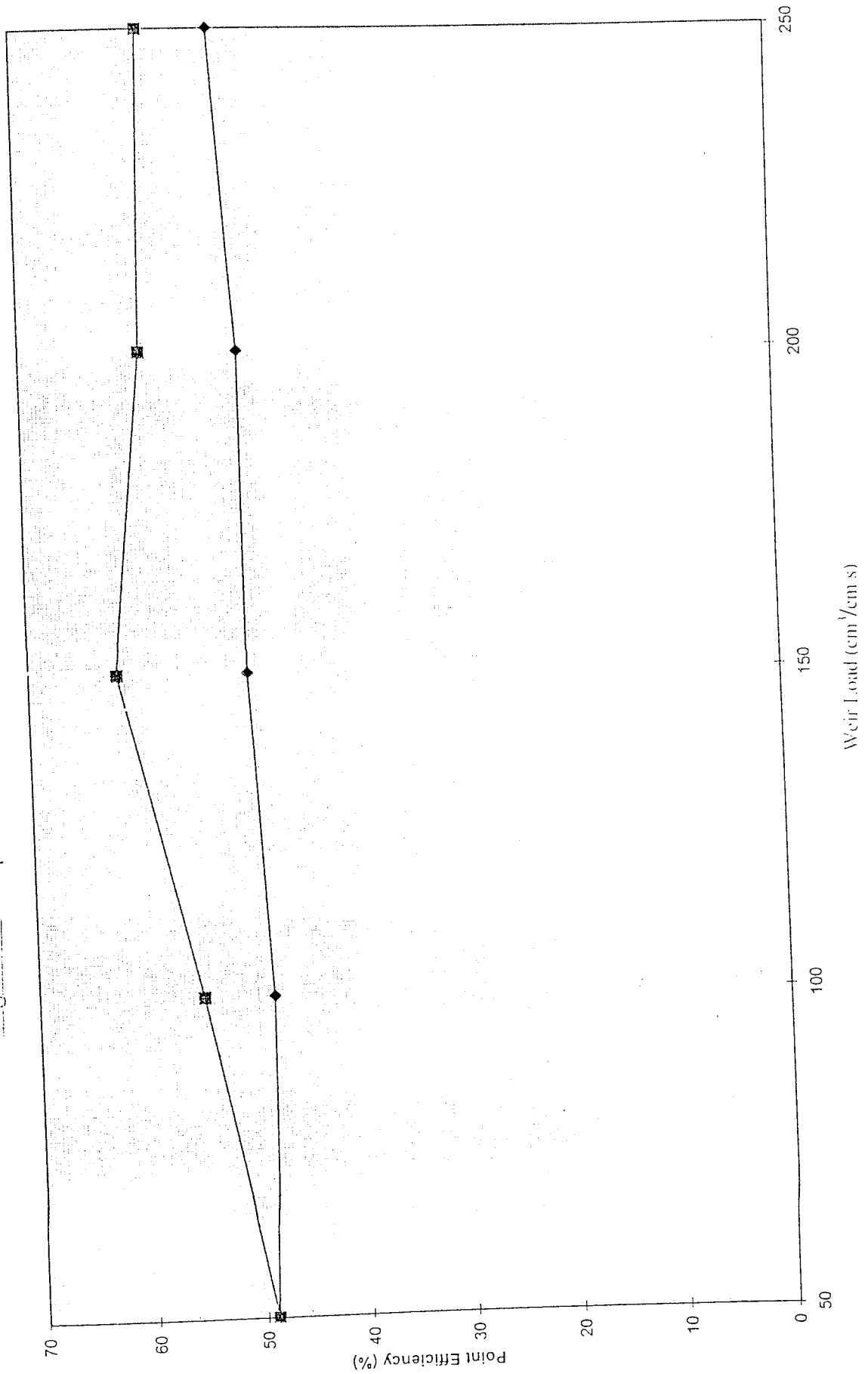
Table 8.2 Measured Murphree Efficiency Data- Normal Tray, IG/OW= 50 mm

Fig. 8.12 Graph of Measured Tray Efficiency Against Weir Load



◆ Slotted
— Unslotted

Fig. 8.13 Graph of Measured Point Efficiency Against Weir Load



◆ Slotted
■ Unslotted

8.5 CONCLUSIONS

From the results obtained in this Chapter, it is clear that the use of vapour-directing slots caused a reduction in both the point and tray efficiencies. The reduction in tray efficiency is due to a reduction in the bubble residence time and the reduction in point efficiency due to the size of the large bubbles passing through each slot.

The next question which needs to be answered is ' How does the tray efficiency of a circular slotted tray compare with the tray efficiency of a normal circular tray ?' This is the basis of the next Chapter.

CHAPTER 9

THE USE OF VAPOUR-DIRECTING SLOTS ON A CIRCULAR TRAY TO REMOVE STAGNANT OR CIRCULATING REGIONS AND INCREASE THROUGHPUT

9.1 INTRODUCTION

The previous Chapters have shown that aluminium vapour-directing slots can be used in obtaining a uniform flow pattern across a rectangular tray and reduce the froth height and hence increase the throughput leading to smaller tray spacing and ultimately lower overall tray pressure drop i.e. smaller columns. There is, however, the possibility of a reduction in both the point and tray efficiencies when using vapour-directing slots. The question that needs to be addressed is ' How does the tray efficiency of a circular slotted tray compare with the tray efficiency of a normal circular tray. The objective of the work in this Chapter is to test the slots on a full circular tray and assess their effectiveness with regards removal of stagnant or circulating regions. In order to do this experiments were carried out using the measurement of the downcomer back-up and also the monitoring of dye across the tray. The water-cooling technique was also used to measure the tray efficiencies.

9.2 Camera Recording of Coloured Dye

The monitoring of liquid flow across a circular tray using a coloured dye, with straight sided chordal weirs, was a highly popular technique among several workers (Weiler et al., 1971, 1973; Porter et al., 1972; Ani, 1988; Hine, 1990). The technique used to show flow non-uniformities on a tray involved the continuous injection of dye from the inlet downcomer until the whole of the single liquid phase or biphase was completely coloured. On stopping the dye injection, the coloured dye in the liquid was removed by fresh clear liquid entering the tray. The rate of coloured dye removal was monitored by camera which showed non-uniform flow as well as regions of longer residence time on the tray.

Ani (1988) and Hine (1990) observed the movement of potassium permanganate dye discharged from a solenoid controlled pulse injection system fitted across the length of the inlet downcomer. In these experiments the coloured dye moved faster in the middle of the tray, whilst at the sides of the tray, it moved very slowly or was forced to circulate.

The dye injection apparatus used in these experiments can be seen from Figure 9.1. It consists of a volume of potassium permanganate solution which is connected to a 20 mm Copper pipe which in turn is connected to an oval shape 15 mm Copper pipe which has a series of 1 mm holes that are 50 mm apart which evenly distributes the dye along the length of the inlet weir.

Dye Injection System
(Not to Scale)

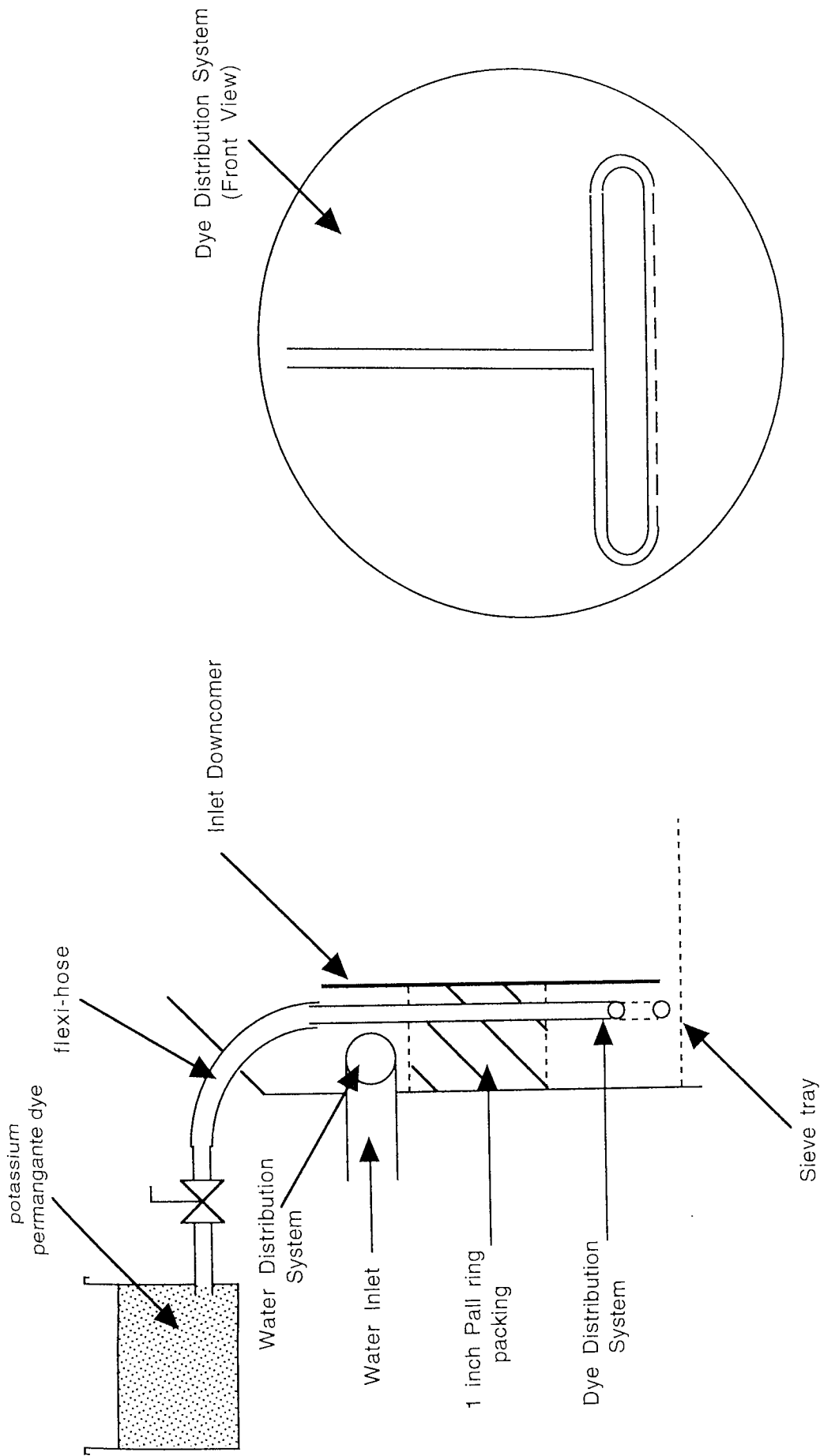


Fig. 9.1 Schematic Diagram Showing the Dye Injection Apparatus

9.3 Vapour-Directing Slot Layout Across Circular Sieve Tray

It should be noted that in order to obtain equal residence time for the liquid on the tray the liquid in the centre of the tray would require less momentum to travel towards the outlet weir. The liquid travelling at the sides of the circular tray has a longer flow path length and would thus need more momentum in order to obtain equal residence time across the whole of the tray. In order to do this the slots were placed in the tray in proportion to the flow path length. Using the figure 9.2 it can be seen that:

If $Z =$ Flow Path Length = 1.9 m

$C =$ Flow Path Length Around the Side of the Tray = 3 m

$t_z =$ residence time across the centre of the tray

$t_c =$ residence time across the sides of the tray

Then if Velocity = $\frac{\text{distance}}{\text{time}}$, then $V_z = \frac{Z}{t_z}$ and $V_c = \frac{C}{t_c}$

Objective : $t_z = t_c$

Therefore $\frac{V_c}{V_z} = \frac{C}{Z} = \frac{3}{2} = 1.5$

ie. $V_c = 1.5V_z$

Hence we need 1.5 times more slots around the sides of the tray than in the centre of the tray.

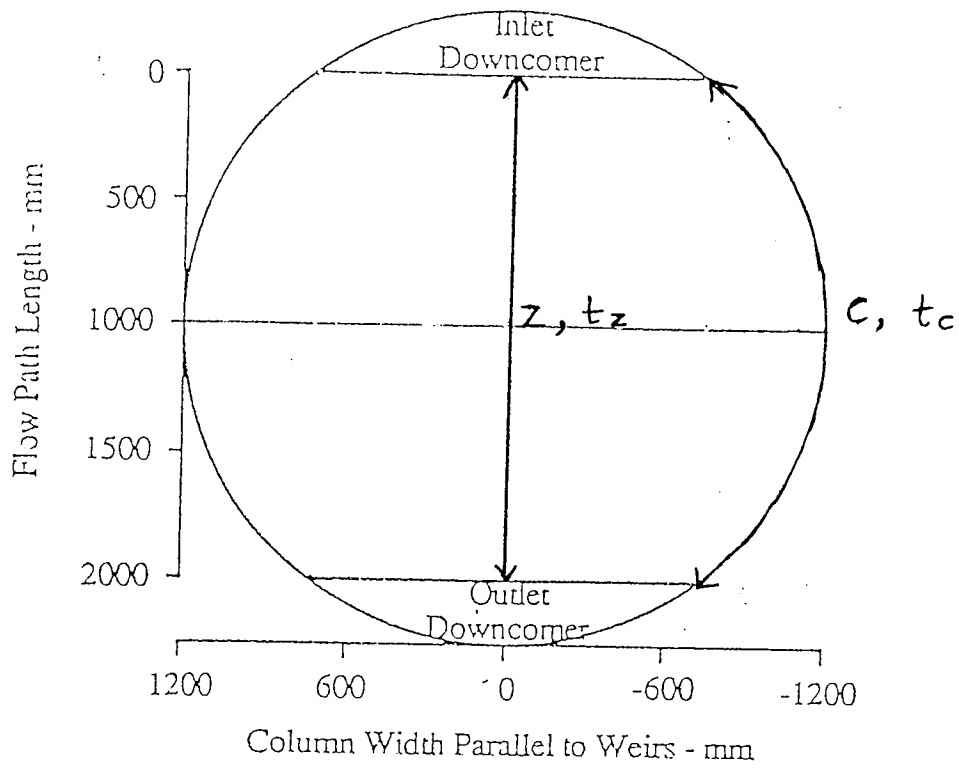


Fig. 9.2 Diagram Showing the Residence Time/ Flow Path Length across a Circular Tray

9.4 EXPERIMENTAL PROCEDURE

The study was performed for inlet gap and outlet weir of 50 mm. The values of the air flowrates used ranged from 0.75 m/s to 2.0 m/s, whilst the water flowrate was varied between 50 cm³/cm s. After steady state was achieved, the potassium permanganate solution was released along the length of the inlet weir. The progress of the dye as it crossed along the length of the tray was monitored by a video camera above the tray and also visual observation. For the slotted tray twenty-four vapour directing slots were positioned over the 2.44 m circular tray as shown in figure 9.3. The arrows denoting the direction that each slot was positioned in. Measurements of the downcomer back-up were noted both for the slotted and unslotted tray.

The water-cooling technique was carried out using the method outlined in Chapter 8.

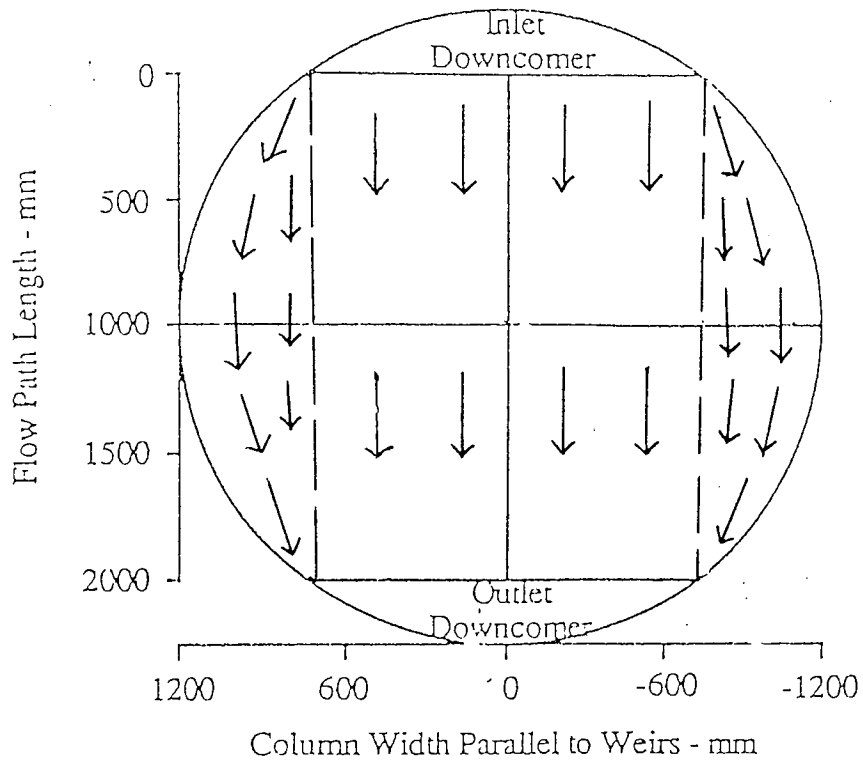


Fig. 9.3 Diagram Showing the 24 Vapour-Directing Slots Positioned Over the 2.44 m Circular Tray

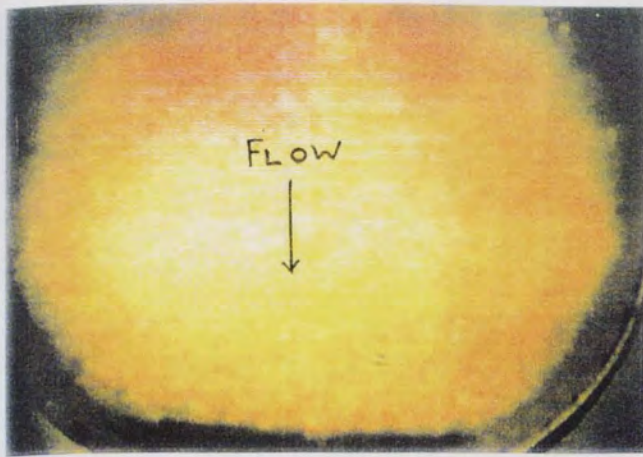
9.5 RESULTS AND DISCUSSION

9.5.1 DYE INJECTION RESULTS

After steady state was achieved, potassium permanganate solution was released along the length of the inlet weir using the apparatus constructed. The progress of the dye, as it crossed the tray from the inlet weir to the outlet weir, was monitored by a video camera 4.5 m above the tray.

Many dye tracer experiments were videoed and studied. Figures 9.4 to 9.6 each present a series of still photographs taken from the video recording of the dye injection studies, see Appendix 5. In the initial experiments with high superficial velocities and high weir loads, difficulties arose with the clarity of the dye in the turbulent froth mixture. It can be seen, however, from the still photographs that using low superficial air velocities and weir loads the dye injection system leads to enhanced clarity of the dye but more importantly the dye is uniformly distributed along the whole of the inlet weir and quickly colours the whole of the biphasic mixture.

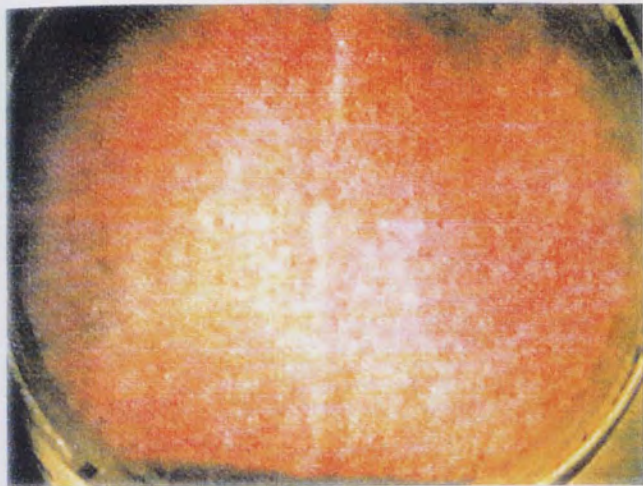
Figure 9.4 a shows an unslotted tray with superficial air velocity of 0.75 m/s and weir load $25 \text{ cm}^3/\text{cm s}$. The photographs show the dye entering the tray and spreading across and eventually completely covering the tray. The photographs also show the dye being slowly removed initially from the centre of the tray working its way towards the sides indicating that the bulk water flows in a straight direction between the inlet and outlet downcomers. The time taken for the sequence of the dye entering the tray and being cleared by fresh water is 2 minutes. With the slotted tray, however, at the same conditions it can be seen from figure 9.4 b, that the fresh liquid is removed quicker from the sides of the tray and also more importantly there is less dye at the sides of the tray indicating that the slots were successful in reducing the size of the stagnant zones. Similar observations were recorded with superficial air velocities of 1m/s and 1.5 m/s, see figures 9.5 to 9.6.



20 SECS



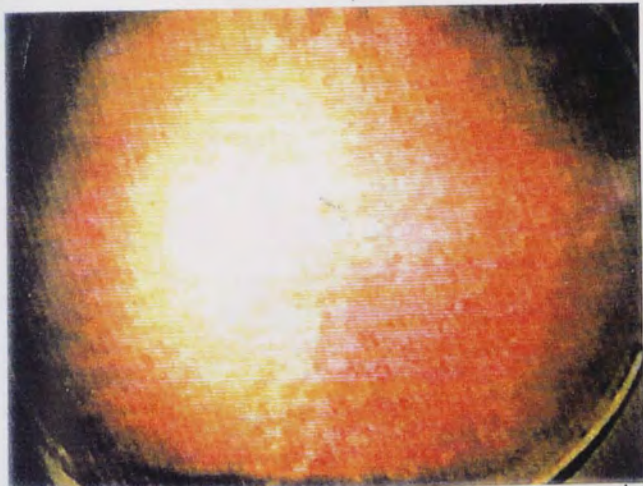
40 SECS



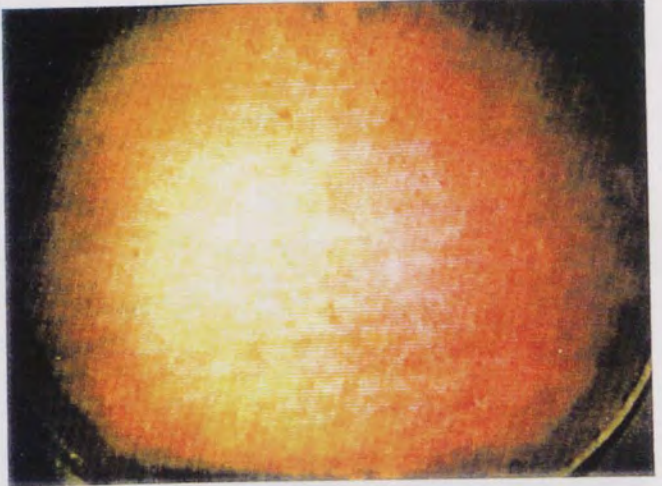
65 SECS



80 SECS

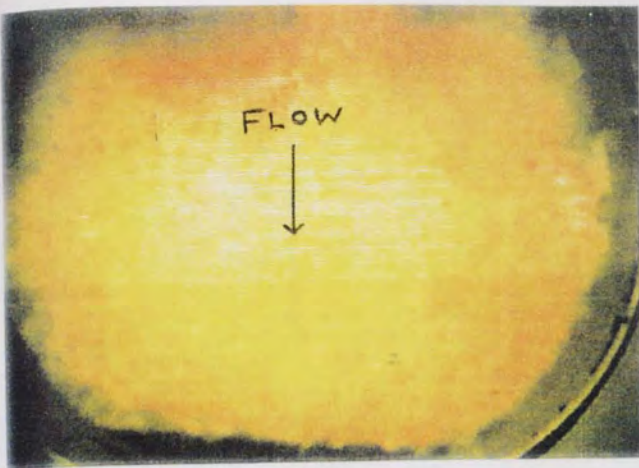


100 SECS



120 SECS

Fig. 9.4 a Still Photograph of an unslotted tray, superficial air velocity = 0.75 m/s, Water Weir Load = 25 cm³/cms



20 SECS



30 SECS



50 SECS



70 SECS

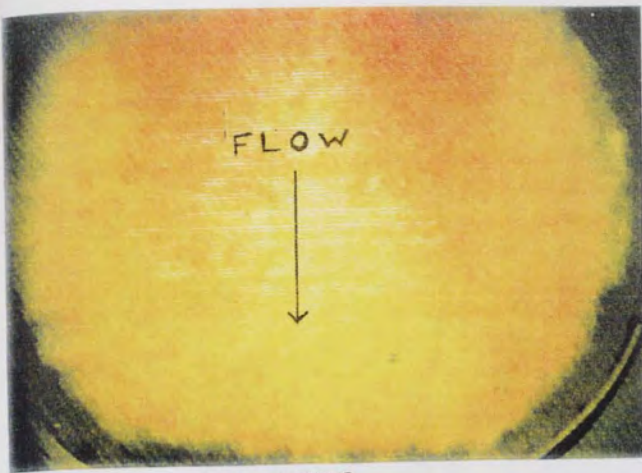


90 SECS



110 SECS

Fig. 9.4 b Still Photograph of a. slotted tray, superficial air velocity = 0.75 m/s,
Water Weir Load = 25 cm³/cms



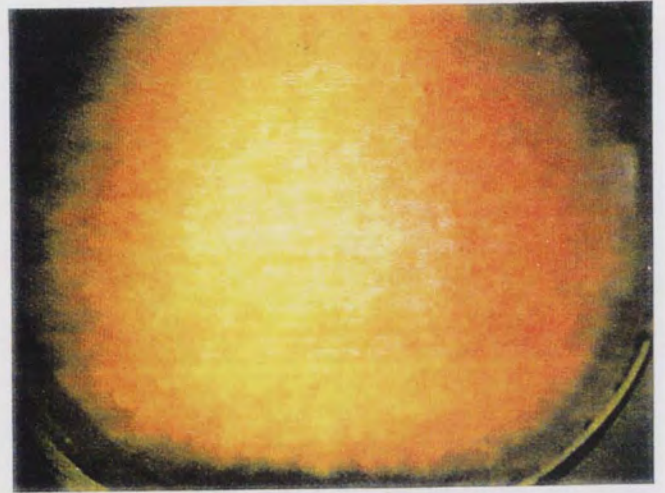
20 SECS



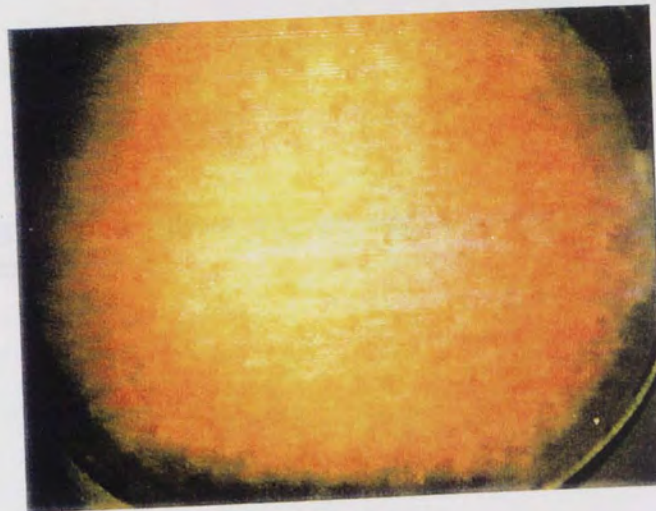
45 SECS



60 SECS

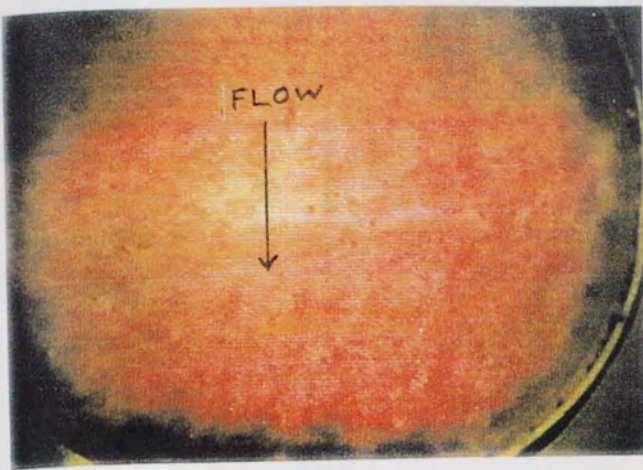


75 SECS

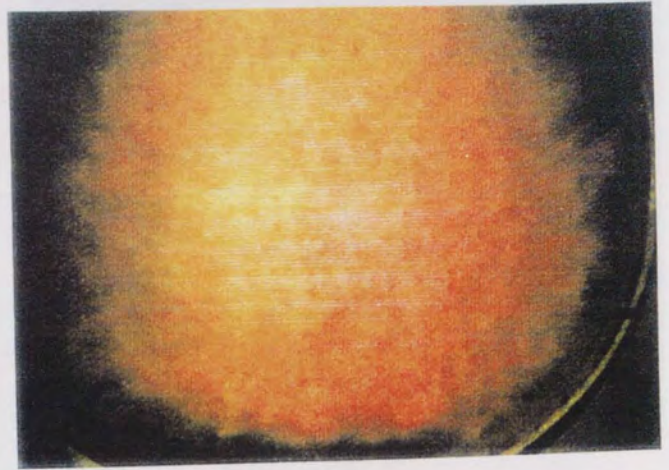


90 SECS

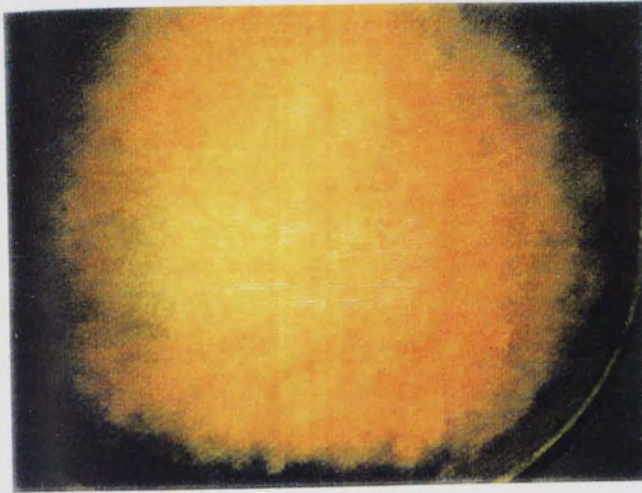
Fig. 9.5 a Still Photograph of an unslotted tray, superficial air velocity = 1.0 m/s,
Water Weir Load = 75 cm³/cms



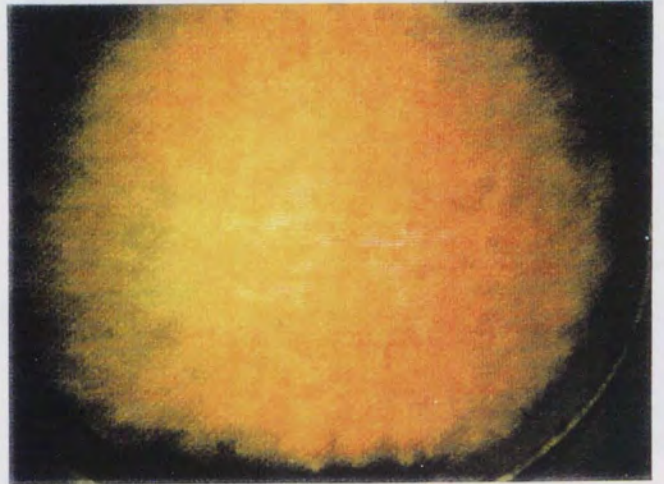
40 SECS



60 SECS

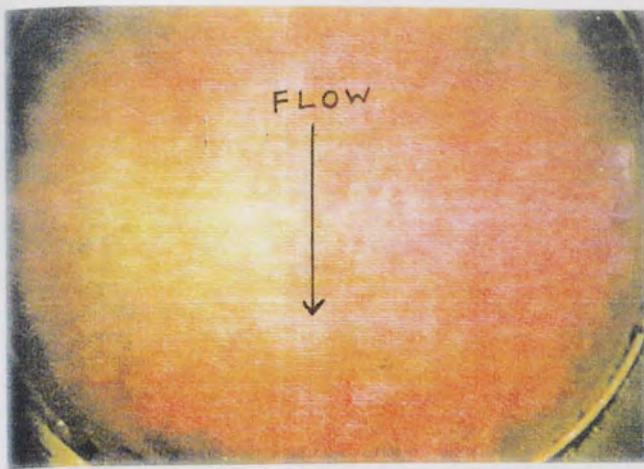


70 SECS

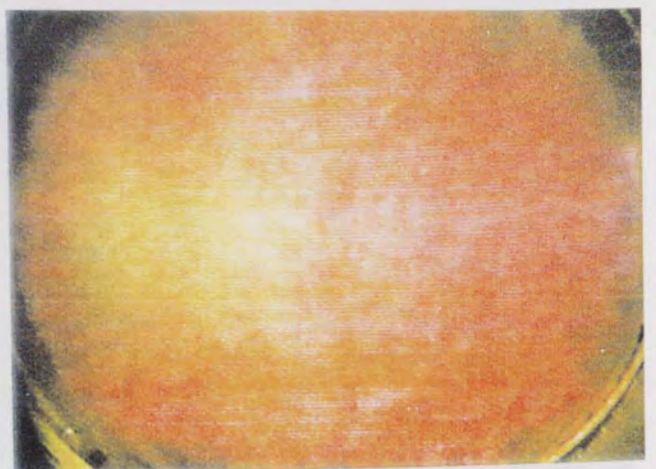


80 SECS

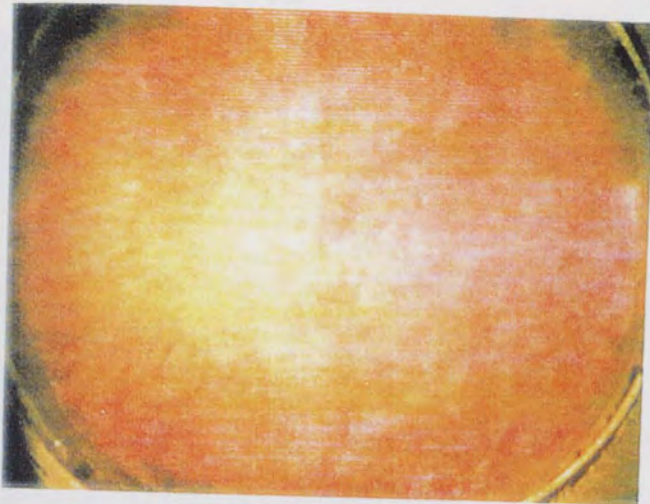
Fig. 9.5 b Still Photograph of a slotted tray, superficial air velocity = 1.0 m/s, Water Weir Load = 75 cm³/cms



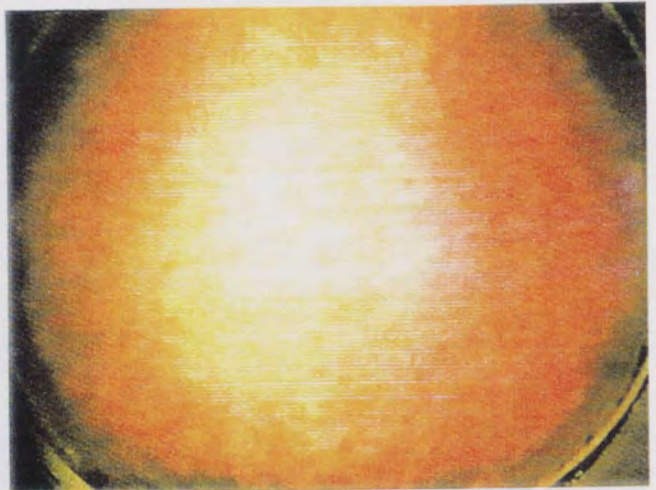
30 SECS



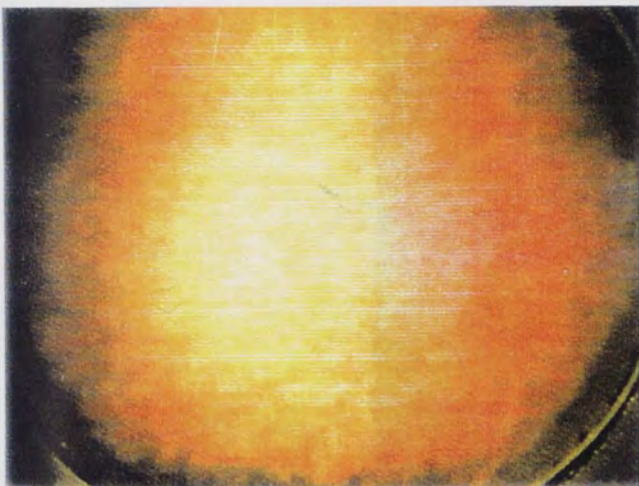
40 SECS



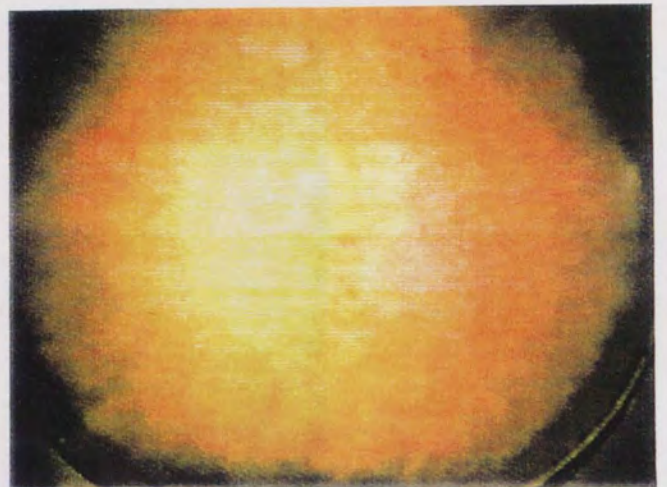
50 SECS



60 SECS

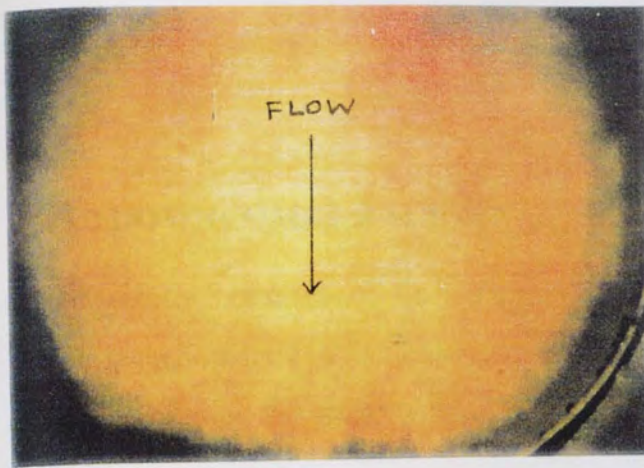


70 SECS

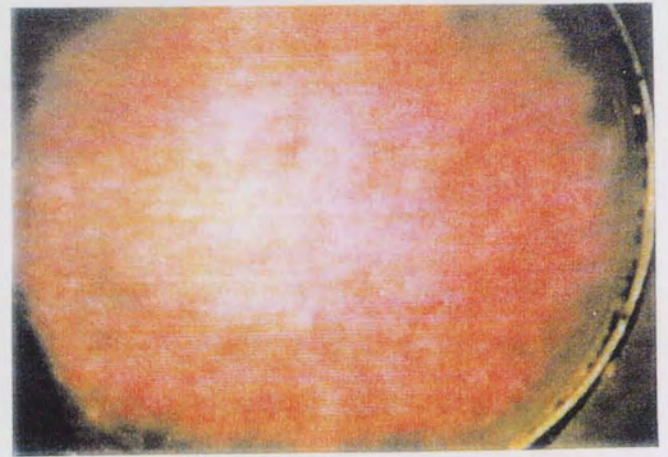


80 SECS

Fig. 9.6 a Still Photograph of an unslotted tray, superficial air velocity = 1.5 m/s, Water Weir Load = 100 cm³/cms



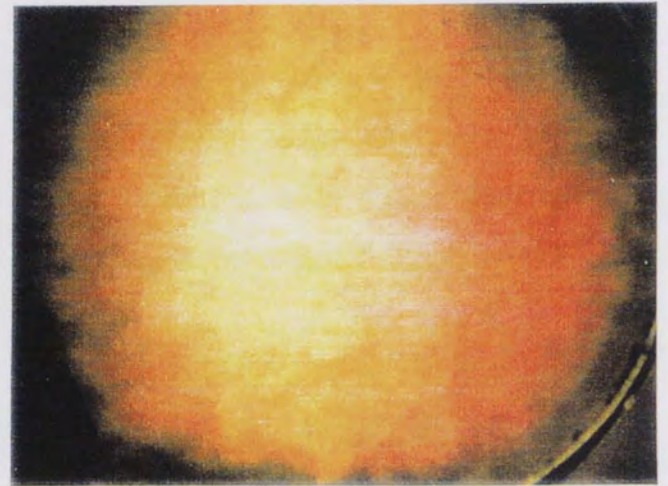
15 SECS



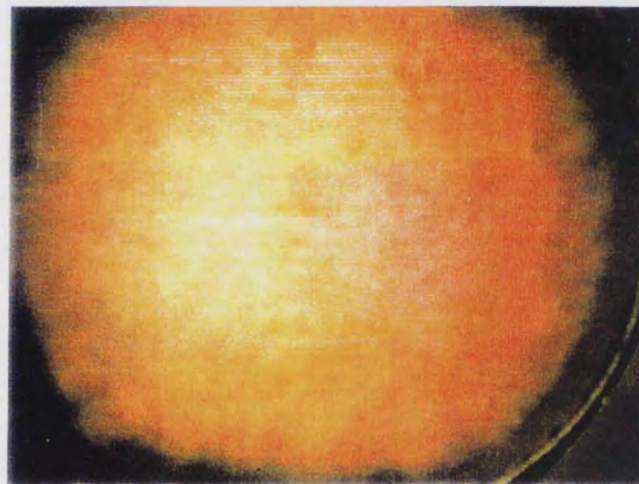
30 SECS



45 SECS



60 SECS



70 SECS

Fig. 9.6 b Still Photograph of a slotted tray, superficial air velocity = 1.5 m/s, Water Weir Load = 100 cm³/cms

9.5.2 DOWNCOMER BACKUP

The results obtained of the height of clear liquid in the downcomer using the six manometers placed in the inlet downcomer can be seen in Appendix 4. The results can be seen in Figures 9.7 to 9.9 where the average downcomer backup is plotted against weir load.

At superficial air velocities of 1.0 m/s and at low weir loads, the value of the average downcomer backup for a normal tray is 6.1 cm which steadily increases with increasing weir load values reaching a figure of 10.5 cm. With the slotted tray, however, at low weir loads, the downcomer back up is 5.5 cm (approximately 0.6 cm less liquid) which rises to a value of 9.9 cm at weir load of $250 \text{ cm}^3/\text{cm s}$.

At higher superficial air velocity a similar pattern is repeated. However, the difference in downcomer backup between a normal tray and a slotted tray increases on average to 1 cm.

Fig. 9.7 Downcomer Hydraulics Full Circular tray: $IG/W = 50$ mm, Sup. Air Vel. = 1.0 m/s

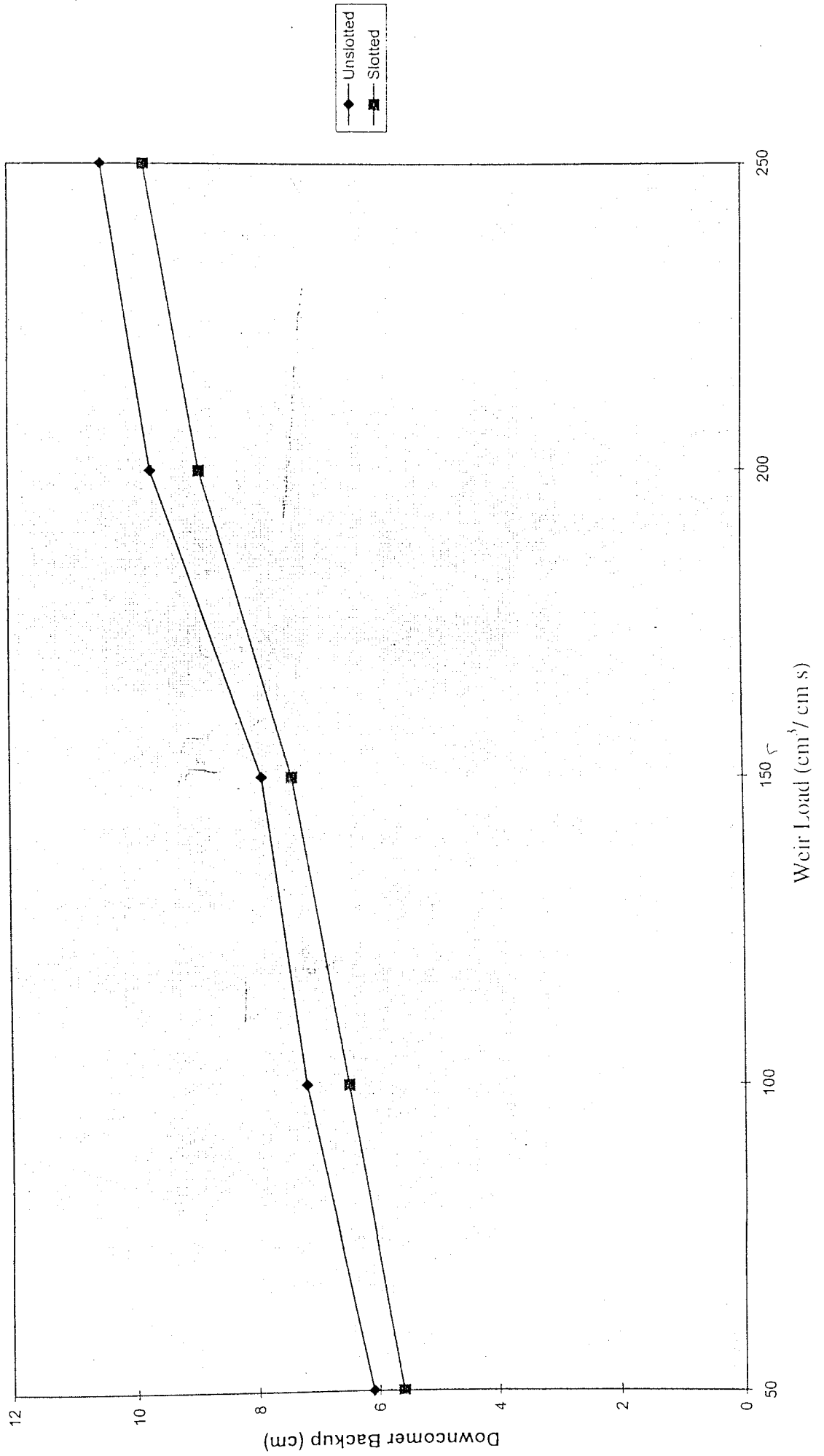


Fig. 9.8 Downcomer Hydraulics Full Circular Tray: IG:OW = 50 mm, Sup. Air Vel. = 1.5 m/s

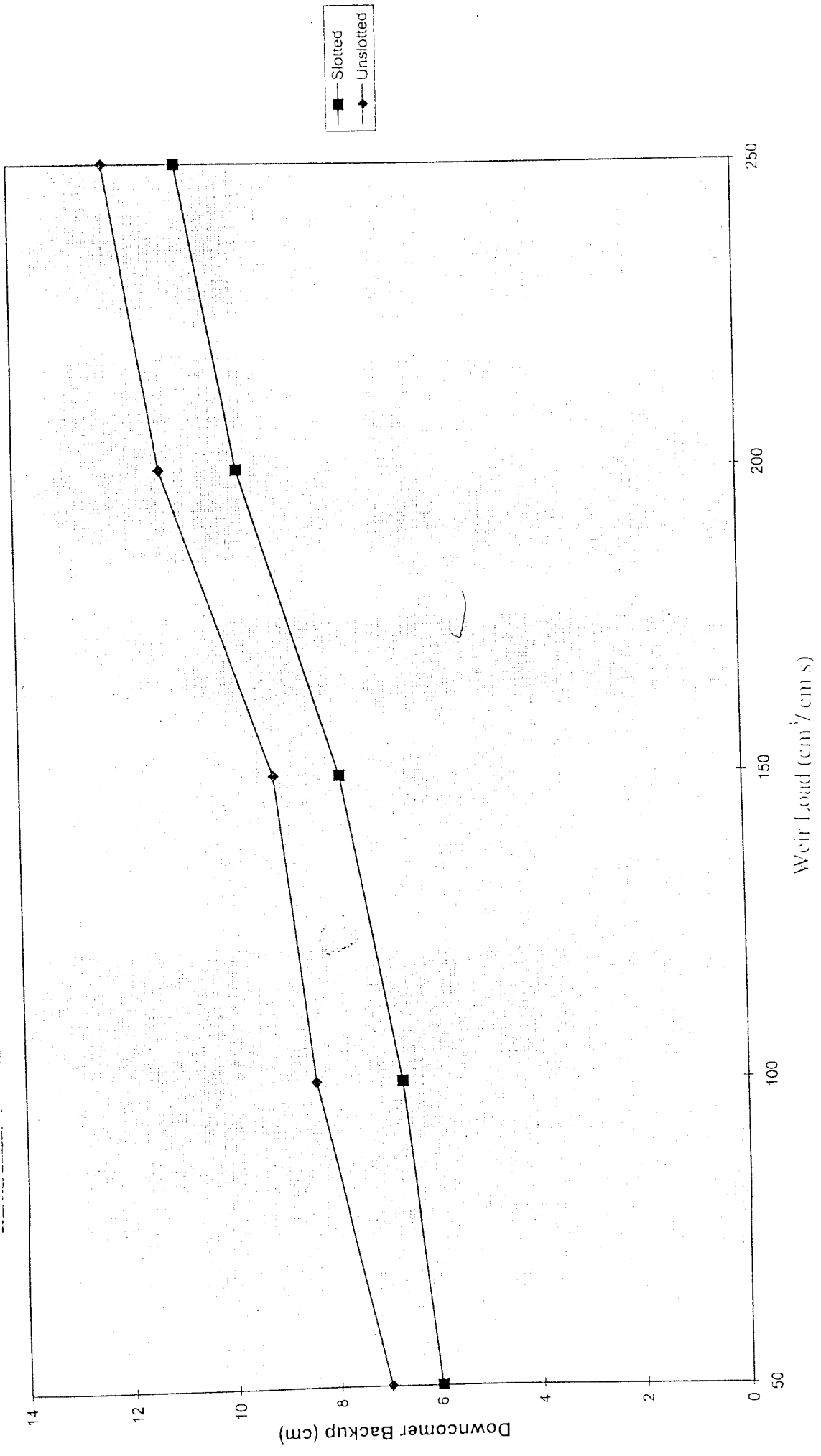
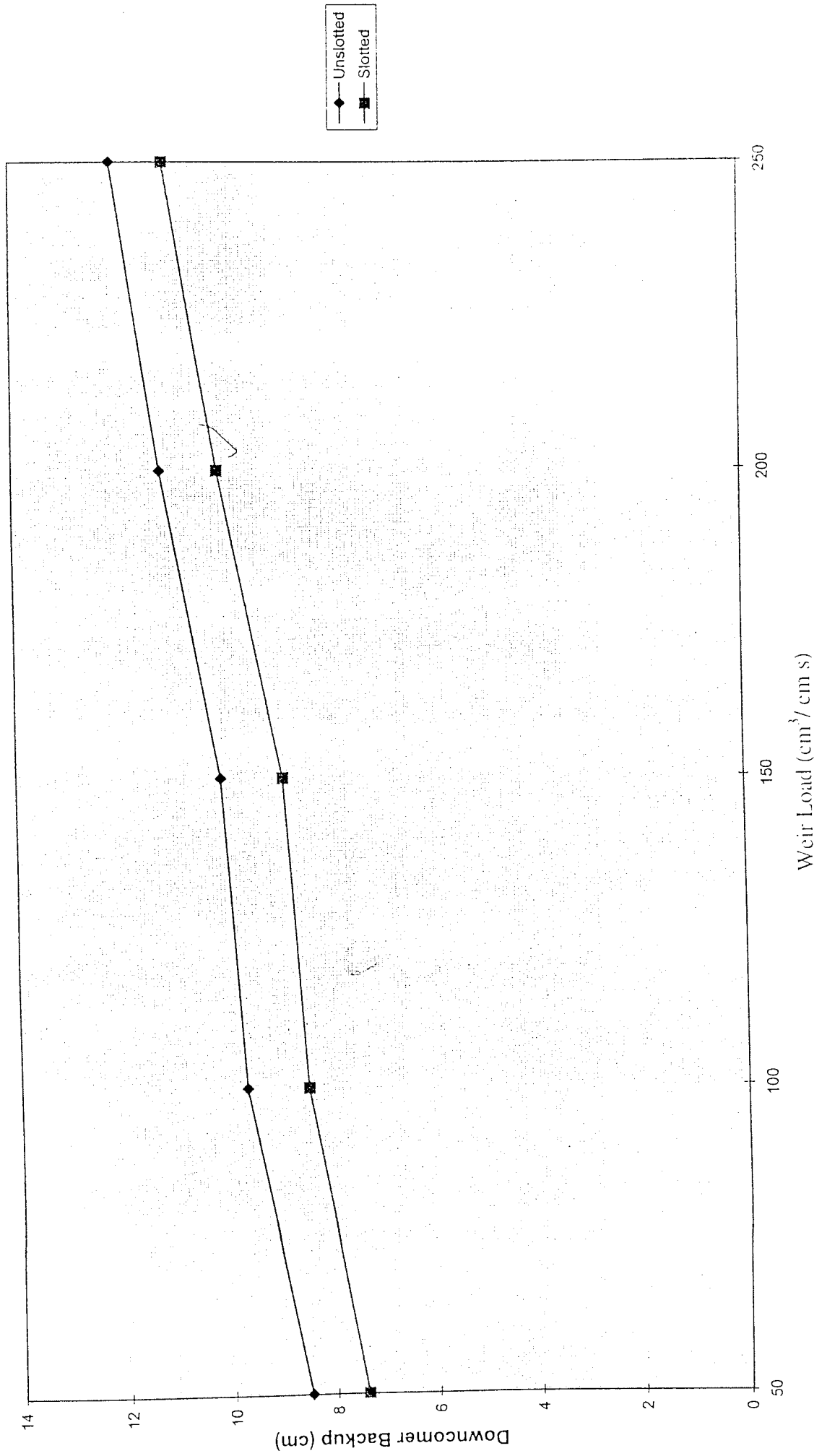


Fig. 9.9 Downcomer Hydraulics Full Circular Tray: IG/IOW =50 mm, Sup. Air Vel.=2.0 m/s



9.5.3 TRAY EFFICIENCY RESULTS

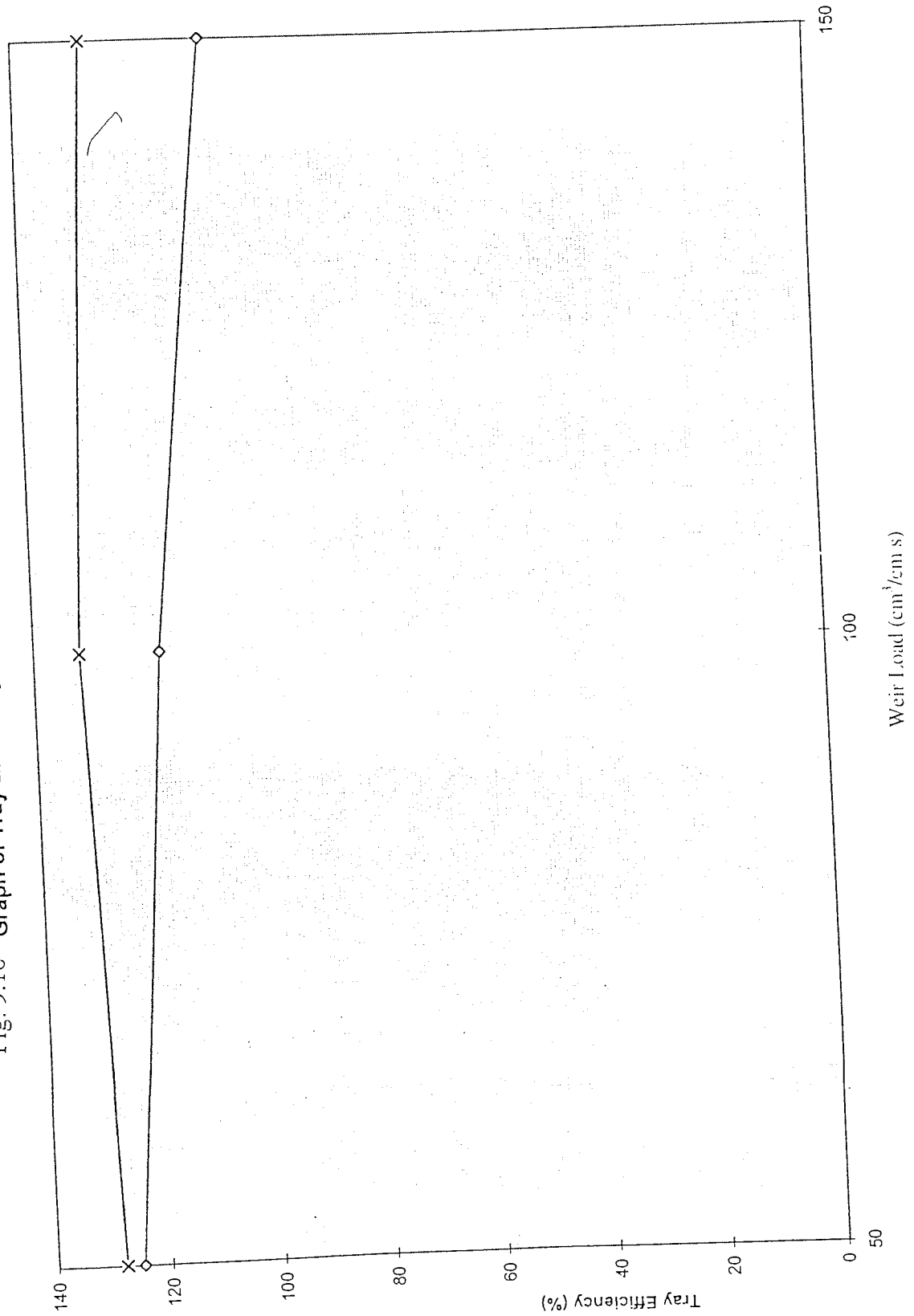
Figures 9.10 to 9.11 show how the Murphree tray efficiencies vary with weir load for a slotted tray compared with a normal tray. Referring to figure 9.11 and for a superficial air velocity of 1.5 m/s at low weir loads of 50 cm³/cm s, the tray efficiency is found to be 124 % which steadily decreases to 113 % as the weir load increases to 150 cm³/cm s. For the slotted tray, however, at the low weir loading of 50 cm³/cm s, the efficiency was 134 % (an increase in 10 %) which reaches a value of 152 % at a weir load of 100 cm³/cm s before decreasing to 132 % at the weir loading of 150 cm³/cm s.

At the superficial air velocity of 2.0 m/s, at low weir loads, it can be seen from figure 9.11 that there is little difference in tray efficiencies between a normal and slotted tray. With increasing weir load, however, the difference in efficiencies increases to 20 %.

It is clear from the results obtained that the vapour-directing slots were successful in reducing the stagnant/ slow moving liquid which had the effect of increasing the tray efficiency.

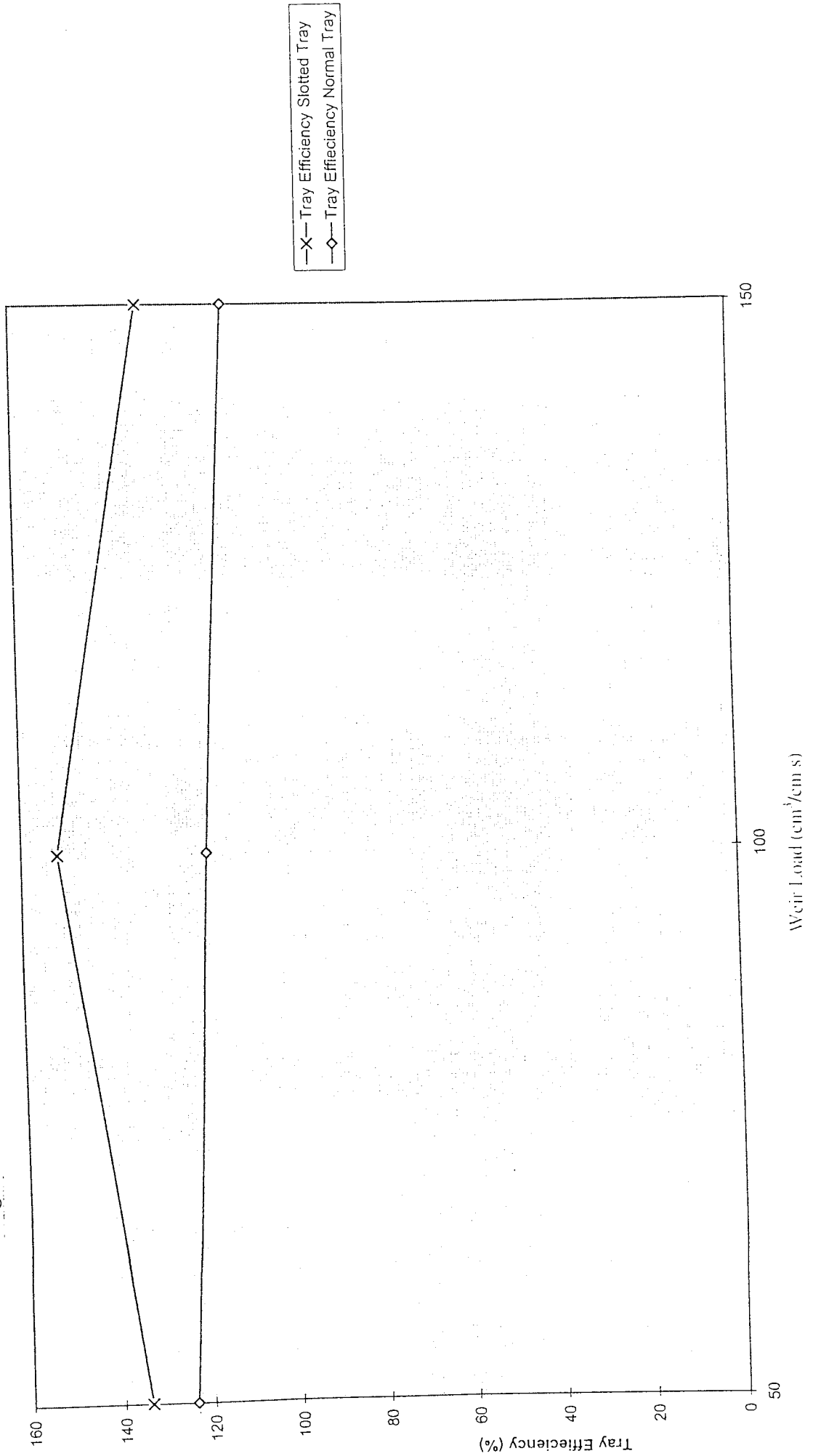
These tray efficiency results compare well with those results obtained by Hines (1990) on the same 1mm circular sieve tray. Further experiments could be carried out to obtain the comparison of the point efficiency (unlikely to change) and a more detailed comparison of the flow patterns across a rectangular and circular tray.

Fig. 9.10 Graph of Tray Efficiency Against Weir load, Superficial Air Velocity = 2.0 m/s



—x— Tray Efficiency Slotted Tray
—o— Tray Efficiency Normal Tray

Fig. 9.11 Graph of Tray Efficiency Against Weir Load, Superficial Air Velocity = 1.5 m/s



9.6 CONCLUSIONS

In a cross-type sieve plate, the liquid emerging from the inlet downcomer tends to flow directly towards the outlet downcomer without appreciable spreading towards the side of the plate. The liquid channelling produced affects the plate efficiency and the effect becomes more prominent as the plate diameter is increased.

It is clear from the results obtained in this Chapter that the use of vapour-directing slots distributed across a large circular sieve tray helps to reduce the size of the areas of slow moving/ stagnant liquid, in turn, this leads to more uniform flow of liquid across the tray and to an increase in the tray efficiency. It is also clear from the results obtained from the video camera that the liquid in the centre of the tray is travelling much faster than that at the sides of the tray i.e. it has a shorter residence time.

It is interesting to note that in Chapter 8 , the rectangular normal tray had better efficiencies than the slotted rectangular tray whereas the work in this Chapter has shown that a slotted circular tray has better efficiencies than a normal circular tray. The reasons for the former have been discussed in 8.4.2 whilst the reasons for the latter are due mainly to the reduction in the stagnant/ slow moving liquid by the vapour-directing slots. There is, however, more improvement in the tray efficiency of a circular slotted tray as an optimum slot layout could be investigated which would allow the liquid to have equal residence time over the whole of the tray coupled with the elimination of the stagnant/ slow moving liquid.

CHAPTER 10

EXPERIMENT TO MEASURE THE VELOCITY OF AIR THROUGH A SINGLE VAPOUR-DIRECTING SLOT

10.1 INTRODUCTION

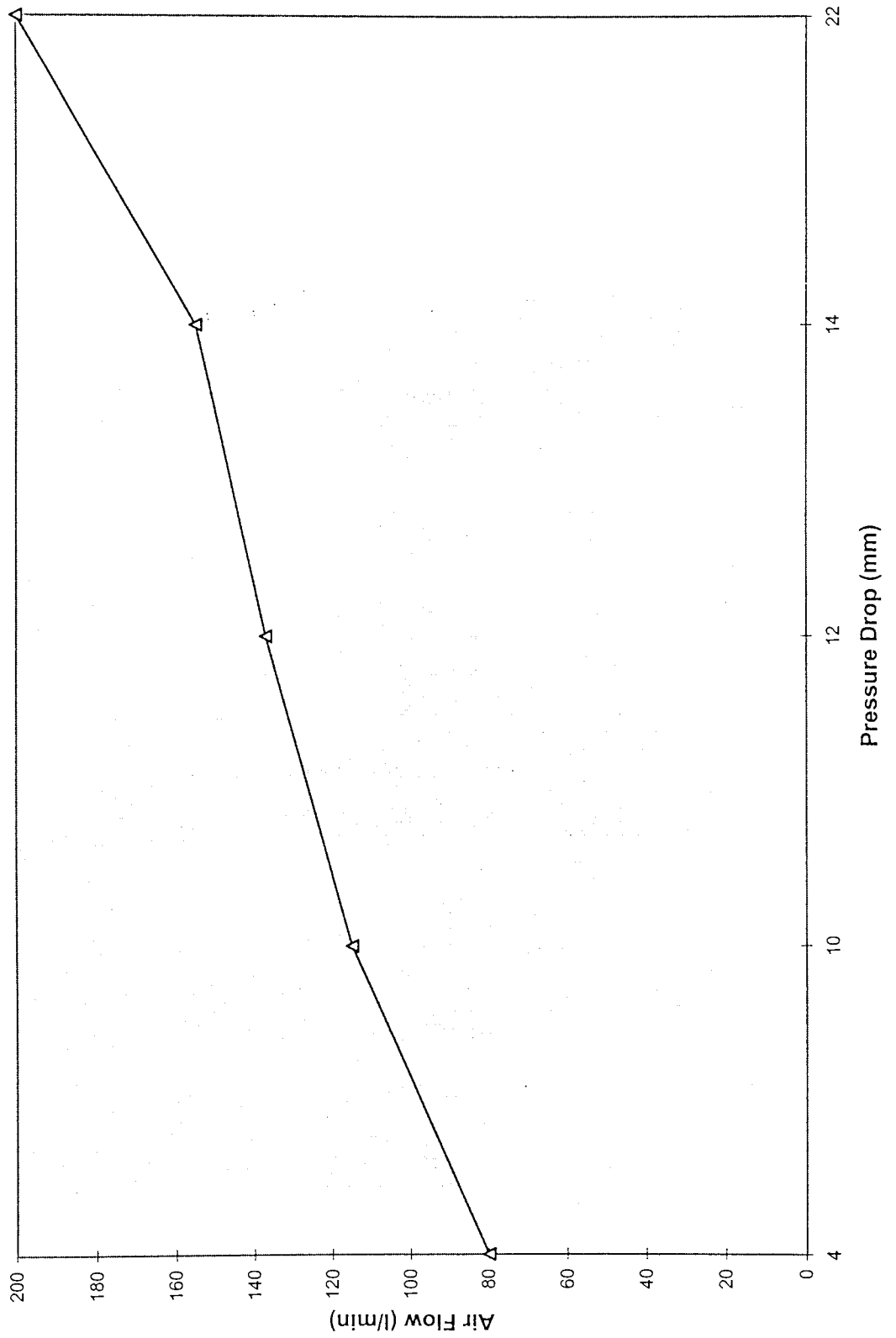
The previous Chapters have shown that it is possible to use vapour-directing slots on a sieve tray in order to improve the throughput and to eliminate slow moving/ stagnant zones. The rising vapour is given a horizontal velocity component in the direction of liquid flow by the slots, consequently there is an interchange of momentum between the vapour and liquid during the phase-contact and this accelerates the liquid across the sieve plate. The hydraulics of a slotted tray are mainly controlled by the slot vapour-velocity, slot vapour-pressure and the average liquid flowrate on the sieve tray. When designing such trays, it is important to know how much momentum is being transferred to the liquid. The aim of this work is to measure the slot vapour-velocity in order to relate it to the reduced liquid depth on the tray. This will ultimately enable the designer of trays to understand how much momentum transfer is needed (and hence slot vapour-velocity) for a particular reduction in froth height under different operating conditions.

it is also important to understand the hydraulics of the slot in terms of the bubble formation and distribution from the slots and the effect of any liquid inside the slotted section. The precise mechanisms of bubble formation at adjacent orifices, coalescence and break up within frothy mixture aren't well established. This is mainly due to the difficulty of observing the departure of bubbles from orifices deep in the flow field and their subsequent motion to the horizon of interfacial coalescence. At low gas velocities froths are characterised by a range of bubble sizes and velocities whose characteristics are difficult to predict. As gas velocities increase, gas jetting from the holes plays an increasingly important role. The theoretical analysis of bubbling from multiple holes is further complicated by the interaction of the pressure fields around neighbouring holes.

10. 2 EXPERIMENTAL PROCEDURE AND PROGRAMME

A single vapour-directing slot, Design 3 (see figure 7.3) , was pop-riveted onto the circular tray for which the inlet gap and outlet weir were each set at 50 mm . This was constructed from PVC to aid visual observation of gas and liquid behaviour inside the slot. The slot was positioned on the tray at a distance of 40 cm from the inlet gap and 160 cm from the outlet weir. The calibrated pitot tube was positioned in the middle of the vapour directing slot as close to the upper surface to prevent the pitot tube measuring the hole velocity.. This was held in position by means of a clamp stand. The pitot tube was connected to a U-tube manometer in order to measure the pressure drop. The range of superficial air- velocities used was 1 m/s to 2.5 m/s. Once the superficial air velocity had been fixed and steady state conditions had been achieved, pressure drop measurements were recorded: these readings were then converted, using the calibration curve, to the actual velocity of air through the slot. In order to investigate whether there was uniform air flowing through the slot, the position of the pitot tube was changed to the end of the slot and the above procedure repeated.

Fig. 10.1 Calibration Curve of Air-Flow Against Pressure Drop



10.3 Measurement Technique and Calibration

A pitot tube was used to measure the velocity of air passing through a single vapour-directing slot. It was constructed from 16 gauge needle tube and measured 10 cm in length.

Before the pitot tube could be used to measure the velocity of air through a single slot, it needed to be calibrated. In order to do this an experiment was set up which involved passing a known volume of air via a rotameter (tube size 24) through PTFE tubing straight section (the pitot tube was placed in the middle of the PTFE section). The pitot tube was connected to a U- tube manometer from which the corresponding pressure drop was noted. It should be noted that the pitot tube was placed inside the PTFE tubing which was connected to the rotameter in order to obtain a more accurate pressure drop reading over an even flow area.

A calibration curve was obtained, see figure 10.1 from which the velocity of air flowing through the slot could be estimated.

Note: Average values of pressure drop were plotted which produced a calibration curve which is not linear.

10.4 RESULTS AND DISCUSSION

The data obtained can be seen in Table 10.1 below:

Superficial Air Velocity (m/s)	Slot Velocity (m/s)
1.0	11.22
1.5	16.13
2.0	28.3
2.5	36.5

Table 10.1 : Superficial Air Velocity and Corresponding Slot Velocity

At low superficial air velocity, 1 m/s, the corresponding slot velocity is 11.22 m/s which is approximately equal to the hole velocity (10 m/s). Further increase in the superficial air velocity leads to a further increase in the slot velocity. There was little difference in the above results when the experiment was repeated with the pitot-tube placed at different positions under the slot.

With respect to the visual observations of the slot hydraulics there was no liquid underneath the slot whilst it was in operation under different air velocity and weir loads.

NO PAGE

223

Liquid and Vapour Momentum and Kinetic Energy

The vapour-directing slots work on the principle of an interchange of momentum between the vapour and liquid which is accelerated across the sieve plate. It is important therefore to try and understand how much momentum and kinetic energy both the liquid and vapour possess.

Data: Superficial Air Velocity = 1 m/s

Tray Area = 4.9 m²

Weir Length = 1.5 m

Free Area = 10 %

Density of Air = 1.2 kg/ m³

Density of Liquid = 1000 kg/ m³

Weir Load = 150 cm³/cms

Inlet Gap = 50 mm

Vapour:

$$\text{Hole Velocity} = \frac{\text{Superficial Air Velocity}}{\text{Free Area}}$$

$$\begin{aligned}\text{Vapour Flowrate} &= \text{Sup. Air Velocity} * \text{Tray Area} \\ &= 1 * 4.9 = 4.9 \text{ m}^3/\text{s}\end{aligned}$$

$$\begin{aligned}\text{Mass Flowrate} &= \text{Vapour Flowrate} * \text{Density of Air} \\ &= 4.9 * 1.2 = 5.88 \text{ kg/s} \\ &= 5.88 \text{ kg/s}\end{aligned}$$

$$\begin{aligned}\text{Kinetic Energy at orifices} &= \frac{1}{2} mv^2 = 0.5 * 5.88 * 10^2 \\ &= \underline{\underline{294 \text{ J/s}}}\end{aligned}$$

$$\begin{aligned}\text{Momentum at orifices} &= \text{Mass} * \text{Velocity} \\ &= 5.88 * 10 = \underline{\underline{58.8 \text{ kg m/s}^2}}\end{aligned}$$

LIQUID:

$$\begin{aligned}\text{Volumetric Flowrate} &= \text{Weir Load} * \text{Weir Length} \\ &= 150 * 1.5 = 22500 \text{ cm}^3/\text{s}\end{aligned}$$

$$\begin{aligned}\text{Mass Flowrate} &= \text{Vol. Flow} * \text{Density of Liq.} \\ &= 0.0225 * 1000 = 22.5 \text{ kg/s}\end{aligned}$$

$$\text{Liquid Velocity} = \frac{\text{Volumetric Flowrate}}{\text{Area Flow}}$$

$$= \frac{0.0225}{0.075} = 0.3 \text{ m/s}$$

$$\begin{aligned}\text{Kinetic Energy} &= \frac{1}{2}mv^2 \\ &= 0.5 * 22.5^2 * 0.3 = 1.0125 \text{ J/s}\end{aligned}$$

$$\begin{aligned}\text{Momentum} &= \text{Mass} * \text{Velocity} \\ &= 22.5 * 0.3 = 6.75 \text{ kgm/s}^2\end{aligned}$$

It can be concluded from the above calculations that the vapour has approximately 8 times more momentum than the liquid.

It is evident that the process of momentum transfer from the vapour to the liquid is important for understanding how slotted trays work. Little work has been done in this area with only one paper being published on the subject that by Bruin (1974). He derived an equation for the required free area of the slots on the tray to maintain a constant froth height across the tray in doing so, he assumed that the vapour issuing from the slots slowed down to the froth velocity as it passed through the froth. This latter assumption was made in the absence of any other information, but it is unlikely that all the available horizontal vapour momentum would be transferred to the liquid. Subsequent work by Lockett and Uddin (1976) who investigated momentum transfer from a single slot showed that, with clear liquid flowing across the tray, the reduction in liquid height after the slot is between 50 and 85 % of the reduction which is expected if complete momentum transfer occurs. This was equivalent to a utilisation of from 30 to 70 % of the initial momentum and pressure force of the gas issuing from the slot. It should be noted that a complete momentum balance on the slotted tray was not possible in a froth system due to the complicated nature of the pressure distribution in the froth.

10.5 CONCLUSION

The work carried out in this Chapter has shown that inside the slotted section there was no presence of liquid. It has also shown that at low superficial air velocities the corresponding slot velocity is approximately equal to the hole velocity.

CHAPTER 11

CONCLUSIONS

The work covered in this Thesis was aimed at modifying the flow pattern using flow control devices to try to improve the efficiency and throughput of sieve trays by reducing or eliminating stagnant zones or slow moving liquid. A reasonable success can be claimed with regard to the underlying engineering objectives. The main conclusions from the experimental work can be summarised as follows :

- (1) The purpose of the intermediate weirs is to deflect some of the liquid towards the sides of the circular tray providing a constant flow of liquid and hence reduce the stagnant zones. In the experiments using intermediate weirs which were placed in the centre of the sieve tray between the inlet downcomer and outlet weir, it was found that in general the effect of an intermediate weir depends on the depth of liquid or froth downstream of the weir. If the weir is deeper than the downstream depth it will cause the upstream liquid to be deeper than the downstream liquid. If the weir is not as deep as the downstream depth it may have little or no effect on the upstream depth. The depth of liquid (or froth) at a point on the tray in the froth regime depends on the liquid flow rate and height of inlet gap/ outlet weir.

- (2) A submerged weir set at an angle to the main direction of flow increases the flow of liquid towards the sides of the tray without causing an increase in the liquid hold-up/froth height. The maximum proportion of liquid caused to flow sideways by the weir is between 5 % and 10 %. It is concluded that intermediate weirs are only partially successful (not enough lateral movement.)

(3) The use of flow directing baffles on conventional sieve trays only addresses the flow pattern problem and does not bring the additional advantage of improved throughput. Work in this Thesis has shown that it is possible to use vapour-directing slots (pop-riveted to the tray) to remove stagnant zones and also increase the throughput of sieve trays. The use of a slotted tray helps to eliminate the hydraulic gradient and provide a more uniform froth height on the tray.

(4) Experimental work has shown that the horizontal momentum that is imparted to the liquid is dependent upon the size of the vapour-directing slot. In, use of a slot with dimensions $L = 20$ cm and $W = 20$ cm caused hydraulic jumps to occur at a short distance from the outlet of the slot. This was coupled with entrainment of liquid droplets directly above the outlet of the slot. Increasing the superficial air velocity causes the slot velocity to increase which in turn increases the distance and height of the hydraulic jump and also leads to an increase in the distance of the entrained liquid.

(5) The testing of a smaller slot, $L = 10$ cm and $W = 10$ cm, proved to be successful in that hydraulic jumps did not occur at the outlet of the slot. There was a sharp deflection of vapour as it passed along the tray with a reduction in the froth height. Experimental work carried out with the smaller slots placed evenly across a rectangular sieve tray (16 in total) produced interesting results. The placements of the slots was found not to be critical as long as the direction of the thrust of the vapour rising through the slots imparts a horizontal momentum to the froth and liquid upon the tray in the general direction of the outlet weir. At low weir loads the slotted tray provided too much momentum and some of the liquid was clearly blowing off the tray. At higher weir loads, however, there was complete vertical mixing of the biphasic with a uniform froth height across the tray. As the hydraulic gradient, which plays a main role in fixing the liquid flowrate on the plate, is eliminated the tray can handle higher liquid rates without weeping.

- (6) The hydraulics of a slotted tray are mainly controlled by the slot vapour-velocity and the slot vapour-pressure. The aim of the work in Chapter 10 was to measure the slot vapour velocity and tray and understand the hydraulics of the slot in terms of the bubble distribution and formation and the effect of any liquid inside the slotted section. Experiments show that firstly there was no liquid underneath the slot whilst it was in operation under different air velocity and weir loads. Results show that generally the slot vapour-velocity measured is approximately equal to that of the hole velocity.
- (7) The primary requirement of the downcomer is that its height must be sufficient to accommodate the liquid backup to avoid flooding . The data collected from the 6 manometers placed in the downcomers clearly show that the slotted tray has approximately 1.5 cm less liquid in the downcomer indicating that the tray has the potential to handle an increase in liquid throughput.
- (8) In order for a slotted tray to be considered commercially the effect of the slots on the point and tray efficiencies need to be investigated. It is of little use to develop a High Throughput tray which lowers the tray efficiency. The water-cooling technique was used to obtain the data required using a total of 70 platinum resistance thermometers evenly distributed across a rectangular sieve tray. Experimental results obtained show that the tray and point efficiencies of a slotted tray were 10 % less than an unslotted tray. It is likely that the reduction in froth height on a slotted tray causes an increase in the liquid velocity which in turn leads to a reduction in the liquid residence time which would account for the reduction in tray efficiency. With regard to the decrease in the point efficiency, this would seem to suggest that the large bubbles of vapour passing through the slots were the likely cause. It is important to note that this reduction in tray efficiency would not be apparent on a circular tray due to the increase in tray efficiency by the removal of the stagnant zones.

(9) The effectiveness of using vapour-directing slots on a full circular tray was investigated by using potassium permanganate dye to completely colour the biphasic and monitoring the removal of the dye by clear liquid entering the tray. With the initial experiments using high superficial air velocities and weir loads, the camera recorder did not reveal the dye as it crossed the tray due to the turbulent froth mixture. Using lower values of both superficial air velocities and weir loads, the results obtained show that for a normal tray the coloured dye was being removed faster in the middle of the tray, whilst at the sides of the tray the dye was being moved very slowly. With the slotted tray (the slots were placed according to the flow path length) the coloured dye in the middle of the tray was removed even quicker than an unslotted tray but more importantly more of the dye was removed from the sides i.e. reduction in the amount of dye in the slow moving areas. The net effect of this is an increase in the tray efficiency.

RECOMMENDATIONS FOR FUTURE WORK

The present investigation has opened a number of potential projects in this field for future studies. These include :

- (1) Experimental work has shown that the liquid hold-up on the tray decreases when the velocity of the gas through the slot is increased. This achievement of the slotted tray helps to eliminate the hydraulic gradient on the tray which can otherwise produce vapour-liquid maldistribution. Hence higher slot vapour-velocity results in a more uniform vapour-liquid distribution on the tray and thus the tray efficiency is increased. But at a very high slot velocity the tray efficiency will decrease as the vapour-liquid contact time decreases. Entrainment might also cause a problem at the higher slot vapour-velocity. Therefore for design purposes an optimum slot velocity must be found for a particular flow rate.
- (2) To try and develop the use of Expanded Metal on the tray as a means of transferring momentum to the liquid. The basic principle behind using Expanded Metal would still make use of the vapour to push the liquid uniformly across the tray from inlet to outlet. However, the use of fine expanded metal grid, the holes of which are narrow slots, would thus reduce the size of the gas bubbles being produced and hence have a negligible effect on the point efficiency. The use of expanded metal is not new, it has been recently used by Biddulph and Lavin (1990) in their paper entitled 'A New High Performance Flow Control Tray'. In their version developed for use in cryogenic distillation, the expanded metal slots are typically about 2.5 mm long and less than 1 mm wide. The angle of deflection of the slots is about 30 degrees to the horizontal. By developing a tray using Expanded Metal this would then have the characteristics of high throughput, good point and tray efficiencies and plug flow across the tray.
- (3) Improve the experimental techniques, in particular (a) replace the present method of measuring the water temperature (platinum resistance thermometers shielded by cylindrical containers) by a temperature probe which causes less disturbance to the flow pattern e.g. Small thermocouples near the tray floor (b) replace tray floor manometers by pressure transducers for rapid continuous measurement (c) obtain or devise a means of measuring the horizontal liquid velocity at any position on the tray.

REFERENCES

- AIChemE, Bubble Tray Design Manual, New York, 1958.
- Ali, Q.H., 1984., 'Gas distribution in shallow large diameter packed beds', PhD Thesis, Aston University.
- Ani, C. C., 1988, 'Flow Patterns, Performance and Scale-Up of Distillation Trays', Ph.D. Thesis, University of Aston in Birmingham, England.
- Bell, R.L., 1972, 'Experimental determination of residence time distributions on commercial scale distillation trays using a fibre optic technique', *AIChE J.*, **18** (3) 491.
- Bell, R.L., 1972, 'Residence time and fluid mixing on commercial scale sieve trays', *AIChE J.*, **18**, (3), 498.
- Bell, R.L. and Solari, R.B., 1974, 'Effect of non-uniform velocity fields and retrograde flow on distillation plate efficiency', *AIChE J.*, **20**, (4), 688
- Biddulph, M.W., Kler, S.C. and Lavin, J.T., 1990, 'Double expanded metal distillation tray', US Patent 5091 119.
- Bruin, S. and Freize, A.D., 1974, 'A simple liquid mixing model for distillation plates with stagnant zones', *Trans. IChemE.*, **52**, 75.
- Chambers, S., 1993, PhD Thesis, University of Aston In Birmingham, 'Observations of Gas Distribution Effects On The Liquid Flow Pattern'.
- Coulson, J.M. and Richardson, J.F. 'Chemical Engineering 3rd Edition' 1983, Pergamon Press Plc
- Darton, R.C., 1992, 'Distillation and absorption technology: current market and new developments', Closing address, *IChemE.*, **52**, 75.
- Diener, D.A., 'Calculation of Effect of Vapour Mixing on Tray Efficiency', *I.E.C. Process Design and Development*, 6 No. 4, 1967, 499.
- Enjugu, B.A., 1986, 'Flow Patterns and Performance of Distillation Trays', Ph.D. Thesis, University of Aston in Birmingham, England.
- Fair, J.R., Smith, B.D., *Design of Equilibrium Stage Processes*, 1963, pp551, McGraw Hill, New York.
- Fenwick, K.W., 1996, 'Liquid Distribution and Mass Transfer on a 2.44 m Distillation Tray', PhD Thesis, University of Aston in Birmingham.
- Gautreaux, M.F. and O'Connell, H.E., 1955, 'Effect of length of liquid path on plate efficiency', *Chem. Engng. Prog.*, **51**, (5), 232.
- Gerster J.A. et al, 'Tray Efficiencies in Distillation Columns', Final Report, University of Delaware, AIChE, New York, 1958.
- Hine, C.J., 1990, 'Effect of Liquid Flow Patterns on Distillation Trays', Ph.D. Thesis, University of Aston in Birmingham, England.
- Holhuis, P.A.M. and Zuiderweg, F.J., 1979, 'Sieve trays: Dispersion density and flow regimes', *IChemE. Symp.Ser.*, **56**, 2.2/1-2.2/27.

- Kafarov, V.V., Shestopalov, V.V and Komissarov, Y.A., 1979. 'Vapour-Liquid Flow structure on bubbler plates'. IChemE Symp. Ser., n56, 2.3/79.
- Keller, J.T., 'Improvements in Inlet Downcomer and Outlet Weir', Chem. Engng. Prog., 58, 1973.
- Kirkpatrick, R.D. and Weiler, D.W., 1978. 'Liquid-gas contacting tray', US Patent 4 101 610.
- Kirschbaum, E., Distillation and Rectification, p276, Brooklyn Chemical Publishing Co.1958.
- Kirschbaum, E., Forsch. Geb. Ingenieurw., 1934, 5, 245.
- Kister H.Z, Pinczewski, W.V. and Fell, C.J.D., 'Entrainment from sieve tray operating in the spray regime', American Chemical Society, Ind. Eng. Chem. Proc. Des. Dev., 20 (3), 528-532, 1981
- Kister, H.Z. and Haas, J.R., 'Sieve tray entrainment prediction in the spray regime', IChemE, No.104, Vol.1 A483, 1979.
- Kouri, R.J. and Sohlo, J.J., 1985, 'Effect of developing liquid flow patterns on distillation plate efficiency', Chem. Eng. Res. Des., **63**, (2), 117.
- Lavin, J.T., Distillation Trays with non-circular holes: expanded metal trays, Gas Separation and Purification, 6 (1), 3, 1986.
- Lewis, W.K., 'Plate Efficiency of Bubble Cap Columns', I.E.C., 28, 1936,399.
- Lim, C.T., Porter, K.E. and Lockett, M.J., 1974, 'The effect of liquid channelling on two pass distillation plate efficiency', Trans. IChemE., **52**, 193.
- Lockett, M.J., 1986, 'Distillation Tray Fundamentals', Cambridge University Press.
- Lockett, M.J., 1981, 'The froth to spray transition on sieve trays', Trans IChemE., **59**, 26.
- Lockett, M.J., and Dhulesia, H.A., 1980, 'Murphree plate efficiency with non-uniform vapour distribution', Chem. Engng. J. **19**, 183.
- Lockett, M.J., Lim, C.T. and Porter, K.E, 1973, 'The effect of liquid channelling on distillation column efficiency in the absence of vapour mixing', Trans. IChemE., **51**, 61.
- Lockett, M.J., Porter, K.E. and Bassoon, K.S., 1975, 'The effect of vapour mixing on distillation plate efficiency when liquid channelling occurs', Trans. I ChemE., **53**, 125.
- Lockett, M.J. and Safekourdi, A., 1976, 'The effect of the liquid flow pattern on distillation plate efficiency', Chem. Engng. J. **11**, 111
- Lockett, M.J., Uddin, M.S., (1978), Slotted Distillation Trays, Momentum Transfer From a Single Slot, Trans. Inst. Chem. Engrs., **56**, 194.
- Matsch, L.C., 1973. Liquid -gas contact tray', US Patent 3 759 498.
- Monovyan, B.H., Gaivanskii, T.E., 'Inclined Counter-Current Contact Tray', Trans. IChemE., 50, 152, 1980.
- Mix, J.E. 1980., Trans. IChemE., 55, 191.
- Murphree, E. V. , 1925, 'Rectifying column calculations', Ind.Engng Chem., 17(7), 747.

Perry R.H., 'Perry's Chemical Engineering Handbook 6th Edition, McGraw Hill Book Co, 1984.

Pinczewski, W.V. and Fell, C.J.D., 1972, 'The transition from froth-to-spray regime on commercially loaded sieve trays', Trans. IChemE., **50**, 102.

Porter, K.E., Lockett, M.J., and Lim, C.T., 'The Effect of Liquid Channelling on Distillation Plate Efficiency', T.I.Ch.E., 50, 1972, 91.

Porter, K.E., Discussion Meeting of EFCE Working Party on Distillation, Absorption and Extraction, June 1975.

Porter, K.E., Davies, B., Enjugu, B. A. and Ani, C.C., 1987, 'Investigating the effect of the liquid flow pattern on sieve tray performance by means of the water-cooling technique', IChemE. Symp. Ser., **n104**, 569.

Porter, K.E. and Jenkins, J.D., 1979, 'The interrelationship between industrial practice and academic research in distillation and absorption', IChemE. Symp. Ser., **n56**, 5.1/1.

Porter, K.E., and Lan, R., 1991, 'Gas driven liquid circulation on perforated trays', Aston university Internal Report on Advanced Studies in Distillation.

Porter, K.E., O'Donnell, K.A. and Latipifour, M., 1982, 'The use of water-cooling to investigate flow pattern effects on tray efficiency', IChemE. Jubilee Symp. Ser., **No. 73**: L33.

Porter, K.E., Safekourdi, A., and Lockett, M.J., 1977, 'Plate efficiency in the spray Regime', TransIChemE., **55**, 190.

Porter, K.E., Yu, K.T., Chambers, S. and Zhang, M.Q., 1992, 'Flow patterns and temperature profiles on a 2.44 m sieve tray', I. ChemE. Symposium Series **No 128**: A257.

Porter, K.E., Fletcher, J.P., Walton A.G., The IChemE Research Event Vol 2, 1193, 1996.

Raper, J.A., Hai, N.T., Pinczewski, W.V. and Fell, C.J.D., 1984, 'Liquid Passage on sieve trays operating in the spray regime', Chem. Eng. Res. Des., 62(2), 111.

Robinson. Private Communication, 1997.

Rush, F.E. Jr., 1979, 'Energy saving alternatives to conventional distillation', IChemE Symp. Ser., **56**, 4.1/1.

Sakata, M. and Yanagi, T., 1979, 'Performance of a commercial scale tray', IChemE Symp. Ser., **n56**, 3.2/21.

Smith, V.C. and Delnicki, W.V., 1975, 'Optimum sieve tray design', Chem. Engng Prog. **71** (8) 6.

Sohlo, J.J. and Kinnunen, S., 1977, 'Dispersion and flow phenomena on a sieve plate', Chem. Engng. Sci., **55**, (2) 71.

Solari, R.B. and Bell, R.L., 1986, 'Fluid flow patterns and velocity distribution on commercial scale sieve trays', AIChEJ., **32**, (4), 640.

Solari, R., Saez, E., D'Apollo, I. And Bellet, A., 1982, 'Velocity distribution and liquid flow patterns on industrial sieve trays', Chem. Engng. Comm. **13**, 369.

Stichlmair, J. and Ulbrich, S., 1987, 'Liquid channelling on trays and its effect on plate efficiency' IChemE. Symp. Ser., **n104**, 555.

Urua, I.J., Lavin, J.T. and Biddulph M.W., 1992, 'A new high performance flow control tray', IChemE. Symp. Series, **No. 128**: A345.

- Weiler, D.W., Bonnet, F.W. and Leavitt, F.W., 1971, 'Slotted sieve trays', Chem. Engng. Prog., **67**, (9), 86.
- Weiler, D.W., Delnicki, W.V. and England, B.L., 1973, 'Flow hydraulics of large diameter trays', Chem. Engng. Prog., **69**, (10), 67.
- Williams, B. and Yendall, E.F., 1968, 'Apparatus for liquid-gas contacting tray', US Patent 3 417 975.
- Winter B., Urti J.S. Chem Eng Prog., **50**, Sept 1976.
- Yanagi, T. and Scott, B.D., 1973, 'Effects of liquid mixing on commercial scale sieve tray efficiency', AIChEJ., Meeting, March, New Orleans.
- Yu, K.T., Huang, J., Li, J.L. and Song, H.H., 1990, 'Two-dimensional flow and eddy diffusion on a sieve tray', Chem. Engng Sci., 45(9), 2901.
- Yu, K.T., Huang, J. and Zhang, Z.T., 1991, 'Residence time profile and plate efficiency for a large tray with single-pass or two-pass liquid flow', J.Chem.Ind. Engng (China), 2,151.
- Yu, K.T., Huang, J., Zhang, Z., Residence Time Distributions and Efficiencies of Large Trays, Beijing, China, 1992.

APPENDIX 1A

HEIGHT OF CLEAR LIQUID MEASUREMENTS (mm), NO INTERMEDIATE WEIR, RECTANGULAR TRAY

(Results Described in Chapter 5)

Below are the values of the height of clear liquid (mm), measured over the 2.44 m diameter tray with **no intermediate weir**.

IG/OW = 10 mm

Superficial Air Velocity = 1.5 m/s
Water Weir = 50 cm³/cm s

20	20	23	26	17	20
19	18	21	20	16	21
17	17	20	18	19	19
14	15	18	17	17	16
12	17	14	14	14	13
10	11	10	11	11	9

Superficial Air Velocity = 1.5 m/s
Water Weir = 150 cm³/cms

14	13	16	16	11	15
28	30	29	32	28	28
28	30	29	31	29	29
28	30	29	31	29	29
25	23	22	22	22	19
16	14	4	15	14	13

Superficial Air Velocity = 1.5 m/s
Water Weir = 250 cm³/cm s

11	12	14	13	9	10
27	29	31	30	28	32
31	32	34	35	32	31
34	35	33	36	34	35
23	25	24	22	21	24
15	13	10	12	13	14

IG/OW = 10 mm

Superficial Air Velocity = 2.5 m/s
Water Weir = 50 cm³/cm s

8	10	13	10	3	11
9	12	12	15	9	12
12	11	13	13	11	13
12	13	11	13	12	11
8	7	11	11	10	8
7	7	5	7	5	7

Superficial Air Velocity = 2.5 m/s
Water Weir = 150 cm³/cms

8	6	8	5	2	9
19	20	19	22	21	18
21	23	24	21	23	23
21	19	18	17	20	17
15	16	17	16	18	18
13	14	12	12	9	10

Superficial Air Velocity = 2.5 m/s
Water Weir = 250 cm³/cm s

10	9	11	12	13	8
24	25	24	25	23	26
27	29	28	30	30	29
28	30	27	29	31	30
22	23	21	22	20	21
14	13	12	10	9	11

IG/OW = 20 mm

Superficial Air Velocity = 1.5 m/s
Water Weir = 50 cm³/cm s

21	21	26	29	20	23
19	22	22	21	20	21
21	20	24	23	20	22
21	19	22	21	19	19
16	20	16	18	18	17
16	18	16	18	16	16

Superficial Air Velocity = 1.5 m/s
Water Weir = 150 cm³/cms

25	23	22	25	18	20
31	31	34	34	31	33
32	30	34	34	31	33
29	25	30	29	27	27
21	27	24	25	26	24
20	20	22	21	20	18

Superficial Air Velocity = 1.5 m/s
Water Weir = 250 cm³/cm s

14	14	15	15	9.0	10
34	35	38	38	32	31
38	40	41	37	38	39
41	37	43	39	33	32
26	30	26	26	32	29
19	23	21	21	22	19

IG/OW = 20 mm

Superficial Air Velocity = 2.5 m/s
Water Weir = 50 cm³/cm s

14	14	16	15	12	14
16	14	15	19	15	12
14	14	17	15	17	16
16	14	14	11	13	12
14	12	13	16	16	14
11	13	13	12	13	14

Superficial Air Velocity = 2.5 m/s
Water Weir = 150 cm³/cm s

9.0	11	9.0	10	8.0	11
19	25	24	24	22	18
21	24	24	22	21	21
21	20	17	19	18	18
17	17	18	18	19	20
14	17	14	16	14	14

Superficial Air Velocity = 2.5 m/s
Water Weir = 250 cm³/cm s

10	13	8.0	9.0	2.0	10
26	27	25	27	23	22
30	34	32	29	30	29
28	31	27	27	29	25
25	26	30	29	28	24
19	20	16	16	19	17

IG/OW = 50 mm

Superficial Air Velocity = 1.5 m/s
Water Weir = 50 cm³/cm s

32	30	29	34	26	33
28	28	31	31	28	31
28	30	33	32	31	29
29	29	34	29	27	31
26	26	27	27	27	26
27	28	27	26	25	26

Superficial Air Velocity = 1.5 m/s
Water Weir = 150 cm³/cms

55	44	37	38	25	31
35	38	38	37	34	35
38	40	40	40	41	40
33	34	39	38	34	33
32	32	35	35	35	32
31	36	36	33	34	32

Superficial Air Velocity = 1.5 m/s
Water Weir = 250 cm³/cm s

58	59	52	41	53	45
53	56	49	44	41	43
40	46	48	43	47	41
38	39	45	41	40	40
36	36	33	37	40	32
33	37	33	36	38	31

IG/OW = 50 mm

Superficial Air Velocity = 2.5 m/s
Water Weir = 50 cm³/cm s

24	25	28	28	29	26
26	27	25	27	30	29
27	28	29	30	28	31
26	25	28	27	25	27
23	22	24	21	22	24
21	20	23	20	19	21

Superficial Air Velocity = 2.5 m/s
Water Weir = 150 cm³/cms

44	41	38	29	32	40
37	36	33	30	34	35
33	34	35	31	30	32
31	29	32	33	29	31
27	28	26	28	30	27
25	26	27	23	24	25

Superficial Air Velocity = 2.5 m/s
Water Weir = 250 cm³/cm s

56	55	58	54	60	53
52	51	50	51	52	49
47	45	46	43	44	42
41	40	39	37	41	38
37	35	36	34	37	35
34	32	33	31	33	31

APPENDIX 1B

HEIGHT OF CLEAR LIQUID MEASUREMENTS (mm), 10 mm INTERMEDIATE WEIR, RECTANGULAR TRAY

(Results Described in Chapter 5)

Below are the values of the height of clear liquid (mm), measured over the 2.44 m diameter tray with a **10 mm intermediate weir** placed on the tray.

IG/OW = 10 mm

Superficial Air Velocity = 1.5 m/s
Water Weir = 50 cm³/cm s

20	19	17	26	18	20
22	24	19	21	20	22
19	20	13	21	15	16
27	33	23	24	26	25
16	23	17	19	17	16
11	8.0	9.0	17	10	14

Superficial Air Velocity = 1.5 m/s
Water Weir = 150 cm³/cms

15	17	14	13	11	15
26	25	27	24	27	23
28	27	30	28	29	25
31	32	33	31	34	29
25	24	23	22	26	23
11	14	113	10	14	15

Superficial Air Velocity = 1.5 m/s
Water Weir = 250 cm³/cm s

13	12	9.0	10	14	11
26	25	28	27	25	27
30	31	32	30	29	31
36	37	35	36	34	37
27	26	28	25	23	26
17	16	15	14	18	17

IG/OW = 10 mm

Superficial Air Velocity = 2.5 m/s
Water Weir = 50 cm³/cm s

18	16	17	19	20	18
20	21	20	22	21	20
22	23	21	22	23	21
26	28	25	27	28	27
22	23	21	24	22	21
14	17	18	16	15	13

Superficial Air Velocity = 2.5 m/s
Water Weir = 150 cm³/cms

13	12	11	10	14	11
20	19	22	21	22	18
24	23	26	24	25	23
27	25	26	27	28	27
21	20	19	21	20	18
10	9.0	11	12	8.0	10

Superficial Air Velocity = 2.5 m/s
Water Weir = 250 cm³/cm s

9.0	8.0	10	11	14	12
21	23	20	22	21	19
27	26	26	27	26	27
30	32	31	30	29	30
24	23	22	23	22	21
14	13	15	12	13	14

IG/OW = 20 mm

Superficial Air Velocity = 1.5 m/s
Water Weir = 50 cm³/cm s

17	16	20	19	18	17
18	18	19	20	24	21
19	20	17	18	20	15
22	21	19	16	19	17
20	19	17	14	16	15
14	17	10	10	13	12

Superficial Air Velocity = 1.5 m/s
Water Weir = 150 cm³/cms

23	21	22	19	23	20
30	36	32	24	27	29
30	29	28	23	27	26
31	26	28	29	29	32
24	25	21	23	22	24
21	18	19	20	17	20

Superficial Air Velocity = 1.5 m/s
Water Weir = 250 cm³/cm s

13	12	11	10	12	14
29	28	30	31	32	33
34	33	35	32	34	35
36	37	37	35	37	36
24	22	23	22	21	23
17	18	16	15	19	17

IG/OW = 20 mm

Superficial Air Velocity = 2.5 m/s
Water Weir = 50 cm³/cm s

16	15	17	16	18	17
17	18	19	20	17	19
19	20	18	22	21	20
21	23	20	21	22	23
18	21	17	18	16	17
15	14	13	13	12	11

Superficial Air Velocity = 2.5 m/s
Water Weir = 150 cm³/cms

18	17	19	20	21	17
25	26	24	27	25	28
27	28	25	28	24	27
26	29	27	29	27	28
20	21	22	21	19	21
17	18	16	17	15	18

Superficial Air Velocity = 2.5 m/s
Water Weir = 250 cm³/cm s

10	9.0	11	12	10	8.0
24	23	22	25	22	23
29	28	27	29	26	27
31	32	33	32	29	30
22	21	20	18	19	21
16	15	14	17	16	19

IG/OW = 50 mm

Superficial Air Velocity = 1.5 m/s
Water Weir = 50 cm³/cm s

29	30	28	31	29	30
27	29	30	31	28	29
26	29	27	30	29	30
27	28	30	29	27	28
26	25	26	27	28	26
23	24	22	23	24	21

Superficial Air Velocity = 1.5 m/s
Water Weir = 150 cm³/cm s

49	51	46	48	52	50
41	42	38	40	43	44
37	40	39	36	39	41
33	34	35	32	33	34
29	31	30	28	30	31
27	28	31	27	26	30

Superficial Air Velocity = 1.5 m/s
Water Weir = 250 cm³/cm s

52	53	50	47	46	53
47	48	46	45	42	45
43	42	41	40	39	42
38	37	39	40	38	37
35	34	36	35	35	32
33	31	32	29	31	28

IG/OW = 50 mm

Superficial Air Velocity = 2.5 m/s
Water Weir = 50 cm³/cm s

27	26	29	25	27	30
26	25	27	24	28	29
24	23	26	24	27	28
23	22	24	22	24	23
21	21	22	20	22	23
20	19	20	18	17	21

Superficial Air Velocity = 2.5 m/s
Water Weir = 150 cm³/cms

43	44	37	38	42	46
33	35	34	32	37	38
34	36	35	31	34	37
29	30	32	30	32	34
28	27	29	26	28	29
27	25	28	25	27	26

Superficial Air Velocity = 2.5 m/s
Water Weir = 250 cm³/cm s

44	43	39	47	48	49
46	42	40	43	41	39
39	37	41	38	37	35
36	34	35	33	34	33
32	33	31	30	32	29
27	28	25	27	26	25

APPENDIX 1C

HEIGHT OF CLEAR LIQUID MEASUREMENTS (mm), 50 mm INTERMEDIATE WEIR, RECTANGULAR TRAY

(Results Described in Chapter 5)

Below are the values of the height of clear liquid (mm), measured over the 2.44 m diameter tray with a **50 mm intermediate weir** placed on the tray.

IG/OW = 10 mm

Superficial Air Velocity = 1.5 m/s
Water Weir = 50 cm³/cm s

26	33	32	37	39	33
34	33	38	36	35	39
31	29	36	34	36	35
23	19	15	22	29	25
21	18	14	16	19	19
12	11	12	10	14	15

Superficial Air Velocity = 1.5 m/s
Water Weir = 150 cm³/cms

18	17	20	16	17	18
32	33	35	30	34	32
33	36	33	34	35	33
18	19	17	22	20	17
17	16	18	20	19	15
16	14	14	16	17	13

Superficial Air Velocity = 1.5 m/s
Water Weir = 250 cm³/cm s

13	11	10	12	14	11
54	57	52	53	51	52
51	55	51	47	53	49
24	23	24	20	21	23
22	19	20	18	20	21
19	18	17	19	16	17

IG/OW = 10 mm

Superficial Air Velocity = 2.5 m/s
Water Weir = 50 cm³/cm s

30	31	32	29	33	28
31	29	33	32	32	30
32	31	31	33	30	31
18	17	19	16	15	17
17	16	17	18	16	17
14	13	15	16	14	15

Superficial Air Velocity = 2.5 m/s
Water Weir = 150 cm³/cm s

16	15	17	14	15	16
31	32	33	34	31	30
34	35	36	36	34	35
20	21	19	17	20	18
17	18	20	18	17	19
15	14	17	16	15	17

Superficial Air Velocity = 2.5 m/s
Water Weir = 250 cm³/cm s

12	13	14	9.0	11	13
46	49	52	48	49	48
49	50	48	49	50	48
21	22	20	22	21	22
19	20	21	20	19	21
18	19	18	17	18	19

IG/OW = 20 mm

Superficial Air Velocity = 2.5 m/s
Water Weir = 50 cm³/cm s

28	26	25	27	28	29
30	29	28	26	27	28
29	28	30	27	28	27
18	17	16	17	19	20
17	16	15	14	17	16
14	15	113	12	14	13

Superficial Air Velocity = 2.5 m/s
Water Weir = 150 cm³/cms

18	19	20	17	16	20
32	31	30	33	29	30
31	32	30	31	30	29
19	20	22	21	18	20
18	17	19	18	17	19
13	14	15	16	15	17

Superficial Air Velocity = 2.5 m/s
Water Weir = 250 cm³/cm s

13	11	9.0	10	8.0	11
46	45	47	46	47	43
48	46	46	47	45	46
27	26	25	27	28	29
24	25	23	24	26	27
24	24	22	21	23	24

IG/OW = 50 mm

Superficial Air Velocity = 1.5 m/s
Water Weir = 50 cm³/cm s

31	27	36	24	28	29
28	29	32	26	27	31
27	25	30	27	22	28
32	30	34	29	28	30
24	27	30	25	24	22
22	25	24	20	21	23

Superficial Air Velocity = 1.5 m/s
Water Weir = 150 cm³/cms

47	44	38	39	43	39
41	37	35	34	39	36
38	35	35	35	37	34
43	39	39	39	41	40
39	35	37	36	34	32
33	31	34	29	30	29

Superficial Air Velocity = 1.5 m/s
Water Weir = 250 cm³/cm s

57	55	51	55	49	50
53	56	50	52	48	47
46	45	47	43	44	46
49	50	51	48	49	50
38	41	39	42	41	40
34	36	34	35	34	32

IG/OW = 50 mm

Superficial Air Velocity = 2.5 m/s
Water Weir = 50 cm³/cm s

30	31	30	26	25	24
26	28	27	28	23	20
24	25	23	24	24	22
30	27	26	28	28	28
27	22	21	23	20	22
21	20	19	21	21	20

Superficial Air Velocity = 2.5 m/s
Water Weir = 150 cm³/cms

37	41	37	36	35	34
33	32	34	31	29	30
31	33	30	28	27	28
36	38	35	33	32	34
32	33	31	28	30	31
28	27	28	26	27	28

Superficial Air Velocity = 2.5 m/s
Water Weir = 250 cm³/cm s

51	48	47	52	50	47
48	47	44	46	45	43
42	41	40	41	39	38
47	46	44	48	43	42
40	37	36	37	36	37
32	33	31	34	31	32

APPENDIX 2

FLOW OVER OUTLET WEIR MEASUREMENTS (cm)

(Results Described in Chapter 6)

Flow Over The Outlet Weir Measurements

When the liquid flow over the outlet weir was investigated, the depth of water in six compartment boxes was recorded- the outlet weir being divided into six equal lengths. Below are the recorded depths of water (cm) in the compartments for the range of air and water flowrates.

INLET GAP = 10mm

OUTLET GAP = 10mm

No Intermediate Weir

AIR (m/s)	WATER (cm ³ /cm s)	COMPARTMENT NUMBER					
		2	3	4	5	6	7
0.7	25	2.9	2.2	2.0	2.5	2.7	2.2
	35	3.6	3.1	3.8	3.5	3.6	3.9
	55	10.0	9.3	9.0	8.8	9.5	9.7
0.9	25	2.5	2.1	2.4	2.5	2.7	2.1
	35	3.5	3.9	4.2	3.6	3.7	4.2
	55	9.7	9.1	9.0	8.9	9.2	9.8
	75	18.5	14.5	15.5	15.7	16.5	19.0
	110	42.5	39.5	38.0	37.0	38.5	41.4
1.2	25	2.4	2.8	3.0	2.4	2.5	2.9
	35	4.0	3.5	3.3	3.8	3.1	3.9
	55	10.5	9.0	9.5	8.9	9.2	10.0
	75	18.8	16.0	15.5	17.8	18.1	20.5
	110	41.8	40.0	37.5	38.4	38.7	40.0
1.5	25	2.7	3.0	2.2	2.5	2.7	2.8
	35	4.1	3.8	3.2	3.3	3.4	3.9
	55	10.16	9.4	9.3	9.0	9.4	10.5
	75	19.0	16.5	15.8	17.0	18.1	20.5
	110	43.7	39.0	36.0	37.5	38.5	42.5

INLET GAP = 10mm
 OUTLET GAP = 10mm

10mm Intermediate Weir

		COMPARTMENT NUMBER						
AIR (m/s)	WATER (cm ³ /cm s)	2	3	4	5	6	7	
0.7	25	2.9	2.7	2.8	2.3	2.2	2.5	
	35	4.1	3.8	4.0	3.4	3.1	3.5	
	55	10.8	10.3	9.9	8.1	7.5	8.4	
0.9	25	3.0	3.2	2.9	2.5	2.3	2.2	
	35	4.0	3.6	3.9	3.5	3.3	3.4	
	55	10.9	10.0	9.8	7.8	6.5	8.0	
	75	20.5	17.5	15.5	13.5	12.0	17.0	
	110	44.0	41.9	40.5	36.5	34.5	41.0	
1.2	25	2.8	2.5	2.6	1.9	2.1	2.0	
	35	4.2	3.9	4.0	3.6	3.2	3.5	
	55	10.5	9.8	10.0	8.0	7.2	8.5	
	75	21.0	19.5	17.9	13.0	12.0	18.0	
	110	43.5	42.0	41.0	36.0	35.5	42.0	
1.5	25	3.3	2.8	3.0	2.7	2.3	2.4	
	35	3.9	4.0	3.8	3.2	3.5	3.3	
	55	11.0	10.5	9.8	7.5	8.0	8.9	
	75	21.5	18.0	17.0	14.3	12.5	17.9	
	110	44.4	41.5	40.8	36.9	34.0	40.0	

APPENDIX 3

HEIGHT OF CLEAR LIQUID MEASUREMENTS IN DOWNCOMER RECTANGULAR TRAY

(Results Described in Chapter 7)

Height of Clear Liquid Measurements In Downcomer

Below are the values of the height of clear liquid (cm) measured over the 6 manometers placed in the inlet downcomer of a rectangular sieve tray.

IG/OW 50mm

Superficial Air Velocity 1.5 m/s

Unslotted Tray

Weir Load (cm ³ /cm s)	Manom 1 (cm)	Manom 2 (cm)	Manom 3 (cm)	Manom 4 (cm)	Manom 5 (cm)	Manom 6 (cm)
50	5.5	6.0	5.5	4.9	6.1	6.4
100	7.6	7.2	6.6	6.7	7.5	7.7
150	9.3	7.9	7.2	6.3	8.2	8.7
200	10.0	8.6	8.3	6.8	8.4	9.7
250	10.9	13.3	11.0	7.7	10.0	10.7

IG/OW 50 mm

Superficial Air Velocity

1.5 m/s

Slotted Tray

Weir Load (cm ³ /cm s)	Manom 1 (cm)	Manom 2 (cm)	Manom 3 (cm)	Manom 4 (cm)	Manom 5 (cm)	Manom 6 (cm)
50	4.5	4.6	4.4	4.5	4.5	5.0
100	5.2	5.3	5.0	4.9	5.2	5.7
150	7.6	6.3	5.8	5.5	6.2	7.5
200	8.2	7.6	7.5	6.3	7.2	8.5

Below are the values of the height of clear liquid (cm) measured over the 6 manometers placed in the inlet downcomer of a rectangular sieve tray.

IG/OW 50mm

Superficial Air Velocity 2.0 m/s

Unslotted Tray

Weir Load (cm³/cm s)	Manom 1 (cm)	Manom 2 (cm)	Manom 3 (cm)	Manom 4 (cm)	Manom 5 (cm)	Manom 6 (cm)
50	5.8	6.0	6.1	5.5	5.8	6.3
100	7.3	6.6	6.1	5.8	6.5	6.8
150	8.0	7.4	6.3	6.2	6.9	8.8
200	8.4	8.5	7.9	7.4	8.1	9.5
250	9.8	10.6	9.9	9.2	9.6	10.0

IG/OW 50 mm

Superficial Air Velocity 2.0m/s

Slotted Tray

Weir Load (cm³/cm s)	Manom 1 (cm)	Manom 2 (cm)	Manom 3 (cm)	Manom 4 (cm)	Manom 5 (cm)	Manom 6 (cm)
50	5.1	5.2	5.4	4.8	5.3	5.7
100	5.6	5.8	5.8	5.0	6.0	6.2
150	7.5	6.6	6.4	5.7	6.5	8.0
200	8.3	8.2	7.8	6.5	7.9	8.8
250	9.3	10.4	10.1	8.5	9.1	9.7

APPENDIX 3

HEIGHT OF CLEAR LIQUID MEASUREMENTS IN DOWNCOMER FULL CIRCULAR TRAY

(Results Described in Chapter 9)

Height of Clear Liquid Measurements In Downcomer, Full Circular Tray

Below are the values of the height of clear liquid (cm) measured over the 6 manometers placed in the inlet downcomer.

IG/OW 50mm

Superficial Air Velocity 1.0 m/s

Unslotted Tray

Weir Load (cm ³ /cm s)	Manom 1 (cm)	Manom 2 (cm)	Manom 3 (cm)	Manom 4 (cm)	Manom 5 (cm)	Manom 6 (cm)
50	6.3	6.1	6.4	5.9	6.1	5.8
100	8.6	7.1	6.9	6.2	7.2	7.4
150	8.8	7.6	7.4	6.2	7.6	9.4
200	10.3	10.2	9.9	8.4	9.7	10.1

IG/OW 50 mm

Superficial Air Velocity 1.0 m/s

Slotted Tray

Weir Load (cm ³ /cm s)	Manom 1 (cm)	Manom 2 (cm)	Manom 3 (cm)	Manom 4 (cm)	Manom 5 (cm)	Manom 6 (cm)
50	5.4	5.4	6.0	5.3	5.6	5.8
100	8.4	6.0	5.9	5.4	6.5	7.1
150	8.4	7.0	6.7	5.5	7.4	9.4
200	9.3	8.7	9.1	7.7	9.2	9.7

IG/OW 50mm

Superficial Air Velocity 1.5 m/s

Unslotted Tray

Weir Load (cm ³ /cm s)	Manom 1 (cm)	Manom 2 (cm)	Manom 3 (cm)	Manom 4 (cm)	Manom 5 (cm)	Manom 6 (cm)
50	6.6	6.9	7.1	7.0	7.4	7.4
100	10.7	7.7	8.0	6.6	8.3	9.4
150	10.2	8.1	8.6	7.3	9.0	11.0
200	11.5	11.0	11.5	9.9	11.2	12.0

IG/OW 50 mm

Superficial Air Velocity 1.5 m/s

Slotted Tray

Weir Load (cm ³ /cm s)	Manom 1 (cm)	Manom 2 (cm)	Manom 3 (cm)	Manom 4 (cm)	Manom 5 (cm)	Manom 6 (cm)
50	6.2	6.0	5.9	5.9	5.4	6.5
100	7.5	6.5	6.3	5.8	6.1	7.4
150	9.1	7.4	7.6	5.8	7.0	9.6
200	9.9	10.7	10.0	8.4	9.2	10.2

IG/OW 50mm

Superficial Air Velocity 2.0 m/s

Unslotted Tray

Weir Load (cm³/cm s)	Manom 1 (cm)	Manom 2 (cm)	Manom 3 (cm)	Manom 4 (cm)	Manom 5 (cm)	Manom 6 (cm)
50	8.2	8.3	9.1	8.7	7.7	9.0
100	12.7	9.1	9.4	8.4	8.4	10.4
150	11.2	9.4	9.8	8.8	9.2	12.2

IG/OW 50 mm

Superficial Air Velocity 2.0 m/s

Slotted Tray

Weir Load (cm³/cm s)	Manom 1 (cm)	Manom 2 (cm)	Manom 3 (cm)	Manom 4 (cm)	Manom 5 (cm)	Manom 6 (cm)
50	7.1	7.3	8.4	7.4	6.5	7.9
100	11.4	7.9	8.2	7.1	7.2	9.2
150	10.0	8.1	8.4	7.5	8.0	11.0